

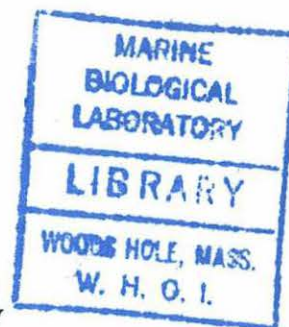
Nitrogen Isotopes in Chlorophyll and the Origin of Eastern Mediterranean  
Sapropels

by

Julian P. Sachs

B.A., Williams College  
(1989)

B.S., Massachusetts Institute of Technology  
(1991)



SUBMITTED IN PARTIAL FULFILLMENT  
OF THE REQUIREMENTS FOR THE DEGREE OF  
DOCTOR OF PHILOSOPHY

at the

MASSACHUSETTS INSTITUTE OF TECHNOLOGY  
and the  
WOODS HOLE OCEANOGRAPHIC INSTITUTION

February, 1997

© Julian P. Sachs, 1997. All rights reserved.

The author hereby grants to MIT and WHOI permission to reproduce and to distribute copies of  
this thesis document in whole or in part.

Signature of Author \_\_\_\_\_

Department of Earth, Atmospheric and Planetary Sciences,  
Massachusetts Institute of Technology and the Joint Program in  
Oceanography, Massachusetts Institute of Technology/Woods  
Hole Oceanographic Institution, November, 22, 1996.

Certified by \_\_\_\_\_

Daniel J. Repeta  
Thesis Supervisor

Accepted by \_\_\_\_\_

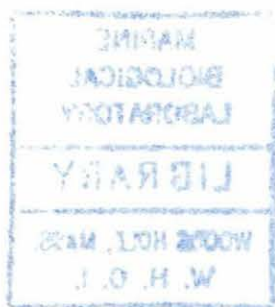
Edward A. Boyle  
Chairman, Joint Committee for Chemical Oceanography,  
Massachusetts Institute of Technology/Woods  
Hole Oceanographic Institution

GC  
7.1

, 522  
1997

1998

WHOI





# Nitrogen Isotopes in Chlorophyll and the Origin of Eastern Mediterranean Sapropels

by Julian P. Sachs

Submitted on November 22, 1996, in partial fulfillment of the requirements for the degree of Doctor of Philosophy at the Massachusetts Institute of Technology and the Woods Hole Oceanographic Institution.

## Abstract

The goals of this thesis were: (1) to establish methods for the determination of nitrogen and carbon isotope ratios in marine particulate and sedimentary chlorophyll derivatives; (2) to establish chlorophyll  $\delta^{15}\text{N}$  and  $\delta^{13}\text{C}$  as proxies for the nitrogen and carbon isotopic composition of marine phytoplankton; and (3) to use chlorophyll nitrogen isotopic ratios to understand the origin of Late Quaternary Eastern Mediterranean sapropels.

Techniques are presented for the determination of chlorin nitrogen and carbon isotopic ratios in marine particles and sediments with a precision greater than 0.15 per mil for both isotopes. The procedure can be performed in about 4 hours for particulate and 8 hours for sediment samples, and relies on multiple chromatographic purifications. About 20 g of a moderately organic-rich sediment are required.

A technique is also presented for the determination of chlorin nitrogen and carbon isotopic ratios by isotope-ratio monitoring gas chromatography-mass spectrometry (irmGC-MS) by synthesizing bis-(*tert.*-butyldimethylsiloxy)Si(IV) chlorin derivatives. However, yields for the 4-step synthesis were only about 5-6% and there was a net isotopic depletion of  $1.2 (\pm 0.3)$  per mil in the derivative, relative to the starting material.

These techniques are then used to show that the nitrogen isotopic difference between chlorophyll and whole cells in six species of marine phytoplankton is  $5.16 \pm 2.40$  per mil. For carbon, the isotopic difference between chlorophyll and whole cells in five species of marine phytoplankton is  $-0.02 \pm 2.12$  per mil. A model of the distribution of  $^{15}\text{N}$  in phytoplankton is constructed and it is demonstrated that the interspecies variability observed for the nitrogen isotopic difference between chlorophyll and whole cells can be attributed to differences in

the partitioning of cellular nitrogen between non-protein biochemicals. In the field, where mixed assemblages of phytoplankton prevail, the isotopic difference between chlorophyll and whole cells is expected to tend toward the average value of 5.16 per mil.

Finally, the average nitrogen isotopic composition of chlorins from six Late Quaternary Eastern Mediterranean sapropels ( $-5.01 \pm 0.38$  per mil) was found to be very similar to the  $\delta^{15}\text{N}$  of chlorophyll from the modern deep chlorophyll maximum ( $-6.38 \pm 1.80$  per mil) in the Eastern Mediterranean. In addition, sapropel photoautotrophic material, calculated from the chlorin  $\delta^{15}\text{N}$ , had the same isotopic composition (0.15 per mil) as both bulk sapropel sediments ( $-0.08 \pm 0.53$  per mil) and deep water nitrate ( $-0.05$  per mil). These data suggest (a) that bottom waters were anoxic, (b) that organic matter burial efficiency was enhanced, and (c) that oligotrophic conditions similar to today persisted, in the Eastern Mediterranean during sapropel deposition. These results contradict earlier interpretations of Late Quaternary bulk sedimentary  $\delta^{15}\text{N}$  in the Eastern Mediterranean. The latter concluded that the pattern of high  $\delta^{15}\text{N}$  values in intercalated marl oozes and low values in sapropels was the result of decreased nutrient utilization, and hence, increased primary production, during sapropel events. The low  $\delta^{15}\text{N}$  of deep water nitrate in the Eastern Mediterranean suggests a significant source of new nitrogen from biological  $\text{N}_2$ -fixation.

It is suggested that attempts to reconstruct the nitrogen isotopic composition of marine organic matter in the past by measuring the  $\delta^{15}\text{N}$  of whole sediments may be subject to misinterpretation due to the alteration of isotopic ratios during diagenesis. The partial oxidation of marine organic matter can result in significant isotopic enrichment of the preserved residual. The magnitude of this enrichment appears to be large when bottom waters are well-oxygenated, and small when bottom waters are anoxic. Environments where large temporal redox changes have occurred are expected to be the most problematic for the interpretation of bulk sedimentary  $\delta^{15}\text{N}$ . In these environments, the diagenetic signal can be at least as large as the primary isotopic signal being sought. The Eastern Mediterranean Sea during the Late Quaternary appears to be one such environment.

Thesis Supervisor: Daniel J. Repeta



## Acknowledgements

I am indebted to Daniel J. Repeta, my thesis supervisor, for guidance, support and friendship. His unfailing optimism and expertise as an organic chemist made this work possible. I am also grateful to Timothy I. Eglinton for his poignant comments throughout this work and for the use of his laboratory and equipment. Edward A. Boyle and Joseph P. Montoya also served as gracious members of my advisory committee. Ed first brought the fascinating issue of the origin of Eastern Mediterranean sapropels to my attention many years ago when he served as my undergraduate advisor and thesis supervisor at MIT. His rigorous standards for scientific research have served as a paradigm to which I have strived. Joe's knowledge of the controls on the nitrogen isotopic composition of phytoplankton and the techniques for growing algal cultures proved most beneficial. Finally, discussions with Ralf Goericke over the last five years have been instrumental in the development of the techniques and conclusions described in this thesis.

Most of the isotopic measurements presented in this thesis were performed by Kris Tholke at the Marine Biological Laboratory. Her skill at operating mass spectrometers for high precision measurements on small samples was invaluable. She always produced high quality results in a very short period of time. I am most indebted to her for her graciousness during the final months of this work when almost 200 isotope analyses were performed in less than 2 weeks.

Another instrumental figure during this work was Brian Fry. Brian offered important insights about nitrogen isotopic systematics on numerous occasions. Furthermore, his development of a cryofocussing technique for measuring nitrogen isotopic ratios on sub-micromolar samples made it possible to measure the isotopic composition of phytoplankton in the modern Eastern Mediterranean. He graciously spent the better part of a weekend making those measurements for me on a recent trip to the laboratory of Robert Michener at Boston University. Bob then used the technique to kindly generate chlorin isotopic values from two sapropel samples that would not otherwise have been possible.

Additional guidance and inspiration came from Mark A. Altabet. Mark has been a pioneer in the field of nitrogen isotopic biogeochemistry. His work

laid the foundation for many of the ideas presented in this thesis. He and Roger Francois were instrumental in the establishment of nitrogen isotopes as a tool for paleoceanographers.

There are numerous people to thank for their help in obtaining samples for this research. I am greatly indebted to Patrick Rimbault, the chief scientist of the Minos Cruise aboard R/V *Le Suroit*, in the Mediterranean Sea in May and June of 1996. He provided many hours of ship time for my sampling of sediments, particles and water. I am also grateful to Herve Claustre for his friendship and for facilitating my participation on that cruise.

Additional Mediterranean Sea samples came from the Ocean Drilling Program. I especially would like to thank Mimi Bowman and Walter Hale for rushing replacement sediment samples to me after a mishap with a drying oven.

I would also like to thank Susumu Honjo for providing me with ship time and logistical support on cruise TN 041 of R/V Thomas G. Thompson in the Arabian Sea in October and November of 1994.

Finally I owe much gratitude to my friends and family for support during this long, strange trip.

Funding for this work came from an Office of Naval Research Graduate Fellowship, the Woods Hole Oceanographic Institution Ocean Ventures Fund, and a Petroleum Research Grant (# 30124-AC2).



## Table of Contents

Abstract.....	iii
Acknowledgements.....	v
Table of Contents.....	vii
List of Figures.....	xv
List of Tables.....	xix

### **Chapter 1: Introduction .....1**

1.1 Goals of the Thesis.....	1
1.2 Overview of the Marine Nitrogen Cycle.....	1
1.3 Nitrogen Isotopic Ratios.....	3
1.4 Diagenetic Alteration of Nitrogen Istopic Ratios.....	4
1.5 Chlorophyll: A Universal Algal Biomarker.....	5
1.6 Origin of Eastern Mediterranean Sapropels.....	8
1.7 The Black Sea: A Modern Analog for Sapropel Depositional Conditions.....	11
1.8 Organization of the Thesis.....	11
References for Chapter 1.....	13

### **Chapter 2: Analytical Methodology I. Purification of Chlorins for Nitrogen and Carbon Isotopic Analysis .....17**

2.1 Abstract.....	17
2.2 Introduction.....	18
2.3 Methods.....	20
2.3.1 General Laboratory Procedures.....	20
2.3.2 Handling of Chlorin Pigments.....	21
2.3.3 Instrumentation.....	21
2.3.3.1 Spectrophotometry.....	21
2.3.3.2 Mass Spectrometry and Gas Chromatography-Mass Spectrometry.....	22

2.3.3.3 Nuclear Magnetic Resonance Spectroscopy (NMR) .....	23
2.3.3.4 High-Performance Liquid Chromatography (HPLC) .....	24
2.3.3.5 Elemental Analysis (CHN) .....	25
2.3.3.6 Isotope-Ratio Mass Spectrometry (irMS) .....	27
2.3.4 Beer's Law and Spectrophotometric Quantifications .....	28
2.3.5 Synthesis of Chlorin Standards .....	31
2.3.5.1 Methyl pheophorbide <i>a</i> .....	31
2.3.5.2 Methyl pyropheophorbide <i>a</i> .....	33
2.3.5.3 9-Deoxo-methyl-pyropheophorbide <i>a</i> .....	35
2.3.6 The Purification of Particulate Chlorophyll <i>a</i> for Isotopic Analysis .....	37
2.3.6.1 Particulate Sample Collection .....	37
2.3.6.2 Particulate Sample Extraction .....	38
2.3.6.3 Particulate Chlorophyll Chromatographic Purification .....	39
2.3.7 The Purification of Sedimentary Chlorins for Isotopic Analysis .....	41
2.3.7.1 Sediment Extraction .....	41
2.3.7.2 Solid-Phase Extraction (SPE) .....	41
2.3.7.3 Preparative Reverse-Phase High-Performance Liquid Chromatography (HPLC) .....	43
2.3.7.4 Size Exclusion Chromatography (SEC) .....	46
2.3.7.5 Normal-phase (SiO <sub>2</sub> ) High-performance Liquid Chromatography .....	48
2.4 Results .....	50
2.4.1 Purity of Particulate Chlorophyll <i>a</i> .....	50
2.4.2 Purity of Sedimentary Chlorins .....	54
2.4.3 Precision of Chlorin Isotopic Determinations .....	55
2.4.3.1 Precision of Particulate Chl <i>a</i> N and C Isotopic Determinations .....	56
2.4.3.2 Precision of Sedimentary Chlorin N and C Isotopic Determination .....	57
2.4.3.3 Reproducibility of Chlorin Isotopic Determinations .....	58



2.5 Discussion.....	60
2.5.1 Minimum Purification Required for Isotopic Analysis of Chlorins.....	60
2.5.2 Implications of Different N and C Isotopic Values in Sedimentary Chlorins.....	63
2.5.2.1 N Isotopic Differences Between PTNa and PPTNa.....	63
2.5.2.2 N Isotopic Difference Between Pheophytin Epimers .....	64
2.5.2.3 C Isotopic Differences Between Sedimentary Chlorins .....	65
2.5.3 Novel Sedimentary Pigments.....	66
2.5.3.1 Chl686.....	66
2.5.3.2 The Purple Compound.....	72
2.5.4 Sedimentary Chlorin Yields from Dried and Acidified Sediments.....	73
2.6 Conclusion .....	76
References for Chapter 2.....	78

### **Chapter 3: Analytical Methodology II. Synthesis of Chlorophyll**

#### **Derivatives for Gas Chromatography .....**

3.1 Abstract.....	83
3.2 Introduction.....	83
3.3 Background .....	85
3.3.1 Precursors to Volatile Chlorin Derivatives .....	85
3.3.2 Phthalocyanines.....	85
3.3.3 Porphyrins.....	87
3.4 Methods .....	88
3.4.1 General Laboratory Procedures.....	88
3.4.1.1 Handling of Moisture-Sensitive Reagents.....	88
3.4.1.2 Solvent Drying and purification.....	90
3.4.1.3 Instrumentation.....	90
3.4.1.3.1 Gas Chromatography.....	90
3.4.1.3.2 Mass Spectrometry and Gas	

Chromatography-Mass Spectrometry.....	91
3.4.1.3.3 Isotope-Ratio Monitoring Gas	
Chromatography-Mass Spectrometry.....	92
3.4.1.3.4 Nuclear Magnetic Resonance	
Spectroscopy (NMR).....	93
3.4.1.3.5 Spectrophotometry.....	93
3.4.2 Synthesis of Volatile Chlorin Si(IV) Complexes.....	94
3.4.2.1 9-Deoxy-methyl-pyropheophorbide <i>a</i> .....	94
3.4.2.2 Chlorin Dichlorosilicon Complexes [PhSiCl <sub>2</sub> ].....	96
3.4.2.2.1 Dichlorosilicon (IV) Methyl	
Pyropheophorbide <i>a</i> .....	96
3.4.2.2.2 Dichlorosilicon (IV) 9-Deoxy-Methyl	
Pyropheophorbide <i>a</i> .....	99
3.4.2.3 Chlorin Dihydroxysilicon	
Complexes [PhSi(OH) <sub>2</sub> ].....	100
3.4.2.3.1 Dihydroxysilicon (IV) Methyl	
Pyropheophorbide <i>a</i> .....	100
3.4.2.3.2 Dihydroxysilicon (IV) 9-Deoxy-Methyl	
Pyropheophorbide <i>a</i> .....	100
3.4.2.4 Chlorin bis( <i>tert.</i> -butyldimethylsiloxy)Si(IV)	
Complexes [PhSi(OTBDMS) <sub>2</sub> ].....	104
3.4.2.4.1 bis( <i>tert.</i> -butyldimethylsiloxy)Si(IV) Methyl	
Pyropheophorbide <i>a</i> .....	104
3.4.2.4.2 bis( <i>tert.</i> -butyldimethylsiloxy)Si(IV) 9-	
Deoxy-Methyl Pyropheophorbide <i>a</i> .....	107
3.4.3 Aromatization and Nickel Insertion Reactions of	
Chlorins .....	110
3.4.3.1 Aromatization of 9-Deoxy	
Methylpyropheophorbide <i>a</i> .....	110
3.4.3.2 Insertion of Nickel Into 9-Deoxy- Chlorins .....	111
3.5 Results.....	111
3.5.1 irmGC-MS Analysis of Derivatized Chlorins.....	113
3.5.2 Isotopic Fractionation During Derivatization of	
Methyl Pyropheophorbide <i>a</i> .....	116
3.6 Discussion.....	119
3.6.1 Chlorin C-9 Ketone Reduction .....	121



3.6.2 Chlorin Dichlorosilicon Complex.....	122
3.6.3 Hydrolysis of the Chlorin Dichlorosilicon Complex.....	123
3.6.4 Silylation of the Chlorin Dihydroxysilicon Complex.....	124
3.6.5 Direct High-Temperature GC of Chlorins.....	129
3.7 Conclusion .....	134
References for Chapter 3.....	136
 <b>Chapter 4: Nitrogen and Carbon Isotopic Ratios in Chlorophyll.....</b>	<b>141</b>
4.1 Abstract.....	141
4.2 Introduction.....	142
4.3 Methods .....	144
4.3.1 Culturing Procedures.....	144
4.3.2 Chlorophyll Purification.....	148
4.3.3 Purity of Chlorophyll Isolated from Phytoplankton.....	149
4.3.4 Isotope Analyses.....	149
4.3.5 Precision of the Analysis.....	151
4.4 Results.....	152
4.4.1 Nitrogen Isotopes.....	152
4.4.2 Carbon Isotopes .....	156
4.5 Discussion.....	159
4.5.1 Nitrogen Isotopes.....	159
4.5.1.1 Overview of Chlorophyll Biosynthesis .....	160
4.5.1.2 Isotopic Fractionation During Chlorophyll Biosynthesis .....	160
4.5.1.2.1 Transamination .....	163
4.5.1.2.2 ALA Condensation to PBG.....	163
4.5.1.2.3 PBG Condensation to Form Hydroxymethylbilane .....	164
4.5.1.2.4 Mg Insertion of Protoporphyrin IX to Form Mg-Protoporphyrin IX.....	165
4.5.1.2.5 Fe Insertion to PTP and the Heme/Bilin Branch.....	167
4.5.1.2.6 Summation of Chlorophyll Biosynthesis and Isotopic Fractionation Discussion.....	167

4.5.1.3 Variability in Chlorophyll $^{15}\text{N}$ -Depletion Between Algal Species .....	168
4.5.1.3.1 A Model of the Distribution of Nitrogen Isotopes in Phytoplankton.....	170
4.5.1.3.2 Interspecies Differences in $\Delta\delta^{15}\text{N}$ Based Upon Branching Ratios of Glutamate.....	173
4.5.1.4 Growth Rate and Nitrogen Isotopic Fractionation.....	175
4.5.1.5 Nutrient Source and Chlorophyll-Cell N Isotopic Differences.....	177
4.5.2 Carbon Isotopic Differences Between Chlorophyll and Algae.....	179
4.6 Conclusion.....	181
References for Chapter 4.....	183

## **Chapter 5: The Origin of Eastern Mediterranean Sapropels.....189**

5.1 Abstract.....	189
5.2 Introduction.....	190
5.3 Methods .....	194
5.3.1 Sample Collection.....	195
5.3.2 Nitrogen Isotopic Measurements on Small Samples: Cryofocussing.....	200
5.3.3 Preparation of Nitrate Samples for Isotopic Analysis.....	201
5.3.4 Precision of Isotopic Measurements.....	201
5.4 Results.....	202
5.4.1 Nitrogen and Carbon Isotopes in the Mediterranean Sea .....	202
5.4.1.1 Water Column Particulate Samples.....	202
5.4.1.2 Water Samples .....	205
5.4.1.3 Sediment Samples.....	206
5.4.2 Nitrogen and Carbon Isotopes in the Black Sea.....	211
5.5 Discussion.....	214
5.5.1 Prior Nitrogen Isotope Studies in the Eastern Mediterranean.....	214

5.5.2 N Isotopic Fractionation During Biological Transformations .....	216
5.5.2.1 Nitrogen Isotopes as Tracers of Nutrient Utilization .....	216
5.5.3 Diagenetic Alteration of Nitrogen Isotopic Ratios .....	218
5.5.3.1 Eastern Mediterranean Sedimentary $\delta^{15}\text{N}$ : An Artefact of Diagenesis.....	219
5.5.3.2 Preservation of Sedimentary $\delta^{15}\text{N}$ Under Anoxic Bottom Water.....	223
5.5.3.3 Origin of Diagenetic $^{15}\text{N}$ -Enrichment in Sediments.....	226
5.5.4 The Origin Of Eastern Mediterranean Sapropels.....	226
5.5.4.1 Persistence of Oligotrophic Conditions in the E. Mediterranean During the Past 200 kyr.....	227
5.5.4.2 Higher Carbon Accumulation Through Improved Preservation .....	228
5.5.4.3 Toward a Unified Picture of Eastern Mediterranean Sapropel Formation.....	230
5.5.4.4 Comparison of E. Mediterranean Sapropels to the Modern Black Sea.....	232
5.5.4.4.1 The Effect of Denitrification and Nitrification on $\delta^{15}\text{N}$ Values in the Black Sea and in Eastern Mediterranean Sapropels.....	235
5.5.4.5 The Origin of Sedimentary Chlorins.....	237
5.5.5 Origin of Low Nitrogen Isotopic Ratios in the Eastern Mediterranean .....	238
5.5.6 Carbon Isotopic Ratios in Eastern Mediterranean Sapropels.....	242
5.6 Conclusion .....	244
References for Chapter 5.....	248
 <b>Chapter 6: Conclusion.....</b>	 <b>267</b>
6.1 General Conclusions.....	267
6.1 Directions for Future Research.....	269





## List of Figures

Figure 1.1: The global nitrogen cycle.....	2
Figure 1.2: Structure of chlorophyll <i>a</i> .....	5
Figure 1.3: Possible transformation pathways for chlorophyll <i>a</i> to DPEP.....	6
Figure 1.4: Typical example of sapropels recovered from the Eastern Mediterranean. ....	9
Figure 1.5: Overview map of the Eastern Mediterranean Sea and schematics showing the widespread occurrence of sapropels in that basin. ....	10
Figure 2.1: Visible spectra of (a) a whole sediment extract and (b) a purified chlorin from Unit II sediments in the Black Sea.....	30
Figure 2.2: Synthesis of methyl pheophorbide <i>a</i> from chlorophyll <i>a</i> .....	32
Figure 2.3: Progress of ketone reduction reaction. ....	36
Figure 2.4: Analytical C18 HPLC chromatograms of a surficial Black Sea sediment after (a) solvent extraction, (b) solid-phase extraction, and (c) size-exclusion chromatography. ....	44
Figure 2.5: Size-exclusion chromatograms of a surface Peru Margin sediment extract. ....	47
Figure 2.6: Purity of algal pheophytin <i>a</i> following each step of the procedure for the purification of particulate chlorins for isotopic analysis. ....	52
Figure 2.7: Purity of a Black Sea surficial sedimentary chlorin (pyropheophytin <i>a</i> ) after successive purification steps. ....	55
Figure 2.8: Visible (a) and mass (b) spectra of Chl686. ....	67
Figure 2.9: Analytical C18 HPLC chromatograms of (a) the pheophytin fraction and (b) the Chl686 fraction collected from a size-exclusion column. ....	68
Figure 2.10: Visible spectrum of Chl686 after standing in methylene chloride at -20°C for 20 days.....	70
Figure 2.11: Visible spectrum of purple compound in acetone.....	70
Figure 2.12: Results of an experiment to determine the effects of sediment drying and acidification on the recovery of chlorins. ....	75
Figure 3.1: Structures of precursors to volatile chlorin silicon complexes. ....	86

Figure 3.2: Schematic of the Finnigan irmGC-MS system for $\delta^{15}\text{N}$ , $\delta^{13}\text{C}$ , $\delta^{18}\text{O}$ .....	92
Figure 3.3: Progress of ketone reduction reaction. ....	95
Figure 3.4: Visible spectra of (a) MPPBDa in acetone, and (b) (MPPBDa)SiCl <sub>2</sub> in MeOH. ....	97
Figure 3.5: Visible spectrum of (9MPPBDa)SiCl <sub>2</sub> in MeOH. ....	99
Figure 3.6: Visible spectrum of (9MPPBDa)Si(OH) <sub>2</sub> in MeCl <sub>2</sub> . ....	103
Figure 3.7: Methane chemical ionization mass spectrum of (9MPPBDa)Si(OH) <sub>2</sub> .....	103
Figure 3.8: GC-CI mass spectrum of (MPPBDa)Si(OTBDMS) <sub>2</sub> .....	106
Figure 3.9: Visible spectrum of (9MPPBDa)Si(OTBDMS) <sub>2</sub> in hexane. ....	108
Figure 3.10: GC-CI mass spectrum of (9MPPBDa)Si(OTBDMS) <sub>2</sub> .....	108
Figure 3.11: (a) GC-CI total ion chromatogram of (9MPPBDa)Si(OTBDMS) <sub>2</sub> .....	109
Figure 3.12: Visible spectrum in acetone of 9MPPBDa after ring IV oxidation with DDQ. ....	110
Figure 3.13: Visible spectra of (a) Ni(II) 9-deoxo-methyl pyropheophorbide <i>a</i> in acetone, and (b) the Ni(II) derivative of ring-IV oxidized 9MPPBDa in acetone .....	112
Figure 3.14: Visible spectrum of Ni(II) deuteroporphyrin dimethyl ester in acetone .....	112
Figure 3.15: Chromatograms from irmGC-MS runs of derivatized 9MPPBDa.....	115
Figure 3.16: Isotopic fractionation resulting from each step of two chlorin derivatizations. ....	117
Figure 3.17: The 4-step synthesis of GC-amenable chlorin derivatives. ....	120
Figure 3.18: Stabilization of free enol by formation of a silyl enol ether.....	121
Figure 3.19: FAB <sup>+</sup> mass spectrum of of the polar band (R <sub>F</sub> =0.56) from alumina TLC of the reaction product of the MPPBDa derivatization. ....	125
Figure 3.20: GC-CI <sup>+</sup> mass spectrum of (MPPBDa)Si(OTBDMS) <sub>2</sub> .....	125
Figure 3.21: GC-CI <sup>+</sup> mass spectrum of compound eluting 19 seconds after (MPPBDa)Si(OTBDMS) <sub>2</sub> . ....	126
Figure 3.23: Gas chromatogram of methyl pyropheophorbide <i>a</i> . ....	129
Figure 3.24: Gas chromatograms of (a) deuteroporphyrin IX dimethyl ester, and (b) 9-deoxo-methyl pyropheophorbide <i>a</i> . ....	131



Figure 3.25: Gas chromatograms of (a) methyl pyropheophorbide <i>a</i> , (b) ring IV-oxidized 9-deoxo-methyl pyropheophorbide <i>a</i> , and (c) a C12-C60 normal alkane standard.....	132
Figure 4.1: Visible absorption spectra of 5 phytoplankton cultures over time.....	147
Figure 4.2: Plot of $\Delta\delta^{15}\text{N}_{\text{cell-Chl}a}$ vs $\delta^{15}\text{N}_{\text{cell}}$ for all 14 phytoplankton cultures grown in this investigation.....	153
Figure 4.3: Plot of $\Delta\delta^{15}\text{N}_{\text{cell-Chl}a}$ vs $\delta^{15}\text{N}_{\text{cell}}$ for all known paired chlorophyll and bulk $\delta^{15}\text{N}$ determinations in (a) plants, (b) marine phytoplankton, and (c) higher plants.....	155
Figure 4.4: Plot of $\Delta\delta^{13}\text{C}_{\text{cell-Chl}a}$ vs $\delta^{13}\text{C}_{\text{cell}}$ for (a) algal cultures grown in this study, (b) all plants and algae from this study and the literature, and (c) only the higher plants from (b). ....	157
Figure 4.5: The conversion of ammonia into the $\alpha$ -amino group of glutamate.....	161
Figure 4.6: The biosynthetic pathway of chlorophyll and other tetrapyrroles.....	161
Figure 4.7: Condensation of 4 PBG molecules to form hydroxymethylbilane. ....	164
Figure 4.8: A plot of the nitrogen isotopic difference between chlorophyll and whole cells (e.g., $\Delta\delta^{15}\text{N}_{\text{cell-Chl}a}$ ) for 8 species of marine phytoplankton. ....	169
Figure 4.9: The distribution of nitrogen in phytoplankton as a percentage of total cellular nitrogen. ....	169
Figure 4.10: A conceptual model for the distribution of $^{15}\text{N}$ in phytoplankton. ....	172
Figure 4.11: Relationship between nitrogen isotopic fractionation during nitrate assimilation and growth rate. ....	176
Figure 4.12: The carbon isotopic difference between chlorophyll and whole cells, $\Delta\delta^{13}\text{C}_{\text{cell-Chl}a}$ , for 7 species of marine phytoplankton. ....	180
Figure 5.1: Schematic diagrams of different Eastern Mediterranean Sea circulation patterns .....	193
Figure 5.2: Overview map of the Eastern Mediterranean Sea with schematics showing the widespread occurrence of sapropels in that basin. ....	196

Figure 5.3: Minos Cruise station locations.....	198
Figure 5.4: Map of the Black Sea showing sample locations.....	199
Figure 5.5: Nitrate and phosphate profiles at Station 11 in the Eastern Mediterranean. ....	205
Figure 5.6: Stratigraphic position of Late Quaternary Eastern Mediterranean sapropels within (a) the SPECMAP stacked $\delta^{18}\text{O}$ record of Imbrie, et al (1984), and (b) the orbital precession index of Berger and Loutre (1991). ....	206
Figure 5.7: Typical reverse-phase HPLC chromatogram of a sapropel solvent extract after solid-phase extraction. ....	210
Figure 5.8: Age versus depth relationship for Unit II sediments from the Black Sea, core KNR 134-08 BC17. ....	213
Figure 5.9: Profiles of (a) organic carbon concentration, (b) sedimentary $\delta^{15}\text{N}$ , and (c) $\delta^{13}\text{C}$ of organic carbon in core MD 84641 from the Eastern Mediterranean. ....	215
Figure 5.10: Nitrogen isotopes in the Equatorial Pacific. ....	217
Figure 5.11: Nitrogen isotopes in (a) the modern Eastern Mediterranean, and (b,c) Late Quaternary Eastern Mediterranean sediments.....	220
Figure 5.12: Nitrogen isotopes in (a) the modern Black Sea, and (b) Unit I and II sediments. ....	234
Figure 5.13: Carbon isotopes in (a) the modern Mediterranean Sea, and (b,c) Late Quaternary Eastern Mediterranean sediments. ....	243



## List of Tables

Table 1.1: Common chlorin abbreviations used in this text.....	7
Table 2.1: Solvent gradient for preparative C <sub>18</sub> HPLC.....	40
Table 2.2: Retention times for common sedimentary chlorins on preparative reverse-phase (C <sub>18</sub> ) HPLC.....	45
Table 2.3: Retention times of reference compounds for size exclusion chromatography.....	48
Table 2.4: Solvent mix for isocratic elution of common sedimentary chlorins on preparative SiO <sub>2</sub> HPLC.....	49
Table 2.5: Purity of algal pheophytin <i>a</i> following each step of the procedure for the preparation of particulate chlorins for isotopic analysis.....	51
Table 2.6: Reproducibility of N and C isotopic determinations on particulate and sedimentary chlorins.....	59
Table 2.7: Isotopic ratios and elemental purities of Black Sea surficial sedimentary chlorins after sequential purification steps.....	61
Table 2.8: N and C isotopic ratios in purified chlorins from surficial Black Sea sediments. ....	63
Table 3.1: Chlorin $\delta^{15}\text{N}$ and $\delta^{13}\text{C}$ values from irmGC-MS.....	114
Table 3.2: Isotopic results for repeat derivatizations of MPPBDa. ....	116
Table 4.1: Description of cultures used in this study.....	144
Table 4.2: Composition of f/2 Medium.....	145
Table 4.3: Compilation of all paired nitrogen and carbon isotopic measurements in plants and algae from this study and the literature.....	154
Table 4.4: Cellular $^{15}\text{N}$ distribution model output.....	174
Table 5.1: Sapropel samples from ODP leg 160 for which chlorin N and C isotopic determinations were made.....	197
Table 5.2: Samples from the Mediterranean Sea collected during R/V <i>Le Suroit</i> Minos Cruise, 5/22/96-6/5/96 and used in this study.....	198

Table 5.3: Description of Black Sea sediment samples used in this study.....	199
Table 5.4: Precision of nitrogen and carbon isotopic determinations in different sample types.....	202
Table 5.5: Nitrogen and carbon isotopic composition of chlorophyll, suspended particulate and nitrate samples from the Mediterranean Sea.....	203
Table 5.6: Nitrogen and carbon isotopic ratios in Eastern Mediterranean sediments.....	207
Table 5.7: Nitrogen and carbon isotopic ratios in chlorins and sediments from Eastern Mediterranean sapropels.....	209
Table 5.8: Nitrogen and Carbon isotopic ratios in sediments and chlorins from the Black Sea.....	212
Table 5.9: The link between bottom water oxygen concentrations and the diagenetic alteration of $^{15}\text{N}/^{14}\text{N}$ ratios in marine organic matter.....	224



### **1.1 Goals of the Thesis**

The goals of this thesis were: (1) to establish methods for the determination of nitrogen and carbon isotope ratios in marine particulate and sedimentary chlorophyll derivatives; (2) to establish chlorophyll  $\delta^{15}\text{N}$  and  $\delta^{13}\text{C}$  as proxies for the nitrogen and carbon isotopic composition of marine phytoplankton; and (3) to use chlorophyll nitrogen and carbon isotopic ratios to understand the origin of Late Quaternary Eastern Mediterranean sapropels.

### **1.2 Overview of the Marine Nitrogen Cycle**

Nitrogen is a limiting nutrient to primary production in the ocean (Dugdale and Goering, 1967; McCarthy and Carpenter, 1983; McElroy, 1983). Phytoplankton productivity is generally high where fixed nitrogen concentrations are elevated and low where they are diminished. Since primary productivity is thought to influence climate--through the uptake of atmospheric carbon dioxide--and the generation of petroleum, it is important to understand nitrogen cycling in the ocean.

The marine nitrogen cycle is complex and not well understood (Codispoti, 1995). Current estimates suggest that the combined oceanic sinks for nitrogen are larger than sources by 75% (Codispoti and Christensen, 1985), but uncertainties of a factor of 2 to 4 exist regarding the magnitude of each term. As summarized

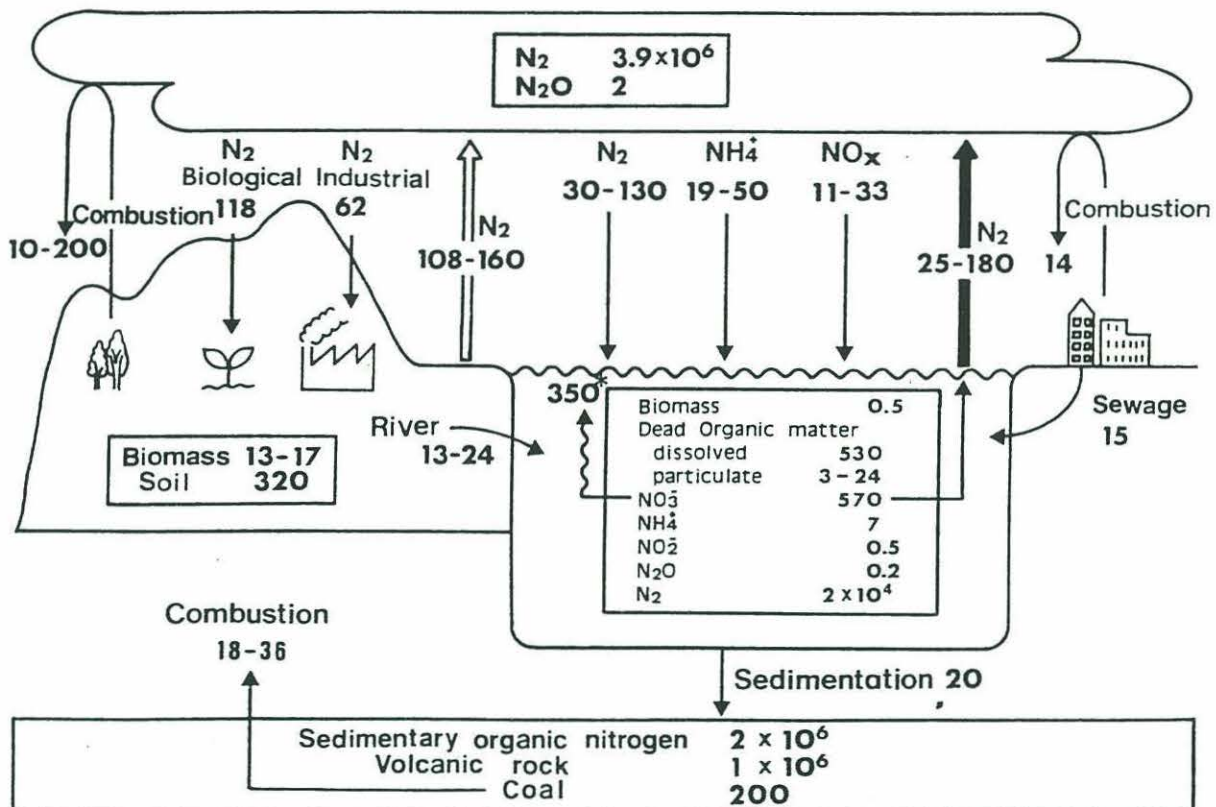


Figure 1.1: The global nitrogen cycle. Inventories are in units of  $10^{15}$  g N. Flows are in units of  $10^{12}$  g N/year. The asterisk denotes a transport from depth to the euphotic zone. Figure from Wada and Hattori (1990).

in figure 1.1, net sources of combined (or fixed) nitrogen to the ocean are (1) nitrogen fixation, (2) atmospheric deposition and (3) river runoff. Net sinks are (1) denitrification (in the water column and in sediments), (2) burial in sediments, and (3) exports of organic nitrogen such as fish catches, guano, and atmospheric transport (Codispoti and Christensen, 1985; McCarthy and Carpenter, 1983). Denitrification is the major sink for fixed nitrogen in the sea, while each of the three source terms is thought to be of a similar magnitude (Codispoti and Christensen, 1985).

### 1.3 Nitrogen Isotopic Ratios

Relatively little is known about the biogeochemistry of nitrogen in the past. One means of studying nitrogen cycling is to measure the natural abundances of its two stable isotopes,  $^{14}\text{N}$  and  $^{15}\text{N}$ . The heavier isotope accounts for 0.37% of all nitrogen (in the solar system). The rates for biological processes involving nitrogenous species are typically greater for  $^{14}\text{N}$  than for  $^{15}\text{N}$  as a result of higher vibrational frequency of bonding in the former (Owens, 1987). This results in isotopic depletion in products relative to substrates. For certain processes, such as denitrification and biological nitrate uptake, this effect can be large, with observed fractionations up to 40 (Cline and Kaplan, 1975) and 23 per mil (Wada and Hattori, 1978), respectively. As a means of examining nitrogen biogeochemistry in the modern and historical ocean, this study sets forth a method for determining the isotopic signature imparted to phytoplankton as a result of these and other processes.



## 1.4 Diagenetic Alteration of Nitrogen Isotopic Ratios

One of the major impediments to interpreting sedimentary nitrogen isotopic records is diagenesis. About 99% of organic matter produced in surface waters is decomposed before reaching the seafloor, and most of the material reaching the seafloor is degraded in the upper few centimeters of the sediment column. It is perhaps not surprising, then, that nitrogen isotopic ratios of algal material are altered prior to burial in sediments (Francois and Altabet, 1992; Schafer and Ittekkot, 1993; Wada, et al., 1987). In many instances, the diagenetic signal is as large or larger than the primary signal being sought.

One way to circumvent the isotopic alteration during diagenesis of bulk organic material is to make N and C isotopic determinations in fossilized biochemicals from phytoplankton. In addition, by comparing the isotopic composition of the bulk phase with that of the biomarker, the magnitude of diagenetic alteration can be determined. This quantity may contain information about the paleo-depositional environment. This has been accomplished (see chapter 5) and it is shown that the Late Quaternary nitrogen isotopic record in Eastern Mediterranean sediments, previously interpreted in terms of changing nutrient availability (Calvert, et al., 1992), is an artefact of diagenesis. A close similarity between algal  $\delta^{15}\text{N}$  and that of bulk sediments exists in sapropels, but the two values differ by more than 5 per mil in modern non-sapropelic environments. The similarity between algal  $\delta^{15}\text{N}$  and that of bulk sediment in sapropels suggests that bottom waters were anoxic during their deposition, since oxic diagenesis tends to elevate sedimentary  $\delta^{15}\text{N}$  values.

## 1.5 Chlorophyll: A Universal Algal Biomarker

The biomarker chosen for isotopic analyses in this study was chlorophyll. Chlorophyll is a ubiquitous photosynthetic pigment found in all photoautotrophs. Its structure consists of a functionalized cyclic tetrapyrrole ( $C_{35}H_{35}O_5N_4$ ) complexed to a magnesium atom, and attached to a phytol-ester ( $C_{20}H_{38}$ ) side-chain (figure 1.2). It is relatively resistant to chemical and biological decomposition, as evidenced by the existence of ancient chlorophyll derivatives (i.e., geoporphyrins (Treibs, 1936)) in the geological record.

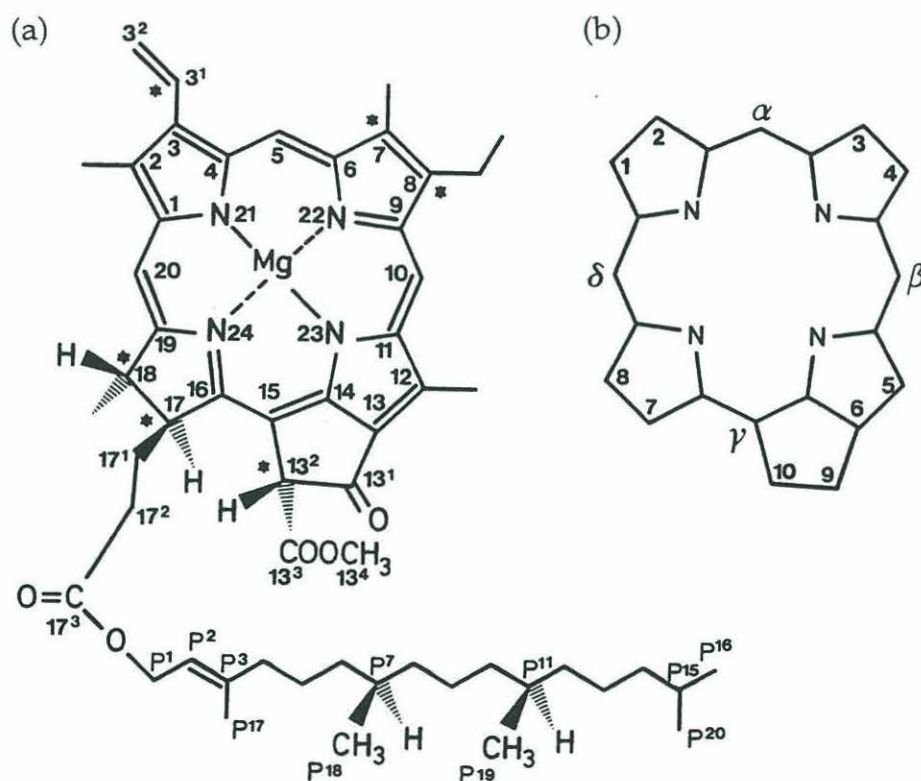


Figure 1.2: Structure of chlorophyll *a* (a), and the Fischer numbering system for chlorins used in this thesis (b).

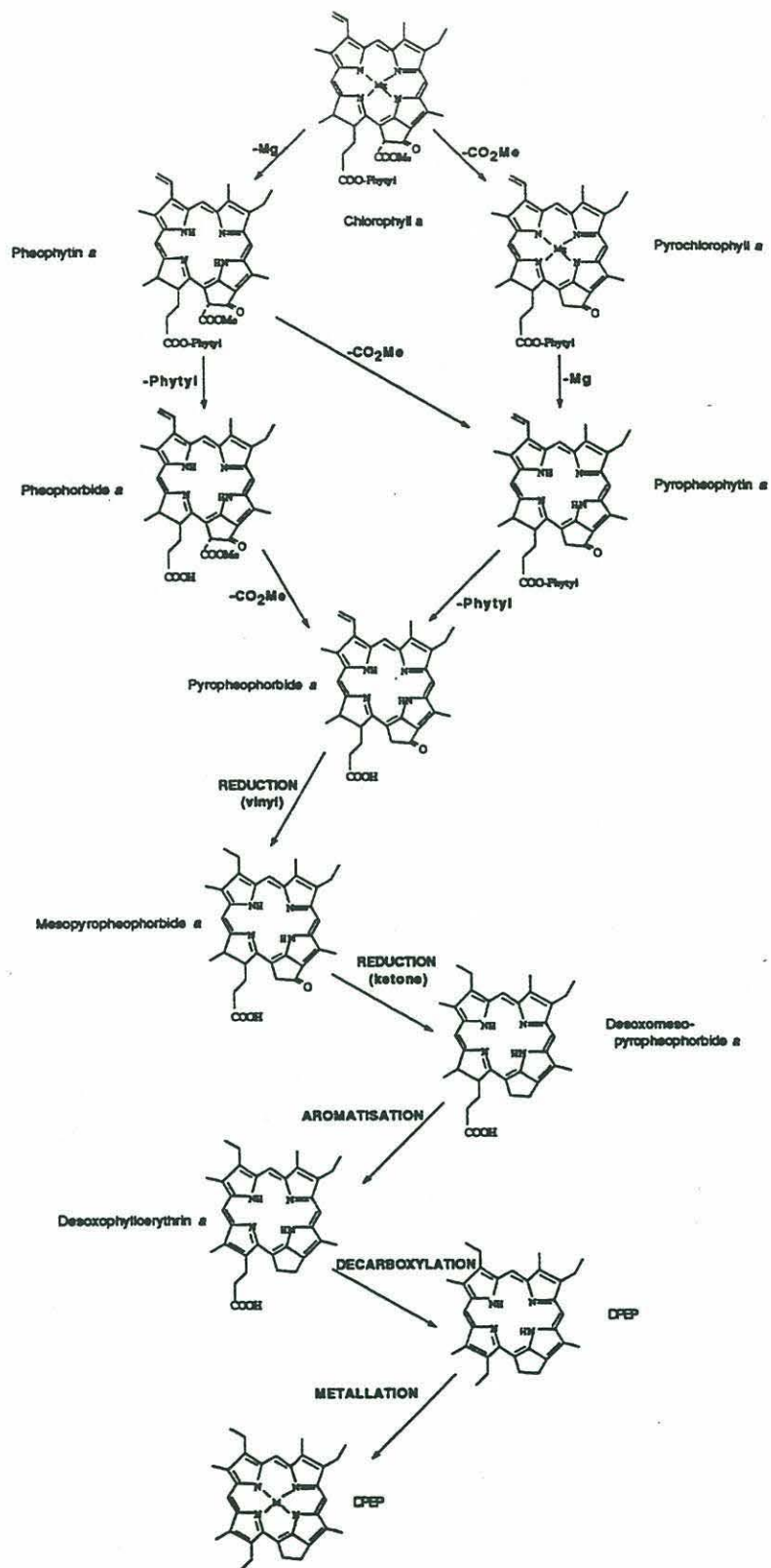


Figure 1.3: Possible transformation pathways for chlorophyll *a* to DPEP. First proposed by Treibs (1936). Figure adapted from Keely (1990) by Huseby (1996).



Before burial in sediments, however, chlorophyll undergoes a sequence of diagenetic transformations (figure 1.3) (Keely, et al., 1990; Treibs, 1936). For instance, it rapidly loses the central Mg atom, and virtually all chlorins found in sediments are demetallated (King, 1993). Additional functional groups are lost on the diagenetic path to completely defunctionalized alkylporphyrins, such as deoxophylloerythroetioporphyrin (DPEP), shown in figure 1.3. However, the most common chlorins encountered in this study of Recent sediments from the Mediterranean and Black Seas and the Peru Margin were pheophytin *a*, pheophorbide *a*, pyropheophytin *a*, pyropheophorbide *a*, and chlorin steryl esters (King and Repeta, 1991).

These and other chlorophyll derivatives will be collectively referred to as chlorins in this thesis. There is a rich nomenclature associated with chlorins and

**Table 1.1: Most common chlorin abbreviations used in this text.**

Chlorin	Abbreviation
Chlorophyll <i>a</i>	Chla
Pheophytin <i>a</i>	PTNa
Pheophytin <i>a'</i> <sup>1,2</sup>	PTNa'
Pyropheophytin <i>a</i>	PPTNa
Pheophorbide <i>a</i>	PBDa
Pheophorbide <i>a'</i> <sup>1,2</sup>	PBDa'
Methyl pheophorbide <i>a</i> <sup>1,3</sup>	MPBDa
Methyl pheophorbide <i>a'</i> <sup>1,2</sup>	MPBDa'
Pyropheophorbide <i>a</i>	PPBDa
Methyl pyropheophorbide <i>a</i> <sup>1</sup>	MPPBDa

<sup>1</sup> Not shown in figure 1.3; <sup>2</sup> The 10(*S*) stereoisomer, called an epimer; <sup>3</sup> Has a methyl ester in place of the carboxylic acid

porphyrins (Scheer, 1991). Much of the (older) literature uses the trivial names of the Fischer nomenclature, while a growing number of investigators are adopting the IUPAC-IUB naming system. We have adopted a mixed nomenclature, for ease of use, that incorporates many of the well-known trivial names from Fischer's system as well as the Fischer numbering system (figure 1.2). The chlorin abbreviations used in the text are listed in table 1.1.

## **1.6 Origin of Eastern Mediterranean Sapropels**

Dark, organic-rich mud layers a few millimeters to 30 cm thick, and having durations of 1-10 kyr, have periodically been deposited in the Eastern Mediterranean since at least the Miocene (Kidd, et al., 1978; Olausson, 1961). Their origin remains the subject of widespread debate. These green-brown to black deposits, called sapropels, have organic carbon contents between 2 and 17%, and are interspersed between grey organic-deficient ( $\sim 0.2\%$  C<sub>org</sub>) nannofossil and foraminiferal marl oozes (figure 1.4). Most Eastern Mediterranean sapropels appear to be basin-wide events at water depths below about 800-1000 m (figure 1.5; Stanley, 1978). The most recent sapropel was deposited from about 9,000 to 7,000 years before present (Troelstra, et al., 1991).

The two competing hypotheses regarding the origin of sapropels call on either increased production or increased preservation of organic matter. Unambiguous evidence supporting one over the other has been elusive since the two are frequently not independent. However, new evidence from nitrogen isotopic measurements in chlorins (presented in chapter 5) supports the formation of sapropels from enhanced preservation of organic matter under anoxic bottom water.



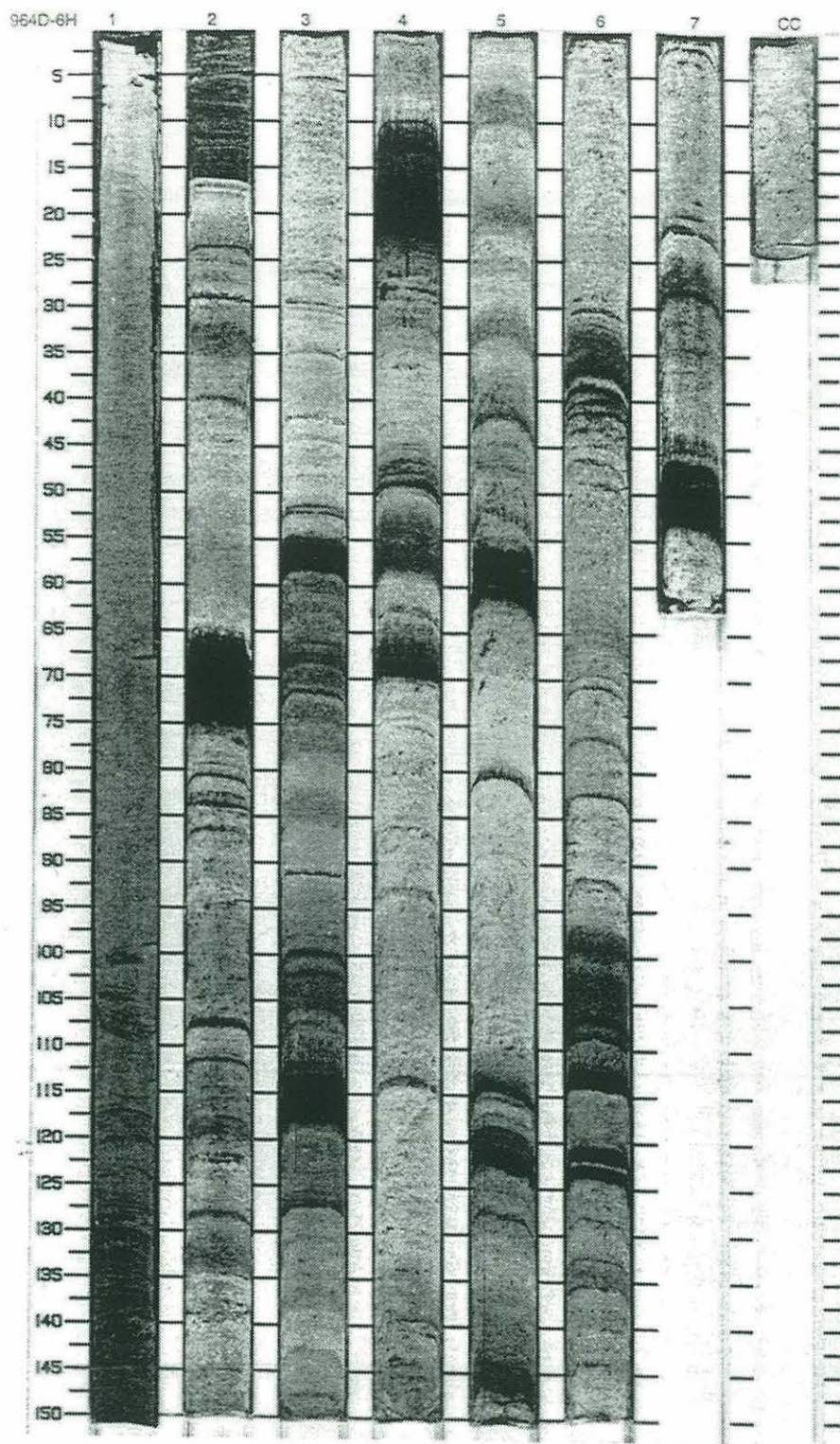


Figure 1.4: Typical example of sapropels recovered from the Eastern Mediterranean. Sapropels are the dark bands.



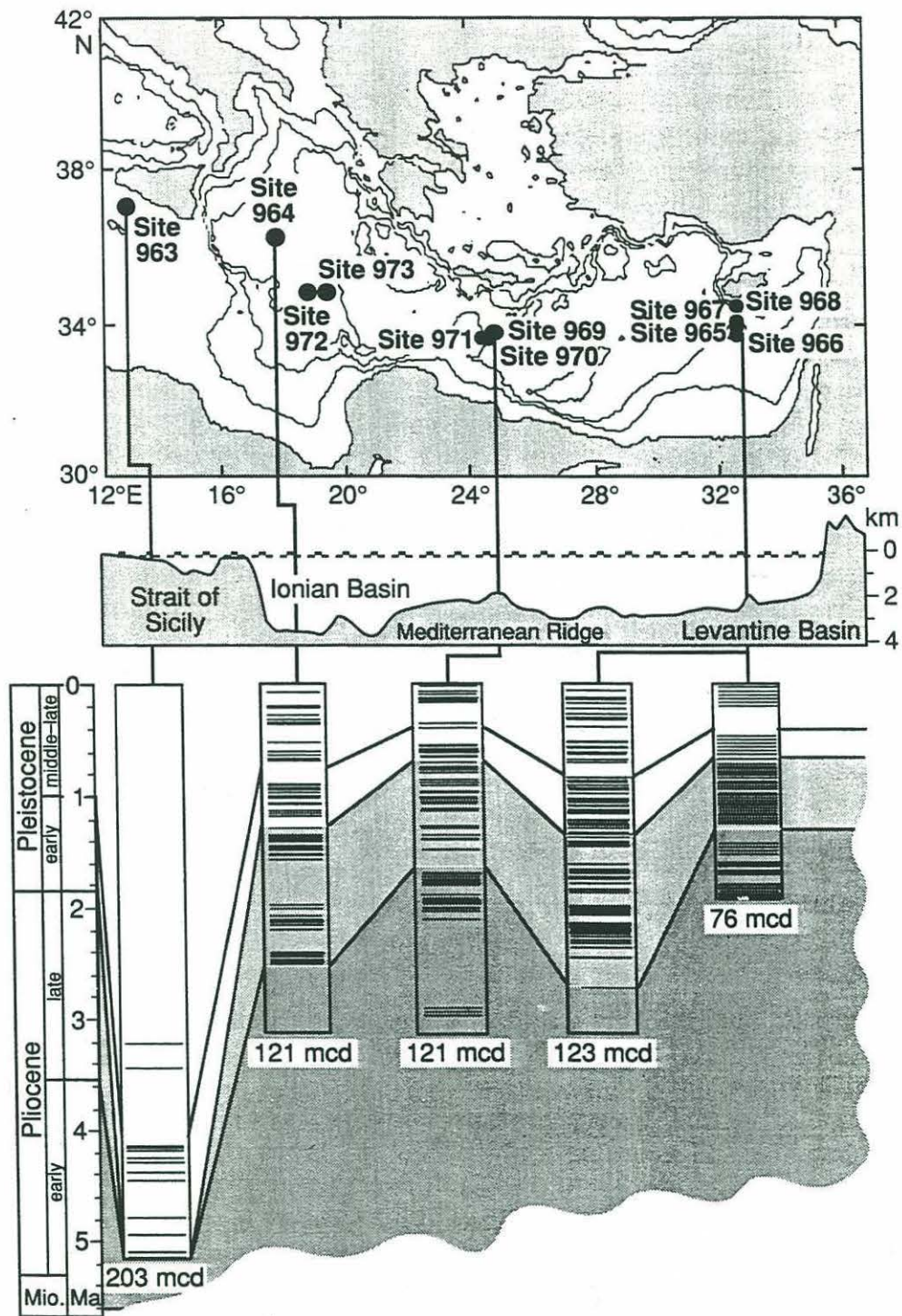


Figure 1.5: Overview map of the Eastern Mediterranean Sea and schematics showing the widespread occurrence of sapropels in that basin. Cores from sites 964 and 969 were used in this study. Figure from Emeis, et al. (1996).

## 1.7 The Black Sea: A Modern Analog for Sapropel Depositional Conditions

The Black Sea is the world's largest anoxic basin. Although the basin is oligotrophic and primary productivity is modest (100-200 g C/m<sup>2</sup>/yr; Deuser, 1971; Sorokin, 1983), surface sediments contain 3-5% organic carbon (Glenn and Arthur, 1985). This richness has been attributed to the increased burial efficiency of organic matter under anoxic bottom water (Canfield, 1989; Demaison and Moore, 1980). Contrary to traditional characterizations, the basin is not stagnant (Southam, et al., 1982). Vertical velocities and deep water residence times are on the order of those in the world ocean. Rather, anoxia results from the excess of oxygen demand over supply in the deep water (Sarmiento, et al., 1988). This excess is maintained by the circulation, independent of high export production.

Nitrogen isotopic evidence from chlorins supports a similar origin for sapropels of the Eastern Mediterranean, and organic-rich sediments of the late Holocene Black Sea. Additional faunal, isotopic and sedimentologic evidence is discussed in chapter 5 that further substantiates this analogy.

## 1.8 Organization of the Thesis

Methods for the purification of particulate and sedimentary chlorins for carbon and nitrogen isotopic analysis are presented in chapter 2. A chemical derivatization procedure for the analysis of chlorin  $\delta^{15}\text{N}$  and  $\delta^{13}\text{C}$  by isotope-ratio monitoring gas chromatography-mass spectrometry (e.g., irmGC-MS) is presented in chapter 3. In chapter 4, experimental evidence from six species of axenic phytoplankton is presented that suggests that chlorophyll is isotopically depleted by about 5 per mil relative to total cellular nitrogen. Cellular carbon is

shown to be isotopically indistinguishable from chlorophyll carbon. Finally, in chapter 5, chlorin nitrogen isotopic evidence is presented that suggests Late Quaternary Eastern Mediterranean sapropels formed as a result of enhanced preservation of organic matter, much like the organic-rich sediments of the modern Black Sea.



## References for Chapter 1

- Calvert, S.E., B. Nielsen and M.R. Fontugne (1992) Evidence From Nitrogen Isotope Ratios for Enhanced Productivity During Formation of Eastern Mediterranean Sapropels. *Nature*, **359**(6392): 223-225.
- Canfield, D.E. (1989) Sulfate Reduction and Oxidic Respiration in Marine Sediments: Implications for Organic Carbon Preservation in Euxinic Environments. *Deep-Sea Research*, **36**(1): 121-138.
- Cline, J.D. and I.R. Kaplan (1975) Isotopic Fractionation of Dissolved Nitrate During Denitrification in the Eastern Tropical North Pacific Ocean. *Marine Chemistry*, **3**: 271-299.
- Codispoti, L.A. (1995) Is the Ocean Losing Nitrate? *Nature*, **376**: 724.
- Codispoti, L.A. and J.P. Christensen (1985) Nitrification, Denitrification and Nitrous Oxide Cycling in the Eastern Tropical South Pacific Ocean. *Marine Chemistry*, **16**: 277-300.
- Demaison, G.J. and G.T. Moore (1980) Anoxic Environments and Oil Source Bed Genesis. *The American Association of Petroleum Geologists Bulletin*, **64**(8): 1179-1209.
- Deuser, W.G. (1971) Organic-Carbon Budget of the Black Sea. *Deep-Sea Research*, **18**: 995-1004.
- Dugdale, R.C. and J.J. Goering (1967) Uptake of New and Regenerated Forms of Nitrogen in Primary Productivity. *Limnology and Oceanography*, **12**: 196-206.
- Emeis, K.-C., A.H.F. Robertson, C. Richter, et al. (1996) Paleoceanography and Sapropel Introduction. In: *Proceedings of the Ocean Drilling Program, Initial Reports*, (E. Kapitan-White, ed.), Ocean Drilling Program, College Station, Texas, pp. 21-26.

Francois, R. and M.A. Altabet (1992) Glacial to Interglacial Changes in Surface Nitrate Utilization in the Indian Sector of the Southern Ocean as Recorded by Sediment  $\delta^{15}\text{N}$ . *Paleoceanography*, 7(5): 589-606.

Glenn, C.R. and M.A. Arthur (1985) Sedimentary and Geochemical Indicators of Productivity and Oxygen Contents in Modern and Ancient Basins: The Holocene Black Sea as the "Type" Anoxic Basin. *Chemical Geology*, 48: 325-354.

Huseby, B. (1996) A Study of Porphyrins in Petroleum Source Rocks. PhD, University of Bergen.

Keely, B.J., W.G. Prowse and J.R. Maxwell (1990) The Treibs Hypothesis: An Evaluation Based on Structural Studies. *Energy & Fuels*, 4: 628-634.

Kidd, R.B., M.B. Cita and W.B.F. Ryan (1978) The Stratigraphy of Eastern Mediterranean Sapropel Sequences Recovered During DSDP Leg 42A and Their Paleoenvironmental Significance. In: *Initial Reports of the Deep Sea Drilling Project*, (R. B. Kidd and P. J. Worstel, ed.), U.S. Government Printing Office, Washington, D.C., pp. 421-443.

King, L.L. (1993) Chlorophyll Diagenesis in the Water Column and Sediments of the Black Sea. PhD, Massachusetts Institute of Technology / Woods Hole Oceanographic Institution.

King, L.L. and D.J. Repeta (1991) Novel Pyropheophorbide Steryl Esters in Black Sea Sediments. *Geochimica et Cosmochimica Acta*, 55: 2067-2074.

McCarthy, J.J. and E.J. Carpenter (1983) Nitrogen Cycling in Near-Surface Waters of the Open Ocean. In: *Nitrogen in the Marine Environment*, (E. J. Carpenter and D. G. Capone, ed.), Academic Press, Inc., New York, pp. 487-512.

McElroy, M.B. (1983) Marine Biological Controls on Atmospheric  $\text{CO}_2$  and Climate. *Nature*, 302: 328-329.

Olausson, E. (1961) Sediment Cores from the Mediterranean and the Red Sea. *Reports of the Swedish Deep Sea Expedition*, 8(6): 337-391.



- Owens, N.J.P. (1987) Marine Variation in  $^{15}\text{N}$ . *Advances in Marine Biology*, **24**: 390-451.
- Sarmiento, J.L., T.D. Herbert and J.R. Toggweiler (1988) Causes of Anoxia in the World Ocean. *Global Biogeochemical Cycles*, **2**(2): 115-128.
- Schafer, P. and V. Ittekkot (1993) Seasonal Variability of  $\delta^{15}\text{N}$  in Settling Particles in the Arabian Sea and Its Palaeogeochemical Significance. *Naturwissenschaften*, **80**: 511-513.
- Scheer, H. (1991) *Chlorophylls*. CRC Press, Boca Raton, 1257 pp.
- Sorokin, Y.I. (1983) The Black Sea. In: *Ecosystems of the World 26--Estuaries and Enclosed Seas*, (B. Ketchum, ed.), Elsevier, pp. 253-307.
- Southam, J.R., W.H. Peterson and G.W. Brass (1982) Dynamics of Anoxia. *Palaeogeography, Palaeoclimatology, Palaeoecology*, **40**: 183-198.
- Stanley, D.J. (1978) Ionian Sea Sapropel Distribution and Late Quaternary Paleoceanography in the Eastern Mediterranean. *Nature*, **274**: 149-152.
- Treibs, A. (1936) Chlorophyll and Hemin Derivatives in Organic Mineral Substances. *Angew. Chem.*, **49**(38): 682-686.
- Troelstra, S.R., G.M. Ganssen, K. van der Borg and A.F.M. de Jong (1991) A Late Quaternary Stratigraphic Framework for Eastern Mediterranean Sapropel S1 Based On AMS  $^{14}\text{C}$  Dates and Stable Oxygen Isotopes. *Radiocarbon*, **33**(1): 15-21.
- Wada, E. and A. Hattori (1978) Nitrogen Isotope Effects in the Assimilation of Inorganic Nitrogenous Compounds by Marine Diatoms. *Geomicrobiology Journal*, **1**: 85-101.
- Wada, E., M. Terazaki, Y. Kabaya and T. Nemoto (1987)  $^{15}\text{N}$  and  $^{13}\text{C}$  Abundances in the Antarctic Ocean with Emphasis on the Biogeochemical Structure of the Food Web. *Deep-Sea Research*, **34**(5/6): 829-841.



Wada, E. and A. Hattori (1990) *Nitrogen in the Sea: Forms, Abundances, and Rate Processes*. CRC Press, Boca Raton, 208 pp.

## Chapter 2: Analytical Methodology I. Purification of Chlorins for Nitrogen and Carbon Isotopic Analysis

### 2.1 Abstract

A method is presented for the measurement of chlorin nitrogen and carbon isotopic ratios in marine particles and sediments that yields products that are at least 88% pure, with a precision greater than 0.15 per mil for both N and C. The purification procedure can be performed in about 4 hours for particulate samples, and 8 hours for sediment samples, when two samples are processed in tandem.

The procedure for particulate samples includes extraction with solvents, two phase separations, and reverse- and normal-phase high-performance liquid chromatographic separations (HPLC). The procedure for sedimentary chlorins includes extraction by solvent, solid-phase extraction on silica gel, reverse-phase HPLC, size-exclusion chromatography, and normal-phase HPLC. If only nitrogen isotopic ratios are sought, the last two steps of the sediment procedure may be omitted, as well as the last step of the particulate procedure.

Overall chlorin recoveries for particulate samples averaged 88%, while those for sediment samples averaged 18%. The low recovery from sediments, relative to particulate samples, is primarily a result of the complex distribution of chlorins in sediments relative to particles, and the fact that only the one or two most abundant chlorins from a sample are purified. It is also a result of the additional steps required to purify sedimentary, relative to particulate, chlorins. Nevertheless, both chlorin  $\delta^{15}\text{N}$  and  $\delta^{13}\text{C}$  values can be obtained with 20 g of a moderately organic-rich ( $\sim 2\%$   $\text{C}_{\text{org}}$ ) sediment.

Finally, different chlorins from a surficial Black Sea sediment were found to have different N and C isotopic ratios. The  $\delta^{15}\text{N}$  differences are interpreted in terms of changes in the seasonal flux of material out of the euphotic zone. The  $\delta^{13}\text{C}$  differences are thought to derive from the presence or absence of the chlorin phytyl side-chain.

## 2.2 Introduction

There are surprisingly few reports in the literature describing the purification of chlorophyll-related pigments from natural samples for stable isotopic analysis (Bidigare, et al., 1991). This, in part, is a result of the difficulty in purifying these compounds from complex mixtures of organic material. Chlorin pigments are non-volatile, thermally unstable, light- and oxygen-sensitive, and chemically-reactive. Facing these problems, we have developed both an on-line protocol utilizing isotope-ratio-monitoring gas chromatography-mass spectrometry (irmGC-MS), and an off-line purification using high-performance liquid chromatography (HPLC) followed by traditional dual-inlet mass spectrometry. The liquid chromatographic procedures are described in this chapter, while the gas chromatographic approach is discussed in chapter 3.

The goal of the analytical development was to develop protocols for the purification of chlorins from marine sedimentary and particulate matter for nitrogen and carbon stable isotopic analysis. The criteria for doing so were (1) to maintain isotopic integrity of the chlorins, (2) to minimize sample size requirements, and (3) to minimize time and labor per analysis.

The only published procedure for the purification of chlorins for N and C isotopic analysis is a report by Bidigare, et al (1991). However, that method was



developed for chlorophyll *a* purification from terrestrial higher plants. It relies on the precipitation of Chla with dioxane (Iriyama, et al., 1974), followed by preparative reverse-phase high-performance liquid chromatography (Watanabe, et al., 1984). Since sedimentary chlorins are predominantly demetallated (e.g., magnesium-free) and tend to be in a lipid-rich matrix, it was thought that the dioxane precipitation would be unsuccessful. Indeed, the dioxane precipitation fails even with Chla when the pigment extract is lipid-rich, as was the case with certain algal cultures (R. Bidigare, personal communication).

Furthermore, partial chlorophyll demetallation occurred during sample collection, storage and handling that resulted in substantial nitrogen isotopic fractionation. For example, in three instances where harvested algal cultures were stored at -20°C for 9 months, 53-65% of the Chla was converted to pheophytin *a* and the demetallated product was found to be enriched in <sup>15</sup>N by 2.0 (± 0.4) per mil relative to the intact Chla. Thus, in order to avoid isotopic alteration resulting from partial demetallation, a procedure was developed for the rapid and complete demetallation of algal chlorophyll directly following the pigment extraction.

The methods described in this chapter should be suitable or adaptable to the entire range of chlorins commonly found in marine particles and sediments. Discussions with Dr. Ralf Goericke during my first two years in Dr. Repeta's laboratory were instrumental in the development of these techniques.

## 2.3 Methods

### 2.3.1 General Laboratory Procedures

All solvents were HPLC-grade except for those used for GC and GC-MS, which are GC/GC-MS grade. Unless otherwise noted, all glassware was cleaned with Micro (Cole-Parmer, Chicago, IL) and rinsed with tap water (3x), distilled water (3x), MeOH (3x), and acetone (3x). Pasteur pipets, Na<sub>2</sub>SO<sub>4</sub>, glass vials, glass fiber filters, sand, aluminum foil, and glass wool were combusted at 450°C for >8 hours. Teflon cap liners, cotton, and boiling chips (Hengar Granules, Hengar Co., Philadelphia, PA) were soxhlet extracted in 7/93 MeOH/MeCl<sub>2</sub>.

Preparative thin-layer chromatography (TLC) plates were prepared as follows. Alumina (Alumina G, 20 x 20 cm, 1000 µm phase, Analtech, Inc., Newark, DE) plates were activated at 90°C for 45-60 minutes, then eluted with 100% acetone and allowed to air-dry for >2 hours. Silica plates (Silica G, 20 x 20 cm, 1000 µm phase, Analtech, Inc., Newark, DE) were eluted with 100% acetone and allowed to air-dry for >2 hours before being activated for >4 hours in an oven at 180°C.

Analytical silica TLC plates (Polygram SIL G/UV254, 4x8 cm, 0.25 mm layer, Macherey-Nagel GmbH & Co. KG, Duren, Germany) were activated at 110°C for >4 hours. Alumina (Aluminum Oxide IB, 2.5x7.5 cm sheets, J.T. Baker Inc, Phillipsburg, NJ) and reversed phase (MKC18F, 1" x 3", 200 µm phase, Whatman International, Ltd., Maidstone, England) TLC plates were used as received.

Column chromatography packings were prepared as follows. Alumina (Neutral Alumina AG 7, 100-200 mesh, BioRad, Richmond, CA) was soxhlet-

extracted for 24 hours in 7/93 (v/v) MeOH/MeCl<sub>2</sub>, then dried in an oven at 180°C for >4 hours. Flash silica (Matrex Silica Si, 60 A Pore Diameter, Amicon Corp., Danvers, MA) was either soxhlet-extracted for 24 hours in 7/93 (v/v) MeOH/MeCl<sub>2</sub> and activated in an oven at 180°C for >4 hours, or combusted (and activated) at 450°C for >8 hours.

### *2.3.2 Handling of Chlorin Pigments*

Chlorophyll-related pigments are light and air-sensitive. Therefore, exposure to both was minimized by a few simple practices. First, all manipulations of pigments were carried out under low-light conditions. Samples were stored dry, in the dark, at -20°C under a nitrogen atmosphere. If a sample was stored dissolved in solvent for more than a few minutes it was kept in the dark under a nitrogen atmosphere. Exposure to polar solvents, such as methanol, was minimized to prevent allomerization and epimerization reactions from occurring (Hynninen, 1979; Otsuki, et al., 1987; Zapata, et al., 1987).

### *2.3.3 Instrumentation*

#### *2.3.3.1 Spectrophotometry*

Visible spectra of the pigments were taken on either a Varian Techtron DMS-200 Spectrophotometer (Varian Techtron Limited, Springvale Road, Mulgrave, Victoria 3170, Australia) or a Hewlett-Packard HP8452A Diode Array Spectrophotometer (Rockville, Maryland). The instruments were referenced against the appropriate solvent contained in a 1-cm quartz cuvette. The



resolution of the HP8452A was 2 nm, while that of the Varian was 0.1 nm. A spike at 656 nm occasionally interfered with the red band absorbance determination while using the diode array spectrophotometer. This interference was minimized by acquiring the sample spectrum immediately after taking the reference spectrum. A discussion of spectrophotometric quantitation calculations and baseline correction can be found in section 2.3.4.

#### 2.3.3.2 *Mass Spectrometry and Gas Chromatography-Mass Spectrometry*

All mass spectrometry was performed in Fye Laboratory (WHOI) on a VG AutoSpecQ connected to an Opus data system on a DEC Alpha workstation. The instrument can be operated in any of three ionization modes: electron impact (EI), chemical ionization (CI) or fast-atom bombardment (FAB). All three ionization modes were employed during this work.

The GC-MS work employed a Hewlett Packard 5890 Series II gas chromatograph connected to the VG AutoSpecQ. The GC was equipped with a Hewlett Packard 7673 autoinjector.

For static FAB<sup>+</sup>-MS, nitrobenzyl alcohol (NBA) was used as a matrix, source temperature was 250°C, source pressure was  $3.5 \times 10^{-4}$  mb, accelerating voltage was 8 kV, resolution was set at 2000, scan time at 5.74 s/dec, and delay at 1.00 secs.

For CI-MS runs, CH<sub>4</sub> was used as ionization gas, source temperature was 250°C, source pressure was  $3.5 \times 10^{-5}$  mb, filament emission was 1 mA, electron energy was 35 eV, and the electron multiplier was set at 425.

For GC-CI-MS work, a 12 m SGE HT5 Aluminum Clad column (SGE Incorporated, Austin, Texas) was used. The column had a 0.1 µm apolar phase

(similar in polarity to DB-5), an i.d. of 0.33 mm and an o.d. of 0.43 mm. A deactivated silica bridge was used (1 m x 0.15 mm i.d.) to span the distance between the GC and the source of the mass spectrometer due to the metallic coating of the column. Automatic pressure programming was employed to maintain a constant linear flow rate of 26.5 cm/sec of helium carrier gas. Unless otherwise noted, the temperature program used was 50-80°C at 35°/min, then 80-275°C at 20°/min, then 275-320°C at 6°/min, followed by a 30 minute isothermal step.

#### 2.3.3.3 Nuclear Magnetic Resonance Spectroscopy (NMR)

<sup>1</sup>H NMR spectra were obtained on a 300 MHz Bruker AC 300 spectrometer (Bruker Instruments, Inc., Manning Park, Billerica, MA) in conjunction with an Aspect 3000 data system (Spectrospin AG, Industriestrasse 26, CH-8117 Faellanden, Switzerland). The field strength of the superconducting magnet was 7.1 Tesla.

NMR tubes were thin-walled 5 mm x 9" tubes from Wilmad (cat. # 535-PP-9, Wilmad Glass Company, Buena, NJ). They were washed with MeOH (3x), MeCl<sub>2</sub> (3x) and acetone (3x), before being dried first under a N<sub>2</sub> stream, and then in an oven at 180°C for >1 hour. NMR pipets were useful for transferring samples to the tubes (cat. # 803A, Wilmad Glass Co.).

Solvents for NMR spectroscopy were ≥ 99.5% deuterated (Aldrich Chemical Company, Milwaukee, WI).



#### 2.3.3.4 *High-Performance Liquid Chromatography (HPLC)*

High-performance liquid chromatography was performed using either a Waters 600E Multisolvent Delivery System with a Waters 990 Photodiode Array Detector and Software (Waters Corporation, Milford, MA), or a pair of Waters 510 Pumps connected to a Hitachi F-1000 Fluorescence detector (Hitachi Ltd., Tokyo, Japan) and controlled by a ChemResearch Chromatographic Data Management/System Controller (v. 2.4) (Isco, Inc., Lincoln, NE). The injector for both configurations was a Rheodyne 7125 Syringe Loading Sample Injector (Rheodyne, Inc., Cotati, CA), fitted with either a 200 or 1000  $\mu$ L sample loop. A Gilson FC 203 Fraction Collector was used for preparative work (Gilson Medical Electronics, Middleton, WI).

The standard reverse-phase analytical column and conditions used in this work to "fingerprint" all sample were as follows. An Adsorbosphere HS C18 3 Micron column with dimensions of 4.6 mm I.D. x 150 mm and 3  $\mu$ m particle size (cat # 28787, Alltech Associates, Inc, Deerfield, IL) was connected to the Waters 600E pumps and 900 photodiode array detector. A gradient from 100% A to 100% B in 30 minutes, followed by a 30 minute isocratic elution of solvent B, was used. Solvent A was 20% 0.5 N ammonium acetate (aq) in MeOH. Solvent B was 20% acetone in MeOH. The flow rate was maintained at 1.5 mL/min.

This gradient was optimized by Dr. Repeta from previously published methods (Mantoura and Llewellyn, 1983; Wright, et al., 1991; Zapata, et al., 1987) to resolve the entire suite of pigments found in marine phytoplankton. It was used in this work because the retention times of most algal pigments eluting during this gradient are well-known and documented. It is not optimized for the analysis of sedimentary chlorins, which often include non-polar chlorins, such as



the chlorin steryl esters (King and Repeta, 1991). Those compounds are not eluted under these conditions.

Aside from the standard analytical reverse-phase conditions described, the columns and solvent systems varied with the nature of the separation. They will be described in later sections in association with the application they were designed for.

#### 2.3.3.5 *Elemental Analysis (CHN)*

CHN analyses were performed on an EA 1108 elemental analyzer with Eager 200 data acquisition software (Fisons Instruments, Inc., Beverly, MA). A Sartorius Micro balance was used for mass determinations (Sartorius AG, Gottingen, Sweden). Organic samples--i.e., whole or partially purified extracts and chlorins--were prepared by placing 50-1000  $\mu\text{g}$  of sample, dissolved in  $< 200 \mu\text{L}$  acetone or  $\text{MeCl}_2$ , via syringe, into an 8 x 6 mm tin cup (Smooth Wall Tin Capsules, cat. # D4066, Elemental Microanalysis Ltd, Manchester, MA). The solvent was then evaporated by heating from above with a 60 W lamp. Smooth walled Sn cups were used because solvent creeping and leakage occurred with "pressed" cups. When dry ( $\sim 5$  minutes), the cups were folded with forceps and stored in a dessicator until analysis.

Sediment samples, which had to be decarbonated before analysis, were prepared using a modified "cup and saucer" technique (Cowie and Hedges, 1991). 10-100 mg of dry sediment, or 50-200 mg of wet sediment was placed into an 8 x 5 mm pressed silver cup (cat # D2009, Elemental Microanalysis Ltd, Manchester, MA), which was then placed into a silver saucer--an unfolded 8 x 5 mm Ag cup. After drying the sediment in an oven at  $50^\circ\text{C}$  for  $>12$  hours, one

drop of 2 N HCl was added to the cup with a pre-combusted (450°C, > 8 hrs) glass Pasteur pipet. The saucer caught any material that overflowed during the effervescence. The sample was then dried for > 4 hours before being treated again with 1 drop of 2 N HCl. This procedure was repeated until effervescence ceased, at which time the sample was dried at 50°C for > 24 hours. The silver capsules were used for samples that were to be decarbonated because Sn becomes brittle in HCl. The dry, decarbonated sample was then folded with forceps (both Ag cups together) and stored in a dessicator until analysis. (The decarbonated samples were highly hygroscopic, being rich in CaCl<sub>2</sub>, so exposure to air was minimized.)

Cowie and Hedges (1991) reported some loss of nitrogen in certain carbonate-rich sediment samples decarbonated in a similar procedure. The comparison between total N in decarbonated and non-decarbonated sediments was not performed in this study. However, of more relevance to this work was the comparison of  $\delta^{15}\text{N}$  values for decarbonated and non-decarbonated sediments. For carbonate-rich surface sediments from the Black Sea (~ 60% CaCO<sub>3</sub> (Ross and Degens, 1974)) there was no isotopic difference between the treated and untreated sediment samples.

All values were blank-corrected for C and N associated with the sample cups. This value was normally < 0.1 nmol N, and ranged between 0.2% and 7% of the sample carbon. In addition, "procedural blanks" were prepared in order to correct organic samples for C and N associated with the sample dissolution, transfer and drying. These values were, again, normally < 0.1 nmol N and ranged between 0.3 and 10% of the sample carbon. Finally, procedural blanks were prepared in order to correct purified chlorins for C and N associated with the chromatography. This was accomplished by collecting eluant at the typical chlorin retention times from HPLC runs of solvent-only injections, and treating



the blanks like other samples during preparation for CHN (or isotope) analysis. Again, the nitrogen blank was < 0.1 nmol N, but the carbon blank ranged from 13 to 30% of the sample carbon. (This carbon blank had a  $\delta^{13}\text{C}$  of -25.1 per mil.)

Samples for irMS were prepared in an identical fashion to those for elemental analysis.

### 2.3.3.6 Isotope-Ratio Mass Spectrometry (irMS)

Most isotope values (unless otherwise noted) were obtained at the Stable Isotope Laboratory at the Marine Biological Laboratory, Woods Hole, MA 02543. The facility consists of a Heraeus CHN Rapid Elemental Analyzer and a Finnigan MAT delta S isotope ratio mass spectrometer coupled by an automated "trapping box" for the sequential cryogenic purification of  $\text{CO}_2$  and  $\text{N}_2$  (Fry, et al., 1992). This system allows the determination of both  $\delta^{15}\text{N}$  and  $\delta^{13}\text{C}$  on the same sample.

Samples are prepared for irMS analysis in the same manner as described above for CHN analysis.

Standard delta notation is used for reporting stable isotopic ratios of nitrogen and carbon. It is defined as

$$\delta^n X \equiv \left[ \frac{\left( \frac{{}^n X / (n-1) X}{\text{Sample}} \right)}{\left( \frac{{}^n X / (n-1) X}{\text{Std.}} \right)} - 1 \right] \times 1000 \text{ per mil}$$

where  $nX = {}^{15}\text{N}$  or  ${}^{13}\text{C}$ . The carbon isotopic standard is Peedee Belemnite (Craig, 1953), a limestone that has been assigned a  $\delta^{13}\text{C}$  value of 0.0 per mil. The isotopic standard for nitrogen is atmospheric  $\text{N}_2$  (i.e., air; Hoering, 1955), which has been assigned a  $\delta^{15}\text{N}$  value of 0.0 per mil. Therefore, positive delta values



arise when a sample is enriched in the heavy isotope relative to the standard, and negative delta values occur when a sample is depleted in the heavy isotope relative to the standard.

Differences of delta values are reported in "delta-del" notation.

Specifically,

$$\Delta\delta^nX \equiv \delta^nX_{Bulk} - \delta^nX_{Biomarker}$$

where  $nX=^{15}N$  or  $^{13}C$ . Bulk refers to the unaltered material from which the biomarker was extracted (i.e., plant, sediment or filtered particulate matter), and the biomarker is the purified pigment (i.e., chlorophyll *a* or other chlorin).

#### 2.3.4 Beer's Law and Spectrophotometric Quantifications

The relationship describing the amount of light transmitted by a solution to the concentration of a light-absorbing solute is the Beer-Lambert Law, or Beer's Law (Jenkins, et al., 1980):

$$\text{Log } I_0/I = A = \epsilon b c$$

where

$I$  = intensity of monochromatic light transmitted through the test solution

$I_0$  = intensity of light transmitted through the reference solution (e.g., the blank)

$A$  = absorbance (dimensionless)

$\epsilon$  = molar absorptivity, or "extinction coefficient" (a constant for a given solute/solvent system and a given wavelength)

$b$  = light path length (usually in cm; always 1 cm in this thesis)

$c$  = concentration of solute (in mol/L when molar absorptivity is used).

Beer's Law states that the absorbance of a solution is directly proportional to the light path length and the concentration of light-absorbing solutes. By rearranging the terms of Beer's Law and solving for concentration,

$$c = A/(\epsilon b).$$

Beer's Law in this form allows, for a given wavelength, the determination of a solute's concentration, assuming the molar extinction coefficient for the solute is known. Path length ( $b$ ) is always 1 cm in this study, and the absorbance ( $A$ ), at a given wavelength, is read from the spectrophotometer.

It is customary to choose wavelengths where maximum light absorption occurs ( $\lambda_{\max}$ ) in order to attain maximum sensitivity. For the demetallated chlorins the two most prominent  $\lambda_{\max}$  are 410 nm and 666 nm. In impure samples the absorption at 666 nm (the red band), rather than at 410 nm (the Soret band), was used because the ultraviolet end of the spectrum was generally more affected by contamination than the infrared end (figure 2.1). If the extinction coefficient for the chlorin at 666 nm was not known, then the absorbance at 666 nm was multiplied by the published (King, 1993; Svec, 1978) S/R (i.e., Soret/red band) ratio to calculate the theoretical absorbance at 410 nm.

In addition, the shape of the contamination spectrum was approximately logarithmic, sloping smoothly down from the UV to the IR (figure 2.1.a). The continuation of this curve was free-drawn under the red band and assumed to be the actual baseline for quantifications of highly impure samples (King and Repeta, 1994a). The absorbance thus calculated led to lower limit estimations of pigment concentration.

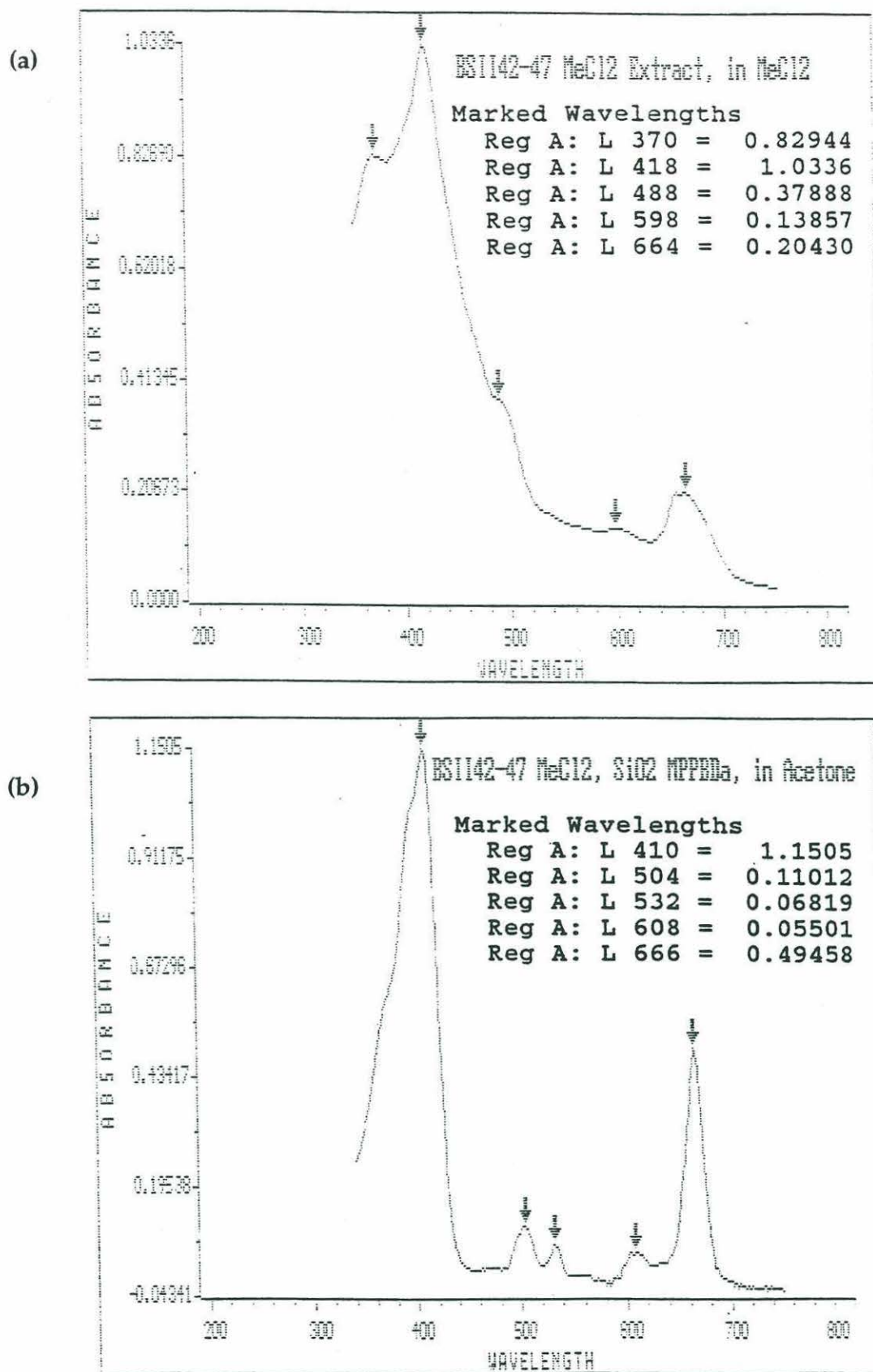


**Figure 2.1: Visible spectra of (a) a whole sediment extract from Unit II of the Black Sea, and (b) the most abundant chlorin in that extract (e.g., MPPBDa) after purification according to procedures developed in this study.**



### 2.3.5 Synthesis of Chlorin Standards

The synthesis of chlorin standards from *Spirulina* relied upon published (King, 1993) and unpublished (Simpson and Repeta, unpubl.; Repeta, pers. comm.) procedures optimized in Dr. Repeta's laboratory from standard protocols (Falk, 1964; Fuhrhop and Smith, 1975; Scheer, 1991; Svec, 1978).

#### 2.3.5.1 Methyl pheophorbide *a*

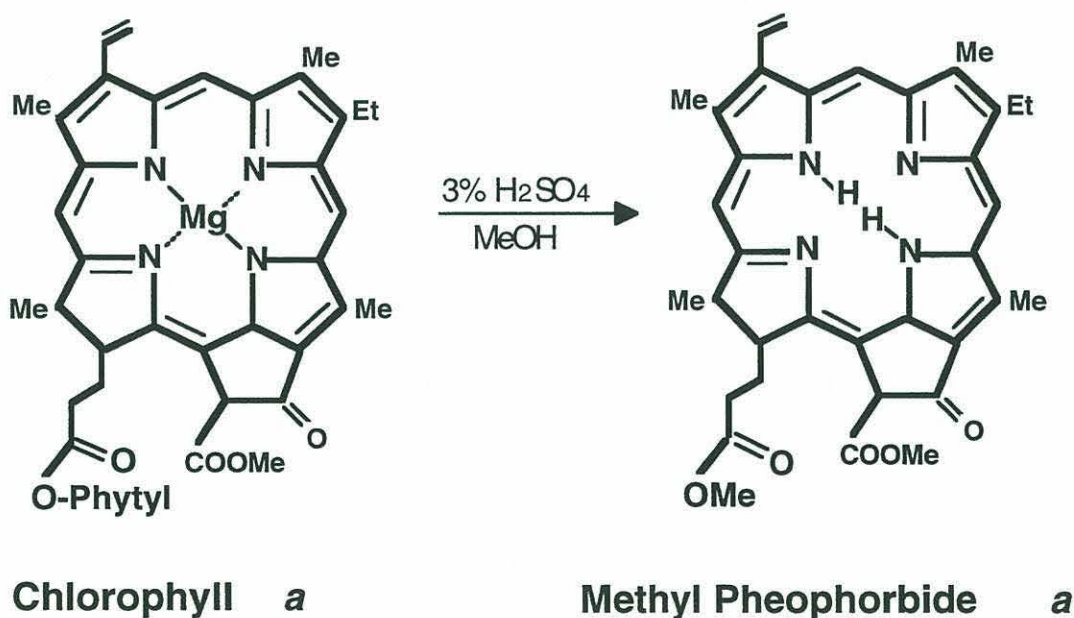
Methyl pheophorbide *a* was synthesized from spirulina chlorophyll *a*. *Spirulina* powder (100 g, Earthrise, Petaluma, CA) was placed in a 1 L flask with 50 mg NaHCO<sub>3</sub> (Aldrich, Milwaukee, WI) and a 2" magnetic stirring bar and extracted with 300 mL degassed MeOH under a nitrogen atmosphere. The extraction was accomplished by first placing the sealed flask in an ultrasonic bath (Cavitator 5.5, Mettler Electronics Corp., Anaheim, CA) for 25 minutes, then stirring at room temperature for 2 hours. The reaction mixture was then filtered (Whatman GF/F, 47 mm) under vacuum. The spirulina was then re-extracted twice in an ultrasonic bath for 20 minutes with 300 mL degassed acetone, filtering after each extraction. The combined extracts were rotary evaporated (Buchi RE-111, Buchi Laboratoriums-Technik AG, Flawil/Schweiz, Switzerland) to dryness.

To the dried extract which contained chlorophyll *a* (Chl<sub>a</sub>) was added 100 mL N<sub>2</sub>-sparged (2 hours) 3/97 (w/v) H<sub>2</sub>SO<sub>4</sub>/MeOH and a magnetic stirring bar. The demetallation/trans-esterification reaction was stirred in the dark under a nitrogen atmosphere and allowed to proceed overnight. The reaction mixture was then diluted with 100 mL MeCl<sub>2</sub> and neutralized by washing (2x) with 500

mL saturated  $\text{NaHCO}_3$  (aq) and (1x) with 500 mL water in a 2 L separatory funnel. The aqueous phases were back-extracted (3x) with  $\text{MeCl}_2$  and the combined organic extracts rotary-evaporated to dryness.

Severe emulsions formed during the water wash and during the back-extractions. The formation of emulsions apparently is common when handling "natural porphyrins in organic solvents" (Falk, 1964). Thus, the emulsions were allowed to settle for many hours, but never completely cleared; some product was inevitably lost. Analytical silica TLC, spotted with authentic standards and eluted with 2/98 (v/v)  $\text{MeOH}/\text{MeCl}_2$ , demonstrated that methyl pheophorbide *a* (MPBDa) (figure 2.2) was the major product, with some pheophytin *a* present and at least four more polar chlorins in minor amounts.

**Figure 2.2: Synthesis of methyl pheophorbide *a* from chlorophyll *a*.**



The extract was then redissolved in a small volume of  $\text{MeCl}_2$  and chromatographed on a 2.5 cm x 15 cm flash  $\text{SiO}_2$  column with 2/98 (v/v)  $\text{MeOH}/\text{MeCl}_2$  as eluant. The first band to elute was reddish orange, the second

band was brownish green, the third was brown, and the fourth was yellow. Analytical SiO<sub>2</sub> TLC spotted with chlorin standards and eluted with 2/98 MeOH/MeCl<sub>2</sub> demonstrated that band 2 contained all of the chlorins. These were shown to be predominately MPBDa with some pheophytin *a* (PTNa) and small quantities of more polar chlorins. Band 1 contained predominantly  $\beta$ -carotene, and bands 3 and 4 contained various carotenoids.

The chlorin-containing fraction was rotary-evaporated to dryness, redissolved in 25 mL MeCl<sub>2</sub> and transferred to a 1 L erlenmeyer flask to which was added 500 mL hexane. Recrystallization of MPBDa was accomplished by allowing the flask to stand at room temperature for 4 days, after which time the supernatant was poured off and the crystals were washed with hexane. The total yield of methyl pheophorbide *a* from 100 g of spirulina was 1.9 mmol (1.1 g).

#### 2.3.5.2 Methyl pyropheophorbide *a*

Pyrolization, or removal of the  $\beta$ -keto ester at C-10 of MPBDa, to form methyl pyropheophorbide *a* (MPPBDa) was accomplished by refluxing the MPBDa under a N<sub>2</sub> atmosphere in 20 mL collidine, to which was added 2 drops H<sub>2</sub>O (as a proton donor), for 2.5 hours. The collidine was then vacuum-distilled off, and the MPPBDa residue was redissolved in 125 mL MeCl<sub>2</sub>. The extract was then neutralized by washing (1x) with 200 mL 1 N HCl, (2x) with 200 mL H<sub>2</sub>O, and (1x) with 50 mL saturated NaHCO<sub>3</sub> (aq) in 100 mL H<sub>2</sub>O. Emulsions were problematic, especially with the water washes, and were left to settle, in some instances, for many hours. The neutral organic extract was then dried over Na<sub>2</sub>SO<sub>4</sub>, filtered (47 mm Whatman GF/F), and rotary-evaporated to dryness.



Analytical alumina and silica TLC (eluted with 10/90 acetone/hexane and 2/98 MeOH/MeCl<sub>2</sub>, respectively) spotted with authentic standards showed MPPBDa to be the major product, with a small amount of PTNa or PPTNa, but a significant quantity of green pigment remained at the origin on both plates. It was hypothesized that this material was comprised of chlorin free-acids derived from hydrolysis of the methyl ester on the propionic acid side-chain (i.e., pheophorbide *a* (PBDa) and pyropheophorbide *a* (PPBDa)), either during the pyrolysis reaction, since water was added, or during the neutralization with 1 N HCl.

Consequently, methylation of the free acids was attempted by repeating the transesterification procedure described earlier, only this time with 4/96 (w/v) H<sub>2</sub>SO<sub>4</sub>/MeOH. Neutralization of the reaction mixture was accomplished by diluting the 100 mL acidic methanol with 100 mL MeCl<sub>2</sub> and pouring onto 500 mL saturated NaHCO<sub>3</sub>(aq). One washing neutralized the extract, which was then washed (1x) with 500 mL water. The aqueous layer was then back-extracted (3x) with 25 mL MeCl<sub>2</sub>. Surprisingly, emulsions did not form.

Analytical silica TLC (2/98 MeOH/MeCl<sub>2</sub>) spotted with authentic standards showed MPPBDa to be the major product, with no detectable PPTNa or PTNa, but with substantial green color at the origin. The organic extracts were then combined, dried over Na<sub>2</sub>SO<sub>4</sub>, and rotary-evaporated to dryness. The dried extract weighed 1.0 g.

The MPPBDa was separated from the polar material by flash silica column chromatography (5 x 15 cm) and 2/98 tetrahydrofuran (THF)/ MeCl<sub>2</sub> as eluant. Carotenoids eluted first (orange/red color) followed by the chlorins (green). Some green color also remained on the silica. The green fraction, shown by silica TLC to contain predominantly MPPBDa with very minor amounts of some more polar chlorins, was rotary-evaporated to dryness. The total amount of MPPBDa

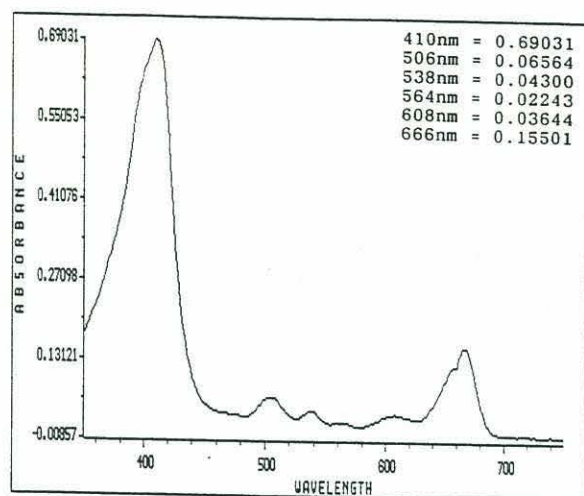
synthesized was 0.39 mmol (214 mg), giving a yield of 21% for the pyrolysis, and 2.1 mg MPPBDa/g Spirulina.

#### 2.3.5.3 9-Deoxo-methyl-pyropheophorbide *a*

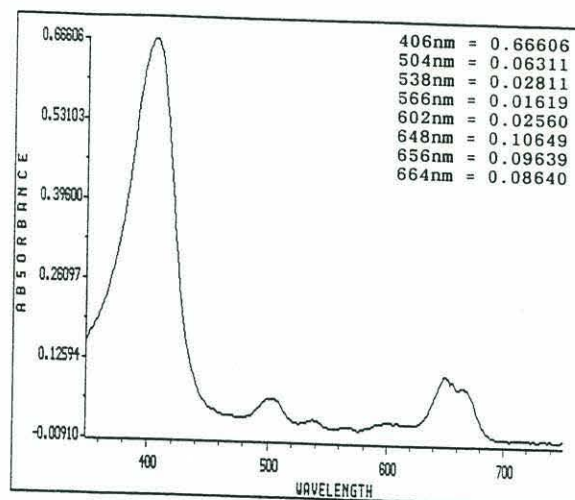
The synthesis of 9-deoxo-methyl-pyropheophorbide *a* (9MPPBDa) from MPPBDa is based on previously published ketone reduction procedures using sodium borohydride in trifluoroacetic acid (Gribble, et al., 1978; Gribble, et al., 1977; Jeandon, et al., 1993; Smith and Smith, 1990). Sodium borohydride ( $\text{NaBH}_4$ , 100 mg, Fisher Scientific, Fair Lawn, NJ) was slowly added to 10 mL dry trifluoroacetic acid (TFA,  $\text{CF}_3\text{COOH}$ , Sigma Chemical Co., St. Louis, MO) with stirring at 0°C under a rapid  $\text{N}_2$  stream (in order to prevent  $\text{H}_2$  buildup). The MPPBDa (212  $\mu\text{mol}$ , 116 mg), dissolved in 10 mL dry TFA, was then added to the  $\text{NaBH}_4$ /TFA mixture slowly via syringe. The ice bath was then removed and the reaction was allowed to proceed under a  $\text{N}_2$  atmosphere for 5 hours.

The progress of the reaction was monitored occasionally by withdrawing 0.5  $\mu\text{L}$  of the reaction mixture by syringe and adding it to  $\text{MeCl}_2$  in a cuvet to which was added 1-2 drops of triethylamine (TEA,  $(\text{CH}_3\text{CH}_2)_3\text{N}$ , Aldrich, Milwaukee, WI) (Smith and Smith, 1990) to neutralize the solution. During the course of the reaction the Soret band migrated from 410 to 404 nm and the red band migrated from 666 to 648 nm. The reaction was complete when there was no shoulder evident at 666 nm (figure 2.3).

(a) 1 Hour



(b) 2 Hours



(c) 5 Hours

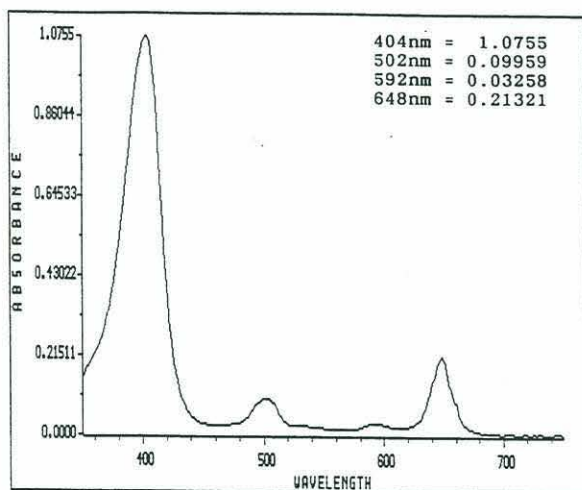


**Figure 2.3: Progress of ketone reduction reaction. MPPBDa is converted to 9-deoxo-methyl-pyropheophorbide *a* by reaction with sodium borohydride in trifluoroacetic acid. After (a) 1 hour, (b) 2 hours, and (c) 5 hours.**



The reaction mixture was then poured into a 500 mL separatory funnel containing 200 mL water. The 9MPPBD was partitioned (3x) into 20 mL MeCl<sub>2</sub>, until the MeCl<sub>2</sub> layer was colorless. The combined organic layers, which were a deep purple color, were then neutralized (1x) with 200 mL saturated NaHCO<sub>3</sub>(aq), and the aqueous layer was back-extracted (2x) with 10 mL MeCl<sub>2</sub>, until it was colorless. The combined organic extracts, which were a deep emerald green color, were then washed (2x) with 200 mL water, back-extracting the aqueous layer each time with (2x) 10 mL MeCl<sub>2</sub>. The combined organic extracts were dried over Na<sub>2</sub>SO<sub>4</sub> and rotary-evaporated to dryness. The reaction product weighed 110 mg (206 μmol 9MPPBD) giving a yield for the ketone reduction of 97%.

### *2.3.6 The Purification of Particulate Chlorophyll a for Isotopic Analysis*

#### *2.3.6.1 Particulate Sample Collection*

The procedures for the purification of Chla for stable N and C isotopic analysis from cultured phytoplankton and marine suspended particulates are described here. The protocol for purifying sedimentary chlorins for isotopic analysis can be found in section 2.3.7.

Culture and marine particulate samples were collected by filtration through a pre-combusted (450°C, > 8 hours) 293 mm Gelman A/E filter. The culture samples were vacuum-filtered, while the marine particulate samples were pumped from depth with garden hoses connected to a pneumatic pump (Lutz Pumps, Inc., Norcross, GA). Filters were immediately stored at -20 to -40°C

(field samples and 3 culture samples), or in liquid nitrogen (remaining culture samples), until extraction.

#### 2.3.6.2 *Particulate Sample Extraction*

Just prior to extraction, filters were thawed at room temperature and 2 x 1 cm subsamples were removed for whole-cell  $\delta^{15}\text{N}$  and  $\delta^{13}\text{C}$  determinations using a cork-borer. Filters were ultrasonically extracted by probe (3x) in 125 mL degassed acetone to which had been added approximately 5 g  $\text{NaHCO}_3$  (for neutralization of extract to prevent chlorophyll demetallation). The extracts were filtered through a 47 mm GF/F filter, and the filtrate was sparged with  $\text{N}_2$  during subsequent extractions. The combined extracts (500 mL) were poured into a 2 L separatory funnel containing 125 mL water, and the chlorophyll was partitioned (3x) into 200 mL hexane. The chlorophyll in both the combined hexane fractions and the aqueous fraction was then quantified spectrophotometrically. Typically, no chlorophyll *a* remained in the aqueous fraction.

The combined hexane fractions (800 mL) were then back-extracted (1x) with 200 mL 15/85  $\text{H}_2\text{O}/\text{MeOH}$  to remove carotenoids. The chlorophyll was then re-quantified in both the hexane and aqueous fractions.

Demetallation of the chlorophyll, to form pheophytin, was accomplished in a third phase separation by adding 200 mL 10%  $\text{HCl}$  (aq) to the hexane fraction and shaking for 1 minute. The color of the hexane solution changed from emerald to pine green. The aqueous fraction was poured off and the hexane neutralized with 100 mL 2% (w/v)  $\text{NaHCO}_3$  (aq). The hexane phase was then dried over  $\text{Na}_2\text{SO}_4$ , and rotary-evaporated to dryness. A final

spectrophotometric quantification was performed before the dried extract was stored under nitrogen at -20°C.

#### 2.3.6.3 *Particulate Chlorophyll Chromatographic Purification*

Further purification of the pheophytin *a* was achieved using preparative reversed-phase (C<sub>18</sub>) HPLC, followed by isocratic normal-phase (SiO<sub>2</sub>) HPLC on an analytical column.

The dried extracts were dissolved in a small (100-500 µL) amount of MeCl<sub>2</sub> before being injected into the HPLC. Injections were between 50 and 200 µL. The preparative C<sub>18</sub> column was a Kromasil Kr100-5-C18 with dimensions of 10 mm I.D. x 250 mm, and a particle size of 5 µm (Eka Nobel, Bohus, Sweden). A Kromasil 10 mm I.D. x 50 mm guard column packed with 5 µm C<sub>18</sub> was placed in front of the preparative column. Normally, 2 to 5 injections of between 1 and 25 mg of extract (amounting to 0.5 to 4 µmol PTNa) were performed, depending on the size of a sample.

The solvent gradient for the two-solvent (e.g., MeOH/acetone) system is shown in table 2.1. The flow rate varied between 6 and 7 mL/min. The chromatogram was typically monitored at 666 nm. Pheophytin *a* and *a'* peaks, eluting at about 20 and 21 mins, respectively, were detected with a photodiode array detector or a fluorescence detector, and collected into 18 mL glass vials with a fraction collector. The chlorins were then rotary-evaporated to dryness and stored at -20°C until the normal-phase chromatography was performed. The column was cleaned between samples with 90 mL 100% MeCl<sub>2</sub> (e.g., 15 minutes at 6 mL/min).



**Table 2.1: Solvent gradient for preparative C<sub>18</sub> HPLC. Time is in minutes, solvent A is methanol, solvent B is acetone, and flow rate is in mL/min.**

Time	% A	% B	Flow
0	95	5	6
10	70	30	6
15	65	35	7
30	0	100	6
35	0	100	6

Samples for SiO<sub>2</sub> HPLC were redissolved in 100-400  $\mu$ L 10/90 acetone/hexane before being injected (50 to 200  $\mu$ L) into the HPLC. This corresponded to 0.5 to 2 mg PTNa per injection. An Alltech Spherisorb Silica 3 Micron analytical column with a 3  $\mu$ m particle size and dimensions of 4.6 mm I.D. x 100 mm (cat # 8556, Alltech Associates, Inc, Deerfield, IL) was used to purify the pheophytins. Isocratic elution of 4/96 acetone/hexane, at 2 mL/min resulted in PTNa' and PTNa retention times of about 11 and 13 minutes, respectively. The chromatogram was usually monitored at 666 nm. The peaks were collected into 4 mL glass vials with a fraction collector, then dried under a N<sub>2</sub> stream, and stored at -20°C until isotopic or CHN analysis.

Care was taken to collect the entire chlorin peak during chromatography in order to prevent isotopic alteration of a sample resulting from across-peak isotopic variations (Bidigare, et al., 1991).

The column was cleaned between samples with 60 mL 100% acetone (e.g., 30 minutes at 2 mL/min). Re-equilibration of the column with 4/96 acetone/hexane was accomplished in 30 minutes (at 2 mL/min).

The pheophytin recoveries for the purification were 88% ( $\pm$  18%), or about 90-95% for each step. No isotopic fractionation was imparted during the

purification (as will be discussed in detail in section 2.4.3). Two samples, prepared in tandem, can be processed in about 8 hours.

### *2.3.7 The Purification of Sedimentary Chlorins for Isotopic Analysis*

#### *2.3.7.1 Sediment Extraction*

Frozen sediments (50-125 g wet wt or 20-50 g dry wt) were thawed at room temperature, transferred to 800 mL centrifuge tubes, and successively sonic-extracted (Vibra Cell, 70% duty cycle, output control 8; Sonics and Materials, Inc., Danbury, CT) with an immersion probe for 9 minutes each in 700 mL 100% MeOH, 50/50 MeOH/MeCl<sub>2</sub>, 25/75 MeOH/MeCl<sub>2</sub>, 100% MeCl<sub>2</sub>. The centrifuge tube was immersed in an ice water bath during extraction to mitigate both pigment decomposition and solvent evaporation. After each of the 4 extractions, the samples were immediately centrifuged (Model 2K, Needham Heights, MA) for 10 minutes at 1200 r.p.m. The supernatants were then decanted, combined and rotary-evaporated to dryness.

#### *2.3.7.2 Solid-Phase Extraction (SPE)*

The dried sediment extracts (typically containing 2 to 7  $\mu$ mol chlorin) were then redissolved in 10 mL 7/93 MeOH/MeCl<sub>2</sub> and applied, via pipet, onto a 5 x 10 cm flash SiO<sub>2</sub> column (Matrex Silica Si, 60 A Pore Diameter, Amicon Corp., Danvers, MA).



The column was prepared by pouring a slurry of 75 g unactivated silica in MeCl<sub>2</sub> into a 5 x 45.7 cm flash chromatography column (cat. # 5872-20, Ace Glass, Inc., Vineland, NJ) containing a plug of glass wool and a thin (5 mm) layer of sand at the bottom. The column was then eluted, under N<sub>2</sub> pressure of 2-5 p.s.i., with 600-1000 mL 7/93 MeOH/MeCl<sub>2</sub>. This both packed and washed the silica. A thin layer (5 mm) of sand was then applied to the top of the silica by slowly pouring it into 200-400 mL 7/93 MeOH/MeCl<sub>2</sub>.

The sample was eluted from the column with 600 mL 7/93 MeOH/MeCl<sub>2</sub>. The first ~100 mL to elute were orange and contained  $\beta$ -carotene and other carotenoids. The next ~200 mL to elute contained most of the common chlorins found in marine sediments. They ranged in polarity from chlorin steryl esters (non-polar) to pheophorbide *a* (chlorin free-acid), yet proceeded down the column as one indistinguishable band. This fraction was green/brown or black in visible light, depending on the size of the sample, but was an intense pink/orange under UV light. A hand-held UV lamp was useful for monitoring the chromatography. The chlorin fraction was collected, rotary-evaporated to dryness, and stored at -20°C.

Typically some pink/orange fluorescence (under UV light) remained at the origin. From the color of the material in visible and UV light it was probably chlorin-derived, however recoveries of total chlorin from the column (assuming an extinction coefficient ( $\epsilon_{666}$ ) of  $5 \times 10^4$  for the red band (King and Repeta, 1994a) and a molecular weight (MW) of 550 or 850, depending on the sample) averaged >100%, so it is unlikely that the material remaining on the column accounted for a significant fraction of the total chlorin. Yields greater than 100% can arise from the baseline correction of visible spectra of highly impure samples. (See section 2.3.4 for a discussion of spectrophotometric chlorin quantitation in impure samples.)



The purity of the chlorin fraction ( $\epsilon_{666} = 5 \times 10^4$ , MW = 550 or 850) after SPE was 4.0% ( $\pm 1.2\%$ ) for 7 Mediterranean and 4 Black Sea sediments. This compares to a purity of  $< 1\%$  for the whole extract prior to SPE. Most importantly, though, the procedure removes much of the chromatographic "baseline" that interferes with chlorin detection at 666 nm (figure 2.4.a). In addition, SPE desalted the samples of seasalt collected during the solvent extraction. In so doing, it circumvented the need for cumbersome phase separations which resulted in severe emulsions and loss of sample.

#### 2.3.7.3 Preparative Reverse-Phase High-Performance Liquid Chromatography (HPLC)

Prior to the preparative C<sub>18</sub> chromatography, a "fingerprint" chromatogram of each sample was taken on analytical C<sub>18</sub> HPLC in order to determine the chlorin distribution. The conditions for the chromatography are described in section 2.3.3.4.

Then the dried extract was redissolved in 200 to 1000  $\mu\text{L}$  10/90 MeOH/MeCl<sub>2</sub> and injected (50-200  $\mu\text{L}$  at a time) onto a preparative C<sub>18</sub> HPLC column (Kromasil Kr 100-5-C<sub>18</sub>, 10 mm I.D. x 250 mm, 5  $\mu\text{m}$  particle size; Eka Nobel, Bohus, Sweden), fitted with a 10 mm I.D. x 50 mm guard column (Kromasil 5  $\mu\text{m}$  C<sub>18</sub> packing), and connected to a Waters 600E pump and 900 photodiode array detector. Up to 30 mg of extract and 5  $\mu\text{mol}$  of chlorin was injected at a time, but  $\leq 10$  mg extract and/or 2  $\mu\text{mol}$  chlorin gave the best results. The chromatogram was monitored at 666 nm and prominent chlorin peaks were collected with a fraction collector into 18 mL glass vials.

The solvent gradient was 75% A to 100% B in 15 minutes, then 8 minutes of 100% B. Solvent A was 10/90 H<sub>2</sub>O/MeOH. Solvent B was acetone. The flow

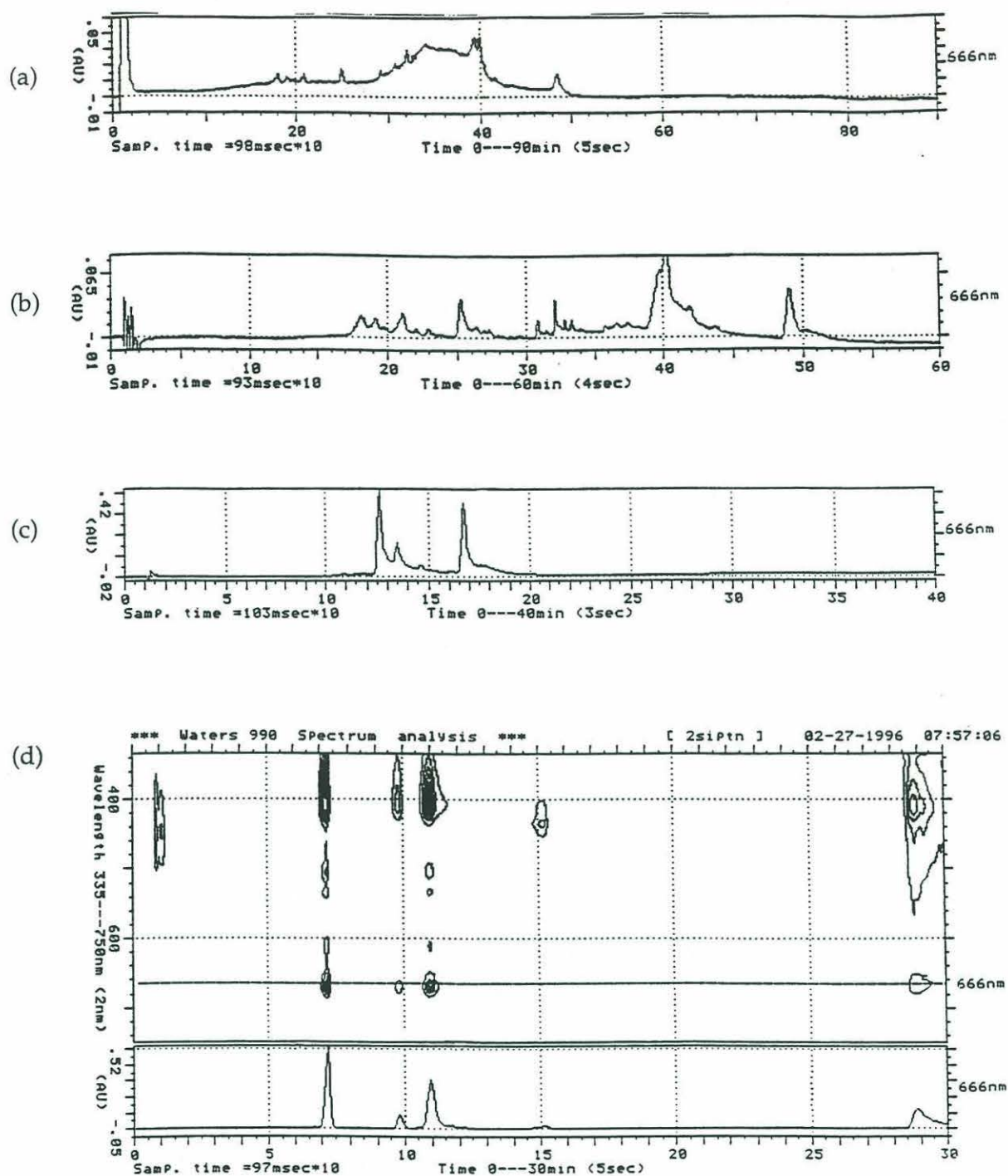


Figure 2.4: Analytical C<sub>18</sub> HPLC chromatograms of a surficial Black Sea sediment after (a) solvent extraction, (b) solid-phase extraction, and (c) size-exclusion chromatography. Chromatogram (d) represents the final purification step and was generated with an analytical SiO<sub>2</sub> column. The gradient was identical for (a) and (b). The three chlorins (in increasing retention time) in (c) and (d) are PTNa, PTNa' and PPTNa (order reversed in (d)).

rate was maintained at 6 mL/min. Approximate retention times for common chlorins are listed in table 2.2.

**Table 2.2: Retention times for common sedimentary chlorins on preparative reverse-phase (C<sub>18</sub>) HPLC.**

Chlorin *	t <sub>R</sub> (mins)
PPBDa	6.5
MPPBDa	9
PTNa	15
PPTNa	17
CSE's	18-20

\* Abbreviations are as follows: pyropheophorbide *a* (PPBDa), methyl pyropheophorbide *a* (MPPBDa), pheophytin *a* (PTNa), pyropheophytin *a* (PPTNa), and chlorin steryl esters (CSE's).

Recoveries for the preparative C<sub>18</sub> HPLC varied widely with the distribution of chlorins in and size of a sample, but averaged 24% ( $\pm 9\%$ ). A sample containing one or two chlorins typically had a higher recovery than one containing a dozen chlorophyll degradation products because it was not practical to collect and purify a dozen chlorins from a single sample. For example, figure 2.4.b shows the distribution of chlorins in a surficial Black Sea sediment extract after solid-phase extraction. Only the two largest peaks, PTNa and PPTNa ( $t_R = 40.3$  and  $49.1$  mins., respectively), accounting for about 50% of the total chlorin in the sample, were collected and purified. (The leading half of the PTNa peak is the unknown chlorin, "Chl686" discussed in section 2.5.3.1.) This alone resulted in recoveries of no better than 50%.

The purity of chlorins collected, based on gravimetry and spectrophotometry, ranged from 12 to 78%, and averaged 43% ( $\pm 22\%$ ).



#### 2.3.7.4 Size Exclusion Chromatography (SEC)

Size exclusion (or gel permeation) chromatography was used to remove impurities having similar polarities to the chlorins. This technique separates compounds on a styrene-divinyl benzene gel, based on the effective length of their longest dimension. Previous researchers have successfully used SEC to separate carotenoids from chlorins (King and Repeta, 1994b; Repeta and Gagosian, 1984; Repeta and Gagosian, 1987), and to separate metalloporphyrins from crude oil (Fish and Komlenic, 1984). In this study, a Shodex GPC K-801 column (8 mm I.D. x 300 mm length; Showa Denko K.K., Tokyo, Japan), having an exclusion limit of  $1.5 \times 10^3$  Daltons, and fitted with a Shodex K-G guard column (8 mm I.D. x 100 mm length) was eluted with degassed  $\text{MeCl}_2$  at 1.0 mL/min. The sample (0.25-4  $\mu\text{mol}$  chlorin, 0.5-3 mg), dissolved in 200  $\mu\text{L}$   $\text{MeCl}_2$ , was injected in 20 to 80  $\mu\text{L}$  aliquots, such that  $\leq 0.5$  mg of sample and  $< 0.5$   $\mu\text{mol}$  chlorin were injected at a time. The chromatogram was monitored at 666 nm, chlorin peaks were collected with a fraction collector into 4 mL vials, then dried under an  $\text{N}_2$  stream and stored at  $-20^\circ\text{C}$ .

Retention times (equal to retention volumes, for the flow rate of 1.0 mL/min) for some common pigments are given in table 2.3. A size-exclusion chromatogram of a surface Peru margin sediment extract is shown in figure 2.5. Good separation between pheophytins and pheophorbides was observed (figure 2.5.b), with carotenoids tending to elute between them (figure 2.5.a). The chlorin peak preceding the pheophytins are the chlorin steryl esters (CSE's), and the peak preceding them is high molecular weight chlorin material (King and Repeta, 1994a). In practice, for preparative-scale work, the following retention times were typical: CSE's, 5.3-5.6 mins.; PTN's and carotenoids, 5.8-7.0 mins.; pheophorbides, 7.0-8.4 mins.

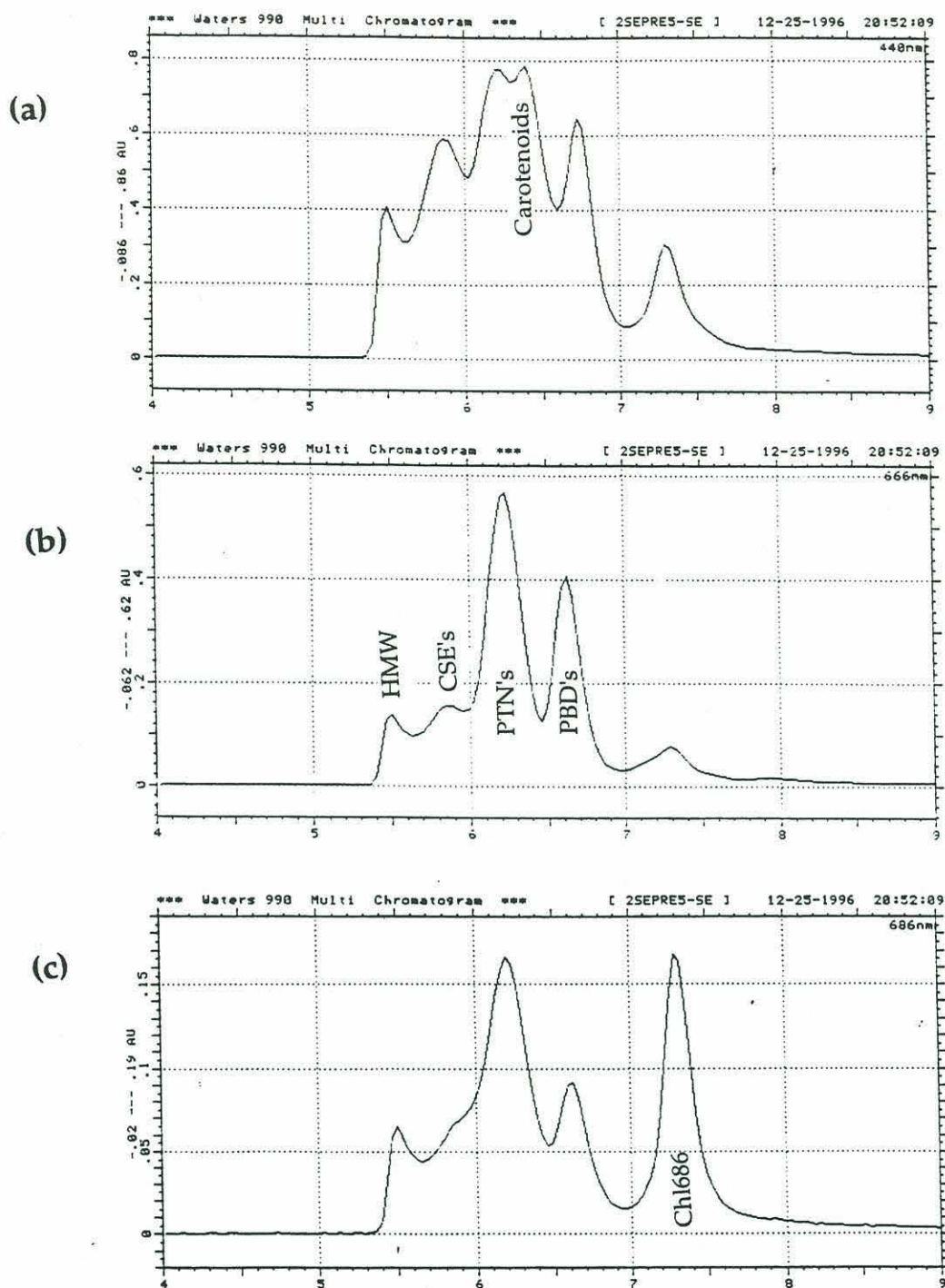


Figure 2.5: Size-exclusion chromatograms of a surface Peru margin sediment extract at (a) 440 nm, (b) 666 nm, and (c) 686 nm. The column was a Shodex GPC K-801 (8 mm I.D.  $\times$  300 mm length; Showa Denko K.K., Tokyo, Japan), the eluant was  $\text{MeCl}_2$ , and the flow rate was 1.0 mL/min. Pigment abbreviations are as follows: HMW=high molecular weight chlorin, CSE=chlorin steryl esters, PTN=pheophytins, PBD=pheophorbides, and Chl686 is an unknown chlorin discussed in section 2.5.3.1.

**Table 2.3: Retention times of reference compounds for size exclusion chromatography.**

Compound	t <sub>R</sub> (mins)
PTNa	6.12
MPBDa	6.53
β-Carotene	6.65
MPPBDa	6.70

The recovery of chlorins from the SEC column averaged 89% ( $\pm 12\%$ ), while the average purity of chlorins recovered (based on gravimetry and spectrophotometry) was 78% ( $\pm 13\%$ ). The chromatogram in figure 2.4.c gives some indication of the purity of chlorins--in this case, pheophytins--after SEC. By comparison with the chromatogram after SPE (just above it) it is clear that much of the chlorin contamination has been removed.

#### *2.3.7.5 Normal-phase (SiO<sub>2</sub>) High-performance Liquid Chromatography*

The final purification step for sedimentary chlorins was isocratic preparative normal-phase (SiO<sub>2</sub>) HPLC. A 10 mm I.D. x 250 mm Kromasil KR100-5-Sil column was used, containing 5  $\mu\text{m}$  packing, and connected to a 10 mm I.D. x 50 mm Kromasil guard column with the same packing. Typical injections were 100  $\mu\text{L}$  and contained 1 mg sample and 0.5  $\mu\text{mol}$  chlorin. The solvent mix varied depending on the chlorin, but was always comprised of acetone and hexane (table 2.4). The flow rate was maintained at 6 mL/min. The chromatogram was monitored at 666 nm, and chlorin peaks were collected into 18 mL glass vials, then rotary-evaporated to dryness.



**Table 2.4: Solvent mix for isocratic elution of common sedimentary chlorins on preparative SiO<sub>2</sub> HPLC. Values are ratios of acetone to hexane. Also listed are the approximate retention times for the chlorins.**

Chlorin	Acet/Hex	t <sub>R</sub> (mins)
PPTNa	5/95	9.5
PTNa'	5/95	12
PTNa	5/95	13
MPPBDa	20/80	7
PPBDa	30/70	6.5

Recoveries for the SiO<sub>2</sub> chromatography averaged 67% ( $\pm$  7.6%). The primary reason for the low recoveries was the separation, from the chlorin peak of interest, of structural isomers and allomers that had coeluted on both C<sub>18</sub> and size exclusion chromatography.

Chlorin purities after SiO<sub>2</sub> HPLC averaged 88% based on both gravimetry and elemental analysis (see discussion in section 2.4.2). Figure 2.4.d shows a typical SiO<sub>2</sub> HPLC chromatogram of a sample containing PPTNa, PTNa', and PTNa. The purity of the chlorins is attested to by the absence of other visible-light-absorbing material.

The entire purification procedure can be accomplished in one day if two samples are processed simultaneously. Chlorin recoveries for the entire procedure averaged 18%.

## 2.4 Results

The procedure for N and C isotopic determination in particulate and sedimentary chlorins was designed for most common chlorophyll degradation products. In this work it was used successfully to measure  $\delta^{15}\text{N}$  and  $\delta^{13}\text{C}$  of particulate Chla and Chla' (i.e., the 10(S)- stereoisomer of chlorophyll *a*), and sedimentary PTNa, PTNa', PPTNa, PPBDa, and MPPBDa. Aside from the requirements of having broad applicability and high recoveries, the technique had to produce highly pure products and maintain isotopic integrity. This section describes results of experiments to determine elemental and isotopic purity of the chlorins thus prepared.

### 2.4.1 Purity of Particulate Chlorophyll *a*

The purity of particulate Chla samples was determined by performing elemental analysis on the products of successive purification steps. Six algal cultures, grown as described in chapter 4, were used for this experiment. The cultures and the results of the elemental analyses are listed in table 2.5. The average chlorin purities are shown graphically in figure 2.6. Since the procedure required the demetallation of Chla to form PTNa, the purities are for PTNa. The three steps of the purification were: (1) solvent extraction and phase separations, (2) reverse-phase (C<sub>18</sub>) HPLC, and (3) normal-phase (SiO<sub>2</sub>) HPLC.

Elemental purities were determined based on spectrophotometric quantification of the PTNa, at 666 nm, using an extinction coefficient of  $1.01 \times 10^5$  and a Soret/ red (S/R) band absorbance ratio of 2.22 (King, 1993). Purities are

lower limits since S/R ratios of purified PTNa in this work were normally between 2.40 and 2.45.

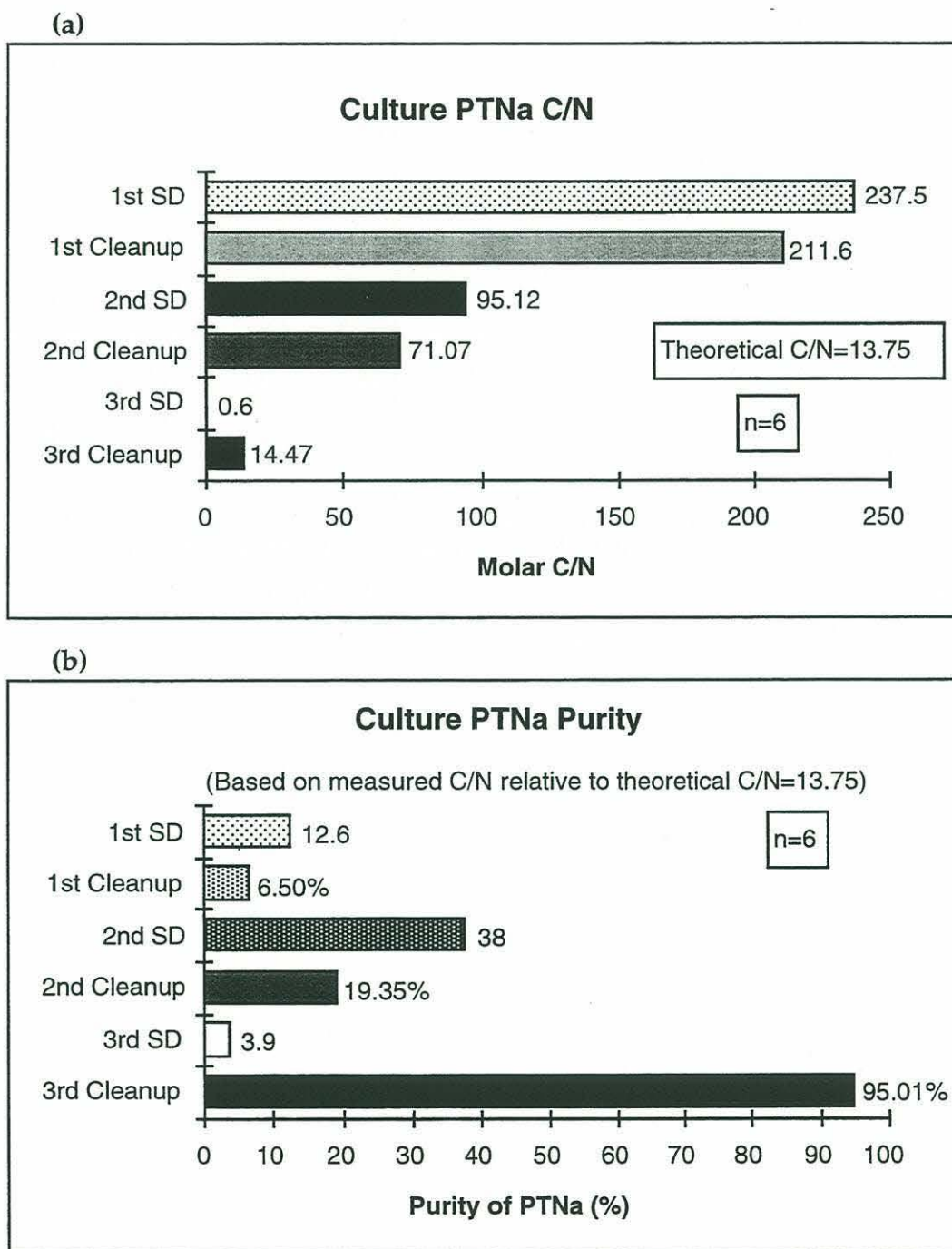
**Table 2.5: Purity of algal pheophytin *a* following each step of the procedure for the preparation of particulate chlorins for isotopic analysis. The theoretical C/N ratio of PTNa is 13.75. Values are in percent.**

Culture <sup>*</sup>	1st N Purity	1st C Purity	2nd N Purity	2nd C Purity	3rd N Purity	3rd C Purity
TW4	33	11	99	99	99	95
PHA4	62	18	98	83	95	96
PAV4	28	1	71	4	97	95
AMP4	62	7	95	41	97	87
DUN4	55	2	89	14	97	90
TW3			91	63	89	86
EH3	96	19				

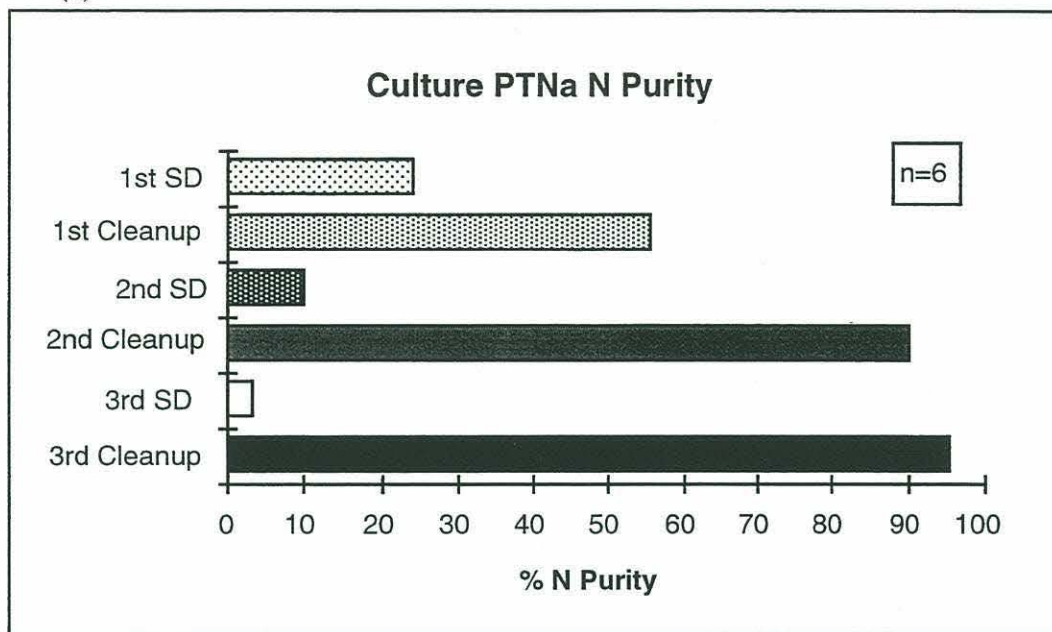
<sup>\*</sup> Culture abbreviations are as follows: TW=*Thalassiosira weissflogii*, PHA=*Phaeodactylum tricornutum*, PAV=*Pavlova lutheri*, AMP=*amphidinium carterae*, DUN=*Dunaliella tertiolecta*, EH=*Emiliana huxleyi*.



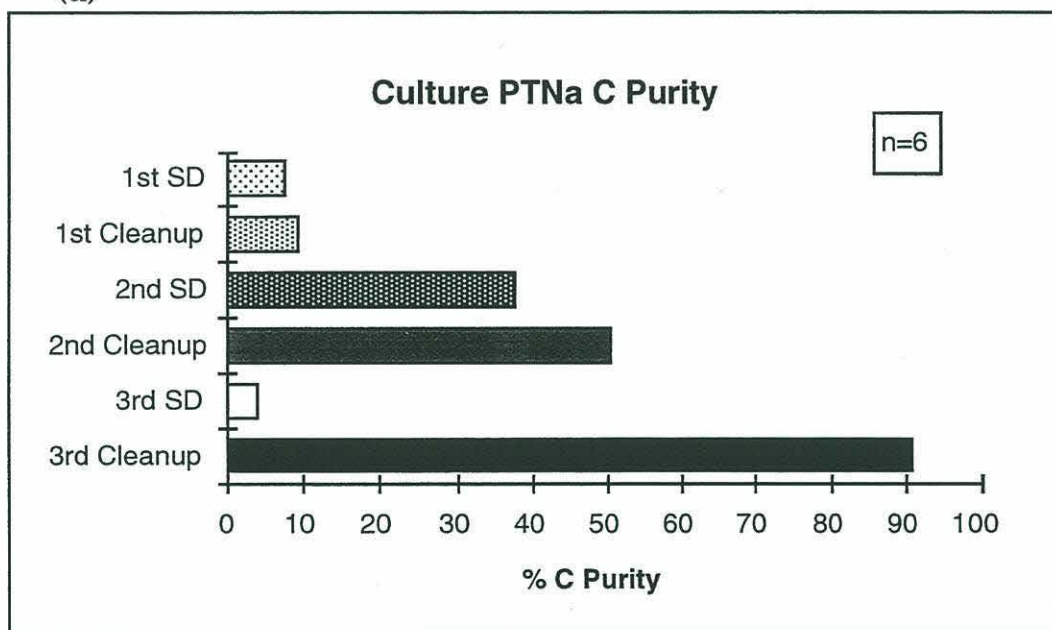
Figure 2.6: Purity of algal pheophytin *a* following each step of the procedure for the purification of particulate chlorins for isotopic analysis. Figure (a) shows the average C/N ratio of the products, (b) shows pheophytin *a* purity based upon the measured versus theoretical C/N ratio, and (c) and (d) show nitrogen and carbon purities of the pheophytin *a*, respectively. All values are averages of 6 cultures, and standard deviations (SD) are plotted. See text for an explanation of the purification steps.



(c)



(d)



As is evident from the chart of N purity (figure 2.6.c), the second chromatography step is not required if only  $\delta^{15}\text{N}$  measurements are sought. The nitrogen purity of the PTNa was 90.4% ( $\pm 10.4\%$ ) after the  $\text{C}_{18}$  HPLC, which should be sufficient for isotopic analysis. It improved to 95.9% ( $\pm 3.4\%$ ) after the  $\text{SiO}_2$  HPLC step. On the other hand, PTNa carbon was only 50.6% ( $\pm 37.8\%$ )

pure after the first chromatography step, but improved to 91.2 % ( $\pm 4.3\%$ ) purity after performing SiO<sub>2</sub> HPLC.

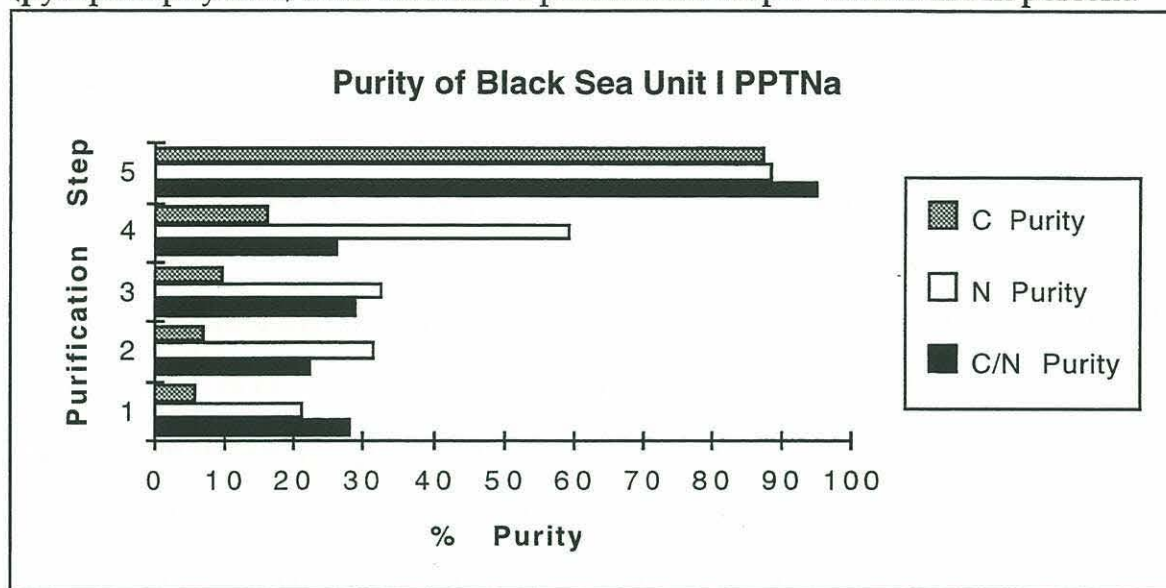
#### 2.4.2 Purity of Sedimentary Chlorins

The purity of sedimentary chlorins, treated as outlined above, was determined by performing elemental analyses on the products of successive purification steps. The sediment sample used for this experiment was surface (0-10 cm) sediment from the Black Sea (2129 m water depth, Stn. 2, Box Core 2, R/V Knorr 134-9, May 14-28, 1988). Pyropheophytin *a* was the most abundant chlorin in the sample. Figure 2.7 is a chart of the PPTNa purity after each step of the procedure.

The nitrogen and carbon purities of PPTNa from surficial Black Sea sediments reached 89% and 88%, respectively, after the 5-step purification procedure. These values are considered lower limits, as discussed above, since the S/R ratio used in spectrophotometric quantitations is believed to be 10% too low. Two other chlorins from the same sediment, PTNa and PTNa', had purities (based on C/N ratio) of 84% and 87%, respectively. These results compared favorably with those obtained by gravimetry for three E. Mediterranean and one Black Sea sapropel sample prepared in the same manner. The average purity of PPBDa and MPPBDa isolated from those samples was 88%.



Figure 2.7: Purity of a Black Sea surficial sedimentary chlorin (pyropheophytin *a*) after successive purification steps. Values are in percent.



**Purification Steps:**

- #1: Solvent Extraction
- #2: Solid Phase Extraction
- #3: Preparative C<sub>18</sub> HPLC
- #4: Size Exclusion Chromatography
- #5: Preparative SiO<sub>2</sub> HPLC

### 2.4.3 Precision of Chlorin Isotopic Determinations

Previous investigators have suggested that nitrogen isotopic compositions of chlorophyll *a* can be altered during reverse-phase chromatography if the entire chlorin peak is not collected (Bidigare, et al., 1991). The results of at least five different experiments in which HPLC was used to purify a variety of chlorins from different natural samples suggest that such alteration did not affect the results of this work. The precision for isotopic determinations of particulate and sedimentary chlorins was 0.12 per mil for nitrogen and 0.09 per mil for carbon.

These values are pooled standard deviations of experiments involving repeated measurements.

#### 2.4.3.1 Precision of Particulate Chla N and C Isotopic Determinations

The most direct test of the reproducibility of chromatographic separations performed in this study was the repeated purification of *Fucus sp.* Chla on C<sub>18</sub> HPLC. In that experiment, 4 individual aliquots of the whole lipid extract were chromatographed on an analytical reversed-phase (C<sub>18</sub>) column, collected, and submitted for N isotopic analysis. One of the aliquots was large enough to be split into 3 subsamples for  $\delta^{15}\text{N}$ . The average  $\delta^{15}\text{N}$  of the 4 aliquots (the 3 subsamples of the large one being averaged) was  $4.33 \pm 0.10$  per mil. The average  $\delta^{15}\text{N}$  of the 3 subsamples of one aliquot was  $4.33 \pm 0.07$  per mil. The first standard deviation represents the chromatographic precision, while the second represents the measurement precision of the  $^{15}\text{N}/^{14}\text{N}$  ratio in purified Chla.

A more comprehensive test of the precision of the particulate Chla isotopic determination came from 6 sets of duplicate phytoplankton cultures (representing 6 different species) that were grown and purified at different times over an 18 month period. These results are discussed in detail in chapter 4. In brief, the precision of Chla  $\delta^{15}\text{N}$  determinations was better than 0.57 per mil. This value is the pooled standard deviation (see definition in section 2.4.3.3) of the isotopic difference between the whole cells and the Chla (e.g.,  $\Delta\delta^{15}\text{N}_{\text{cell-Chla}}$ ). It is used because absolute  $\delta^{15}\text{N}_{\text{Chla}}$  values varied from one experiment to another. Thus, the measurement includes the additional errors associated with the bulk PON  $\delta^{15}\text{N}$  determination (e.g., 1 SD = 0.23 per mil) and the natural

variability of the cell-chlorophyll isotopic difference. It is therefore an upper limit on the precision of the Chla  $\delta^{15}\text{N}$  determination. The precision for carbon, based on 5 sets of repeat culture experiments, was 1.25 per mil. This value also includes the errors associated with the  $\delta^{13}\text{C}_{\text{POC}}$  determination (e.g., 1 SD = 0.61 per mil) and the natural variability in  $\Delta\delta^{13}\text{C}_{\text{cell-Chla}}$ , and is therefore an upper limit on the precision of the Chla  $\delta^{13}\text{C}$  determination.

#### 2.4.3.2 Precision of Sedimentary Chlorin N and C Isotopic Determination

The precision of the sedimentary chlorin isotopic determinations was assessed by comparing repeated analyses of sample splits, as well as by comparing the isotopic composition of structurally related (i.e., epimers, allomers, etc.) chlorins purified simultaneously.

Fractions of PPTNa and PTNa from surficial Black Sea sediment (the same sample used in the purity experiment discussed above) were collected off a size exclusion column and split. Each duplicate was independently chromatographed on  $\text{SiO}_2$  HPLC. Both PTNa samples had identical  $\delta^{15}\text{N}$  and  $\delta^{13}\text{C}$  values after the chromatography. Furthermore, one of the PPTNa samples was then re-chromatographed on  $\text{C}_{18}$  HPLC. The isotopic difference between the two PPTNa samples after the additional chromatography step was 0.05 per mil for both N and C. Finally, a fraction from the SEC column containing both PTNa and PTNa' (a C-10 stereoisomer of PTNa) was chromatographed on  $\text{SiO}_2$  HPLC and the purified epimers were found to have  $\delta^{15}\text{N}$  values that differed by 0.5 per mil. (As discussed below in section 2.5.2, though, chlorin epimers may have different N isotopic compositions).



In another experiment, MPPBDa and its allomer (e.g., 10-hydroxy-MPPBDa, or alMPPBDa) were purified from a surficial (2-10 cm) Peru margin sediment (250 m water depth, R/V Seward Johnson 92, Stn 36, 11/15/92, core BC-153, 11°03.7'S, 78°04.4'W). The procedure differed slightly from that outlined above, with the two chlorins being fractionated on preparative reverse-phase TLC, then independently chromatographed on C<sub>18</sub> HPLC, SiO<sub>2</sub> HPLC, and again on C<sub>18</sub> HPLC. The purified MPPBDa was then split into two for  $\delta^{15}\text{N}$  analysis. The isotopic composition of the purified MPPBDa (splits averaged) and its allomer differed by 0.25 per mil. The isotopic difference between the two splits of purified MPPBDa was 0.3 per mil, again suggesting that the chromatographic purification of chlorins results in little or no N isotopic alteration.

The final experiment to determine the precision of sedimentary chlorin isotopic determinations was the comparison of chlorin  $\delta^{15}\text{N}$  and  $\delta^{13}\text{C}$  values from splits of an Eastern Mediterranean sapropel. Sapropel S4 (~95 Kyr BP, ODP Leg 160, Hole 964F, Core 2H/01/40-58) was split into two sections and each was independently processed according to the procedure described above. The purified PPBDa from the two sections differed in  $\delta^{15}\text{N}$  by 0.1 per mil, while the  $\delta^{13}\text{C}$  values differed by 0.3 per mil.

#### 2.4.3.3 *Reproducibility of Chlorin Isotopic Determinations*

Table 2.6 summarizes the precision data presented in the previous two sections, excluding those for the replicate culture experiments (since they are not comparable). The standard deviations of the replicate measurements are listed for both nitrogen and carbon isotopes (when the latter are available). Also

shown are the chromatographic procedures performed on the replicates in each experiment. At the bottom of the table the pooled standard deviation for all the measurements is shown. This quantity is defined as

$$\text{pooled standard deviation} = \sqrt{\frac{\sum (n_i - 1) \sigma_i^2}{\sum (n_i - 1)}}.$$

**Table 2.6: Reproducibility of N and C isotopic determinations on particulate and sedimentary chlorins. See text for sample descriptions.**

Sample	$1\sigma\text{-}\delta^{15}\text{N}$	n	$1\sigma\text{-}\delta^{13}\text{C}$	n	Chromatographic Steps
Fucus	0.10	4			C <sub>18</sub> HPLC
Black Sea PTNa	0	2	0	2	SiO <sub>2</sub> HPLC
Black Sea PPTNa	0.03	2	0.05	2	SiO <sub>2</sub> HPLC, C <sub>18</sub> HPLC
Black Sea PTNa,a'	0.25	2			SiO <sub>2</sub> HPLC
Peru MPPBDa,al	0.13	2			C <sub>18</sub> TLC, 2xC <sub>18</sub> , 1xSiO <sub>2</sub> HPLC
Med Sea PPBDa	0.05	2	0.15	2	SPE, SEC, C <sub>18</sub> & SiO <sub>2</sub> HPLC
Pooled SD	0.12		0.09		

These data indicate that sedimentary and particulate chlorin  $\delta^{15}\text{N}$  and  $\delta^{13}\text{C}$  can be determined with a precision of 0.12 and 0.09 per mil, respectively. There does not appear to be any substantial N or C isotopic alteration of chlorins during their purification with the methods described in this work.

## 2.5 Discussion

The procedure outlined above for the measurement of chlorin  $\delta^{15}\text{N}$  and  $\delta^{13}\text{C}$  in marine particles and sediments has been shown to yield products that are at least 88% pure, with a precision better than 0.15 per mil for both C and N.

### 2.5.1 *Minimum Purification Required for Isotopic Analysis of Chlorins*

It has been suggested (Macko, 1981) that sediment and particulate lipid extracts may contain primarily chlorin nitrogen, and therefore may be used as surrogates for chlorophyll  $\delta^{15}\text{N}$  analyses. This appears not to be the case for particles or sediments. For instance, the average Chla nitrogen purity for solvent extracts of phytoplankton cultures in this work was 56% ( $\pm 24\%$ ), while that for carbon was 9.5% ( $\pm 7.6\%$ ). In a solvent extract of surficial sediments from the Black Sea the chlorin N purity was 21%, while chlorin C purity was 6%. In addition, in 7 Eastern Mediterranean sapropel and 4 Black Sea sediment samples, chlorin purity was 4% ( $\pm 1.2\%$ ) after solvent and solid-phase extraction, based on gravimetry. This suggests that chlorin purity in lipid extracts is low.

Since the impurities appeared to have significantly different N and C isotopic ratios than the chlorins, the extract  $\delta^{15}\text{N}$  and  $\delta^{13}\text{C}$  values were not suitable substitutes for the purified pigments. For instance, in surficial Black Sea sediments, the purified chlorins had  $\delta^{15}\text{N}$  values ranging from -3.4 to -4.9 per mil, while the whole sediment extract had a  $\delta^{15}\text{N}$  value of -2.55 per mil (table 2.7). Furthermore, the  $\delta^{13}\text{C}$  of the chlorins fell between -24.9 and -25.0, while the  $\delta^{13}\text{C}$  of the whole extract was -27.4 per mil (table 2.7).



**Table 2.7: Isotopic ratios and elemental purities of Black Sea surficial sedimentary chlorins after sequential purification steps**

Sample	$\delta^{15}\text{N}$	% N Purity	$\delta^{13}\text{C}$	% C Purity
Whole Sediment	1.2		-23.3	
Lipid Extract	-2.6	21	-27.4	6
SPE Chlorins	-3.6	32	-26.7	7
C <sub>18</sub> HPLC PPTNa	-4.4	33	-26.7	10
C <sub>18</sub> HPLC PTNa	-4.6	39	-25.7	18
SEC PTNa+PPTNa		60		16
SiO <sub>2</sub> Chlorins*	-4.5	89	-24.1	88

\*  $\delta^{15}\text{N}$  value is a weighted average for PPTNa, PTNa, PTNa', and an unknown chlorin (discussed below).  $\delta^{13}\text{C}$  value is a similar weighted average, excluding PTNa', for which no  $\delta^{13}\text{C}$  measurement was available. The N and C purities are for PPTNa, since no elemental purities (only those based on C/N ratio) were available for the other chlorins.

So just how much purification is required for N and C isotopic analysis of chlorins in sediments and particles? As shown in table 2.7, sedimentary chlorin  $\delta^{15}\text{N}$  was closely approximated after the third purification (e.g., C<sub>18</sub> HPLC). Following that step, the  $\delta^{15}\text{N}$  of Black Sea surface sediment PPTNa and PTNa fractions (e.g., -4.4 and -4.6 per mil, respectively) were both within 0.12 per mil (i.e., 1 pooled SD) of the weighted average  $\delta^{15}\text{N}$  (-4.51 per mil) of fully purified chlorins. For  $\delta^{13}\text{C}$ , though, all 5 steps were required. The  $\delta^{13}\text{C}$  of the same C<sub>18</sub> HPLC-purified PPTNa and PTNa fractions (e.g., -26.7 and -25.7 per mil, respectively) was 2.6 and 1.6 per mil depleted in  $^{13}\text{C}$  compared to the weighted average  $\delta^{13}\text{C}$  (-24.1 per mil) of fully purified chlorins.

These results indicate that the non-chlorin component of the lipid extract was depleted in  $^{13}\text{C}$  and enriched in  $^{15}\text{N}$  compared to the chlorins. With increasing purity,  $\delta^{15}\text{N}$  values decreased while  $\delta^{13}\text{C}$  values increased.

The amount of purification required for suitable particulate Chla isotopic ratios can only be estimated, since isotopic determinations were not made on the partially purified algal Chla from culture. As discussed in section 2.4.1, the N purity of Chla from six algal cultures averaged > 90% after the first chromatography step (e.g., C<sub>18</sub> HPLC). Since Chla  $\delta^{15}\text{N}$  is about 5 per mil depleted in  $^{15}\text{N}$  relative to whole cells (see chapter 4), and assuming the < 10% of non-Chla N remaining has  $\delta^{15}\text{N}$  similar to the whole cell, then the partially purified Chla would be enriched in  $^{15}\text{N}$  by < 0.5 per mil, or ~10%. In addition, the average purity of 4 Mediterranean Sea particulate Chla samples after C<sub>18</sub> HPLC was 94% ( $\pm 11\%$ ), again suggesting that only the first chromatographic purification is required for  $\delta^{15}\text{N}$  determinations.

For  $\delta^{13}\text{C}$  determinations of particulate Chla it is recommended that both chromatographic purifications (e.g., C<sub>18</sub> and SiO<sub>2</sub> HPLC) be performed. The Chla from cultured algae averaged only 51% purity for C after C<sub>18</sub> HPLC, and improved to >90% purity after SiO<sub>2</sub> HPLC. Although there was little systematic difference between Chla and cellular  $\delta^{13}\text{C}$  in cultured phytoplankton from this study (see chapter 4), it is widely accepted that lipids are depleted in  $\delta^{13}\text{C}$  relative to whole algal cells (DeNiro and Epstein, 1977; Galimov and Shirinsky, 1975). This suggests that contaminants in partially purified Chla from particulate lipid extracts may have significantly different  $\delta^{13}\text{C}$  values. Furthermore, the cultures grown in this study were prepared axenically. In natural systems, where detritus and non-planktonic carbon can account for significant fractions of the total C, there may be differences between Chla  $\delta^{13}\text{C}$  and POC  $\delta^{13}\text{C}$ .



### 2.5.2 Implications of Different N and C Isotopic Values in Sedimentary Chlorins

The chlorins purified from a surficial Black Sea sediment had different N and C isotopic ratios (table 2.8). These differences may be attributable to primary signals imparted to Chla during different seasons, or they may result from decompositional processes. In either case, they may contain detailed information about historical productivity in the Black Sea.

#### 2.5.2.1 N Isotopic Differences Between PTNa and PPTNa

One interesting inter-chlorin isotopic difference is the 0.9 per mil  $^{15}\text{N}$  depletion in PPTNa relative to PTNa (table 2.8). It is suggested that this difference is a primary signal reflecting changes in the seasonal flux of organic matter out of the euphotic zone.

**Table 2.8: N and C isotopic ratios in purified chlorins from surficial Black Sea sediments.**

Chlorin	$\delta^{15}\text{N}$	$\delta^{13}\text{C}$
PPTNa	-4.8	-24.9
PTNa	-3.9	-25.0
PTNa'	-3.4	
Chl686	-4.9	-23.1

There are two annual phytoplankton blooms in the Black Sea during which times most of the material flux to sediments occurs (Hay, et al., 1990). A large dinoflagellate and diatom bloom occurs in the spring, and a smaller



coccolithophorid-dominated bloom occurs in the fall (Hay, et al., 1990). The spring bloom at our core location is associated with a maximum in the PPTNa flux out of the euphotic zone, while the fall bloom is associated with a maximum in the PTNa flux (King, 1993).

It has been observed that minima in sinking particulate  $\delta^{15}\text{N}$  values coincide with maxima in mass fluxes to sediment traps in both the North Atlantic (Altabet and Deuser, 1985; Altabet, et al., 1991) and the Arabian Sea (Schafer and Ittekkot, 1993). In both locations, multi-year sediment trap deployments suggest that sinking particulate  $\delta^{15}\text{N}$  is inversely related to total mass flux.

The difference in Black Sea sedimentary PPTNa and PTNa  $\delta^{15}\text{N}$  values may therefore result from deposition of these components during the spring and summer blooms, respectively. The larger mass flux associated with the spring bloom, relative to the fall bloom, may result in lower  $\delta^{15}\text{N}$  values of material deposited at that time, including the PPTNa. Whereas the PTNa, deposited in the fall, is expected to be comparatively enriched in  $^{15}\text{N}$  since the material flux associated with that bloom is smaller. The potential may therefore exist to reconstruct seasonal paleo-fluxes (and hence, paleoproductivity) in the Black Sea based on N isotopic studies of sedimentary chlorins.

#### 2.5.2.2 *N Isotopic Difference Between Pheophytin Epimers*

A 0.5 per mil depletion in PTNa was observed relative to PTNa' in surficial Black Sea sediments. This difference in  $\delta^{15}\text{N}$  may be significant in light of the fact that the precision of sedimentary chlorin  $\delta^{15}\text{N}$  determinations is thought to be 0.12 per mil (see section 2.4.3.3). In another instance where the  $\delta^{15}\text{N}$  of the two epimers was measured, PTNa was depleted by 2.0 per mil

relative to the epimer. That sample was a suspended particulate sample from the deep chlorophyll maximum in the E. Mediterranean Sea (see chapter 5). In the Black Sea sediment, the epimer accounted for 23% of the combined PTNa+a', whereas in the Mediterranean Sea particulate sample it accounted for 28% of total PTNa+a'. However, a strict mass balance is not possible since the amount of each compound transformed to other chlorins or to colorless products is not known.

Chlorin epimers can readily arise non-enzymatically (Hynninen, 1979) during pigment handling and natural decomposition processes (Mantoura and Llewellyn, 1983). Furthermore, the C-10 stereoisomerization of PTNa and PBDa, to form 10(S)-pheophytin *a'* and 10(S)-pheophorbide *a'*, is thought to result in significant additional steric strain on the chlorin macrocycle due to the cis arrangement of the C-7 propionic ester group and the carbomethoxy group at C-10 (Hynninen and Sievers, 1981). The relief of that strain through conformational changes in the chlorin macrocycle could conceivably result in nitrogen isotopic fractionation.

#### 2.5.2.3 C Isotopic Differences Between Sedimentary Chlorins

As shown in table 2.8, the unknown chlorin "Chl686" (discussed below in section 2.5.3) is depleted in  $^{13}\text{C}$  by 1.85 per mil relative to PTNa and PPTNa. In addition, it has about the same  $\delta^{15}\text{N}$  as PPTNa. It is therefore suggested that this compound is a derivative of PPTNa (see above discussion, section 2.5.2.1) that lacks the phytyl ester side-chain.

The phytyl ester of chlorophyll is a lipid, and as such is expected to be depleted in  $^{13}\text{C}$  relative to protein (DeNiro and Epstein, 1977; Galimov and



Shirinsky, 1975). In fact, it has been demonstrated that phytol is depleted in  $^{13}\text{C}$  by 1.6 to 5.1 per mil (Bogacheva, et al., 1979). If Chl686 is a "dephytylated" chlorin then it would be expected to be enriched in  $^{13}\text{C}$  relative to intact pheophytins and chlorophylls.

### 2.5.3 *Novel Sedimentary Pigments*

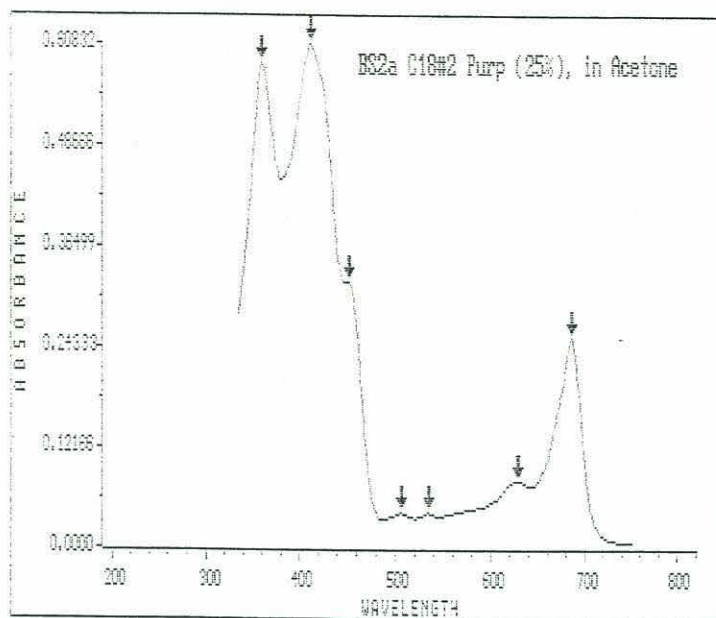
#### 2.5.3.1 *Chl686*

A chlorin-like compound was observed in sediments from Unit I (surface) and Unit II (~3-5 kyr) of the Black Sea, surficial sediments from the Peru margin, and in sapropel S7 (~190 kyr) from the Eastern Mediterranean. This compound, referred to above as Chl686, was characterized by visible absorption maxima (and relative extinction coefficients) in  $\text{MeCl}_2$  at 362 (0.95), 418 (1.0), 508 (0.08), 536 (0.08), 630 (0.15), 686 (0.44) (figure 2.8.a). In acetone the spectrum was similar but the Soret band was at 412, rather than 418 nm. The compound was alluded to in an early report addressing pigments in a Black Sea surface sediment (Peake, et al., 1974), and was attributed to "aberrant types of chlorophyll." Upon reinspection of chromatograms of Black Sea surface sediments from the thesis of L. King, it was also observed. Chl686 is of interest here because it appeared to be the most abundant chlorin in certain samples (i.e., Unit I and II in the Black Sea).

Aside from the unusual visible spectrum, Chl686 has the following characteristics: (1) it is relatively non-polar, eluting just before PTNa on  $\text{C}_{18}$  HPLC (figure 2.9); (2) it is smaller than other chlorins, eluting after MPBDa on size-exclusion chromatography (figure 2.5.c), and having mass peaks at 413 (100%), 429 (76%), 465 (21%), and 517 (20%) on  $\text{CH}_4$  chemical ionization mass



(a)



(b)

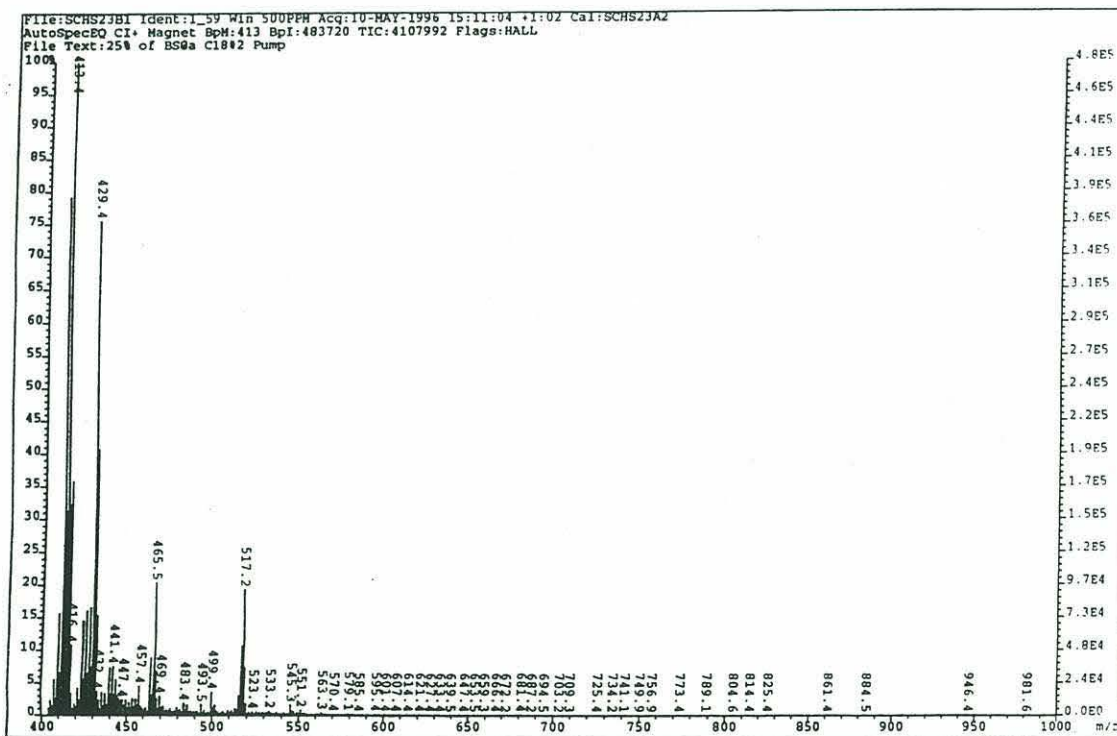


Figure 2.8: Visible (a) and mass (b) spectra of Chl686. Absorbance maxima in acetone are: 360, 412, 506, 534, 628, and 686 nm.

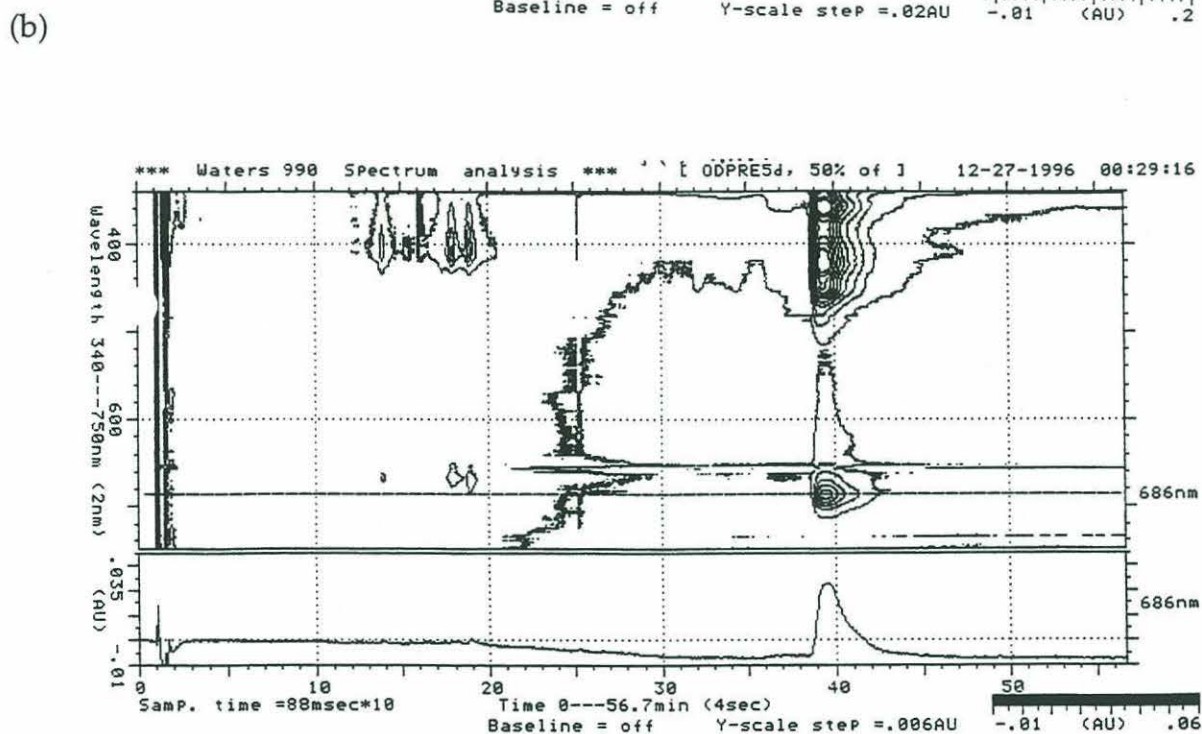
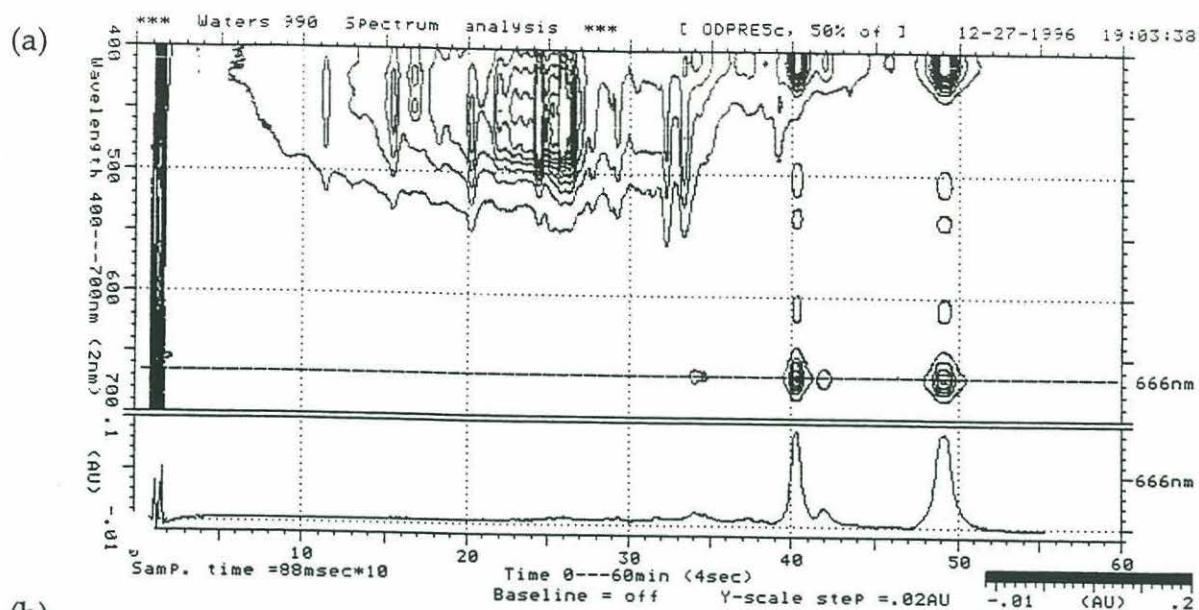


Figure 2.9: Analytical C<sub>18</sub> HPLC chromatograms of (a) the pheophytin fraction and (b) the Chl686 fraction collected from a size-exclusion column. The SEC chromatogram is shown in figure 2.5. An identical gradient was used to generate both chromatograms. Retention times and peak identities are as follows: Chl 686 (39.55 mins), PTNa (40.30 mins), PTNa' (42.00 mins), PPTNa (49.10 mins).

spectra (figure 2.8.b); (3) it appears, from  $^1\text{H}$  NMR (Keely, 1989), not to contain protons at C-7 and C-8 on ring IV, or at C-10 on the isocyclic ring, but to contain the C-2 vinyl group, the C-4 ethyl group and the C-1 methyl group. The NMR data might suggest that Chl686 is a porphyrin (Krane, et al., 1983), with an oxidized ring IV. However porphyrins are normally characterized by S/R ratios in excess of 5 (Baker and Louda, 1986), and Chl686 has an S/R ratio of 2.2.

It is possible that Chl686 is an artefact introduced during sample preparation. However, the compound is observed in samples prepared using a variety of techniques. For instance, Chl686 can be identified in splits of a surficial (0-30 cm, bulk) Peru margin sediment sample (135 m water depth, MW87-08, core BC-5, 7/21/87), one oven-dried, then extracted with 25% (w/v)  $\text{H}_2\text{SO}_4/\text{MeOH}$ ; the other extracted wet, in acetone and  $\text{MeCl}_2$ , by ultrasonic probe. In addition, the compound is observed in surficial Black Sea sediments ultrasonically extracted wet in acetone, then  $\text{MeCl}_2$  (this work and King (1993)), and in those soxhlet-extracted in acetone (Peake, et al., 1974). Furthermore, Chl686 is observed in three intervals from a Black Sea sapropel (e.g., Unit II), and in an Eastern Mediterranean sapropel (S7), each of which was soxhlet extracted in  $\text{MeOH}$ , then  $\text{MeCl}_2$ . Finally, a chlorin with a virtually identical visible absorption spectrum, called "Phorbide-686.5," was reported in sediments from a sub-bottom depth of 31-35 m in the Gulf of California (Baker and Louda, 1982; Louda and Baker, 1986).

One potential explanation for the origin of this compound is that it is a dimer or structural isomer of pheophytin *a*, pheophorbide *a* or their "pyro" derivatives. Upon sitting at  $-20^\circ\text{C}$  for 20 days in  $\text{MeCl}_2$  ( $1.9\ \mu\text{M}$  solution, assuming  $\epsilon_{410} = 10^5$ ), the visible spectrum of the compound reverted to a typical pheophorbide *a*/pheophytin *a* spectrum (figure 2.10). The transformation product was characterized by a loss of the absorption maximum at 362 nm, and a blue-



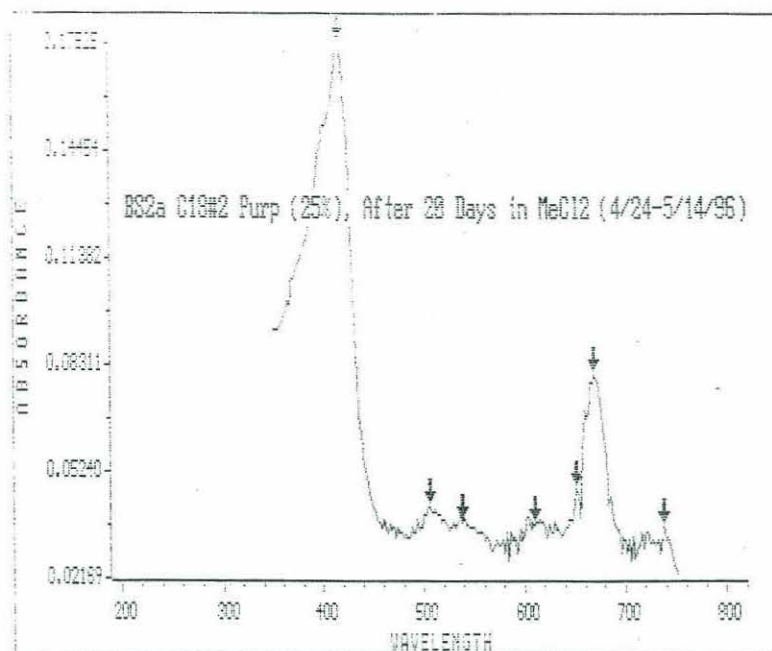


**Figure 2.10: Visible spectrum of Chl686 after standing in methylene chloride at -20°C for 20 days. Absorbance maxima are at 416, 506, 538, 610, and 670 nm.**

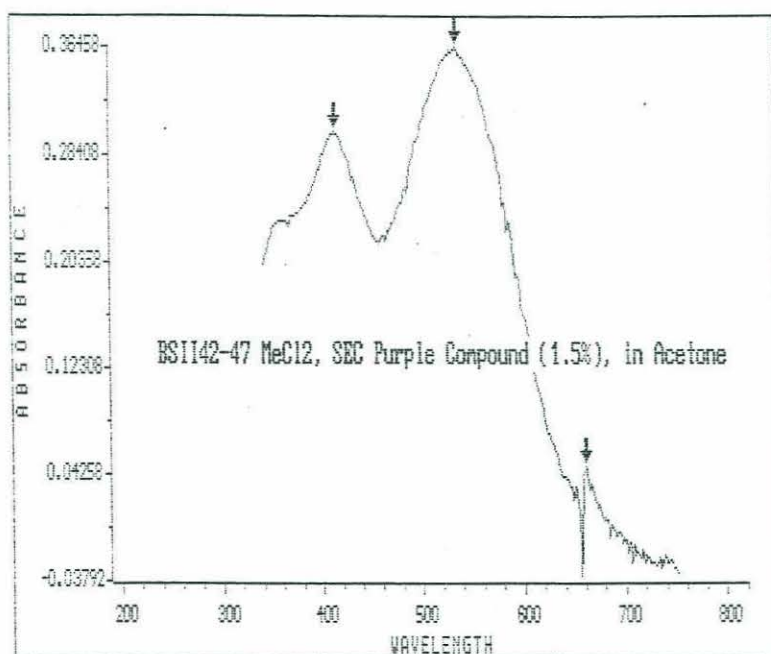


**Figure 2.11: Visible spectrum of purple compound in acetone. Absorbance maxima are at 414 and 536 nm.**

shift of the red band from 686 to 670 nm. However, the Soret band at 418 nm and the minor absorption maxima at 506 and 538 nm remained unchanged (given the 2 nm resolution of the spectrophotometer). Even the absolute absorbances of the Soret and red bands remained essentially unchanged, retaining the same S/R ratio of 2.2. It is noteworthy that this conversion did not occur in acetone under similar experimental conditions, and could not be repeated with a 5.7  $\mu\text{M}$  (assumes  $\epsilon_{410} = 10^5$ )  $\text{MeCl}_2$  solution of Chl686 from a Black Sea Unit II sediment (see chapter 5) left at 4°C for 60 days.

The C/N ratio of Chl686 was 12.4, intermediate between PPTNa (13.25) and MPPBDa (8.5). However, significant lipid contamination was evident in the  $^1\text{H}$  NMR spectrum, which would tend to increase the C/N. Therefore, it is likely that the actual C/N of Chl686 is closer to 8.5. As mentioned above, the  $^{13}\text{C}$ -enrichment of Chl686 relative to pheophytins in the same sample also suggests it is a pheophorbide (e.g., it lacks the phytyl side-chain). Additional support for this interpretation comes from the high retention volume (7.29 mL) of the compound on size exclusion chromatography relative to PTNa (6.19 mL).

Baker and Louda (1982) and Louda and Baker (1986) tentatively identified the chlorin they called Phorbide-686.5 as a 2-acetyl-2-desvinyl derivative of pyropheophytin *a*. They suggested, based on the 35.5 nm hypsochromic shift of the red band in the sodium borohydride-reduced product of Phorbide-686.5 ( $\lambda_{\text{max}}=396, 651.5 \text{ nm}$ ), that the compound contained two conjugated carbonyl moieties, one each on rings I and V. In addition, they attributed the split, or "bifurcated," Soret band to the oxidation of the 2-vinyl group to a 2-acetyl-2-desvinyl or a 2-formyl-2-desvinyl group, although no structural studies other than visible spectrophotometry were performed. Our  $^1\text{H}$  NMR results, however, suggest that the 2-vinyl moiety was intact in Chl686.

In the final analysis, the identity of Chl686 remains unknown. It is difficult to reconcile the small size of the molecule, deduced from size-exclusion chromatography, with the observations from visible spectrophotometry, HPLC and  $^1\text{H}$  NMR studies that Chl686 is likely a derivative of PPBDa. It is recommended that attempts be made to recrystallize the compound and acquire clean  $^1\text{H}$  NMR and mass spectra.

#### 2.5.3.2 *The Purple Compound*

Another unidentified compound encountered in this study, during work on Black Sea sediments, was an intense purple-colored pigment. As with Chl686, such a compound was alluded to in the study by Peake, et al (1974). The "purple compound" has been the subject of ongoing research in the laboratory of Dr. Repeta for many years, being found in sediments from the Black Sea, the Peru Margin and Salt Pond, to name a few. In this work, the purple compound was encountered in high abundance in Unit II sediments from the Black Sea (see chapter 5). The visible spectrum (figure 2.11) of the purple compound is characterized by a broad absorption maximum at 536 nm (this work; Peake, et al., 1974). It is unknown whether the absorption maxima at 414 and 660 nm are real or whether they resulted from contamination by PTNa or MPPBDa.

The purple compound was extracted, along with pheophytins and pheophorbides, from a 42-47 cm section of core BC17, from R/V Knorr cruise 134-08 (see chapter 5) by soxhlet in  $\text{MeCl}_2$ . It was carried through the purification of MPPBDa up through the size-exclusion chromatography step, coeluting with MPPBDa on preparative  $\text{C}_{18}$  HPLC. During size-exclusion chromatography though, the purple compound eluted 0.6 mins (or 0.6 mL) prior



to MPPBDa. This difference in retention volume is identical to that for MPPBDa and PTNa.

The identity of the purple compound remains a mystery. Given its abundance in this sediment sample, though (89% of the MPPBDa by weight), it appears to be an abundant pigment (or pigment transformation product) in certain environments.

#### *2.5.4 Sedimentary Chlorin Yields from Dried and Acidified Sediments*

An experiment was performed to determine the effects on sedimentary chlorin recovery of (1) drying a sample before extraction, and (2) acidifying the extraction solvent. It has been previously shown that up to 50% more chlorin can be extracted from Black Sea sediments with acidic methanol than by solvents (i.e., acetone and  $\text{MeCl}_2$ ) alone (King and Repeta, 1994a). These acid-extractable chlorins were thought to be incorporated into macromolecular material, and possibly hydrolyzed by the acidic  $\text{MeOH}$ .

Regardless of the mechanism, this work was aimed at developing methods for the routine stable isotopic measurements of sedimentary chlorins. This required that sample sizes be minimized. Maximizing chlorin yields from a sediment was therefore a priority. In addition, sediments for geochemical analysis are frequently dried before use. Hence, it sought to determine whether such sediments would be suitable for chlorin isotopic studies.

Toward these ends, a surficial (0-30 cm, bulk) sediment sample from the Peru Margin (135 m water depth, R/V Moana Wave cruise # 87-08, Stn. 8, core BC-5, 7/21/87) was homogenized and split into 6 sections of about 12.5 g (wet wt) each. Two of the sections were freeze-dried for 71 hours, two were oven-

dried at 60°C for 96 hours, and two were extracted wet. One of each pair was extracted with 25% (w/v) H<sub>2</sub>SO<sub>4</sub>/MeOH (2x). The other was first ultrasonically extracted with acetone (3x) and MeCl<sub>2</sub> (1x), then re-extracted with 25% (w/v) H<sub>2</sub>SO<sub>4</sub>/MeOH.

The acidic methanol extractions were performed while sparging with N<sub>2</sub>. The sediments were suspended in 45 mL MeOH for 30 minutes before the acid (3 mL) was added, dropwise, by syringe. The reaction was stirred for one hour at room temperature. A phase separation was then performed by adding 400 mL H<sub>2</sub>O and 80 mL MeCl<sub>2</sub> to the combined filtered extracts, and the chlorins were partitioned into the organic phase. The chlorin fraction was dried over Na<sub>2</sub>SO<sub>4</sub> and rotary-evaporated to dryness.

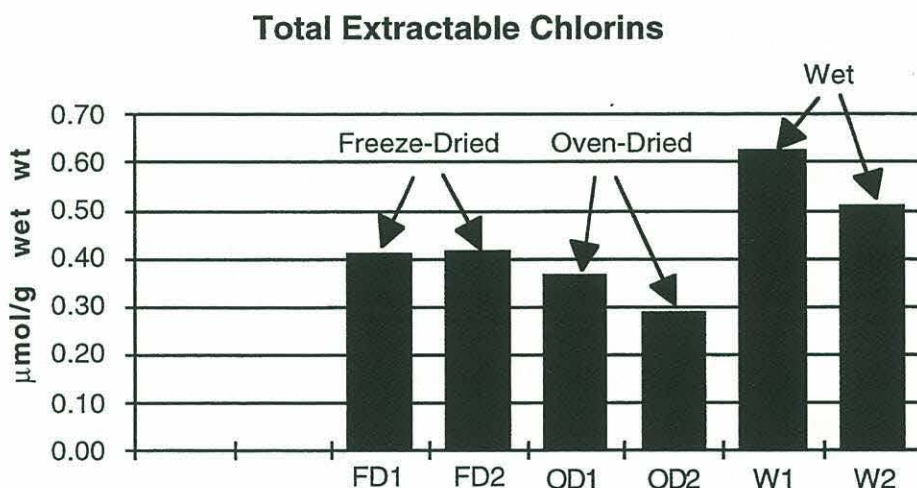
The results of the experiment are shown graphically in figure 2.12. The total amount of chlorin (e.g., acid extraction or solvent plus acid extraction) extracted from each of the 6 splits of sediment, normalized to the starting weight of sediment, is shown in figure 2.12.a. The wet sediment yields larger quantities of chlorin than the freeze- or oven-dried sediments, by 26% and 42%, respectively. In addition, wet and oven-dried sediments that were first extracted with solvents, then acid, yielded 18% and 22% more chlorin, respectively, than those directly acid-extracted. Both freeze-dried sediments yielded about the same amount of chlorin.

Figure 2.12.b, is a bar graph showing the quantities of chlorin (normalized to the starting weight of sediment) extracted by solvents (black) versus those extracted by acid (white) for the 3 samples thus consecutively treated. For the wet sediment, an additional 34% of chlorin was released by the acid, following solvent extraction. In the freeze- and oven-dried sediments, an additional 96% and 153% of chlorin, respectively, was extracted by the acid treatment.

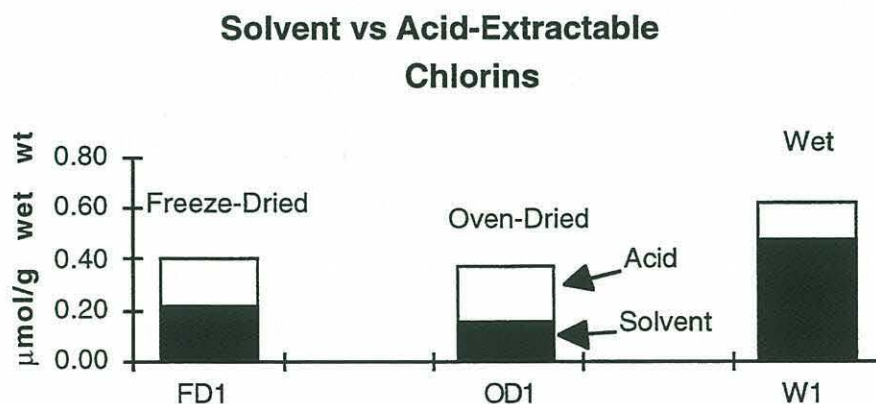
The chlorin distribution is markedly altered by acid extraction. Whereas PPPTNa, PTNa, and PPBDa are the most abundant chlorins in the solvent extracts of both wet and dry sediments, MPPBDa is the dominant chlorin in all acid extracts.

**Figure 2.12: Results of an experiment to determine the effects of sediment drying and acidification on the recovery of chlorins. All 6 samples were ~12.5 g (wet wt.) splits of a homogenized Peru margin surficial sediment.**

(a)



(b)





These results indicate that (1) it is best to leave sediments wet for the analysis of chlorins, (2) an additional 34% of total chlorin can be recovered by subjecting a solvent-extracted sediment to acidic methanol, and (3) the direct acidic-methanol extraction of a wet sediment yields 18% less total chlorin than the two-step procedure, but is less time-consuming and results in a less complex chlorin distribution.

It should be noted, though, that any paleoenvironmental information that can be derived from sedimentary chlorin distributions (King and Repeta, 1994b) is likely to be lost during acid-extraction, since most common chlorins are converted to MPBDa and MPPBDa. In addition, these conclusions are based on results from one surficial sediment. Additional experiments are required on older sediments and those from other environments before these results can be generalized.

## **2.6 Conclusion**

Nitrogen and carbon isotopic ratios in most common chlorins can be determined in marine particulate and sediment samples with a precision better than 0.15 per mil for both isotopes. The entire procedure can be accomplished in about 4 hours for particulate samples and 8 hours for sediment samples. The chlorins thus produced from particulate samples had nitrogen purities of 96% and carbon purities of 91%. Sedimentary chlorins were recovered with N and C purities of 89% and 88%, respectively. The chlorin recovery from particulate samples was 88%, while that for sediment samples was 18%. The low recovery from sediments, relative to particles, is attributed to the complex distribution of chlorins in sediments and to the additional purification steps required.

Using these techniques, different chlorins in a surficial Black Sea sediment had different isotopic ratios. The  $\delta^{15}\text{N}$  variation is attributed to coincident changes in the seasonal flux of material and certain chlorins out of the euphotic zone. The  $\delta^{13}\text{C}$  differences are likely a result of the presence or absence of the phytyl side-chain in different chlorins.

Finally, the presence of two unidentified pigments (both alluded to by Peake, et al., 1974) was discussed. The first, Chl686, was found in sediments from the Peru margin, Unit I and II in the Black Sea, and sapropel S7 from the Eastern Mediterranean. It appeared to be the most abundant chlorin in the Black Sea sediments analyzed in this work. The compound had an unusual visible spectrum, with a red band at 686 nm and a bifurcated Soret band at 360 and 418 nm. Proton NMR and HPLC studies, in addition to N and C isotopic ratios and elemental analyses, suggest that Chl686 is similar to PPBDa. However, size-exclusion chromatography and mass spectrometry suggest the compound is too small to be a PPBDa derivative.

The other unknown pigment is an intense purple compound found in Unit II Black Sea sediments. The pigment has an absorption maximum at 536 nm. It has a polarity similar to MPPBDa, coeluting with that chlorin on reverse-phase ( $\text{C}_{18}$ ) HPLC, but is similar in size to PTNa, coeluting with that compound on size-exclusion chromatography. The "purple compound" has been under investigation for many years in Dr. Repeta's laboratory, having been observed in sediments from the Black Sea, the Peru margin and Salt Pond. The search for its identity continues.



## References for Chapter 2

Altabet, M.A. and W.G. Deuser (1985) Seasonal Variations in Natural Abundance of  $^{15}\text{N}$  in Particles Sinking to the Deep Sargasso Sea. *Nature*, **315**: 218-219.

Altabet, M.A., W.G. Deuser, S. Honjo and C. Stienen (1991) Seasonal and Depth-Related Changes in the Source of Sinking Particles in the North Atlantic. *Nature*, **354**: 136-139.

Baker, E.W. and J.W. Louda (1982) Geochemistry of Tetrapyrrole, Tetraterpenoid, and Perylene Pigments in Sediments from the Gulf of California: Deep Sea Drilling Project Leg 64, Sites 474, 477, 479, and 481, and Scripps Institution of Oceanography Guaymas Basin Survey Cruise Leg 3, Sites 10G and 18G. In: *Initial Reports of the Deep Sea Drilling Project*, (J. R. Curaray and D. G. Moore, ed.), U.S. Government Printing Office, Washington, DC, pp. 789-814.

Baker, E.W. and J.W. Louda (1986) Porphyrins in the Geological Record. In: *Biological Markers in the Sedimentary Record*, (R. B. Johns, ed.), Elsevier, Amsterdam, pp. 125-225.

Bidigare, R.R., M.C. Kennicutt II, W.L. Keeney-Kennicutt and S.A. Macko (1991) Isolation and Purification of Chlorophylls a and b for the Determination of Stable Carbon and Nitrogen Isotope Compositions. *Analytical Chemistry*, **63**: 130-133.

Bogacheva, M.P., L.A. Kodina and E.M. Galimov (1979) Intramolecular Carbon Isotope Distributions in Chlorophyll and Its Geochemical Derivatives. In: *Advances in Organic Geochemistry 1979*, (A. G. Douglas and J. R. Maxwell, ed.), Pergamon Press, Oxford, pp. 679-687.

Cowie, G.L. and J.I. Hedges (1991) Organic Carbon and Nitrogen Geochemistry of Black Sea Surface Sediments from Stations Spanning the Oxidic-Anoxic Boundary. In: *Black Sea Oceanography*, (Izdar and J. W. Murray, ed.), Kluwer Academic Publishers, The Netherlands, pp. 343-359.



Craig, H. (1953) The Geochemistry of the Stable Carbon Isotopes. *Geochimica et Cosmochimica Acta*, 3: 53-92.

DeNiro, M.J. and S. Epstein (1977) Mechanism of Carbon Isotope Fractionation Associated With Lipid Synthesis. *Science*, 197: 261-263.

Falk, J.E. (1964) *Porphyrins and Metalloporphyrins*. Elsevier Publishing Company, Amsterdam, 266 pp.

Fish, R.H. and J.J. Komlenic (1984) Molecular Characterization and Profile Identifications of Vanadyl Compounds in Heavy Crude Petroleums by Liquid Chromatography/Graphite Furnace Atomic Absorption Spectrometry. *Analytical Chemistry*, 56: 510-517.

Fry, B., W. Brand, F.J. Mersch, K. Tholke and R. Garritt (1992) Automated Analysis System for Coupled  $\delta^{13}\text{C}$  and  $\delta^{15}\text{N}$  Measurements. *Analytical Chemistry*, 64: 288-291.

Fuhrhop, J.-H. and K.M. Smith (1975) *Laboratory Methods in Porphyrin and Metalloporphyrin Research*. Elsevier Scientific Publishing Company, Amsterdam, 243 pp.

Galimov, E.M. and V.G. Shirinsky (1975) Ordered Distributions of Carbon Isotopes in Compounds and Components of the Lipid Fraction in Organisms. *Geokhimiya*, 4: 503-528.

Gribble, G.W., W.J. Kelly and S.E. Emery (1978) Reactions of Sodium Borohydride in Acidic Media; VII. Reduction of Diaryl Ketones in Trifluoroacetic Acid. *Synthesis*, **October**: 763-765.

Gribble, G.W., R.M. Leese and B.E. Evans (1977) Reactions of Sodium Borohydride in Acidic Media; IV. Reduction of Diarylmethanols and Triarylmethanols in Trifluoroacetic Acid. *Synthesis*, **March**: 172-176.

- Hay, B.J., S. Honjo, S. Kempe, V.A. Ittekkot, E.T. Degens, T. Konuk and E. Izdar (1990) Interannual Variability in Particle Flux in the Southwestern Black Sea. *Deep-Sea Research*, **37**(6): 911-928.
- Hoering, T. (1955) Variations of Nitrogen-15 Abundance in Naturally Occurring Substances. *Science*, **122**: 1233-1234.
- Hynninen, P.H. (1979) Application of Elution Analysis to the Study of Chlorophyll Transformations by Column Chromatography on Sucrose. *Journal of Chromatography*, **175**: 75-88.
- Hynninen, P.H. and G. Sievers (1981) Conformations of Chlorophylls a and a' and their Magnesium-Free Derivatives as Revealed by Circular Dichroism and Proton Magnetic Resonance. *Zeitschrift fuer Naturforschung*, **36b**: 1000-1009.
- Iriyama, K., N. Ogura and A. Takamiya (1974) A Simple Method for Extraction and Partial Purification of Chlorophyll from Plant Material, Using Dioxane. *Journal of Biochemistry*, **76**(4): 901-904.
- Jeandon, C., R. Ocampo and H.J. Callot (1993) Improved Preparation of Deoxophylloerythroetioporphyrin (DPEP) and its 15'-Methyl Derivative from Chlorophyll a. *Tetrahedron Letters*, **34**(11): 1791-1794.
- Jenkins, D., V.L. Snoeyink, J.F. Ferguson and J.O. Leckie (1980) *Water Chemistry: Laboratory Manual, 3rd Edition*. John Wiley & Sons, New York, 183 pp.
- Keely, B.J. (1989) Early Diagenesis of Chlorophyll and Chlorin Pigments. PhD, University of Bristol.
- King, L.L. (1993) Chlorophyll Diagenesis in the Water Column and Sediments of the Black Sea. PhD, Massachusetts Institute of Technology/Woods Hole Oceanographic Institution.
- King, L.L. and D.J. Repeta (1991) Novel Pyropheophorbide Steryl Esters in Black Sea Sediments. *Geochimica et Cosmochimica Acta*, **55**: 2067-2074.



King, L.L. and D.J. Repeta (1994a) High Molecular weight and acid extractable chlorophyll degradation products in the Black Sea: new sinks for chlorophyll. *Organic Geochemistry*, **21**(12): 1243-1255.

King, L.L. and D.J. Repeta (1994b) Phorbin Steryl Esters in Black Sea Sediment Traps and Sediments: A Preliminary Evaluation of Their Paleoceanographic Potential. *Geochimica et Cosmochimica Acta*, **58**(20): 4389-4399.

Krane, J., T. Skjetne, N. Telnaes, M. Bjoroy and H. Solli (1983) Nuclear Magnetic Resonance Spectroscopy of Petroporphyrins. *Tetrahedron*, **39**(24): 4109-4119.

Louda, J.W. and E.W. Baker (1986) The Biogeochemistry of Chlorophyll. In: *Organic Marine Geochemistry*, (H. L. Sohn, ed.), American Chemical Society, Washington D.C., pp. 107-126.

Macko, S.A. (1981) Stable Nitrogen Isotope Ratios as Tracers of Organic Geochemical Processes. Ph.D., The University of Texas at Austin.

Mantoura, R.F.C. and C.A. Llewellyn (1983) The Rapid Determination of Algal Chlorophyll and Carotenoid Pigments and Their Breakdown Products in Natural Waters by Reverse-Phase High-Performance Liquid Chromatography. *Analytica Chimica Acta*, **151**: 297-314.

Otsuki, A., M.M. Watanabe and K. Sugahara (1987) Chlorophyll Pigments in Methanol Extracts from Ten Axenic Cultured Diatoms and Three Green Algae as Determined by Reverse Phase HPLC With Fluorometric Detection. *Journal of Phycology*, **23**: 406-414.

Peake, E., D.J. Casagrande and G.W. Hodgson (1974) Fatty Acids, Chlorins, Hydrocarbons, Sterols, and Carotenoids from a Black Sea Core. In: *The Black Sea--Geology, Chemistry and biology*, (E. T. Degens and D. A. Ross, ed.), The American Association of Petroleum Geologists, Tulsa, Oklahoma, pp. 505-523.

Repeta, D.J. and R.B. Gagosian (1984) Transformation Reactions and Recycling of Carotenoids and Chlorins in the Peru Upwelling Region (15°S, 75°W). *Geochimica et Cosmochimica Acta*, **48**: 1265-1277.



Repeta, D.J. and R.B. Gagosian (1987) Carotenoid Diagenesis in Recent Marine Sediments--I. The Peru Continental Shelf (15°S, 75°W). *Geochimica et Cosmochimica Acta*, **51**: 1001-1009.

Ross, D.A. and E.T. Degens (1974) Recent Sediments of Black Sea. In: *The Black Sea--Geology, Chemistry, and Biology*, (E. T. Degens and D. A. Ross, ed.), The American Association of Petroleum Geologists, Tulsa, Oklahoma, pp. 183-199.

Schafer, P. and V. Ittekkot (1993) Seasonal Variability of  $\delta^{15}\text{N}$  in Settling Particles in the Arabian Sea and Its Palaeogeochemical Significance. *Naturwissenschaften*, **80**: 511-513.

Scheer, H. (1991) *Chlorophylls*. CRC Press, Boca Raton, 1257 pp.

Smith, N.W. and K.M. Smith (1990) Preparation of Bacteriopetroporphyrins by Partial Synthesis from the *Chlorobium* Chlorophylls. *Energy & Fuels*, **4**: 675-688.

Svec, W.A. (1978) The Isolation, Preparation, Characterization, and Estimation of the Chlorophylls and the Bacteriochlorophylls. In: *The Porphyrins: Physical Chemistry, Part C*, (D. Dolphin, ed.), Academic Press, New York, pp. 341-399.

Watanabe, T., A. Hongu, K. Honda, M. Nakazato, M. Konno and S. Saitoh (1984) Preparation of Chlorophylls and Pheophytins by Isocratic Liquid Chromatography. *Analytical Chemistry*, **56**: 251-256.

Wright, S.W., S.W. Jeffrey, R.F.C. Mantoura, C.A. Llewellyn, T. Bjornland, D. Repeta and N. Welschmeyer (1991) Improved HPLC Method for the Analysis of Chlorophylls and Carotenoids from Marine Phytoplankton. *Marine Ecology Progress series*, **77**: 183-196.

Zapata, M., A.M. Ayala, J.M. Franco and J.L. Garrido (1987) Separation of Chlorophylls and Their Degradation Products in Marine Phytoplankton by Reversed-Phase High-Performance Liquid Chromatography. *Chromatographia*, **23**(1): 26-30.

## Chapter 3: Analytical Methodology II. Synthesis of Chlorophyll Derivatives for Gas Chromatography

### 3.1 Abstract

The analysis of chlorin N and C isotopic ratios by isotope-ratio monitoring gas chromatography-mass spectrometry (irmGC-MS) has been accomplished by synthesizing chlorin bis-(*tert* -butyldimethylsiloxy)Si(IV) derivatives. These volatile chlorin silicon complexes are characterized by elution temperatures of 260°C. Because early attempts at direct gas chromatography of chlorins were unsuccessful, the derivatization was pursued. However, yields for the four-step procedure were low (5-6%), and there was a net N isotopic depletion of 1.2 per mil ( $\pm 0.3$ ) in the derivative, relative to the starting chlorin. Upon further investigation of the feasibility of direct GC of chlorins it was found that methyl pyropheophorbide *a*, a common sedimentary chlorin, was in fact chromatographable. With specialized aluminum-clad fused silica capillary columns thinly coated with chemically-bonded apolar stationary phases, and He carrier gas flow rates of 3.5 mL/min, the model chlorin eluted from the GC at 385°C. Reducing the ketone at C-9 resulted in improved chromatographic peak shape and an elution temperature of 380°C. The ketone reduction is a rapid, high (e.g., 97%) yielding reaction that results in no isotopic fractionation. It is suggested that future work focus on the direct high-temperature irmGC-MS analysis of chlorins.

### 3.2 Introduction

Recent technological developments in analytical chemistry have made it



possible to measure the C, N and O isotopic compositions of individual compounds as they elute from a gas chromatograph (Brand, et al., 1994; Hayes, et al., 1990). The sensitivity of new mass spectrometers combined with the high resolution of capillary GC columns now allows the stable isotopic analysis of nanomolar quantities of individual organic compounds in a complex mixture. The technique seemed well-suited to a study of sedimentary chlorophyll isotopic ratios because (1) sedimentary organic matter is a complex mixture, (2) the concentration of chlorins in sediments is low (typically in the ppm range), (3) the purification of chlorins from sediments for off-line isotopic analysis is time- and labor-intensive, and (4) off-line (dual-inlet irMS) analyses typically require  $>1\mu\text{mol}$  of both N and C.

However, no published accounts of chlorin gas chromatography exist in the literature, and our preliminary work suggested that chlorins thermally decompose before they volatilize and pass through a GC column. This chapter describes the development of a derivatization procedure for the synthesis of GC-amenable chlorins. The technique is then used to produce the first irmGC-MS values for chlorin  $\delta^{15}\text{N}$  and  $\delta^{13}\text{C}$ .

After a brief discussion in the Background section (3.3) about the synthetic precursors to volatile chlorin silicon complexes, a detailed description of their synthesis is presented in the Methods section (3.4). The results from the first-ever irmGC-MS analyses of derivatized chlorins are contained in the Results section (3.5), in addition to a study of isotopic fractionation during the derivatization. A discussion about the synthesis, its drawbacks and recommendations for future work, can be found in the Discussion section (3.6). That section finishes with the results of experiments using direct high-temperature gas chromatography, a promising direction in chlorin irmGC-MS.



### 3.3 Background

#### 3.3.1 *Precursors to Volatile Chlorin Derivatives*

A protocol for the analysis of chlorin  $\delta^{15}\text{N}$  and  $\delta^{13}\text{C}$  by irmGC-MS is desirable in order to take advantage of the high sensitivity of modern mass spectrometers, and the high resolution attainable with today's capillary GC columns. Whereas traditional off-line  $\delta^{15}\text{N}$  analyses require  $>1\ \mu\text{mole N}$  per analysis, irmGC-MS can be accomplished with 20 nmoles N (Brand, et al., 1994), or two orders of magnitude less sample. Furthermore, it was thought that the increased resolution of gas chromatography over HPLC would allow for fewer purification steps before isotopic analysis, decreasing labor and the potential for isotopic fractionation. These advantages seemed significant enough to warrant a concerted effort toward the development of chlorin derivatives that would be amenable to gas chromatography. Initial experiments suggested that free-base chlorins were not GC-amenable, decomposing before eluting from a GC at temperatures approaching  $440^\circ\text{C}$ . Therefore a derivatization protocol was developed to increase chlorin volatility.

#### 3.3.2 *Phthalocyanines*

In the early 1960's the groundwork for the synthesis of volatile cyclic tetrapyrrolic compounds was laid by Kenney and coworkers at Case Institute of Technology (Joyner, et al., 1960; Joyner and Kenney, 1962; Krueger and Kenney, 1963). Those workers synthesized a variety of silicon phthalocyanines (PcSi)

with groups oxygen-bridged to the silicon (figure 3.1.a). They found that Si could be tetravalently bound to the four nitrogen atoms in the center of the phthalocyanine macrocycle. The four planar Si-N bonds formed were found to be highly stable, and the strength of the SiO-R bonds in the characteristic hexagonal geometry of these derivatives is attested to by their inertness to hot

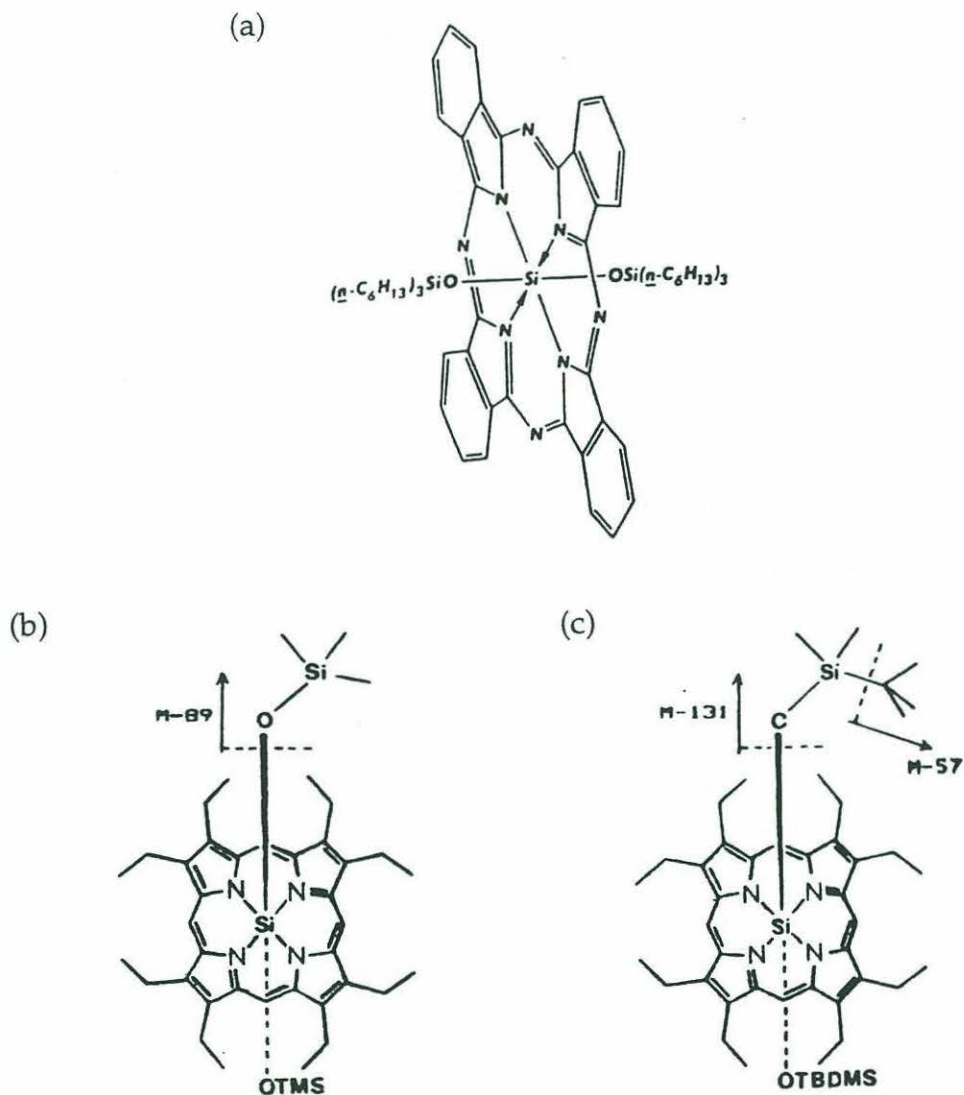


Figure 3.1: Structures of precursors to volatile chlorin silicon complexes. (a) A Silicon phthalocyanine, (b) a bis(trimethylsiloxy)Si(IV) derivative of octaethylporphyrin, and (c) a bis(*tert.*-butyldimethylsiloxy)Si(IV) derivative of octaethylporphyrin.

concentrated sulfuric acid (Krueger and Kenney, 1963). By altering the nature of the siloxy side chains it was possible to markedly change the polarity of the derivatives, with  $\text{PcSi}(\text{OH})_2$  being soluble in aqueous alcohol and  $\text{PcSi}(\text{OC}_{18}\text{H}_{37})$  being soluble in benzene. Concurrent with the observed changes in solubility were changes in volatility, with  $\text{PcSi}(\text{OC}_2\text{H}_5)$  remaining unmelted at temperatures  $>360^\circ\text{C}$  in vacuo, and  $\text{PcSi}(\text{OC}_{18}\text{H}_{37})$  melting at  $152^\circ\text{C}$  (Krueger and Kenney, 1963). This ability to enhance the volatility of  $\text{PcSi}$  derivatives by increasing the molecular flexibility and decreasing the molecular symmetry of the derivative led geochemists to exploit this chemistry later in the 1960's for the structural elucidation of geoporphyrins by GC-MS.

### 3.3.3 *Porphyrins*

By the mid 1960's it had been demonstrated that a number of homologous series of porphyrins existed in certain oils, shales and rocks (Baker, et al., 1967). The determination of the structure of these components was hampered by the inability to conduct gas chromatographic and mass spectrometric analyses due to the low volatility of porphyrins (Boylan and Calvin, 1967). It was therefore undertaken to synthesize GC-amenable porphyrin silicon derivatives (figure 3.1.b) in much the same manner as was done by Kenney, et al. with the phthalocyanines (Boylan, et al., 1969; Boylan and Calvin, 1967). This work was expanded upon in the 1980's by Eglinton and Maxwell's group at the University of Bristol to yield a vast array of petroporphyrin structural data by analyzing GC-MS data from petroporphyrin fractions derivatized to their volatile silicon complexes (Eckardt, et al., 1988; Gill, et al., 1986; Hein, et al., 1985; Marriott, et al., 1984).



Since the Bristol group was interested primarily in increasing porphyrin volatility they introduced the use of silylating reagents as a simple rapid way to add bulky side chains to the oxygen bridges of the porphyrin silicon complex (PSi). In brief, the hybrid procedure (Marriott, et al., 1984) consists of inserting Si into the macrocycle with hexachlorodisilane ( $\text{Si}_2\text{Cl}_6$ ) in toluene to form the dichloro-Si(IV)-porphyrin complex, followed by hydrolysis of the axial chlorines in aqueous KOH, and silylation of the axial hydroxy groups with N-methyl-N-(*tert*.-butyldimethylsilyl)trifluoroacetamide (MTBSTFA) in pyridine (figure 3.1.c). Yields for this synthesis were reported to be >90% (Hein, et al., 1985).

### 3.4 Methods

#### 3.4.1 General Laboratory Procedures

The general laboratory procedures for the synthesis, handling, quantification, and identification of chlorins are described in chapter 2. Therefore, only those techniques specific to chlorin derivatization for gas chromatography will be described here.

##### 3.4.1.1 Handling of Moisture-Sensitive Reagents

Many of the syntheses described in this chapter involve the use of moisture-sensitive reagents. The use of reagents such as hexachlorodisilane ( $\text{Si}_2\text{Cl}_6$ ) and N-methyl-N-(*tert*.-butyldimethylsilyl)trifluoroacetamide

(MTBSTFA), requires that all solvents and glassware be dry, and that all analytical techniques exclude air and water. Two excellent references for performing syntheses with moisture-sensitive reagents are the book Organic Syntheses Via Boranes (Brown, 1975) and the technical report from Aldrich entitled "Handling Air-Sensitive Reagents" (Lane and Kramer, 1977).

In brief, all syringes and glassware must be dried in an oven for at least 4 hours at 110°C, then allowed to cool in a dessicator or under a N<sub>2</sub> stream. Plastic caps, silicone and teflon septa, and rubber septa are to be dried for >24 hours at 60°C. Syringes must be gas-tight and transfers of the moisture-sensitive reagents, especially Si<sub>2</sub>Cl<sub>6</sub>, must be rapid, especially in humid weather, since reaction with water vapor is very fast. I found that Hamilton Gas-Tight syringes (1001RN Syringe, Hamilton Company, Reno, NV) with removable needles worked best. If the reaction of the reagent with water forms a salt that clogs the needle, the syringe can be used again by simply replacing the needle. It is also imperative to have close by a septum-capped vial or flask containing dry toluene under a N<sub>2</sub> atmosphere in which to immediately rinse the syringe after transferring the moisture-sensitive reagent. If not done instantly, the syringe will permanently clog.

Reaction vials in which moisture-sensitive reactions are performed are sealed with a screw-cap fitted with a teflon-lined silicone septum (National Scientific Company, Lawrenceville, GA), then the cap is teflon-taped, and a size 14/20 rubber septum (Aldrich, Milwaukee, WI) is inverted over it and teflon-taped to further protect against moisture.

When withdrawing a dry solvent from a flask or bottle fitted with a septum I found it helpful to insert a needle (#22 or smaller diameter) connected to a N<sub>2</sub> line for flushing the headspace while a syringe is inserted and solvent withdrawn. A plug of N<sub>2</sub> should be drawn into the syringe from the headspace

before removal from the septum. A venting needle should also be inserted to keep the pressure from blowing out the septum.

#### 3.4.1.2 *Solvent Drying and Purification*

The procedures for purifying and drying solvents and reagents for use in moisture-sensitive reactions can be found in the invaluable laboratory reference book, Purification of Laboratory Chemicals (Perrin, et al., 1980). The following procedures came from that source.

The procedure for drying pyridine is to reflux over KOH pellets (Fisher Scientific, Fair Lawn, NJ) for 24 hours, fractionally distill the pyridine, and store over  $\text{CaH}_2$  in the dark at  $4^\circ\text{C}$ .

Trifluoroacetic acid (TFA) is dried by refluxing over  $\text{KMnO}_4$  crystals (J.T. Baker, Phillipsburg, NJ) for at least 12 hours, followed by fractional distillation, and a second reflux for 3 hours over  $\text{P}_2\text{O}_5$  (Fluka AG, Buchs, Switzerland), followed by fractional distillation. The dried TFA is stored under  $\text{N}_2$  at room temperature in the dark.

Toluene is dried by refluxing over  $\text{CaH}_2$  (Aldrich, Milwaukee, WI) for 48 hours, fractionally distilling the dry toluene, and storing over  $\text{CaH}_2$ .

#### 3.4.1.3 *Instrumentation*

##### 3.4.1.3.1 *Gas Chromatography*

All gas chromatography was performed on a Hewlett-Packard 5890 Series II GC, fitted with an HP 7673 GC/SFC automatic injector. The column used was



an SGE HT-5 aluminum-clad 12 m column with a non-polar film thickness of 0.1  $\mu\text{m}$  and an internal diameter of 0.32 mm. On-column injection was used throughout, as was electronic pressure programming (EPP), to maintain constant He carrier gas flow rates throughout a temperature program. Data acquisition was facilitated using Chromperfect 2.0 software (Justice Innovations, Inc.).

#### 3.4.1.3.2 *Mass Spectrometry and Gas Chromatography-Mass Spectrometry*

All mass spectrometry was performed in Fye Laboratory (WHOI) on a VG AutoSpecQ connected to an Opus data system on a DEC Alpha workstation. The instrument can be operated in any of three ionization modes: electron impact (EI), chemical ionization (CI) or fast-atom bombardment (FAB). All three ionization modes were employed during this work.

The GC-MS work employed a Hewlett Packard 5890 Series II gas chromatograph at the front end of the VG AutoSpecQ. The GC was equipped with a Hewlett Packard 7673 autoinjector.

For static FAB<sup>+</sup>-MS, nitrobenzyl alcohol (NBA) was used as a matrix, source temperature was 250°C, source pressure was  $3.5 \times 10^{-4}$  mb, voltage was 8 kV, resolution was set at 2000, time at 5.74 s/dec, and delay at 1.00 secs.

For CI-MS runs, CH<sub>4</sub> was used as ionization gas, source temperature was 250°C, source pressure was  $3.5 \times 10^{-5}$  mb, current was 1 mA, electron energy was 35 eV, and the electron multiplier was set at 425.

For GC-CI-MS work, a 12 m SGE HT5 Aluminum Clad column (SGE Incorporated, Austin, Texas) was used. The column had a 0.1  $\mu\text{m}$  non-polar phase (similar in polarity to DB-5), an i.d. of 0.33 mm and an o.d. of 0.43 mm. A deactivated silica bridge was used (1 m x 0.15 mm i.d.) to span the distance

between the GC and the source of the mass spectrometer due to the metallic coating of the column. Automatic pressure programming with vacuum compensation was employed to maintain a constant linear flow rate of 26.5 cm/sec helium. Unless otherwise noted, the temperature program was 50-80°C at 35°/min, then 80-275°C at 20°/min, then 275-320°C at 6°/min, followed by a 30 minute isothermal period at the maximum temperature.

#### 3.4.1.3.3 Isotope-Ratio Monitoring Gas Chromatography-Mass Spectrometry

The experimental conditions for the irmGC-MS runs were as follows. The mass spectrometer was a Finnigan MAT 252, the GC was a Hewlett-Packard 5890 Series II, and the combustion interface was a Standard GC/C II interface (figure 3.2). The column was an SGE HT-5 aluminum-clad 12 m column with an apolar

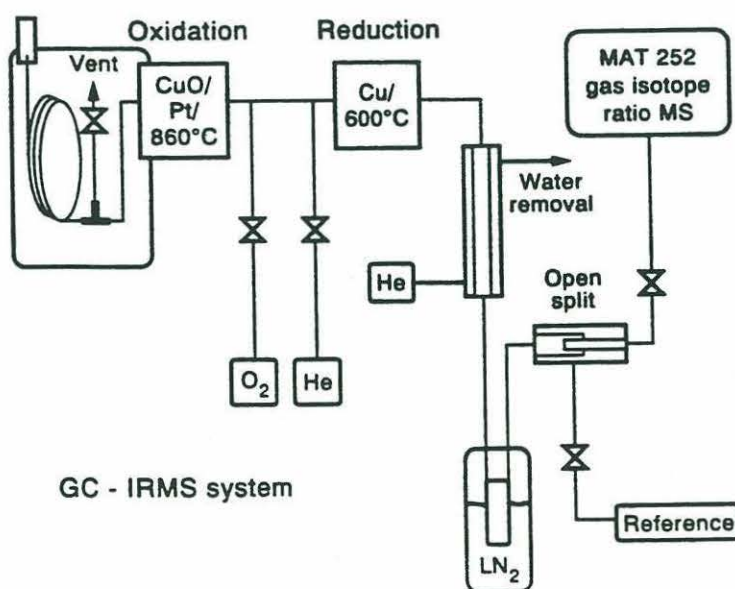


Figure 3.2: Schematic of the Finnigan irmGC-MS system for  $\delta^{15}\text{N}$ ,  $\delta^{13}\text{C}$ ,  $\delta^{18}\text{O}$ .

film thickness of 0.1  $\mu\text{m}$  and an internal diameter of 0.32 mm. The temperature program was 1 min at 40°C, then 35°/min to 80°C, then 20°/min to 275°C, then 6°/min to 315°C, followed by a 10 min isothermal period at 315°C. On-column injection and electronic pressure programming were used, such that the pressure was 10.4 p.s.i. at 40°C.

#### 3.4.1.3.4 *Nuclear Magnetic Resonance Spectroscopy (NMR)*

$^1\text{H}$  NMR spectra were obtained on a 300 MHz Bruker AC 300 spectrometer (Bruker Instruments, Inc., Manning Park, Billerica, MA) in conjunction with an Aspect 3000 data system (Spectrospin AG, Industriestrasse 26, CH-8117 Faellanden, Switzerland). The field strength of the superconducting magnet was 7.1 Tesla.

NMR tubes were thin-walled 5 mm x 9" tubes from Wilmad (cat. # 535-PP-9, Wilmad Glass Company, Buena, NJ). They were washed with MeOH (3x), acetone (3x) and  $\text{MeCl}_2$  (3x), before being dried first under a  $\text{N}_2$  stream, and then in an oven at 180°C for >1 hour. NMR pipets were useful for transferring samples to the tubes (cat. # 803A, Wilmad Glass Co.).

Solvents for NMR spectroscopy were  $\geq 99.5\%$  deuterated (Aldrich Chemical Company, Milwaukee, WI).

#### 3.4.1.3.5 *Spectrophotometry*

Visible spectra of the pigments were taken on either a Varian Techtron DMS-200 Spectrophotometer (Varian Techtron Limited, Springvale Road,



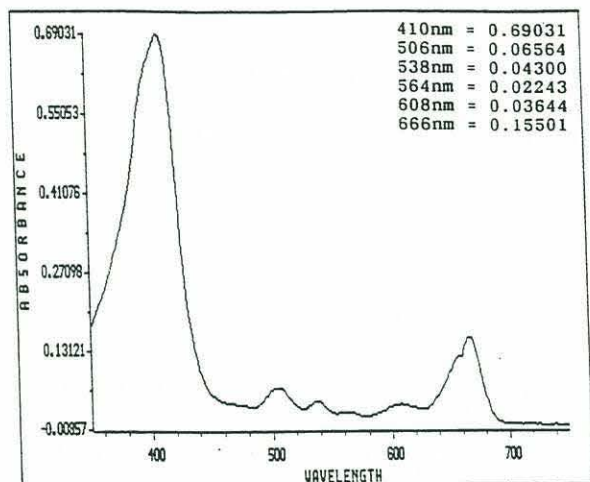
Mulgrave, Victoria 3170, Australia) or a Hewlett-Packard HP8452A Diode Array Spectrophotometer (Rockville, Maryland). The instruments were referenced against the appropriate solvent contained in a 1-cm quartz cuvette. The resolution of the HP8452A was 2 nm, while that of the Varian was 0.1 nm. A spike at 656 nm occasionally interfered with the red band absorbance determination while using the diode array spectrophotometer. This interference was minimized by acquiring the sample spectrum immediately after taking the reference spectrum. A discussion of spectrophotometric quantitation calculations and baseline correction can be found in section 2.3.4.

### 3.4.2 *Synthesis of Volatile Chlorin Si(IV) Complexes*

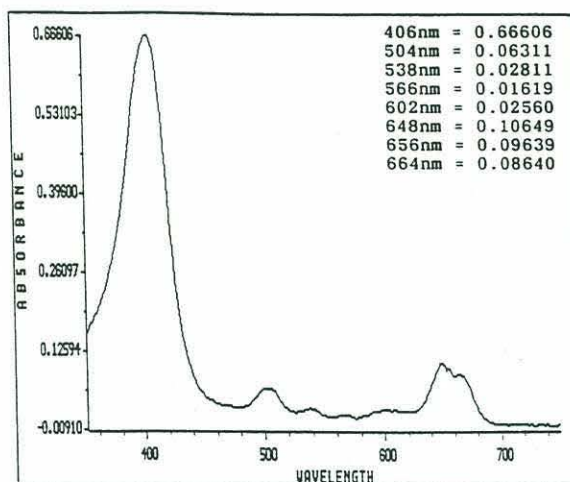
#### 3.4.2.1 *9-Deoxo-methyl-pyropheophorbide a*

The synthesis of 9-deoxo-methyl-pyropheophorbide *a* (9MPPBDa) from MPPDa is based on previously published ketone reduction procedures using sodium borohydride in trifluoroacetic acid (Gribble, et al., 1978; Gribble, et al., 1977; Jeandon, et al., 1993; Smith and Smith, 1990). Sodium borohydride ( $\text{NaBH}_4$ , 100 mg, Fisher Scientific, Fair Lawn, NJ) is slowly added to 10 mL dry trifluoroacetic acid (TFA,  $\text{CF}_3\text{COOH}$ , Sigma Chemical Co., St. Louis, MO) with stirring at 0°C under a rapid  $\text{N}_2$  stream (in order to prevent  $\text{H}_2$  buildup). The MPPBDa (212  $\mu\text{mol}$ , 116 mg), dissolved in 10 mL dry TFA, is then added to the  $\text{NaBH}_4$ /TFA mixture slowly via syringe. The ice bath is then removed and the reaction allowed to proceed at room temperature under a  $\text{N}_2$  atmosphere for 5 hours. The progress of the reaction is monitored occasionally by withdrawing

(a) 1 Hour



(b) 2 Hours



(c) 5 Hours

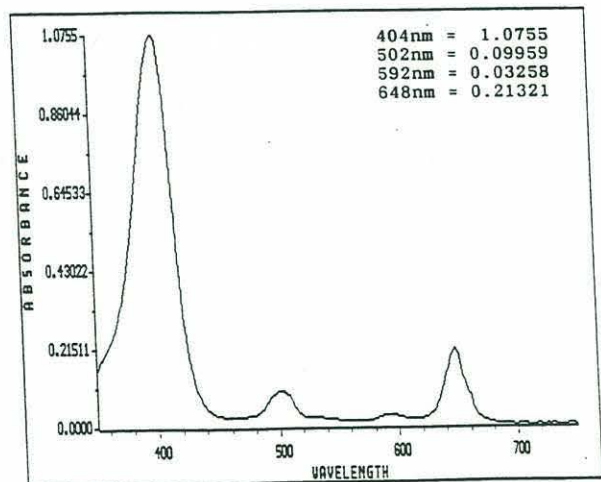


**Figure 3.3: Progress of ketone reduction reaction. MPPBDa is converted to 9-deoxo-methyl-pyropheophorbide *a* by reaction with sodium borohydride in trifluoroacetic acid. Visible absorption spectra after (a) 1 hour, (b) 2 hours, and (c) 5 hours.**

0.5  $\mu\text{L}$  of the reaction mixture by syringe and adding it to  $\text{MeCl}_2$  in a cuvet to which is added 1-2 drops of triethylamine (TEA,  $(\text{CH}_3\text{CH}_2)_3\text{N}$ , Aldrich, Milwaukee, WI) (Smith and Smith, 1990) to neutralize the solution. During the course of the reaction the Soret band migrates from 410 to 404 nm and the red band migrates from 666 to 648 nm. The extinction coefficient for the Soret band was reported by Smith and Smith (1990) to be 153,100 ( $\text{L}/\text{mol}\cdot\text{cm}$ ). The reaction is complete when there is no shoulder evident at 666 nm (figure 3.3).

The reaction mixture is then poured into a 500 mL separatory funnel containing 200 mL water. The 9MPPBD is partitioned (3x) into 20 mL  $\text{MeCl}_2$ , until the  $\text{MeCl}_2$  layer is colorless. The combined organic layers, which are a deep purple color, are then neutralized (1x) with 200 mL saturated  $\text{NaHCO}_3(\text{aq})$ , and the aqueous layer is back-extracted (2x) with 10 mL  $\text{MeCl}_2$ , until it is colorless. The combined organic extracts, which are a deep emerald green color, are then washed (2x) with 200 mL water, back-extracting the aqueous layer each time with (2x) 10 mL  $\text{MeCl}_2$ . The combined organic extracts are dried over  $\text{Na}_2\text{SO}_4$  and rotary-evaporated to dryness. The reaction product weighed 110 mg (206  $\mu\text{mol}$  9MPPBD) giving a yield for the ketone reduction of 97%.

#### 3.4.2.2 Chlorin Dichlorosilicon Complexes [ $\text{PhSiCl}_2$ ]

##### 3.4.2.2.1 Dichlorosilicon (IV) Methyl Pyropheophorbide a

The first synthesis of a chlorin dichlorosilicon complex was achieved by dissolving MPPBDa (24.1  $\mu\text{mol}$ , 13.2 mg) in dry toluene under a  $\text{N}_2$  atmosphere in a 4 mL screw-capped vial fitted with a teflon-lined silicone septum (National



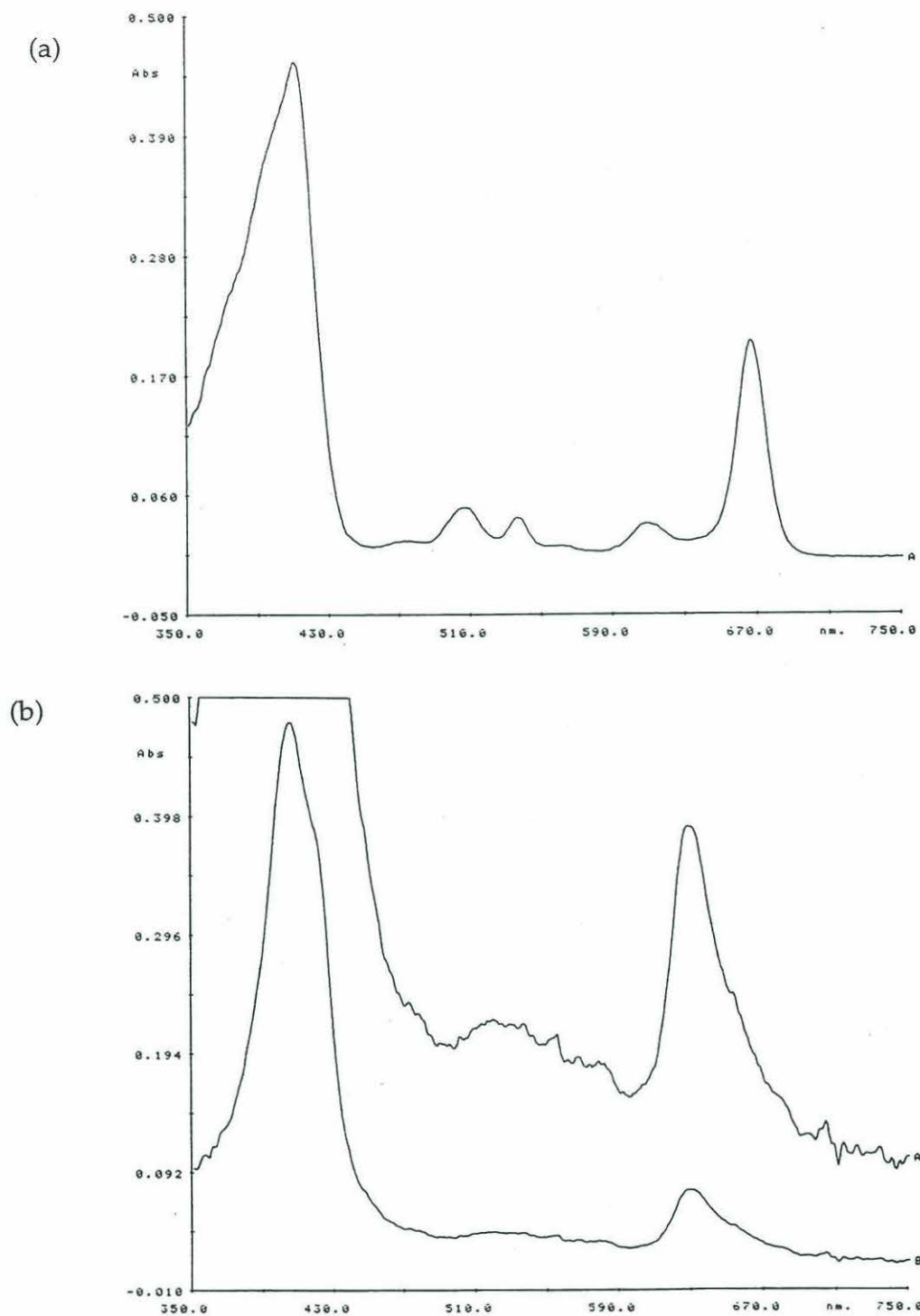


**Figure 3.4: Visible spectra of (a) MPPBDa in acetone, and (b) (MPPBDa)SiCl<sub>2</sub> in MeOH. In the dichlorosilicon complex the red band migrated from 666 to 628 nm, the three satellite bands of MPPBDa at 507, 536 and 610 nm disappeared, and the S/R ratio increased from 2.2 to 5.9.**

Scientific Company, Lawrenceville, GA) and adding 500  $\mu\text{L}$  hexachlorodisilane ( $\text{Si}_2\text{Cl}_6$ ; Aldrich, Milwaukee, WI) via syringe. The reaction was allowed to proceed for at least 2 hours at  $70^\circ\text{C}$ , after which time the vial was opened and dried under a  $\text{N}_2$  stream at  $70^\circ\text{C}$ . The residue was immediately redissolved in 1.0 mL MeOH. Our experience has been that allowing the dried product to stand (even under  $\text{N}_2$ ) for any length of time results in the formation of an insoluble green residue on the walls of the vial (see (9MPPBDa) $\text{SiCl}_2$  synthesis for further discussion of this).

The visible spectrum (figure 3.4) shows a migration of the red band from 666 to 628 nm, and a migration of the Soret band from 410 to 405 nm. The three primary satellite bands at 507, 536, and 610 nm in MPPBDa disappear and the S/R (e.g., Soret/red band) ratio increases from 2.2 to 5.9. The reaction appears to go to completion based on the loss of bands at 410 and 666 nm. The average spectrophotometric yield for this reaction, based on five separate syntheses, was  $44 \pm 14\%$  ( $1\sigma$ ,  $n = 5$ ). It should be noted, though, that the extinction coefficient for (MPPBDa) $\text{SiCl}_2$  is not known. A yield of 88% is possible if the extinction coefficient for both the starting material (MPPBDa) and the reaction product ((MPPBDa) $\text{SiCl}_2$ ) is the same.

The lower yield assumes an extinction coefficient twice that of the product, or 226,000  $\text{L/mol}\cdot\text{cm}$ . This estimation is based on the extinction coefficients for silicon complexes of etioporphyrin (Boylan and Calvin, 1967) and octaethylporphyrin (Fuhrhop and Smith, 1975) which are both about 2x greater than for the corresponding free-base porphyrins. Therefore, extinction coefficients equal to twice that of the free-base were used for all spectrophotometric quantitations involving chlorin silicon complexes.

#### 3.4.2.2.2 Dichlorosilicon (IV) 9-deoxy-methyl pyropheophorbide a

The dichlorosilicon complex of 9MPPBDa is prepared in a similar fashion to (MPPBDa)SiCl<sub>2</sub>, with some minor modifications. The Si<sub>2</sub>Cl<sub>6</sub> (120  $\mu$ L) in this synthesis was added to the dry toluene (1.0 mL) in a 50 mL pear-shaped flask fitted with a 14/20 rubber septum (Aldrich, Milwaukee, WI) before the chlorin (68  $\mu$ mol, 37 mg) was added (dissolved in 0.75 mL dry toluene). That way, in the event any water was present, the pigment would be preserved. (A violent reaction occurred when Si<sub>2</sub>Cl<sub>6</sub> contacted water; smoke and heat were evolved and the mixture turned to a frothy brown substance, destroying the pigment in the process.) The visible spectrum of the product (figure 3.5) has  $\lambda_{\text{max}}$  at 403

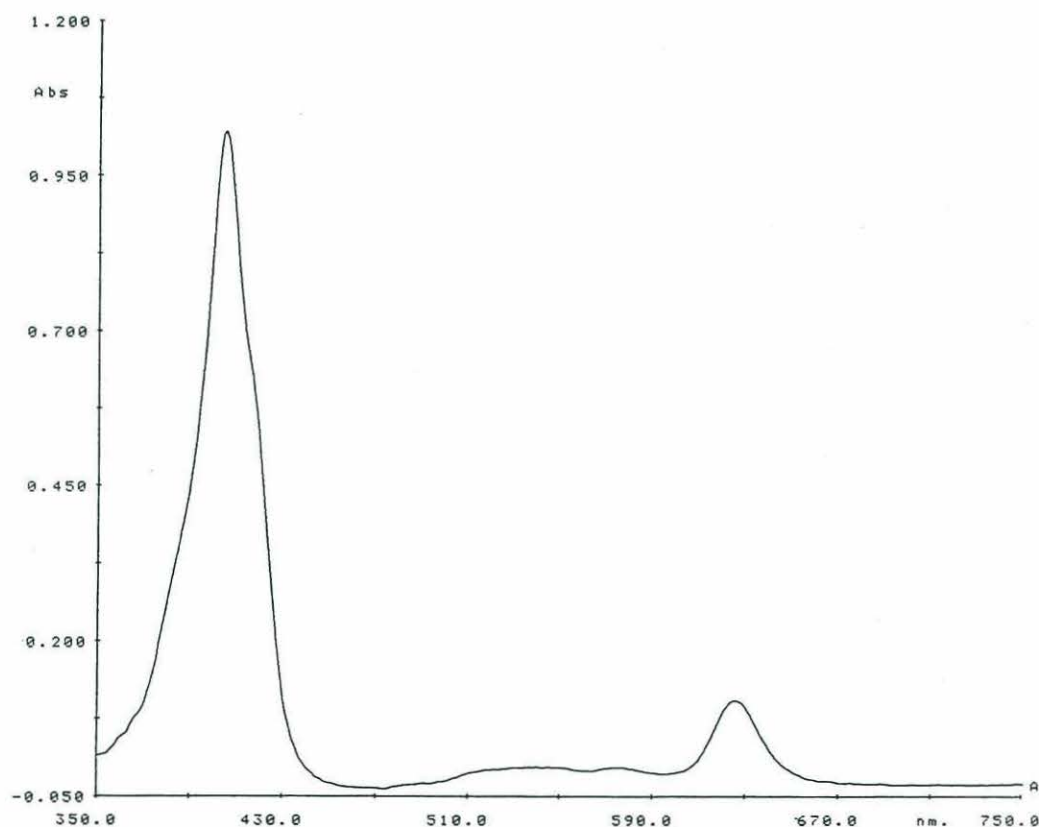


**Figure 3.5: Visible spectrum of (9MPPBDa)SiCl<sub>2</sub> in MeOH. The red band migrated to 624 nm in the dichlorosilicon complex from 648 nm in the free-base .**



and 624 nm. The Soret absorption remains at the same wavelength as in free-base 9MPPBDa, but the red band migrates down 24 nm, from 648 nm. The yield for this reaction was highly variable, ranging from 30 to 85%.

#### 3.4.2.3 Chlorin Dihydroxysilicon Complexes [ $\text{PhSi}(\text{OH})_2$ ]

##### 3.4.2.3.1 Dihydroxysilicon (IV) Methyl Pyropheophorbide a

To dichlorosilicon (IV) methyl pyropheophorbide *a* (9.5  $\mu\text{mol}$ , 6 mg) dissolved in 1 mL MeOH is added 30  $\mu\text{L}$  0.6 mM HCl in MeOH and 0.75  $\mu\text{L}$   $\text{H}_2\text{O}$ , thus bringing the acid content to 18 nmol ( or 17 $\mu\text{M}$ ) and the water content to 42  $\mu\text{mol}$  (or 0.07%) for the acid catalyzed hydrolysis of the 2 axial chlorines. The reaction was mixed with a vortex mixer (Deluxe Mixer S8220, American Scientific Products, McGraw Park, IL) and allowed to stand at 70°C for 1.5 hours, after which time 2 mL dry pyridine was added. The reaction mixture was then repeatedly (3x) blown down with a  $\text{N}_2$  stream, at 70°C, to a volume of ~1 mL, adding 2 mL dry pyridine after each concentration step. The yield for this reaction was roughly 58%. Uncertainty in the yield arises as a result of some free-base MPPBDa being evident in the visible spectrum. The free-base chlorin is only sparingly soluble in MeOH but is quite soluble in pyridine, while the inverse is true for the dihydroxysilicon chlorins.

The purpose of the repeated concentration was to remove water and MeOH without drying the  $\text{PSi}(\text{OH})_2$ . Water (b.p. = 100°C), aqueous HCl (20.24% HCl, b.p. = 110°C) and MeOH (b.p. = 65°C) are more volatile than pyridine (b.p. = 111°C), so it was thought that the MeOH, water, and acid might be removed

after repeated concentrations. If the hydrolysis was complete, then there would have been 1030  $\mu\text{L}$  MeOH, 24  $\mu\text{mol}$   $\text{H}_2\text{O}$ , and 18 nmol HCl remaining to evaporate. Even if small amounts of MeOH and water remained it was thought the silylation might proceed if a large excess of reagent was used. The silylating reagent is significantly less moisture-sensitive than the hexachlorodisilane used earlier. Experience showed that drying this product--hence removing all protic solvents--resulted in the formation of an insoluble residue and complete loss of the  $\text{PSi}(\text{OH})_2$  (see discussion in section 2.6.1).

#### 3.4.2.3.2 *Dihydroxysilicon (IV) 9-Deoxo-Methyl Pyropheophorbide a*

It is likely that the 17  $\mu\text{M}$  HCl in 99.3% MeOH (aq) used for the hydrolysis of MPPBDa (above) was insufficient for complete reaction. This conclusion is based on the significant quantity of unreacted product from the hydrolysis of  $(9\text{MPPBDa})\text{SiCl}_2$  when identical reaction conditions were used. Therefore the  $(9\text{MPPBDa})\text{SiCl}_2$  was dried under a  $\text{N}_2$  stream, at  $60^\circ\text{C}$ , with frequent washing of the vial walls with MeOH, and redissolved in 2 mL 0.1 N HCl in 95% MeOH (aq). After 10 minutes in an ultrasonic bath, some green residue remained on the vial walls and some particulate pigmented material was observed in the solution. The hydrolysis was allowed to proceed for 1 hour at  $60^\circ\text{C}$ .

Two simultaneous workups were attempted upon completion of the reaction in order to determine the optimal procedure. In one, the reaction mixture was added to 20 mL  $\text{H}_2\text{O}$  in a 60 mL separatory funnel and partitioned into 4 mL toluene. The blue organic layer was decanted and the aqueous layer was transferred to a 500 mL separatory funnel for repeated partitionings into  $\text{MeCl}_2$  (1x) and  $\text{CHCl}_3$  (1x). A final partition into chloroform was performed



after the addition of 100 mL saturated  $\text{NaHCO}_3$  (aq). The combined organic layers were dried over  $\text{Na}_2\text{SO}_4$  and rotary-evaporated to dryness. Alumina TLC in 30/70 acetone/hexane demonstrated the formation of the desired blue product, along with some free-base 9MPPBD and a significant quantity of green pigment at the origin. An alternative workup of the hydrolysis product was pursued in order to avoid the severe emulsions encountered during the phase extraction.

In the second workup the hydrolysis product was first neutralized by transferring to a 10 mL pear-shaped flask containing 30 mg  $\text{NaHCO}_3$ , and allowed to stand at  $4^\circ\text{C}$  for 60 hours, before being partitioned into 50 mL chloroform in a 2 L separatory funnel containing 1 L  $\text{H}_2\text{O}$ . The aqueous layer was re-extracted 2 more times with  $\text{CHCl}_3$ , and the combined blue organic layers were dried over  $\text{Na}_2\text{SO}_4$  and rotary-evaporated to dryness. Alumina TLC (30/70 acetone hexane) demonstrated the formation of the desired product, along with some free-base and some green material at the origin. In this workup, emulsions were negligible, probably owing to the neutralization of the acidic reaction mixture prior to the phase extraction.

The products of both workups were then purified on preparative alumina TLC plates eluted with 30/70 acetone/hexane. The blue band corresponding to the dihydroxysilicon 9MPPBDa ( $R_F = 0.43$ ) was scraped and eluted with  $\text{MeCl}_2$  (3x) and acetone (2x) by filtration through a 47 mm Whatman GF/F filter. The solution was then dried under a  $\text{N}_2$  stream at  $60^\circ\text{C}$ , and the reaction product quantified spectrophotometrically. The visible spectrum of  $(9\text{MPPBDa})\text{Si}(\text{OH})_2$  in  $\text{MeCl}_2$  (figure 3.6) contains 4 absorbance maxima at 405, 511, 572, and 617 nm. The Soret/red band ratio was 7.4. The yield for the hydrolysis ranged between 8.6 and 9.3%.



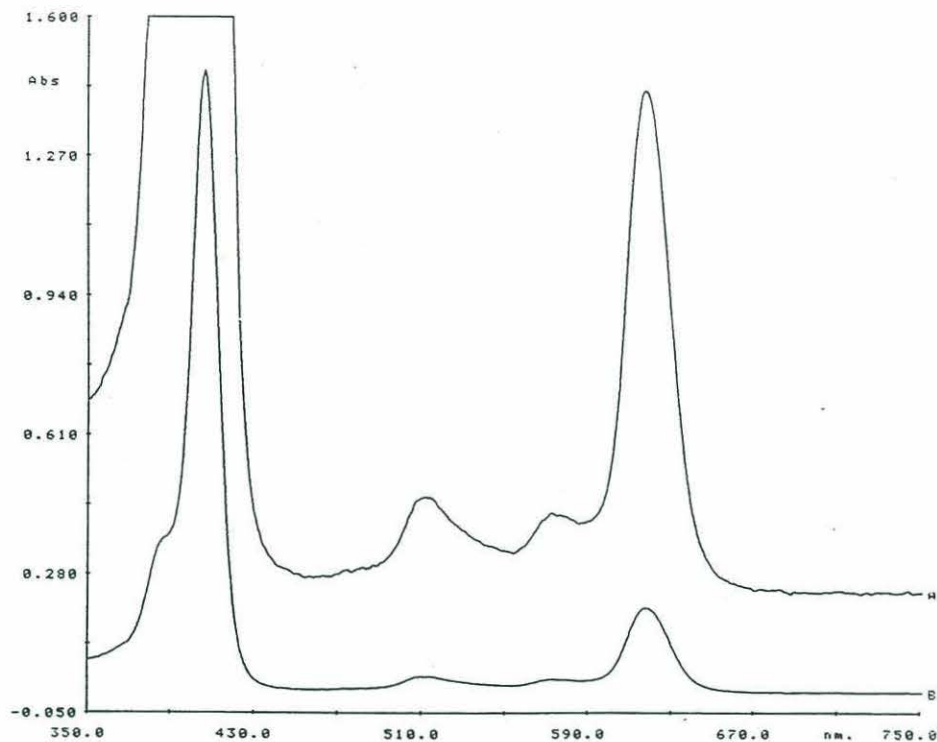


Figure 3.6: Visible spectrum of (9MPPBDa)Si(OH)<sub>2</sub> in MeCl<sub>2</sub>. Absorbance maxima are at 405, 511, 572, and 617 nm.

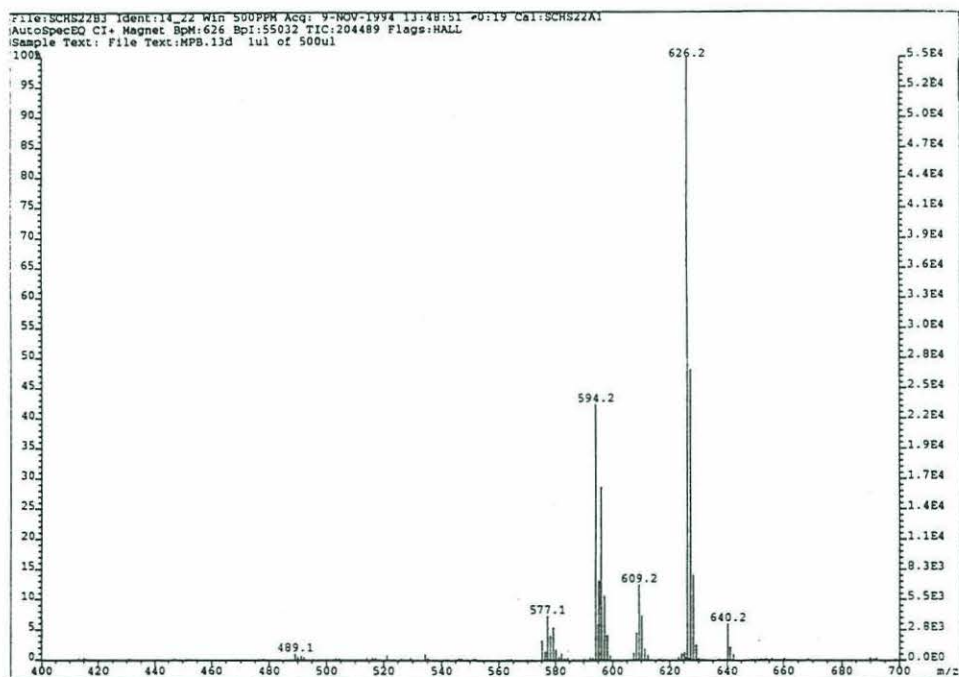


Figure 3.7: Methane chemical ionization mass spectrum of (9MPPBDa)Si(OH)<sub>2</sub> ( $M/Z = 594$  ( $M$ , 40%)). In addition, a product with  $M/Z = 626$  was formed ( $M+32$ , 100%), which corresponds to the addition of CH<sub>4</sub>O. A discussion of this product can be found in section 3.6.4.

The existence of the desired product was confirmed (1) by  $^1\text{H}$ -NMR in  $\text{CD}_2\text{Cl}_2$  in which the highly shielded axial hydroxyl protons appear far upfield: -2.2 ppm (d, 1 H) and -2.3 ppm (s, 1 H), and (2) by  $\text{CH}_4$   $\text{CI}^+$ -MS ( $M/Z = 594$  ( $M$ , 40%)) (figure 3.7). In addition to the desired product, a compound 32 mass units greater was formed ( $M/Z = 626$  ( $M+32$ , 100%)). This corresponds to the addition of methanol, or  $\text{CH}_4\text{O}$ . A discussion on the origin of this side-product can be found in section 3.6.4.

#### 3.4.2.4 Chlorin bis(*tert*.-butyldimethylsiloxy)Si(IV) complexes [ $\text{PhSi}(\text{OTBDMS})_2$ ]

##### 3.4.2.4.1 bis(*tert*.-butyldimethylsiloxy)Si(IV) methyl pyropheophorbide a

The  $(\text{MPPBDa})\text{Si}(\text{OH})_2$  (5.5  $\mu\text{mol}$ , 3.3 mg) dissolved in 2 mL dry pyridine was transferred to a dry 4 mL vial and sealed under a  $\text{N}_2$  atmosphere with a screw-cap fitted with a teflon-lined silicone septum. *N*-methyl-*N*-(*tert*.-butyldimethylsilyl)trifluoroacetamide (150  $\mu\text{L}$ ; MtBSTFA: Regis Chemical, cat # 270241; or Pierce Chemical Co., Rockford, IL, cat # 48925) was added to the reaction vial via syringe, and the reaction was vortex-mixed and allowed to stand at 70°C for 17 hours.

Upon completion of the reaction the mixture was dried at 70°C under a  $\text{N}_2$  stream and redissolved in 500  $\mu\text{L}$  Hexane. Analytical alumina TLC spotted with the free-base MPPBDa and eluted with 10/90 (v/v) acetone/hexane showed 5 fluorescent products ( $R_F = 0.21, 0.30, 0.39, 0.46, 0.59$ ) less polar than the free-base ( $R_F = 0.13$ ), as well as a spot corresponding to the free-base and some green pigment at the origin (presumably unsilylated  $\text{PhSi}(\text{OH})_2$  and/or unhydrolyzed

PhSiCl<sub>2</sub>). These less polar compounds were believed to be various silyl ether derivatives of disiloxysilicon MPPBDa. It should also be noted that a significant amount of green pigment remained undissolved on the walls of the vial, implying incomplete silylation of the dihydroxysilicon complex.

The reaction product was filtered through cotton into a clean vial dried under a N<sub>2</sub> stream and redissolved in 1 mL hexane. This product was then column chromatographed on neutral alumina and eluted with 20 mL 30/70 (v/v) acetone/hexane. A significant quantity of green pigment remained on the top of the column which, when eluted with MeOH, was shown by alumina TLC (20/80 acetone/hexane) to contain some free-base MPPBDa and predominantly PhSi(OH)<sub>2</sub> and/or PhSiCl<sub>2</sub>, as most of the color remained at the origin where both the dihydroxy- and the dichloro- silicon chlorin complexes have been shown to remain on alumina.

The fraction eluted from the column with 30/70 acetone/hexane was dried under N<sub>2</sub> at 70°C, then redissolved in 100 µL hexane, applied to a preparative alumina TLC plate, allowed to dry for 40 minutes, and eluted with 20/80 (v/v) acetone/hexane. The developed plate contained four bands with R<sub>F</sub> values of 0.56, 0.65, 0.70, and 0.79. The most intense band was the least polar with an R<sub>F</sub> = 0.79. Each of the 4 bands was scraped from the plate, eluted with acetone, filtered through a 47 mm Whatman GF/F filter, rotary-evaporated to dryness and stored in a dry vial for at -20°C under a N<sub>2</sub> atmosphere.

Static FAB<sup>+</sup> and GC-CI mass spectrometry confirmed the existence of at least 6 different bis(*tert*.-butyldimethylsiloxy)Si(IV) derivatives of methyl pyropheophorbide *a*. in the 3 least polar bands from the TLC plate. The desired product, (MPPBDa)Si(OTBDMS)<sub>2</sub> had a GC retention time (t<sub>R</sub>) of 18:36 and M/Z = 837 (M+1, 40%), 779 (M-57, 37%), 705 (M-131, 100%) (figure 3.8). This fragmentation pattern is typical of TBDMS derivatives (Gill, et al., 1986; Marriott,



et al., 1984). A discussion of the other reaction products can be found in section 3.6.4.

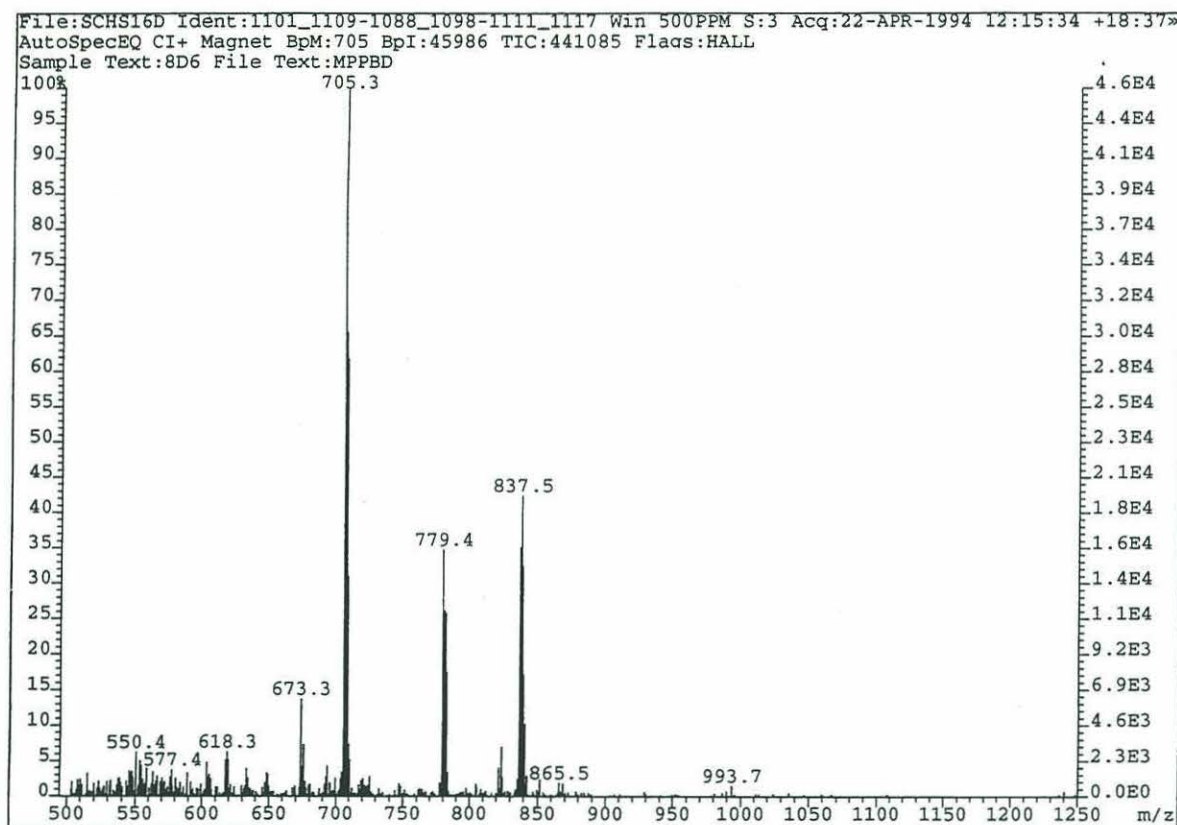


**Figure 3.8:** GC-MS mass spectrum of (MPPBDa)Si(OTBDMS)<sub>2</sub> (M/Z = 837 (M+1 40%), 779 (M-57, 37%), 705 (M-131, 100%). The retention time of the derivative was 18:36 minutes.

The GC column was a 12 m SGE HT5 aluminum clad column with a 0.1  $\mu$ m apolar phase, an inner diameter of 0.33 mm, and an outer diameter of 0.43 mm. On-column injection was used. The temperature program was: 50°-80°C at 35°/min, then 80°-275°C at 20°/min, then 275°-320°C at 6°/min, followed by a 20

min isothermal phase at 320°C. The carrier gas was He and auto pressure programming was used to maintain a constant flow rate of approximately 26.5 cm/sec. A 1 m piece of 0.15 mm ID deactivated silica tubing was used as a bridge from the Al-clad column to the source.

The 4th band from the TLC plate ( $R_F = 0.56$ ) contained primarily unreacted MPPBDa ( $M/Z = 548$  ( $M^+$ , 44%)), and possibly (MPPBDa)Si(OH)<sub>2</sub> ( $M/Z = 608$  ( $M^{++2}$ , 80%)). Since neither the free base or the PhSi(OH)<sub>2</sub> is GC-amenable, GC-CI-MS runs showed nothing for the polar TLC product.

#### 3.4.2.4.2 *bis(tert.-butyldimethylsiloxy)Si(IV) 9-deoxo-methyl pyropheophorbide a*

The dried (9MPPBDa)Si(OH)<sub>2</sub> (2.7 to 3.4  $\mu$ mol, 1.6 to 2.0 mg) was redissolved in dry pyridine in a 4 mL glass vial and fitted with a screw-cap containing a teflon-lined silicone septum. The headspace was filled with N<sub>2</sub>, and 100  $\mu$ L MtBSTFA (+1% *t*-butyl dimethylchlorosilane, Pierce Chemical Co., Rockford, IL) was added via syringe. The reaction was allowed to proceed at 60°C in the dark for 14 hours. The reaction mixture was then dried under a N<sub>2</sub> stream at 60°C. Complete redissolution occurred in 1 mL hexane.

The visible spectrum of the product in hexane had  $\lambda_{max}$  at 403, 508, 568, and 610 nm (figure 3.9). GC-CI mass spectrometry confirmed that (9MPPBDa)Si(OTBDMS)<sub>2</sub> had been synthesized (figure 3.10) ( $t_R = 16:26$ ;  $M/Z = 822$  (M, 100%), 807 (M-15, 25%), 765 (M-57, 25%), 735 (M-87, 15%), 691 (M-131, 65%)). The observed fragmentation pattern is typical of TBDMS derivatives (Gill, et al., 1986; Marriott, et al., 1984), and corresponds to loss of -CH<sub>3</sub>, -C(CH<sub>3</sub>)<sub>3</sub>, -TBDMS, -O(TBDMS), respectively. The GC conditions were the same as those listed above for (MPPBDa)Si(OTBDMS)<sub>2</sub>. The yield for the silylation

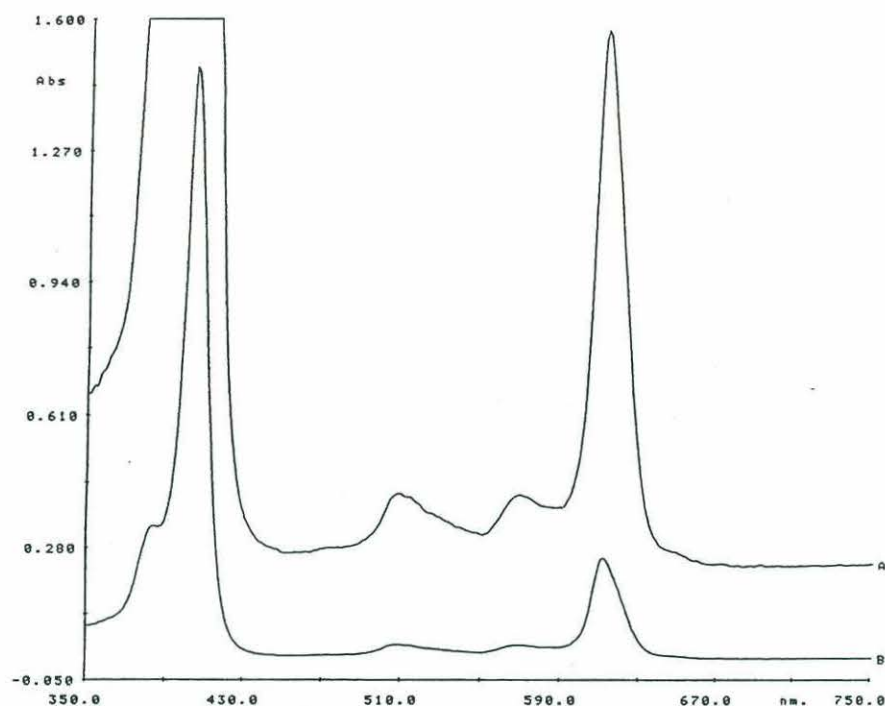


Figure 3.9: Visible spectrum of (9MPPBDa)Si(OTBDMS)<sub>2</sub> in hexane. Absorbance maxima are at 403, 508, 568, and 610 nm.

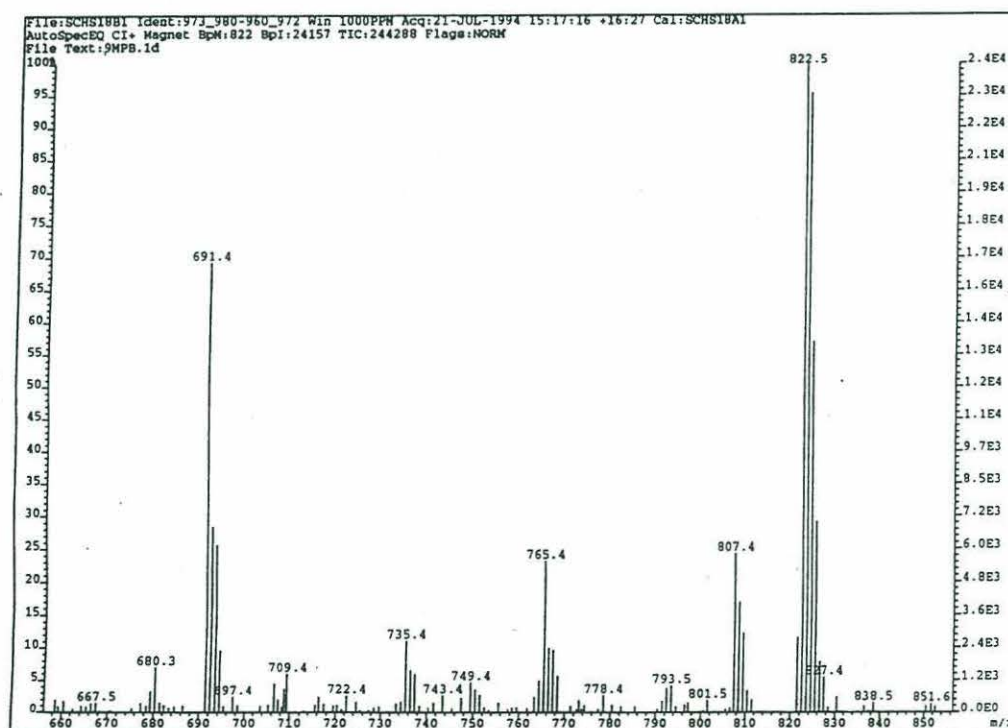


Figure 3.10: GC-MS mass spectrum of (9MPPBDa)Si(OTBDMS)<sub>2</sub> (M/Z=822 (M, 100%), 807 (M-15, 25%), 765 (M-57, 25%), 735 (M-87, 15%), 691 (M-131, 65%)). The GC retention time of the derivative was 16:26 minutes.



ranged between 71 to 86%. The overall yield for the synthesis of (9MPPBdA)Si(OTBDMS)<sub>2</sub> from methyl pyropheophorbide *a* ranged between 5.4 and 5.8%.

A minor product (10-15%) of the synthesis was sometimes observed on gas chromatograms 14 seconds before (9MPBDa)Si(TBDMS)<sub>2</sub> eluted. This product was confirmed by GC-MS to be 2 mass units greater than the primary product (figure 3.11). It is believed to be meso-9-deoxo(MPPBDa)Si(OTBDMS)<sub>2</sub>, the result of vinyl reduction at the C-2 position on the chlorin macrocycle.

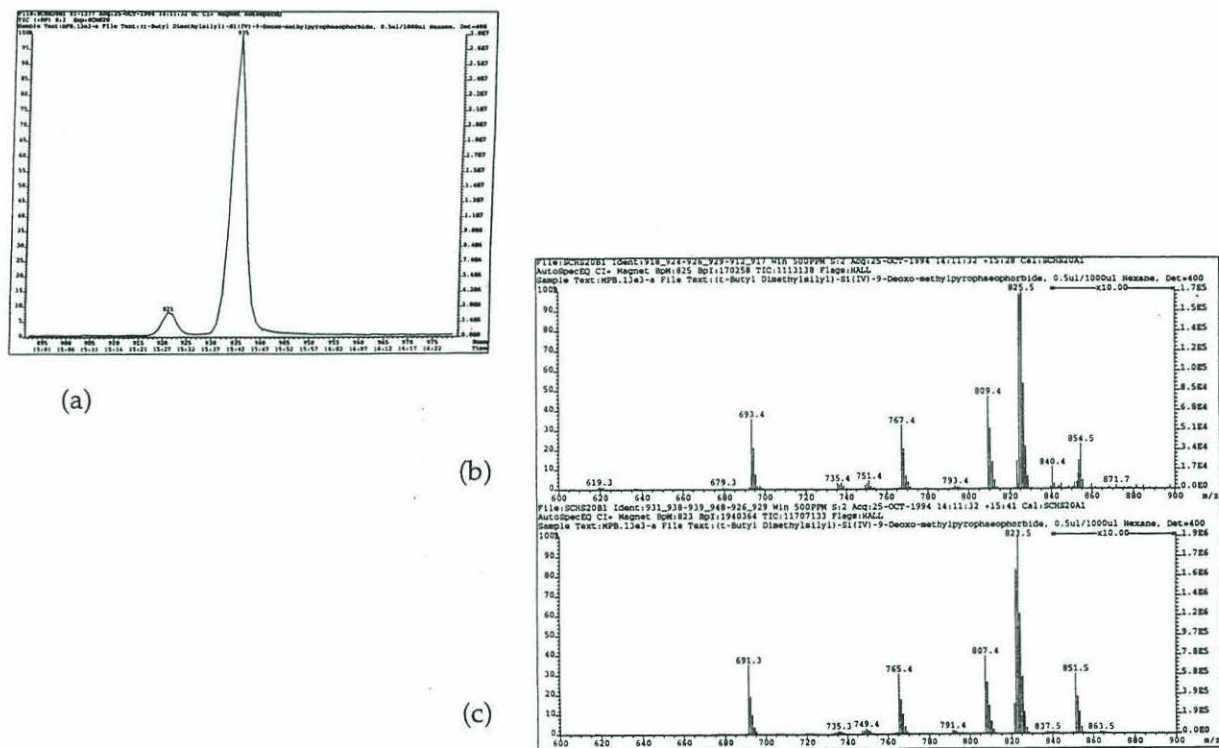
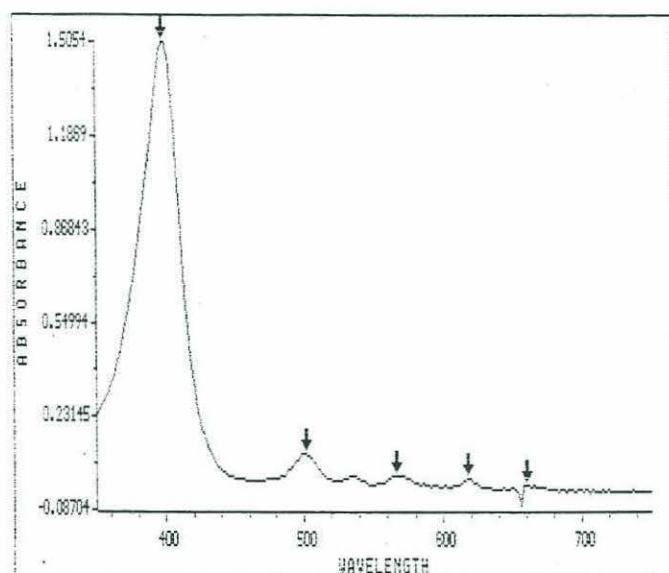


Figure 3.11: (a) GC-MS total ion chromatogram of (9MPPBdA)Si(OTBDMS)<sub>2</sub> showing the minor product, believed to be (meso-9-deoxo-methyl-pyropheophorbide *a*)Si(OTBDMS)<sub>2</sub>, eluting 14 seconds prior to the desired product. The mass spectra of the vinyl-reduced product is shown in (b), while that of the main product is shown in (c).

### 3.4.3 Aromatization and Nickel Insertion Reactions of Chlorins

#### 3.4.3.1 Aromatization of 9-Deoxo Methylpyropheophorbide a

The aromatization, or ring IV oxidation, of 9MPPBDa was achieved by the reaction of 9MPPBDa with 2,3-dichloro-5,6-dicyano-1,4-benzoquinone (DDQ) (Kenner, et al., 1973) in  $\text{MeCl}_2$  (Simpson and Smith, 1988; Smith and Smith, 1990). To 2.01  $\mu\text{mol}$  (1.07 mg) 9MPPBDa, dissolved in 2 mL  $\text{MeCl}_2$ , was added 0.5 mg (1.09 equivalents, or 2.2  $\mu\text{mol}$ ) DDQ dissolved in 0.5 mL benzene (dropwise, via syringe). The solution went from green to burgundy almost immediately with gentle swirling at room temperature. The mixture was rotary evaporated to dryness after 5 minutes. Complete redissolution occurred in 2.0 mL 1:1 acetone: $\text{MeCl}_2$ . The visible spectrum of the product showed complete loss of the



**Figure 3.12:** Visible spectrum in acetone of 9MPPBDa after ring IV oxidation with DDQ. Absorbance maxima are at 398, 502, 566, and 618 nm.

red band and was similar to that of alkyl porphyrins ( $\lambda_{\text{max}} = 398, 502, 566, 618$  nm) (figure 3.12). This suggested the reaction had gone to completion. The spectrophotometric yield for the reaction was 66%.

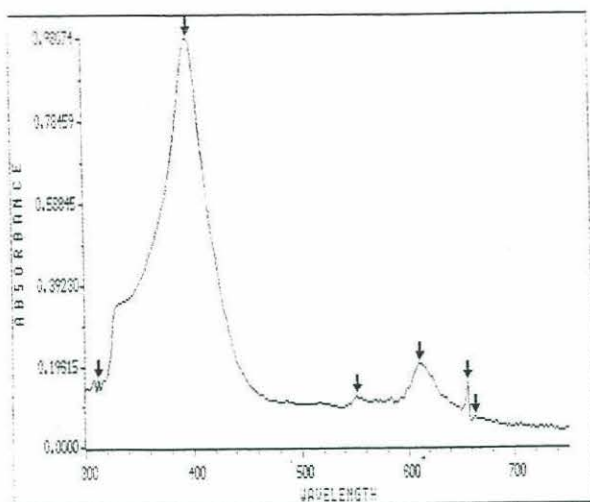
#### 3.4.3.2 Insertion of Nickel Into 9-Deoxo- Chlorins

The overnight reaction of 9MPPBDa and aromatized 9MPPBDa with Ni (II) acetylacetonate (Aldrich) in benzene (Verne-Mismer, 1988) resulted in quantitative conversion of the free-base chlorins to their Ni (II) derivatives. The chlorins (c. 1.0 mg) were dissolved in 10 mL benzene in 25 mL round-bottom flasks, and the vessels were flushed with N<sub>2</sub>. Then c. 5 mg Ni (II) acetylacetonate was added, and the reaction was allowed to reflux overnight. The products were either cleaned up on alumina Sep-Paks or partitioned into MeCl<sub>2</sub>. The visible spectra in acetone suggested quantitative conversion of the free-base chlorins to their Ni(II) derivatives, by the disappearance of the red bands and the appearance of absorption bands at 396, 552, 610 nm, or 394, 518, 552 nm, for 9MPPBDa and its aromatized derivative, respectively (figure 3.13). The aromatized structure also displayed a prominent absorption band at 328 nm. For comparison, the visible spectrum of Ni(II) deuteroporphyrin dimethyl ester (synthesized as above) had  $\lambda_{\text{max}} = 388, 546$  and 510 nm (figure 3.14).

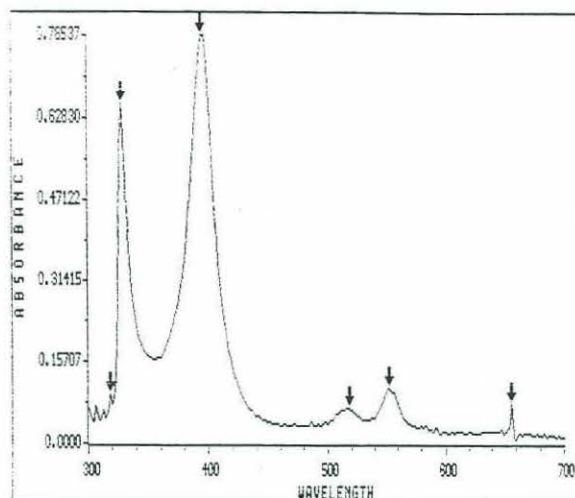
### 3.5 Results

This section begins with the results of the first-ever irmGC-MS analyses of derivatized chlorins. The latter part focuses on the results of a study of nitrogen





(a)



(b)

**Figure 3.13: Visible spectra of (a) Ni(II) 9-deoxo-methyl pyropheophorbide *a* in acetone ( $\lambda_{\text{max}}$ =396, 552 and 610 nm), and (b) the Ni(II) derivative of ring-IV oxidized 9MPPBDa in acetone ( $\lambda_{\text{max}}$ =394, 518 and 552 nm).**

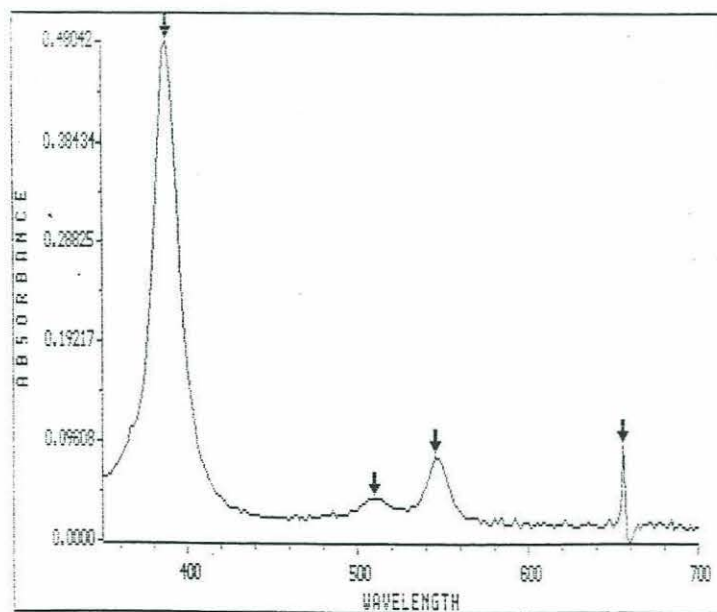


**Figure 3.14: Visible spectrum of Ni(II) deuteroporphyrin dimethyl ester in acetone ( $\lambda_{\text{max}}$ =388, 546 and 510 nm).**

isotopic fractionation during the derivatization of chlorins for gas chromatography and irmGC-MS.

### 3.5.1 *irmGC-MS Analysis of Derivatized Chlorins*

Aliquots of derivatized methyl pyropheophorbide *a* from two separate derivatizations were submitted to A. Hilkert at Finnigan MAT, in Bremen, Germany, for  $\delta^{15}\text{N}$  and  $\delta^{13}\text{C}$  determination via irmGC-MS. The same GC column and conditions were used as those listed above for the GC-MS work. The system was a MAT 252 GC system (Brand, et al., 1994) (figure 3.2). Each of the  $\delta^{15}\text{N}$  runs used between 2.3 and 2.5 nmol, or 1.9 to 2.1  $\mu\text{g}$ , of derivatized chlorin, corresponding to 9.3 to 10.0 nmol of nitrogen. The  $\delta^{13}\text{C}$  runs were performed with 1/10th that amount (e.g., 0.23 to 0.25 nmol, or 0.19 to 0.21  $\mu\text{g}$  chlorin; and 10.6 to 11.5 nmol C.) Two representative mass 28 ( $^{14}\text{N}_2$ ) and mass 44 ( $^{12}\text{C}^{16}\text{O}_2$ ) chromatograms are shown in figure 3.15. The isotope results are presented below in table 3.1. The duplicate derivatizations are termed MPPBDa#1 and MPPBDa#2 in the table.

The irmGC-MS results compared favorably with the  $\delta^{15}\text{N}$  values obtained on the same samples with traditional (off-line) dual-inlet irMS. Those values were 1.2 per mil and 1.8 per mil, respectively, for MPPBDa#1 and MPPBDa#2. This suggests that the determination of derivatized chlorin  $\delta^{15}\text{N}$  values by irmGC-MS has both an accuracy and a precision of  $\pm 0.3$  per mil.

Table 3.1: Chlorin  $\delta^{15}\text{N}$  and  $\delta^{13}\text{C}$  values from irmGC-MS. Values are in per mil.

	MPPBDa#1	MPPBDa#2
$\delta^{15}\text{N}$	1.36	1.54
	1.17	1.50
	1.70	1.10
<b>Average</b>	<b>1.41</b>	<b>1.38</b>
SD	0.27	0.24
$\delta^{13}\text{C}$	-30.28	-30.89
	-30.76	-31.27
<b>Average</b>	<b>-30.52</b>	<b>-31.08</b>
SD	0.24	0.19



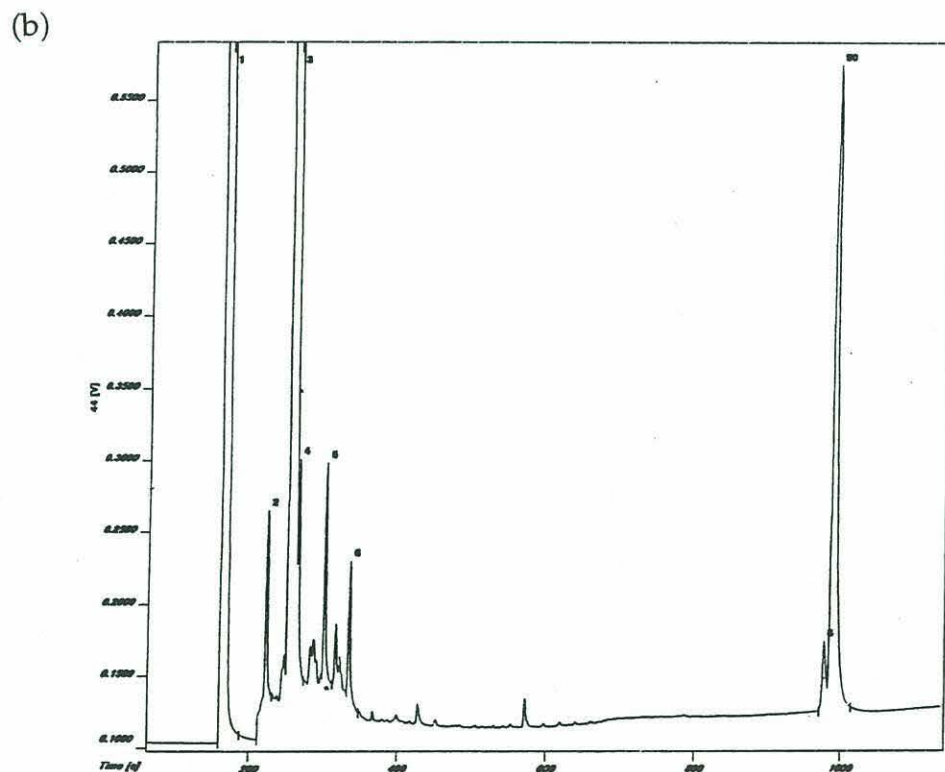
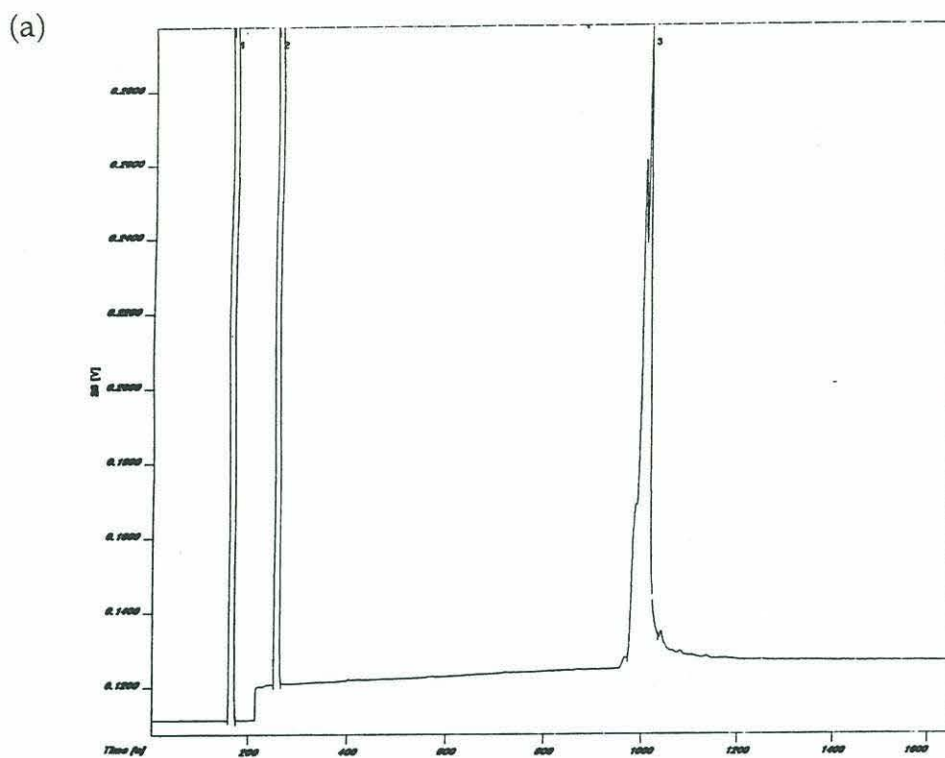


Figure 3.15: Chromatograms from irmGC-MS runs of derivatized 9MPPBDa. The results for  $\delta^{15}\text{N}$  ( $^{14}\text{N}_2$ =mass 28) are shown in (a), while those for  $\delta^{13}\text{C}$  ( $^{12}\text{C}^{16}\text{O}_2$ =mass 44) are shown in (b). The peak splitting in (a) resulted from overloading the GC column.

### 3.5.2 Isotopic Fractionation During Derivatization of Methyl Pyropheophorbide a

Duplicate derivatizations of MPPBDa were performed in order to determine whether nitrogen isotopic fractionation occurred as a result of the synthesis. The results of the isotope analyses are presented in table 3.2. They are shown graphically in figure 3.16.

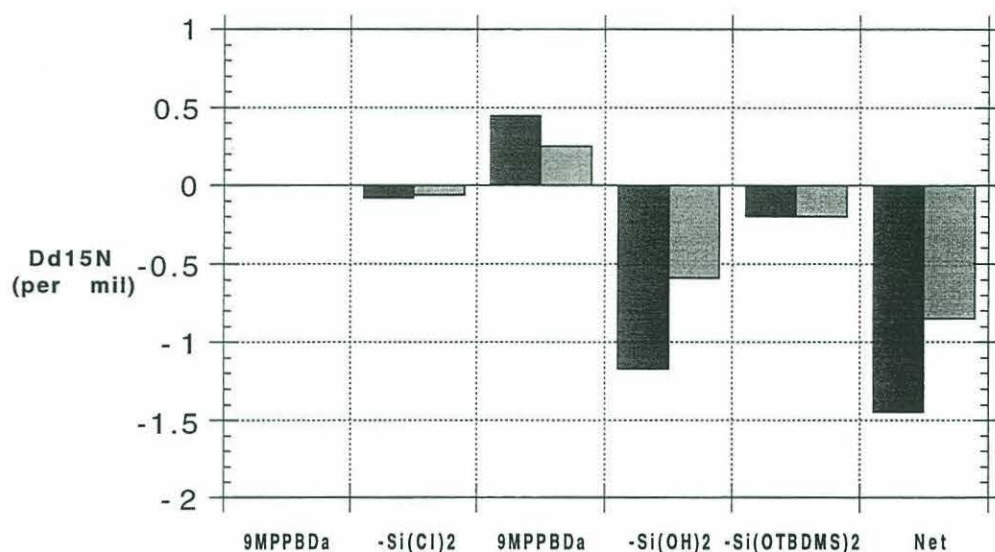
**Table 3.2: Isotopic results for repeat derivatizations of MPPBDa. Yields are in percent.  $\Delta\delta^{15}\text{N}$  values and yields are relative to the immediate precursors.**

	$\delta^{15}\text{N}$ #1	$\Delta\delta^{15}\text{N}$ #1	Yield #1	$\delta^{15}\text{N}$ #2	$\Delta\delta^{15}\text{N}$ #2	Yield #2
MPPBDa	2.65			2.65		
9MPPBDa <sup>1</sup>	2.65	0	97	2.65	0	97
-SiCl <sub>2</sub> <sup>2</sup>	2.57	-0.08	85	2.59	-0.06	80
9MPPBDa <sup>3</sup>	3.10	0.45	15	2.90	0.25	20
-Si(OH) <sub>2</sub>	1.40	-1.17	9.3	2.00	-0.59	8.6
-Si(OTBDMS) <sub>2</sub>	1.20	-0.2	71	1.80	-0.2	86
Net		-1.45	5.4		-0.85	5.8

<sup>1</sup> Duplicate 9MPPBDa syntheses not performed. <sup>2</sup> Values calculated from a mass balance; see text for description. <sup>3</sup> This 9MPPBDa was recovered, unreacted starting material.

There was a net isotopic depletion in the product of both derivatizations. The first had a yield of 5.6%, and was depleted in  $^{15}\text{N}$  by 1.45 per mil relative to the starting material. The second derivative was depleted in  $^{15}\text{N}$  by 0.85 per mil relative to the starting material, and its yield was 5.9%. Most (69 to 81%) of the isotopic alteration occurred during the hydrolysis of the 9MPPBDa dichlorosilicon complex. There was no isotopic fractionation associated with the ketone reduction of MPPBDa, a reaction with a 97% yield.

Figure 3.16: Isotopic fractionation resulting from each step of two chlorin derivatizations. Values plotted are N isotopic differences between product and substrate, or  $\Delta\delta^{15}\text{N}_{\text{product-substrate}}$ .



The silicon insertion step appears to have resulted in little isotopic fractionation. Since this product could not be isolated for isotopic analysis (see Methods section) a mass balance calculation was performed to determine the  $\delta^{15}\text{N}$  values. The mass balance is based upon the assumptions that (1) all of the 9MPPBDa was either converted to the dichlorosilicon complex or left unreacted and carried through the hydrolysis step, and (2) all of the 9MPPBDa recovered after the hydrolysis was unreacted starting material from the Si-insertion step, not reformed starting material resulting from loss of the central Si. (This is a reasonable assumption since the Si complexes of alkyl porphyrins are stable even in 100%  $\text{H}_2\text{SO}_4$  (Fuhrhop and Smith, 1975)). Thus, the following mass balance can be established,

$$\delta_{\text{MPB1}}Y_{\text{MPB1}} = \delta_{\text{SiCl}_2}Y_{\text{SiCl}_2} + \delta_{\text{MPB2}}Y_{\text{MPB2}}$$



where  $\delta_x$  is the  $\delta^{15}\text{N}$  of the product  $x$  (in per mil),  $Y_x$  is the yield of the reaction resulting in product  $x$ , MPB1 is the precursor to the dichlorosilicon complex (9MPPBDa), and MPB2 is the unreacted 9MPPBDa recovered after the hydrolysis step. The equation has two unknowns,  $\delta_{\text{SiCl}_2}$  and  $Y_{\text{SiCl}_2}$ . However, the fraction of starting material recovered as unreacted 9MPPBDa is known, and the assumption is being made that all starting material ended up as either dichlorosilicon complex or unreacted 9MPPBDa. Therefore,

$$Y_{\text{SiCl}_2} = 1 - Y_{\text{MPB2}}.$$

Now the mass balance can be solved for the isotopic composition of (9MPPBDa) $\text{SiCl}_2$  by substituting the second into the first equation, and substituting the appropriate values from table 3.2, and solving for  $\delta_{\text{SiCl}_2}$ . Hence,

$$\begin{aligned}\delta_{\text{SiCl}_2} &= (\delta_{\text{MPB1}}Y_{\text{MPB1}} - \delta_{\text{MPB2}}Y_{\text{MPB2}}) / (1 - Y_{\text{MPB2}}) \\ &= (2.65 \times 1 - 3.1 \times 0.154) / (1 - 0.154) \\ &= 2.57 \text{ per mil for the first derivatization,}\end{aligned}$$

and

$$\begin{aligned}\delta_{\text{SiCl}_2} &= (2.65 \times 1 - 2.9 \times 0.197) / (1 - 0.197) \\ &= 2.59 \text{ per mil for the second derivatization.}\end{aligned}$$

The mass balance calculation therefore indicates that isotopic fractionation of the chlorine associated with Si-insertion with hexachlorodisilane is on the order of 0.1 per mil.

It is the hydrolysis of the axial chlorines that results in significant isotopic fractionation of the derivative. The yield for this step was about 9% in both instances. Incomplete reaction resulting from overly mild hydrolysis conditions

is the likely cause of the low yields (see section 3.6). It is expected that the isotopic fractionation associated with this step will diminish if yields can be increased.

The last step of the derivatization, silylation of the axial hydroxyl groups, resulted in a 0.2 per mil  $^{15}\text{N}$  depletion of the product in both syntheses. The yields for the reaction were 71 and 86%, respectively.

### 3.6 Discussion

With some modifications to procedures developed for the synthesis of volatile alkyl porphyrins (Boylan, et al., 1969; Boylan and Calvin, 1967; Eckardt, et al., 1988; Gill, et al., 1986; Hein, et al., 1985; Marriott, et al., 1984) a synthetic route to volatile chlorin derivatives has been devised (figure 3.17). Methyl pyropheophorbide *a* (MPPBDa), a common chlorophyll *a* degradation product found in marine sediments, was used as a model chlorin in this work. The synthesis of MPPBDa from Chl *a* is described in chapter 2.

Modifications to the earlier procedures were necessary due to the additional functional groups on chlorins relative to alkyl porphyrins. For instance, it was thought that the hydrolysis of the axial chlorines in either 1 N ethanolic (50/50  $\text{H}_2\text{O}/\text{EtOH}$ ) HCl (Boylan, et al., 1969; Boylan and Calvin, 1967) or concentrated KOH (aq) (Marriott, et al., 1984) would result in hydrolysis of the ester on the C-7 propionic side-chain. Therefore dilute (0.1 N) methanolic (5/95  $\text{H}_2\text{O}/\text{MeOH}$ )HCl was used for the hydrolysis. Furthermore, it was suggested (R. Ocampo, personal communication) that reduction of the ketone at the C-9 position (on the isocyclic ring) would increase yields of the dihydroxysilicon chlorins. Solubility issues also arose as a result of the chlorins being more polar than the alkyl porphyrins derivatized by the Bristol group. So, for instance,

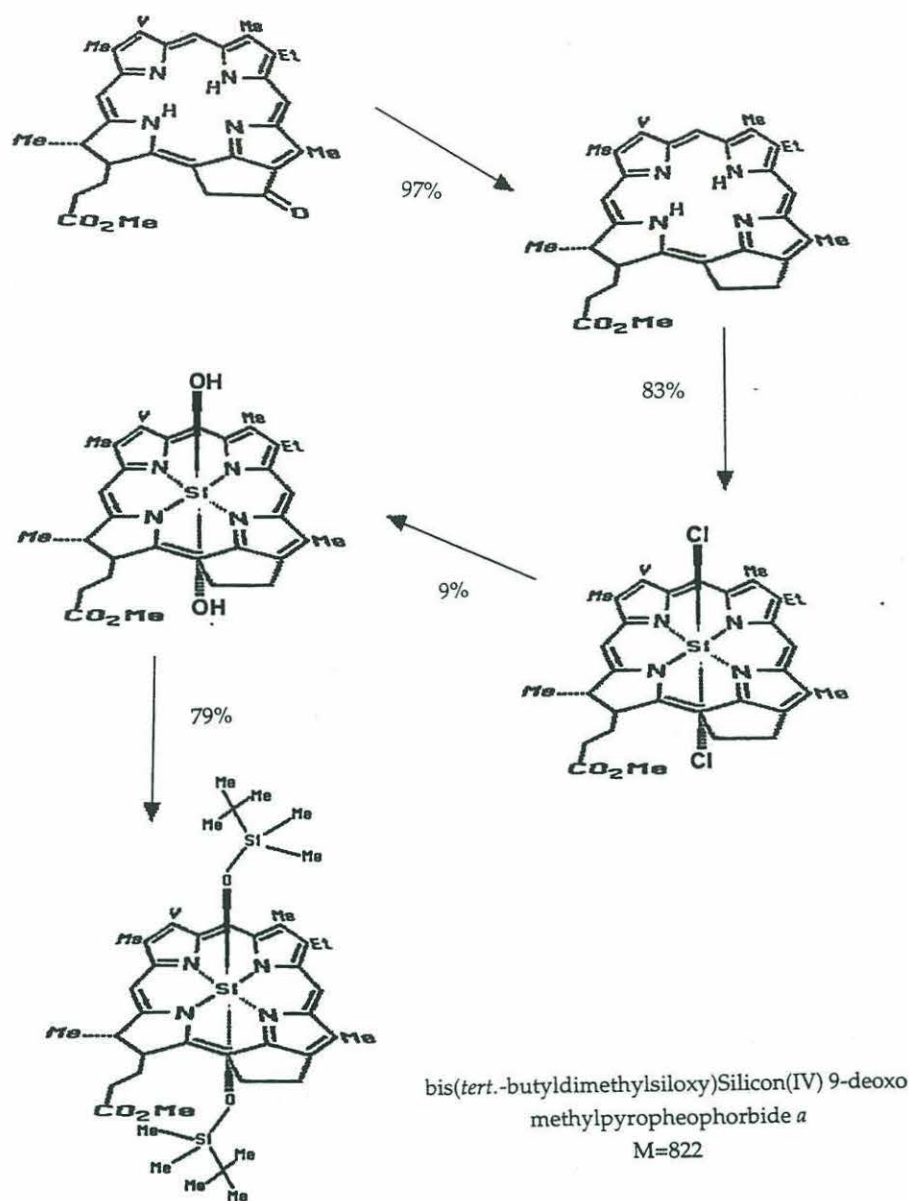


Figure 3.17: The 4-step synthesis of GC-amenable chlorin derivatives. The yields for each reaction are shown.

methanol rather than ethanol was used to dissolve the dichlorosilicon chlorins.

Even with these modifications, yields for the synthesis of volatile silicon chlorin complexes remain low (5-6%). Most of the loss occurs during the handling of the dichlorosilicon complex and the subsequent hydrolysis step. The following discussion focuses on the causes of, and potential solutions to, the low yields for the chlorin derivatization.



### 3.6.1 Chlorin C-9 Ketone Reduction

The ketone reduction of MPPBDa to form 9-deoxo-MPPBDa was pursued as a potential solution to the "polymerization," and resultant loss of product, observed during the synthesis and handling of (MPPBDa)SiCl<sub>2</sub>.

It is known that the C-10 is an active site on the chlorin macrocycle (Hynninen, 1979; Hynninen, et al., 1979) with the C-10 protons being abnormally acidic. This is due (1) to the activation of this site by the two electron-withdrawing carbonyl functionalities at C-9 and C-10 and (2) to the resonance stabilization afforded the benzylic-like anion of a C-10-deprotonized chlorin (Scheer, 1991). Although somewhat reduced, the acidity of the C-10 protons persists even after removal of the  $\beta$ -keto ester to make the "pyro" chlorin (Scheer, 1991). Thus the ketone at C-9 can enolize relatively easily. However, at thermodynamic equilibrium the free enol is expected to be in very low concentrations (Scheer, 1991). The stability, and hence concentration of the free enol can, however, be enhanced by formation of a silyl enol ether (Hynninen, et al., 1979) (figure 3.18).

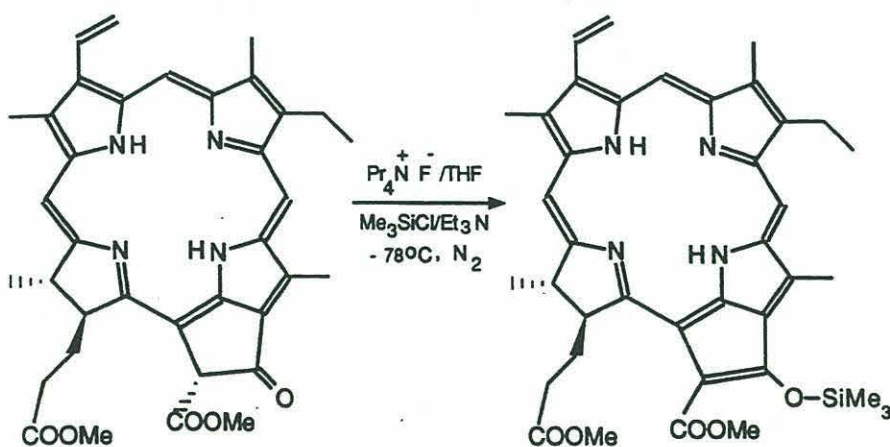


**Figure 3.18:** Stabilization of free enol by formation of a silyl enol ether (Hynninen, 1991).

It is likely, then, that the C-9 enol was stabilized by the synthesis of a chlorosilyl enol ethers during the reaction of MPPBDa with  $\text{Si}_2\text{Cl}_6$ . The chlorosilyl moiety of the enol ether would then be available for insertion into the macrocycle of another chlorin. In this way polymerization could occur (Dr. Ruben Ocampo, personal communication).

### 3.6.2 Chlorin Dichlorosilicon Complex

The reaction of chlorins with hexachlorodisilane ( $\text{Si}_2\text{Cl}_6$ ) to form chlorin dichlorosilicon complexes is a rapid, high yield reaction. The problem with this approach for routine use is the extremely high reactivity of the reagent. Hexachlorodisilane reacts violently with water. Therefore, great care must be taken to insure all solvents, reactants and glassware are dry. In addition, air must be excluded from reaction vessels. Furthermore, transfer of the reagent via syringe was often unsuccessful, especially if the ambient humidity was high. Finally, the product of the reaction appears to be susceptible to self-polymerization. This polymerization is largely responsible for the significant loss of product encountered during chlorin derivatization.

The polymerization is likely to occur even in a completely defunctionalized chlorin. For instance, the dichlorosilicon complex of octaethylporphyrin--an alkyl porphyrin lacking carbonyl functionalities--underwent a similar transformation (this work). Furthermore, phthalocyanine dihydroxy silicon complexes underwent self-polymerizations as well (Joyner and Kenney, 1962). The latter were thought to be essentially linear polymers in the z-direction to form a chain of  $\cdots\text{O-Si-O-Si-O}\cdots$  bonds. This suggests the axial chlorines in our dichlorosilicon complexes may be easily hydrolyzed, after which



time they may be available for the hydrolysis of neighboring axial chlorines, thus producing an insoluble polymer.

As mentioned above, the C-9 enol may also be involved in the polymerization. In this way the polymerization would be similar to that observed with hematin, the dihydroxy complex of heme--an iron porphyrin with carboxylic acid side chains--which forms an insoluble polymer when it is allowed to stand in alcohol (Falk, 1964). That the axial chlorines in our syntheses were hydrolyzed by SiO<sub>2</sub> moieties comprising the glass vial walls was considered unlikely since the same behavior was observed in teflon.

It is therefore recommended that if Si<sub>2</sub>Cl<sub>6</sub> is to be used, it be done in an airtight reactor where transfer of the reagent can be accomplished without contact with air. The simplest approach would be to perform the reaction in an N<sub>2</sub>-filled glove bag. However, there are specialized pieces of equipment designed for the use of moisture-sensitive reagents (Brown, 1975). Furthermore, the dichlorosilicon complex should be hydrolyzed immediately since it is susceptible to rapid self-polymerization.

### 3.6.3 Hydrolysis of the Chlorin Dichlorosilicon Complex

Mild (i.e., 17  $\mu$ M HCl in 99.3% MeOH (aq)) reaction conditions were used for the hydrolysis of chlorin dichlorosilicon complexes because many naturally occurring chlorins contain ester functionalities that are susceptible to hydrolysis in aqueous acid. However, it is likely that the reaction conditions used for this work were too mild for complete reaction. Previous workers have used 1 N HCl in 50% aqueous ethanol (Boylan and Calvin, 1967) or saturated KOH (aq) (Marriott, et al., 1984) for the hydrolysis reaction.



In order to increase the yield of the hydrolysis reaction it is recommended (1) that more aggressive hydrolysis conditions (i.e., 1 N HCl in 75% MeOH (aq)) be employed, and (2) that high dilutions be used during the phase separation of the hydrolysis product from the aqueous solution into organic solvents. Increasing the acidity of the solvent is likely to reduce in partial hydrolysis of the ester functionalities, but this reaction may be minimized by decreasing the reaction time to a few minutes. For example, an experiment showed that methyl pyropheophorbide *a* was stable in 0.1 N HCl in 95% MeOH (aq), with 0.45% degrading in 1 hour and 4.8% degrading in 18 hours. The dilution of the reaction medium (both by increasing the water concentration and making the mixture more dilute) is suggested in order to decrease the likelihood that chlorin axial -OH groups will encounter axial chlorines, thus preventing polymerization.

#### 3.6.4 Silylation of the Chlorin Dihydroxysilicon Complex

Mass spectrometry (static FAB<sup>+</sup> and GC-CI) confirmed the successful synthesis of volatile chlorin silicon complexes of methyl pyropheophorbide *a*. Purification of the reaction products by alumina TLC led to the three blue bands ( $R_F = 0.65, 0.70$  and  $0.79$ ) containing at least 6 different bis(*tert*.-butyldimethylsiloxy)Si(IV) derivatives of methyl pyropheophorbide *a*.

The fourth, and most polar ( $R_F = 0.56$ ), band was shown by FAB<sup>+</sup> MS (figure 3.19) to contain free-base MPPBDa ( $M/Z = 548$  ( $M^+$ , 44%)), and possibly some dihydroxysilicon complex ((MPPBDa)Si(OH)<sub>2</sub>,  $M/Z = 608$  ( $M^+ + 2$ , 80%)), or meso-dihydroxysilicon complex ( $M/Z = 610$  ( $M^+$ , 80%). (The term meso refers to a reduced vinyl group at C-2.) Since neither the free base or the PhSi(OH)<sub>2</sub> is GC-amenable, neither compound was observed in GC-CI-MS runs.

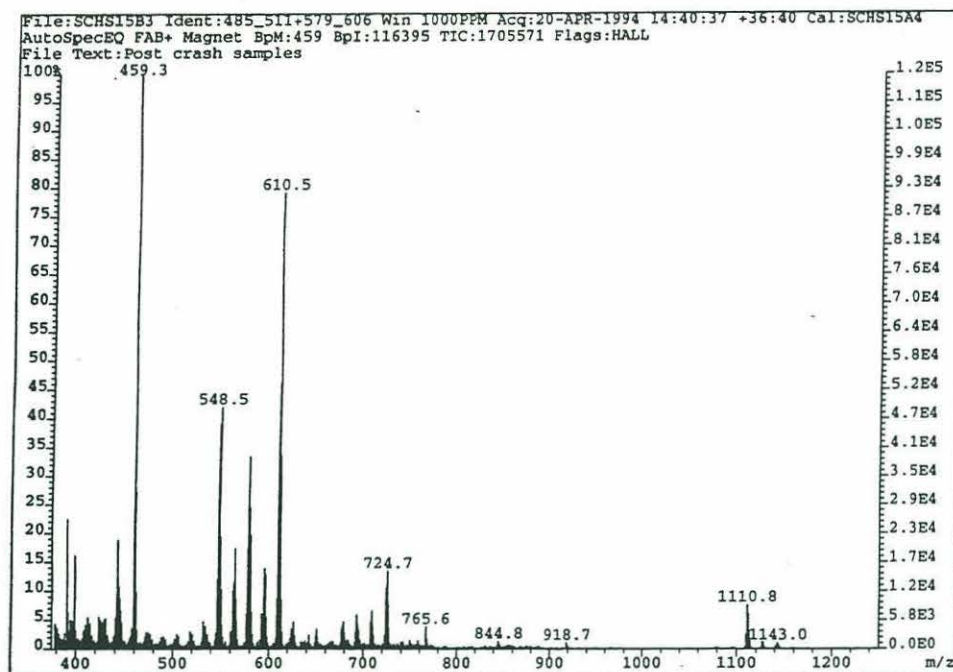


Figure 3.19: FAB<sup>+</sup> mass spectrum of the polar band ( $R_F=0.56$ ) from alumina TLC of the reaction product of the MPPBDa derivatization.

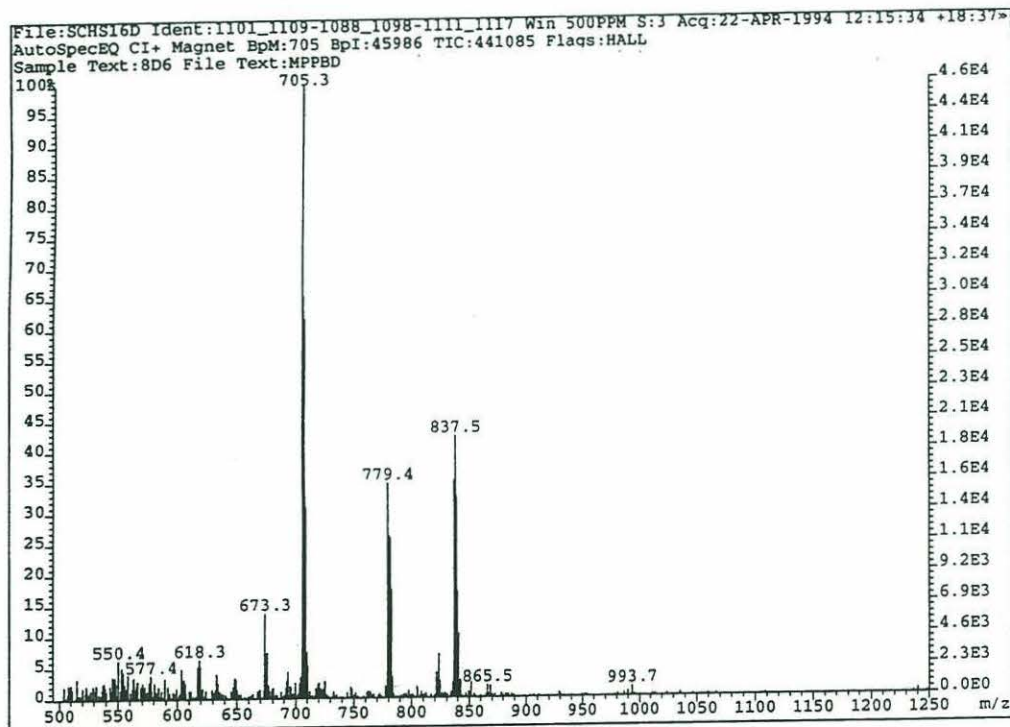


Figure 3.20: GC-CI<sup>+</sup> mass spectrum of (MPPBDa)Si(OTBDMS)<sub>2</sub>. The retention time of the derivative was 18:36 minutes.

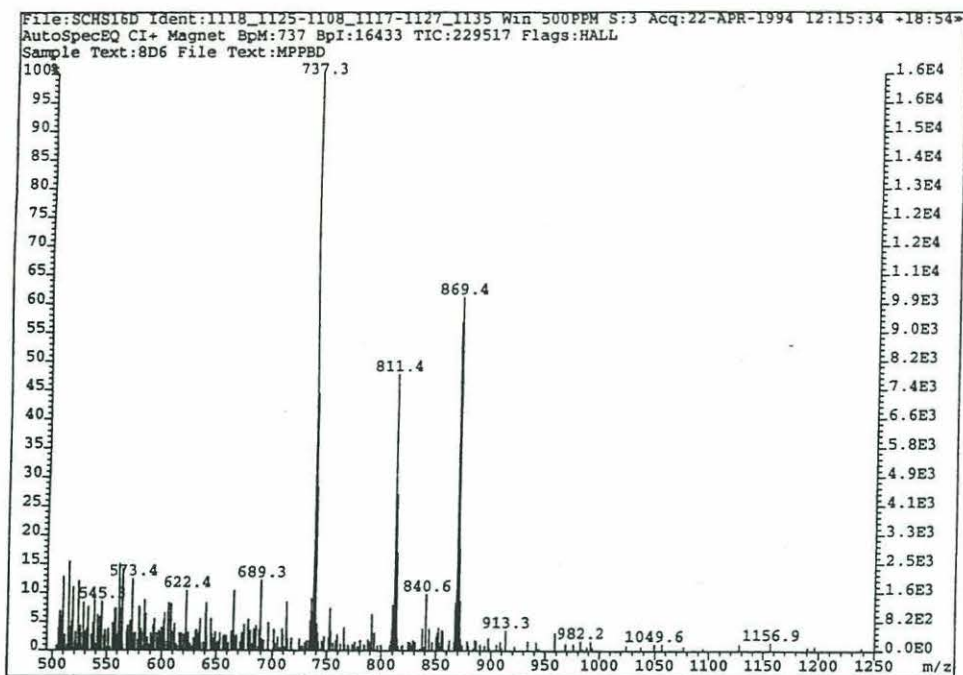


Figure 3.21: GC- $\text{CI}^+$  mass spectrum of compound eluting 19 seconds after  $(\text{MPPBDa})\text{Si}(\text{OTBDMS})_2$ . The fragmentation pattern is virtually identical to that of the desired product (figure 3.20), yet each fragment is 32 mass units greater (see text for discussion).

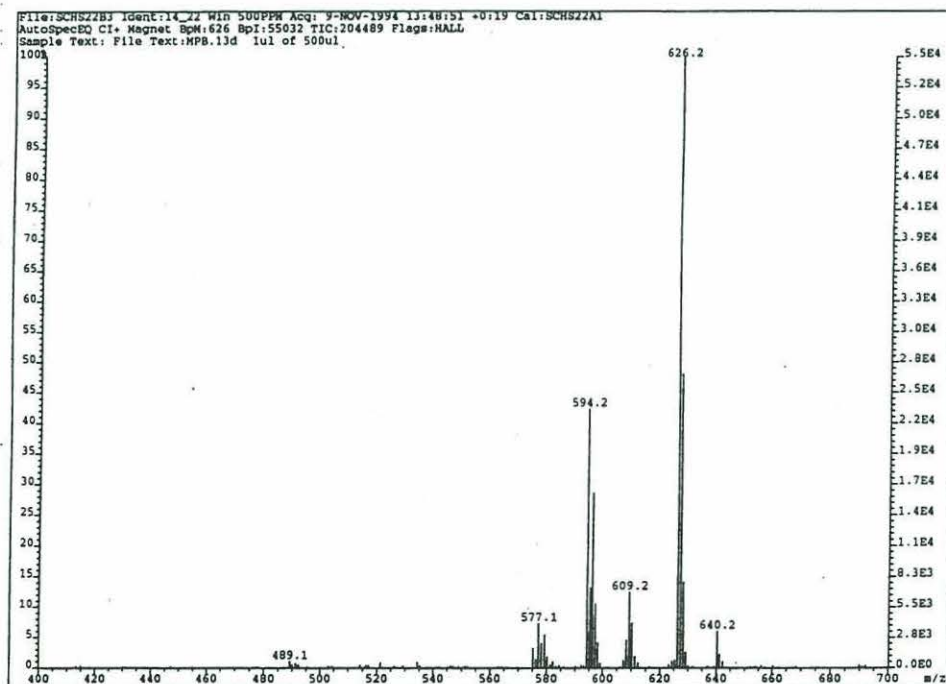


Figure 3.22: Methane  $\text{CI}$ -mass spectrum of  $(9\text{MPPBDa})\text{Si}(\text{OH})_2$  ( $M/Z=594$  ( $M$ , 40%)) showing the high abundance of the  $M+32$  side-product ( $M/Z=626$ , 100%), corresponding to the addition of  $\text{CH}_4\text{O}$ .



The 2 adjacent bands from the TLC plate, with  $R_F = 0.65$  and  $0.70$ , contained two of the same chlorin derivatives, with retention times ( $t_R$ ) of 18:36 and 18:55, respectively. This was 30 and 49 seconds, respectively, into the isothermal part of the temperature program, and therefore corresponded to an elution temperature of  $320^\circ\text{C}$ . The compound eluting at 18:36 was (MPPBDa)Si(OTBDMS)<sub>2</sub>, the desired product ( $M/Z = 836$  ( $M+1$ , 43%), 779 ( $M-57$ , 35%), 705 ( $M-131$ , 100%)) (figure 3.20). The observed fragmentation pattern is typical for *tert*.-butyldimethylsiloxy groups (Gill, et al., 1986; Marriott, et al., 1984), with loss of a -TBDMSO (-131) accounting for the major ion, and the parent ion and loss of a *t*-butyl (-57) group having similar intensities.

The compound eluting at 18:55 was 32 mass units greater than the desired derivative ( $M/Z = 868$  ( $M+1$ , 54%), 811 ( $M-57$ , 41%), 737 ( $M-131$ , 100%)) (figure 3.21) which suggests the addition of methanol (CH<sub>3</sub>OH). High-resolution MS-MS supports this interpretation. The most likely place for the addition of CH<sub>3</sub>O- is at the central silicon atom. This may occur during the hydrolysis of the dichlorosilicon complex in acidic MeOH. The fourth hydrogen would then be a pyrrolic proton.

If the silicon complexed to only 3 of the 4 pyrrolic nitrogens, possibly as a result of the puckered geometry of the chlorin macrocycle, then MeOH could substitute for one or more of the remaining chlorines during the hydrolysis step. It is thought that metals are incorporated into porphyrins via an S<sub>N</sub>2-type displacement, whereby the metal forms an activated complex with the porphyrin, followed by displacement of the two pyrrolic protons by the metal (Falk, 1964). This mechanism--rather than a dissociation of the pyrrolic protons to form the dianion, followed by reaction with the metal--certainly seems more compatible with the "partial reaction" hypothesis. The proposed scenario

requires that a silicon complex formed with only 3 of the pyrrole nitrogens be quite stable.

If MeOH is reacting with the central Si atom, then it might be expected to see  $\text{ChSi}(\text{OCH}_3)(\text{OH})_2$ ,  $\text{ChSi}(\text{OCH}_3)_2(\text{OH})$ , and even  $\text{ChSi}(\text{OCH}_3)_3$  as reaction products of the hydrolysis. The first two products are, in fact observed, with  $\text{ChSi}(\text{OCH}_3)(\text{OH})_2$  actually being the most abundant product in some instances (figure 3.22). The silyl methyl triether has not been observed.

In a similar finding, Boylan and Calvin (1967) showed that the Cl ligands on dichlorosilicon etioporphyrin I could be substituted by alkyl ether groups when the product of the silicon insertion step was treated with acidic ethanol. However, there have not been any reports in the literature of Si complexing with only 3 of the 4 nitrogens in a cyclic tetrapyrrole. Nevertheless, important differences exist in chlorin geometry relative to alkyl porphyrins.

Porphyrins are planar molecules, while chlorins tend to have a puckered macrocycle (Hynninen and Sievers, 1981). The 5-membered isocyclic ring exerts steric strain on the chlorin macrocycle. This strain is relieved by conformational alterations afforded by the enhanced flexibility resulting from the  $\text{sp}^3$  hybridization at C-7 and C-8 in ring IV (Hynninen and Sievers, 1981). Porphyrins tend to be more planar since they contain an oxidized ring IV and therefore lack this added flexibility.

Additional stability would be imparted to a methoxy ligand on the central Si through hydrogen bonding with the proton on the ring II N.

The other potential site for the addition of  $\text{CH}_3\text{O}-$  on the chlorin macrocycle is across the vinyl group at the C-2 position. However, this seems unlikely given the stability of that group in strongly acidic methanol (i.e., 25/75 (w/w)  $\text{H}_2\text{SO}_4/\text{MeOH}$  for up to 3 hours) (Sachs, unpubl.) (King and Repeta, 1994).



Even if silyl methyl ethers are being synthesized as a result of incomplete reaction of the pyrrolic nitrogens with tetravalent Si (from  $\text{Si}_2\text{Cl}_6$ ), they are not significantly diminishing the volatility of the chlorin derivatives. This is evidenced by their elution 49 seconds into the isothermal phase of the temperature program, versus 30 seconds for the desired derivative. Nonetheless, avoiding this side reaction is desirable since it would simplify the chromatography.

### 3.6.5 Direct High-Temp GC of Chlorins

The most promising route to irmGC-MS analysis of chlorins may be direct high-temperature gas chromatography of partially defunctionalized chlorophylls. Initial attempts to chromatograph methyl pyropheophorbide *a* gave poor results (figure 3.23). The broad hump upon which the chlorin peak

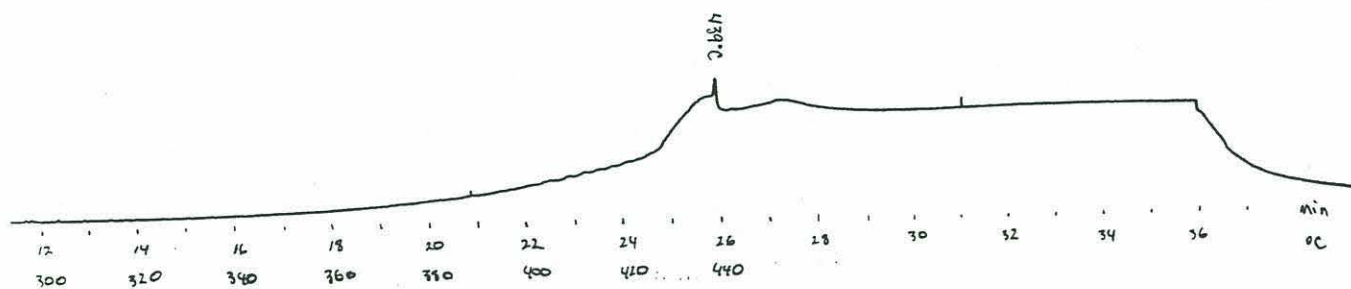


**Figure 3.23:** Gas chromatogram of methyl pyropheophorbide *a*. Partial thermal decomposition of the chlorin occurred prior to its elution at 439°C.



(elution temperature = 439°C) sits was thought to result from partial thermal degradation of the chlorin. Therefore, two approaches were taken to improve the chromatography. The first was to increase the thermal stability of the chlorin. The second was to increase the volatility of the chlorin (without the multi-step derivatization described above).

Increased volatility was achieved by reduction of the methyl pyropheophorbide *a* ketone at C-9. Increased thermal stability was attempted in two ways. First, by aromatizing, and second by inserting Ni into the chlorin macrocycle. The aromatization consisted of D (or IV) ring oxidation. The reaction of 9MPPBDa with 2,3-dichloro-5,6-dicyano-1,4-benzoquinone (DDQ) in MeCl<sub>2</sub> (Smith and Smith, 1990) went to completion at room temperature in roughly 30 seconds (figure 3.12). The reaction of 9MPPBDa and aromatized 9MPPBDa with Ni (II) acetylacetonate (Aldrich) in benzene at reflux overnight (Verne-Mismer, 1988) resulted in quantitative conversion of the free-base chlorins to their Ni (II) derivatives (figure 3.13). Experiments were conducted to determine whether N or C isotopic fractionation occurred as a result of the metallation reaction. None was observed with either deuteroporphyrin IX dimethyl ester or 9MPPBDa.

Using an aluminum-clad capillary GC column (SGE HT-5, 12 m, 0.1 μm non-polar phase), which can be operated at temperatures up to 480°C, it was possible to directly chromatograph 9-deoxo-methylpyropheophorbide *a* (figure 3.24.b). The elution temperature for this compound was 380°C. For the temperature gradient employed--60°(1)/25/350°(0)/10/440°(20)--this corresponded to a retention time of 15.61 minutes. This was similar to the retention time of deuteroporphyrin IX dimethyl ester, which eluted at 15.75 minutes, or 381.4°C (figure 3.24.a).

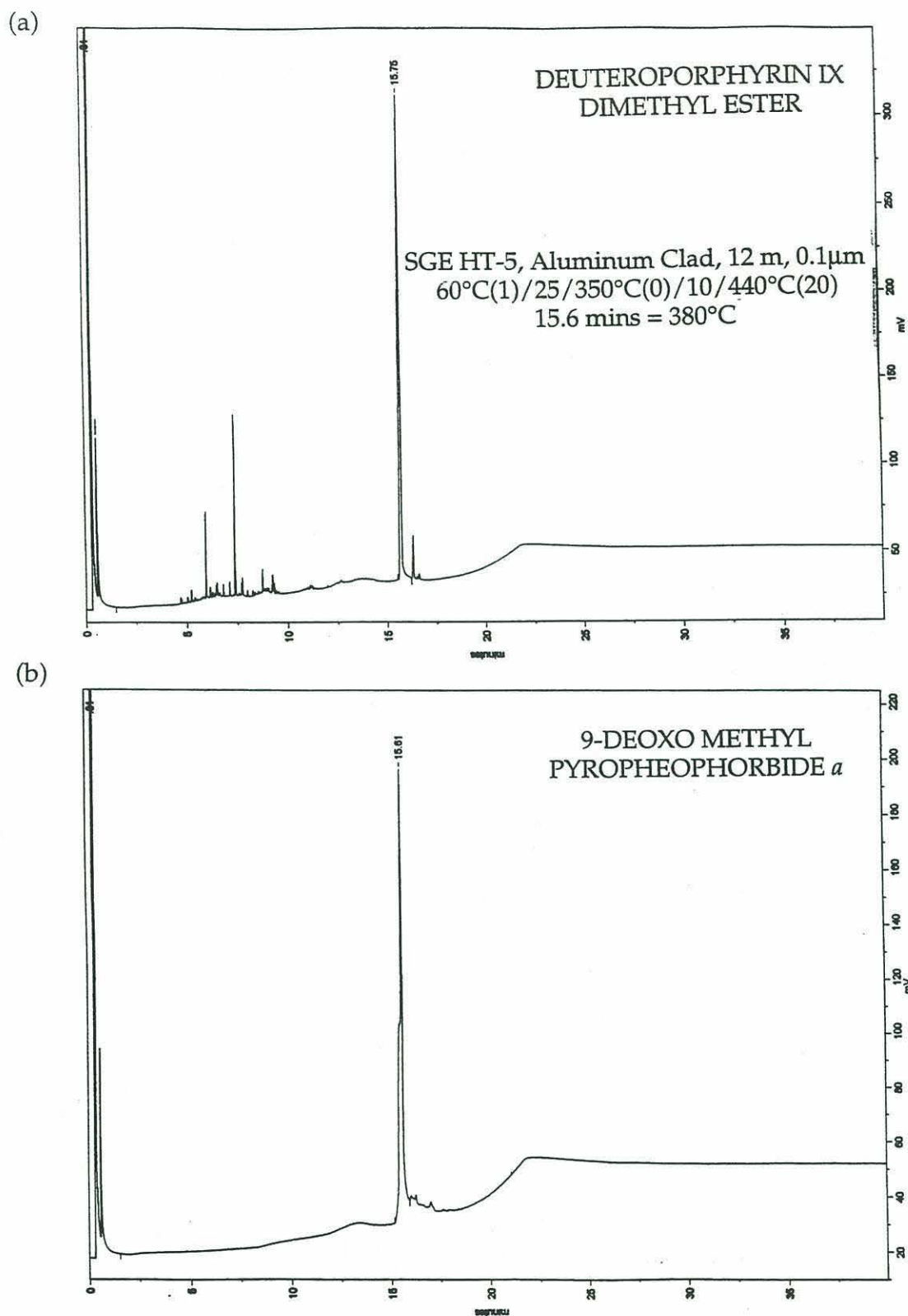


Figure 3.24: Gas chromatograms of (a) deuterioporphyrin IX dimethyl ester, and (b) 9-deoxo-methyl pyropheophorbide *a*.

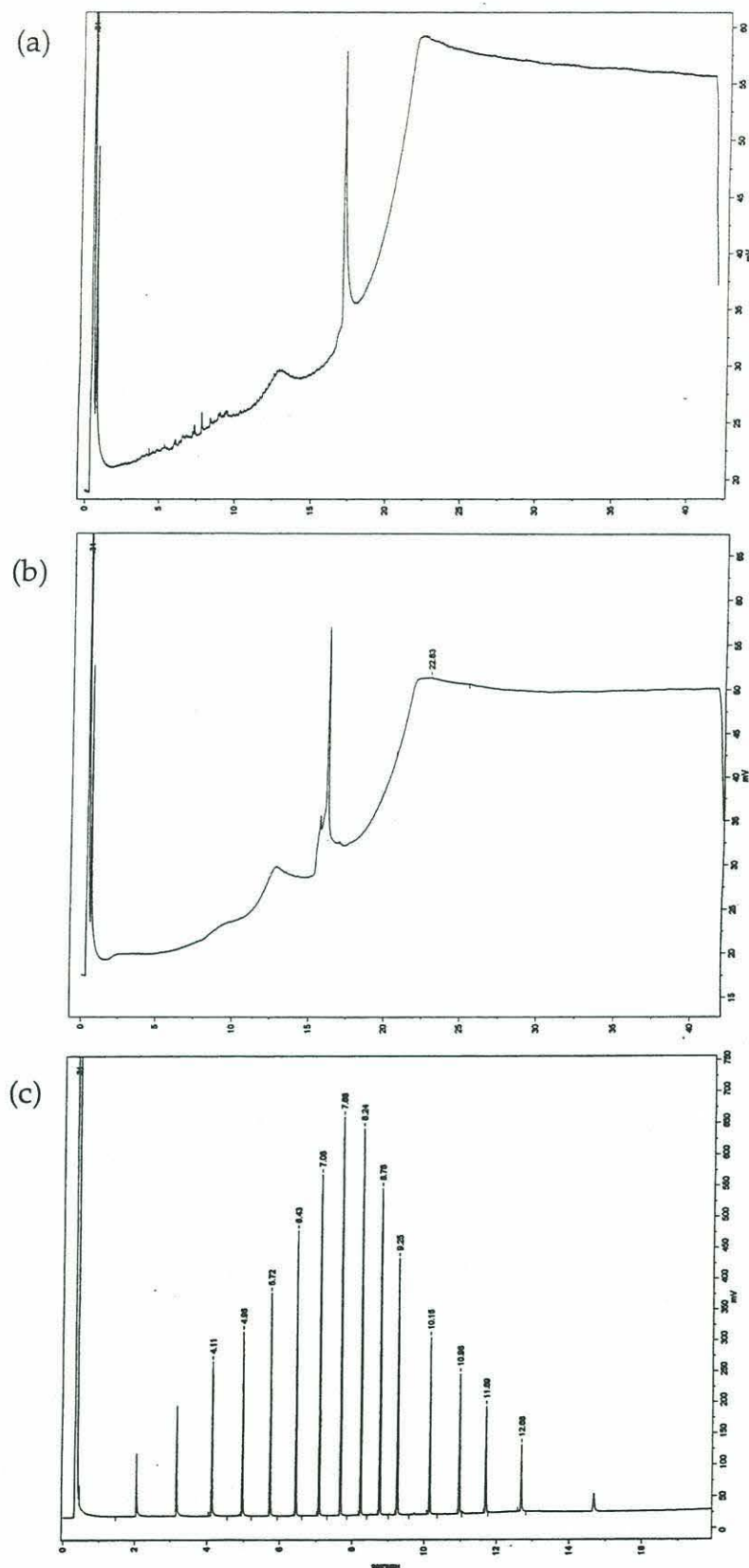


Figure 3.25: Gas chromatograms of (a) methyl pyropheophorbide *a*, (b) ring IV-oxidized 9-deoxo-methyl pyropheophorbide *a* (see section 3.4.3.1), and (c) a C<sub>12</sub>-C<sub>60</sub> normal alkane standard.



The earlier, failed attempts at direct chlorin gas chromatography employed a hydrogen carrier gas at flow rates of 3.0 mL/min (at 110°C). The successful chromatography occurred when the carrier was switched to helium, and the flow rate increased to 3.5 mL/min, and held constant with electronic pressure programming. In addition to the 9-deoxo chlorin, it was possible to chromatograph intact methyl pyropheophorbide *a* with these improved conditions (figure 3.25.a). The retention time was 16.12 minutes, corresponding to an elution temperature of 385.1°C. This is 0.51 mins and 5.1°C greater than observed for the reduced ketone derivative. The chromatographic peak shape was also somewhat diminished relative to the 9-deoxo chlorin.

The gas chromatography of aromatized 9-deoxo chlorin was successful (figure 3.25.b), but the peak shape was also inferior to that of intact 9MPPBDa. The retention time of the aromatized structure was 17.25 minutes, corresponding to an elution temperature of 396.4°C. Furthermore, none of the Ni (II) derivatives--Ni(II)9MPPBDa, Ni(II)-"aromatized"-9MPPBDa, Ni(II) deuteroporphyrin IX dimethyl ester--eluted from the chromatograph during the temperature program employed (i.e., to 440°C, followed by a 20 minute isothermal period).

In conclusion, the direct gas chromatography of underivatized chlorins is possible at temperatures below 400°C. The use of a short (12 m) aluminum-clad column with a thin (0.1 µm) phase, and a high (3.5 mL/min) He flow rate produces good chromatographic results with methyl pyropheophorbide *a* and 9-deoxo-methyl pyropheophorbide *a*. Since the former is a commonly found chlorophyll degradation product in marine sediments, it may be possible to measure chlorin  $\delta^{15}\text{N}$  and  $\delta^{13}\text{C}$  values directly by irmGC-MS of sedimentary lipid extracts. It is expected that some resolution will be lost by the use of short GC columns with thin phases, yet n-C<sub>50</sub> and nC-60 are resolved by 2.2 minutes

using the column and conditions described above (figure 3.25.c). This resolution may be sufficient toward the high end of the chromatogram where there may be fewer co-eluting materials. It is not known, though, whether current irmGC-MS systems will tolerate the higher operating temperatures suggested here.

### 3.7 Conclusion

Stable N and C isotope ratios in chlorophyll may prove to be powerful biogeochemical tracers. Their measurement, though, has been hampered by the inability to purify chlorins to levels suitable for isotopic analysis. In the few instances where this has been done, the number of measurements was small due to the complexity of the chemistry. And there are no published analyses of sedimentary chlorin stable isotopic ratios.

Recent technological advances have now made it possible to measure isotopic composition of nanomolar quantities of nitrogen and carbon on individual compounds as they elute from a gas chromatograph. The high sensitivity of new mass spectrometers combined with the high resolution of today's capillary GC columns make this a very powerful tool. Therefore, we sought to measure chlorin  $\delta^{15}\text{N}$  and  $\delta^{13}\text{C}$  by irmGC-MS.

Since initial attempts at direct gas chromatography of chlorins were unsuccessful, we developed a procedure for the synthesis of volatile bis-(*tert*.-butyldimethylsiloxy)Si(IV) chlorin derivatives. These derivatives eluted from a GC at 260°C. However yields for the synthesis were low (5-6%) and a net nitrogen isotopic depletion of 1.2 per mil was observed in the derivative relative to the starting chlorin. Therefore, the direct GC approach was revisited.

It was found that methyl pyropheophorbide *a*, a common sedimentary chlorin, passed through a GC at 385°C. This occurred when a short (12 m), non-polar thin-phased (0.1  $\mu\text{m}$ ) aluminum-clad glass capillary column was used, and the helium carrier gas flow rate was maintained at a constant 3.5 mL/min. The chromatographic peak shape improved, and the elution temperature decreased by 5°C when the ketone at C-9 on the chlorin isocyclic ring was removed. The reduction is rapid and the yield is high (97%), resulting in no N isotopic alteration.

It is suggested that future work on chlorin irmGC-MS focus on the direct high-temperature route, rather than on the derivatization. Doing so would avoid the cumbersome manipulations required when working with extremely reactive moisture-sensitive reagents. Furthermore, the direct chromatographic approach should result in less isotopic fractionation since little or no chemical alteration of the chlorin is required.



### References for Chapter 3

Baker, E.W., T.F. Yen, R.E. Dickie, R.E. Rhodes and L.F. Clark (1967) Mass Spectrometry of Porphyrins. II. Characterization of Petroporphyrins. *Journal of the American Chemical Society*, **89**(14): 3631-3639.

Boylan, D.B., Y.I. Alturki and G. Eglinton (1969) Application of Gas Chromatography and Mass Spectrometry to Porphyrin Microanalysis. In: *Advances in Organic Geochemistry, 1968*, Pergamon Press, Oxford, pp. 227-240.

Boylan, D.B. and M. Calvin (1967) Volatile Silicon Complexes of Etioporphyrin I. *Journal of the American Chemical Society*, **89**(21): 5472-5473.

Brand, W.A., A.R. Tegtmeier and A. Hilker (1994) Compound-Specific Isotope Analysis: Extending Toward  $^{15}\text{N}/^{14}\text{N}$  and  $^{18}\text{O}/^{16}\text{O}$ . *Organic Geochemistry*, **21**(6/7): 585-594.

Brown, H.C. (1975) *Organic Syntheses Via Boranes*. John Wiley & Sons, New York, 283 pp.

Eckardt, C.B., L. Dyas, P.W. Yendle and G. Eglinton (1988) Multimolecular Data Processing and Display in Organic Geochemistry: The Evaluation of Petroporphyrin GC-MS Data. *Organic Geochemistry*, **13**(4-6): 573-582.

Falk, J.E. (1964) *Porphyrins and Metalloporphyrins*. Elsevier Publishing Company, Amsterdam, 266 pp.

Fuhrhop, J.-H. and K.M. Smith (1975) *Laboratory Methods in Porphyrin and Metalloporphyrin Research*. Elsevier Scientific Publishing Company, Amsterdam, 243 pp.

Gill, J.P., R.P. Evershed and G. Eglinton (1986) Comparative Computerised Gas Chromatographic-Mass Spectrometric Analysis of Petroporphyrins. *Journal of Chromatography*, **369**: 281-312.

Gribble, G.W., W.J. Kelly and S.E. Emery (1978) Reactions of Sodium Borohydride in Acidic Media; VII. Reduction of Diaryl Ketones in Trifluoroacetic Acid. *Synthesis*, **October**: 763-765.

Gribble, G.W., R.M. Leese and B.E. Evans (1977) Reactions of Sodium Borohydride in Acidic Media; IV. Reduction of Diarylmethanols and Triarylmethanols in Trifluoroacetic Acid. *Synthesis*, **March**: 172-176.

Hayes, J.M., K.H. Freeman, B.N. Popp and C.H. Hoham (1990) Compound-Specific Isotopic Analyses: A Novel Tool for Reconstruction of Ancient Biogeochemical Processes. *Organic Geochemistry*, **16**(4-6): 1115-1128.

Hein, C.S., J.P. Gill, R.P. Evershed and G. Eglinton (1985) Reverse Search and Related Processing of Gas Chromatographic/Mass Spectrometric Data from Petroporphyrin Analyses. *Analytical Chemistry*, **57**: 1872-1879.

Hynninen, P.H. (1979) Application of Elution Analysis to the Study of Chlorophyll Transformations by Column Chromatography on Sucrose. *Journal of Chromatography*, **175**: 75-88.

Hynninen, P.H. (1991) Chemistry of Chlorophylls: Modifications. In: *Chlorophylls*, (H. Scheer, ed.), CRC Press, Boca Raton, pp. 145-209.

Hynninen, P.H. and G. Sievers (1981) Conformations of Chlorophylls a and a' and their Magnesium-Free Derivatives as Revealed by Circular Dichroism and Proton Magnetic Resonance. *Zeitschrift fuer Naturforschung*, **36b**: 1000-1009.

Hynninen, P.H., M.R. Wasielewski and J.J. Katz (1979) Chlorophylls. VI. Epimerization and Enolization of Chlorophyll a and Its Magnesium-free Derivatives. *Acta Chemica Scandinavica*, **B 33**: 637-648.

Jeandon, C., R. Ocampo and H.J. Callot (1993) Improved Preparation of Deoxophylloerythroetioporphyrin (DPEP) and its 15'-Methyl Derivative from Chlorophyll a. *Tetrahedron Letters*, **34**(11): 1791-1794.



Joyner, R.D., J. Cekada Jr., R.G. Linck and M.E. Kenney (1960) Diphenoxysilicon Phthalocyanine. *Journal of Inorganic Nuclear Chemistry*, **15**: 387-388.

Joyner, R.D. and M.E. Kenney (1962) Phthalocyaninosilicon Compounds. *Inorganic Chemistry*, **1**(2): 236-238.

Kenner, G.W., S.W. McCombie and K.M. Smith (1973) Pyrroles and Related Compounds. Part XXIV. Separation and Oxidative Degradation of Chlorophyll Derivatives. *Journal of the Chemical Society, Perkin Transactions I*, : 2517-2523.

King, L.L. and D.J. Repeta (1994) High Molecular weight and acid extractable chlorophyll degradation products in the Black Sea: new sinks for chlorophyll. *Organic Geochemistry*, **21**(12): 1243-1255.

Krueger, P.C. and M.E. Kenney (1963) Dialkoxypthalocyaninisilicon Derivatives. *Journal of Organic Chemistry*, **28**: 3379-3381.

Lane, C.F. and G.W. Kramer (1977) Handling Air-Sensitive Reagents. *Aldrichimica Acta*, **10**(1): 11-18.

Marriott, P.J., J.P. Gill, R.P. Evershed, C.S. Hein and G. Eglinton (1984) Computerised Gas Chromatographic-Mass Spectrometric Analysis of Complex Mixtures of Alkyl Porphyrins. *Journal of Chromatography*, **301**: 107-128.

Perrin, D.D., W.L.F. Armarego and D.R. Perrin (1980) *Purification of Laboratory Chemicals, 2nd Edition*. Pergamon Press, Oxford, 568 pp.

Scheer, H. (1991) *Chlorophylls*. CRC Press, Boca Raton, 1257 pp.

Simpson, D.J. and K.M. Smith (1988) Ascorbic Acid Photoreductions of Zinc(II) Chlorophyll Derivatives: Access to Metal-Free Isobacteriochlorins. *Journal of the American Chemical Society*, **110**: 2854-2861.

Smith, N.W. and K.M. Smith (1990) Preparation of Bacteriopetroporphyrins by Partial Synthesis from the *Chlorobium* Chlorophylls. *Energy & Fuels*, **4**: 675-688.



Verne-Mismer, J. (1988) Petroporphyrines Dans les Schistes Bitumineux Marocains de Timahdit et des Oulad Abdoun: Etude Structurale et Signification Geochimique. PhD, De L'Universite Louis Pasteur de Strasbourg.



### 4.1 Abstract

The single published study exploring chlorophyll-whole plant N and C isotopic relationships suggests that both chlorophyll  $\delta^{13}\text{C}$  and  $\delta^{15}\text{N}$  are linearly related to the  $\delta^{13}\text{C}$  and  $\delta^{15}\text{N}$ , respectively, of the whole plant from which the chlorophyll was extracted (Bidigare, et al., 1991; Kennicutt II, et al., 1992). That study included six higher plants. This study was undertaken in order to establish the chlorophyll-cell N and C isotopic relationships for phytoplankton. Fourteen axenic batch cultures of phytoplankton, representing 8 species, were grown under nutrient-replete conditions and the N and C isotopic composition of the chlorophyll from each was compared to the isotopic composition of the whole cells. A constant relationship was found for both isotopes. Chlorophyll nitrogen was depleted in  $^{15}\text{N}$  by 5.0 per mil (SD = 2.1, n = 14), while chlorophyll carbon was depleted in  $^{13}\text{C}$  by 0.1 per mil (SD = 2.9, n = 13) relative to whole cells. The large standard deviation of the average for N is explained in terms of inter-species differences in the partitioning of N between non-protein biochemicals. Repeat culture experiments suggest the precision of the method is 0.57 and 1.25 per mil, respectively, for  $\Delta\delta^{15}\text{N}_{\text{cell-Chla}}$  and  $\Delta\delta^{13}\text{C}_{\text{cell-Chla}}$  determinations in cultured marine phytoplankton. When results are averaged by species,  $\Delta\delta^{15}\text{N}_{\text{cell-Chla}} = 5.16 \pm 2.40$  per mil for N; and  $\Delta\delta^{13}\text{C}_{\text{cell-Chla}} = -0.02 \pm 2.12$  for C.



## 4.2 Introduction

Stable N and C isotope ratios in marine particles and sediments have been used for the past four decades to understand the cycling of the major nutrients between geologic and biologic pools. The timescales of processes studied range from  $10^{-2}$  (e.g., phytoplankton blooms) (Altabet, et al., 1991) to  $10^9$  years (e.g., organic carbon burial since the Precambrian) (Knoll and Walter, 1992). Frequently what is sought with these measurements is the N or C isotopic ratio of primary producers, or phytoplankton--those organisms that exist at the interface between the geologic and the biologic realms. As a result of heterotrophy and diagenetic alteration primary isotopic signals can be altered significantly (DeNiro and Epstein, 1978; DeNiro and Epstein, 1981; Montoya, 1994; Wada, 1980). For this reason biogeochemists interested in nitrogen and carbon cycling have, over the last 10 years, begun to make isotopic measurements on biomarkers, or molecular fossils having known origins (Hayes, et al., 1990; Hayes, et al., 1989; Hayes, et al., 1987).

Sixty years ago Alfred Treibs identified the first biomarker, deoxyphylloerythroetioporphyrin (DPEP), a compound he believed derived from chlorophyll *a* (figure 1.3) (Treibs, 1936). More recent work has confirmed his proposed degradative pathway (Baker and Louda, 1986; Boreham, et al., 1989; Keely, et al., 1990; Krane, et al., 1983). Chlorophyll is a ubiquitous light-harvesting pigment found in all algae. Although rapidly degraded during senescence, light exposure, grazing, and microbial action (Sun, et al., 1991; Sun, et al., 1993; Welschmeyer and Lorenzen, 1985), the colored chlorophyll degradation products shown in figure 1.3, (i.e., chlorophyllides, pheophytins, pheophorbides, and porphyrins) tend to be more resilient than chlorophyll *a*, and can be recovered from marine particles and sediments (Louda and Baker, 1986). Their

ubiquity amongst algae and resistance to decomposition suggest that the chlorins may be an ideal tracer of algal  $\delta^{15}\text{N}$  and  $\delta^{13}\text{C}$  in particulate matter and sediments.

In order to use chlorin  $\delta^{15}\text{N}$  and  $\delta^{13}\text{C}$  as proxies for algae it must be established that a predictable relationship between the biomarker isotopic composition and that of the whole cell exists. This relationship had been explored by Kennicutt, et al (1992) in six terrestrial plants--ragweed, parsley, Brussels sprouts, sorghum, Bermuda grass and Johnson grass--and found to be linear for both nitrogen ( $\delta^{15}\text{N}_{\text{bulk}} = (1.30)\delta^{15}\text{N}_{\text{Chl } a} - 0.40$ ,  $r^2 = 0.90$ ,  $n = 6$ ) and carbon ( $\delta^{13}\text{C}_{\text{bulk}} = (0.97)\delta^{13}\text{C}_{\text{Chl } a} - 1.88$ ,  $r^2 = 0.95$ ,  $n = 6$ ). In addition, R. Goericke performed N isotopic measurements on semi-purified chlorophyll *a* from 5 species of phytoplankton grown in chemostats (e.g., continuous cultures). He, too, found a linear relationship between chlorophyll and whole-cell  $\delta^{15}\text{N}$  ( $\delta^{15}\text{N}_{\text{bulk}} = (1.12)\delta^{15}\text{N}_{\text{Chl } a} + 5.12$ ,  $r^2 = 0.70$ ,  $n = 5$ ). However, no  $\delta^{13}\text{C}$  measurements were performed and information regarding chlorophyll purity was not available. Our objective, then, was to firmly establish whether a predictable relationship exists between chlorophyll and whole-cell  $\delta^{15}\text{N}$  and  $\delta^{13}\text{C}$  in marine phytoplankton.

Toward this end we grew 14 axenic batch cultures of marine phytoplankton and measured the N and C isotopic difference between chlorophyll and whole cells. Results are presented for both carbon and nitrogen isotopes. The focus of the discussion, though, is nitrogen isotopes, since the primary goal of this thesis is to introduce chlorophyll  $\delta^{15}\text{N}$  as a paleoenvironmental tracer.



## 4.3 Methods

### 4.3.1 Culturing Procedures

Fourteen individual batch cultures of marine algae were grown on four occasions over the course of 17 months. Ten of the seed cultures were obtained directly from the Provasoli-Guillard National Center for Culture of Marine Phytoplankton (CCMP) at the Bigelow Laboratory for Ocean Sciences, West Boothbay Harbor, Maine 04575 (table 4.1). Three of the other four seed cultures were provided by Dr. Joseph Montoya (Harvard University), and the fourth was provided by Dr. John Waterbury (WHOI). In all cases but one--synechococcus, for which SN2 medium was used-- f/2 medium (table 4.2) (Guillard, 1975) was used.

Table 4.1: description of cultures and used in this study.

Species	Clone	Class	Common Name	Abbrev.	Name	Origin	Date	Size	Medium	d15N-NO3	L:D	T	SW Origin	Growth Phase	Cell d15N
<i>Thalassiosira weissflogii</i>	TW	Bacillariophyceae	Diatom	TW1	Dr. Montoya	6/22-7/5/94	20 L	f/2	3.6	3.05	12:12	18	Nahant, MA		0.55
<i>Emiliania huxleyi</i>	CCMP1516	Prymnesiophyceae	Coccolithophorid	EH1	Dr. Montoya	6/22-7/5/94	20 L	f/2	3.6	5.8	12:12	18	Nahant, MA		-2.2
<i>Isochrysis galbana</i>	T-Iso	Haptophyceae	Brown Flagellate	IG1	Dr. Montoya	6/22-7/5/94	20 L	f/2	3.6	9.5	12:12	18	Nahant, MA		-5.9
<i>Amphidinium carterae</i>	CCMP1314	Dinophyceae	Dinoflagellate	AMP2	CCMP	5/15-5/26/95	20 L	f/2	2	5.1	12:12	18	Vineyard Sound, MA	Stationary	-3.1
<i>Dunaliella tertiolecta</i>	CCMP1320	Chlorophyceae	Green Alga	DUN2	CCMP	5/11-5/17/95	20 L	f/2	2	6.1	12:12	18	Vineyard Sound, MA	Exponential	-4.1
<i>Pavlova lutheri</i>	CCMP1325	Prymnesiophyceae	Coccolithophorid	PAV2	CCMP	5/11-5/17/95	20 L	f/2	2	0.35	12:12	18	Vineyard Sound, MA	Exponential	1.65
<i>Phaeodactylum tricornutum</i>	CCMP630	Bacillariophyceae	Diatom	PHA2	CCMP	5/11-5/16/95	20 L	f/2	2	3.55	12:12	18	Vineyard Sound, MA		-1.55
<i>Synechococcus</i>	WH7803		Cyanobacterium	SYN2	Dr. Waterbury	5/22-6/6/95	3 X 1 L	SN2	2	-1.88	12:12	18	Vineyard Sound, MA		3.88
<i>Isochrysis galbana</i>	CCMP1323	Prymnesiophyceae	Haptophyte	IG3	CCMP	7/26-8/8/95	2 X 1 L	f/2	2	0.7	24:0	24	Vineyard Sound, MA		1.3
<i>Thalassiosira weissflogii</i>	CCMP1336	Coccolithophyceae	Diatom	TW4	CCMP	11/1-11/8/95	2 X 1.5	f/2	2	2.75	24:0	Rm T	Vineyard Sound, MA	Stationary	-0.75
<i>Phaeodactylum tricornutum</i>	CCMP630	Bacillariophyceae	Diatom	PHA4	CCMP	11/1-11/8/95	3 X 1 L	f/2	2	1.7	24:0	Rm T	Vineyard Sound, MA	Exponential	0.3
<i>Dunaliella tertiolecta</i>	CCMP1320	Chlorophyceae	Green Alga	DUN4	CCMP	11/1-11/8/95	3 X 1 L	f/2	2	2.1	24:0	Rm T	Vineyard Sound, MA	Stationary	-0.1
<i>Pavlova lutheri</i>	CCMP1325	Prymnesiophyceae	Coccolithophorid	PAV4	CCMP	11/1-11/9/95	2 X 1.5	f/2	2	9.3	24:0	Rm T	Vineyard Sound, MA	Stationary	-7.3
<i>Amphidinium carterae</i>	CCMP1314	Dinophyceae	Dinoflagellate	AMP4	CCMP	11/1-11/10/95	2 X 1.5	f/2	2	0.15	24:0	Rm T	Vineyard Sound, MA	Stationary	1.85



Table 4.2 Composition of f/2 Medium (Guillard, 1975)

Nutrient Salt	Concentration
NaNO <sub>3</sub>	883 $\mu$ M
NaH <sub>2</sub> PO <sub>4</sub> ·H <sub>2</sub> O	36.3 $\mu$ M
Na <sub>2</sub> SiO <sub>3</sub> ·9H <sub>2</sub> O	54 $\mu$ M
Na <sub>2</sub> ·EDTA	11.7 $\mu$ M
FeCl <sub>3</sub> ·6H <sub>2</sub> O	11.7 $\mu$ M
CuSO <sub>4</sub> ·5H <sub>2</sub> O	0.04 $\mu$ M
ZnSO <sub>4</sub> ·7H <sub>2</sub> O	0.08 $\mu$ M
CoCl <sub>2</sub> ·6H <sub>2</sub> O	0.05 $\mu$ M
MnCl <sub>2</sub> ·4H <sub>2</sub> O	0.9 $\mu$ M
Na <sub>2</sub> MoO <sub>4</sub> ·2H <sub>2</sub> O	0.03 $\mu$ M
Thiamin·HCl	0.1 mg/L
Biotin	0.5 $\mu$ g/L
Vitamin B <sub>12</sub>	0.5 $\mu$ g/L

Care was taken to ensure cultures remained axenic. (Such precautions were required since the filtered medium at harvest was used for the determination of algal cell isotopic compositions.) For instance, seed cultures were axenic; all glassware, tubing, air filters, stoppers, beakers and bungs were autoclaved before use; seawater for the medium was either 0.2  $\mu$ m-filtered, or 0.2  $\mu$ m-filtered then autoclaved; stock solutions of nutrients, vitamins, and trace metals were autoclaved; culture flasks were inoculated and sampled in a laminar flow bench; stoppers, screw caps, test tubes, forceps, and pipets were flamed before and after use. Large (20 L) carboys were stoppered with silicone rubber stoppers through which glass inlet and vent tubes were inserted.

Fernbach and erlenmeyer flasks were covered with either a gauze-wrapped cotton bung or an inverted beaker. Light microscopy (backlit, 400x magnification) was used occasionally to inspect cultures for the presence of bacteria (D. Kulis, personal communication), which were not observed.

Five of the 14 cultures were harvested during the stationary phase of growth, while 3 of the 14 were harvested during the exponential growth phase (table 4.1). Growth phase was estimated either by *in situ* fluorescence or absorption. The latter consisted of measuring the absorption, at 6 wavelengths in the visible spectrum, of an aliquot of medium. Absorption was assumed to correspond to cell density, and cultures were harvested when a plot of absorption versus time attained a zero slope (figure 4.1).

Eight of the 14 cultures were grown on a 12 hr light-12 hr dark cycle at 18°C, while six were grown on a 24 hour light cycle at room temperature (~20-25°C) (see table).

Culture vessels were either 2.5 L Pyrex low form culture flasks, 2.8 L Fernbach flasks, or 20 L Pyrex carboys. All flasks were leached with 10% HCl for at least 3 days prior to use, then rinsed (3x) with tap water and (3x) with distilled water. The seven cultures grown in 20 L carboys were bubbled vigorously with laboratory air that had been passed sequentially through either (1) activated charcoal and a 0.2 µm filter, or (2) 1 M H<sub>3</sub>PO<sub>4</sub>, glass wool, distilled water, and glass wool. The smaller cultures were agitated by swirling at least twice daily.

For the 20 L cultures, the 15 mL seed cultures received from CCMP (or other sources) were first transferred to 1 L of f/2 medium and incubated for 1-2 weeks before being added to the carboys. Carboys were allowed to equilibrate with the bubbling air for at least 24 hours before the 1 L inoculants were added.



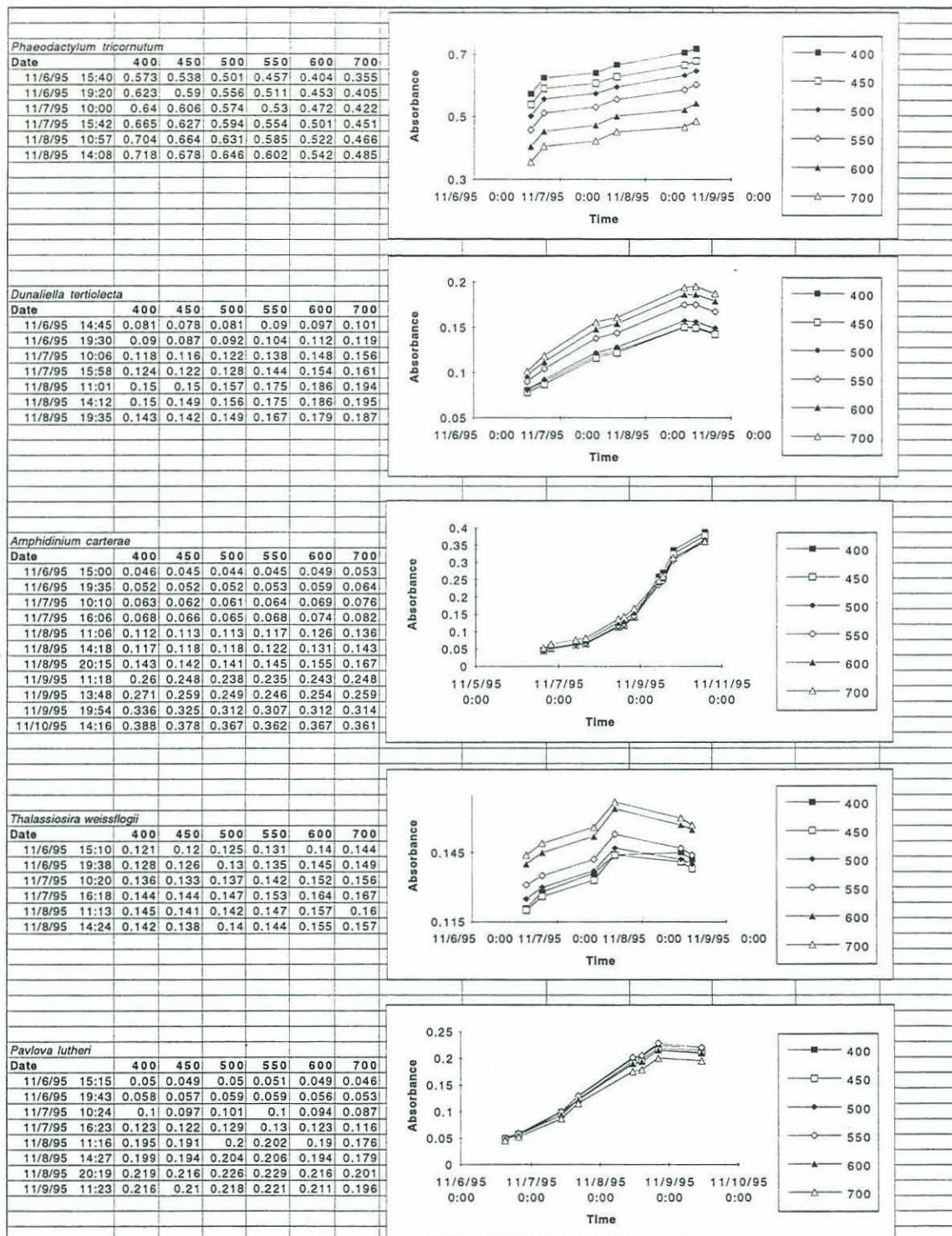


Figure 4.1: Visible absorption spectra of 5 phytoplankton cultures over time. Absorption was measured at 400, 450, 500, 550, 600, and 700 nm and was assumed to correspond to cell density.



#### 4.3.2 Chlorophyll Purification

The procedures for the purification of chlorophyll from cultured phytoplankton are discussed in detail in chapter 2. Therefore only a brief account will be given here.

Cultures were harvested by vacuum-filtration through a pre-combusted (450°C, > 8 hours) 293 mm Gelman A/E filter. In all but 3 cases, filters were immediately stored in liquid nitrogen until extraction. Otherwise they were stored at -20°C. Just prior to extraction, filters were thawed at room temperature and 2x1 cm subsamples were removed for whole-cell  $\delta^{15}\text{N}$  and  $\delta^{13}\text{C}$  determinations using a cork-borer. Filters were ultrasonically extracted by probe (3x) in 125 mL degassed acetone to which had been added approximately 5 g  $\text{NaHCO}_3$  (for neutralization of extract to prevent chlorophyll demetallation). The extracts were filtered through a 47 mm GF/F filter, and the filtrate was sparged with  $\text{N}_2$  during subsequent extractions. The combined extracts (500 mL) were poured into a 2 L separatory funnel containing 125 mL water, and the chlorophyll was partitioned (3x) into 200 mL hexane. The chlorophyll in both the combined hexane fractions and the aqueous fraction was then quantified spectrophotometrically. Typically, no chlorophyll *a* remained in the aqueous fraction.

The combined hexane fractions (800 mL) were then back-extracted (1x) with 200 mL 15/85  $\text{H}_2\text{O}/\text{MeOH}$  to remove carotenoids. The chlorophyll was then re-quantified in both the hexane and aqueous fractions.

Demetallation of the chlorophyll to pheophytin was accomplished in a third phase-separation by adding 200 mL 10%  $\text{HCl}$  (aq) to the hexane fraction and shaking for 1 minute. The color of the hexane solution changed from emerald to pine green. The aqueous fraction was poured off and the hexane

neutralized with 100 mL 2% (w/v) NaHCO<sub>3</sub> (aq). The hexane phase was then dried over Na<sub>2</sub>SO<sub>4</sub>, and rotary-evaporated to dryness. A final spectrophotometric quantification was performed before the dried extract was stored under nitrogen at -20°C.

Further purification of the pheophytin *a* was achieved using preparative reversed-phase (C<sub>18</sub>) HPLC, followed by isocratic normal-phase (SiO<sub>2</sub>) HPLC on an analytical column. (For specific columns and conditions, please refer to chapter 2).

#### 4.3.3 Purity of Chlorophyll Isolated from Phytoplankton

The purity of the chlorophyll isolated from 6 of the 14 cultures was determined by performing CHN analyses on spectrophotometrically-quantified aliquots (see chapter 2). Nitrogen purity (i.e., the total nitrogen in the sample attributable to chlorins) averaged  $95.9 \pm 3.4\%$ . Carbon purity averaged  $91.2 \pm 4.3\%$ .

#### 4.3.4 Isotope Analyses

The procedures for the preparation of samples for isotopic determination are detailed in chapter 3. Therefore, only a brief account will be given here.

Purified chlorophyll was transferred to 8x6 mm smooth wall tin capsules (Elemental Microanalysis, Manchester, MA, cat # D4066) in a small volume (<200 µL) of acetone and dried under a 60 W light bulb. The Sn cups were then folded with forceps and stored in a dessicator until isotopic analysis.



The filter subsamples for whole-cell isotopic analysis were dried at 60°C, then placed into 5x9 mm Sn boats (Elemental Microanalysis, Manchester, MA) which were folded with forceps and stored in a dessicator until isotopic analysis.

All isotope values were obtained at the Stable isotope Laboratory at the Marine Biological Laboratory, Woods Hole, MA 02543. The facility consists of a Heraeus CHN Rapid Elemental Analyzer and a Finnigan MAT delta S isotope ratio mass spectrometer coupled by an automated "trapping box" for the sequential cryogenic purification of CO<sub>2</sub> and N<sub>2</sub> (Fry, et al., 1992). This system allows the determination of both  $\delta^{15}\text{N}$  and  $\delta^{13}\text{C}$  on the same sample.

Standard delta notation is used for reporting stable isotopic ratios of nitrogen and carbon. It is defined as

$$\delta^n X \equiv \left[ \frac{(^n X / ^{(n-1)} X)_{\text{Sample}}}{(^n X / ^{(n-1)} X)_{\text{Std}}} - 1 \right] \times 1000 \text{‰}$$

where  $^n X = ^{15}\text{N}$  or  $^{13}\text{C}$ . The carbon isotopic standard is Peedee Belemnite (Craig, 1953), a limestone that has been assigned a  $\delta^{13}\text{C}$  value of 0.0 per mil. The isotopic standard for nitrogen is atmospheric N<sub>2</sub> (e.g., air; Hoering, 1955), which has been assigned a  $\delta^{15}\text{N}$  value of 0.0 per mil. Therefore, positive delta values arise when a sample is enriched in the heavy isotope relative to the standard, and negative delta values occur when a sample is depleted in the heavy isotope relative to the standard.

Differences of delta values will be reported in "delta-del" notation. Specifically,

$$\Delta \delta^n X \equiv \delta^n X_{\text{Bulk}} - \delta^n X_{\text{Biomarker}}$$

where  $^n X = ^{15}\text{N}$  or  $^{13}\text{C}$ . Bulk refers to the unaltered material from which the biomarker was extracted (i.e., plant, sediment or filtered particulate matter), and the biomarker is the purified pigment (i.e., chlorophyll *a* or other chlorin).



#### 4.3.5 Precision of the Analysis

The precision of the entire procedure for determining  $\Delta\delta^{15}\text{N}_{\text{cell-Chla}}$  -- including culturing steps, chlorophyll purification steps and isotope-ratio determinations of both the particulate and chlorophyll fractions--is 0.57 per mil for N and 1.25 per mil for C. These values represent the pooled standard deviations of replicate cultures of six (five for C) algal species (table 4.3). This quantity is defined as

$$\text{pooled standard deviation} = \sqrt{\frac{\sum (n_i - 1) \sigma_i^2}{\sum (n_i - 1)}}$$

where  $\sigma$  is the standard deviation and  $n$  is the number of replicates of the  $i$ th algal species. The replicates, always cultured on separate occasions, were conducted over a 17 month period. The culturing took place in 3 locations: The Harvard Biological Laboratories (Dr. Joseph Montoya's laboratory), Redfield Laboratory, WHOI (Dr. Don Anderson's laboratory), and Fye Laboratory, WHOI (Dr. Daniel Repeta's laboratory). The only factor held constant over the time period was the composition of the growth medium (table 4.1). No attempt was made to hold light intensity, temperature, pH, culture density, growth phase at harvest, culture flask geometry, light-dark cycle, or aeration rate constant from one experiment to the next. The isotopic composition of the  $\text{NO}_3^-$  used for the first three cultures listed in the table was 3.6 per mil. In the other 11 culture experiments the nitrate  $\delta^{15}\text{N}$  was 2.0 per mil.

The measurement precision for  $\delta^{15}\text{N}$  determinations is 0.72 per mil. This is a pooled standard deviation of 21 replicate analyses of PON and purified chlorophyll samples (table 4.3). The measurement precision for  $\delta^{13}\text{C}$  determinations is 1.10 per mil, which is a pooled standard deviation of 23 POC and purified chlorophyll replicates (table 4.3). The replicates are either (1) subsamples of a glass fiber filter (Gelman A/E or Whatman GF/F) used to

harvest the cultures, or (2) splits of the purified chlorophyll (after chromatography). Thus, it represents the combined errors and artefacts introduced during sample preparation for mass spectrometry--e.g., drying, placement into and folding of Sn cup, evaporation of solvent, storage, and internal machine precision.

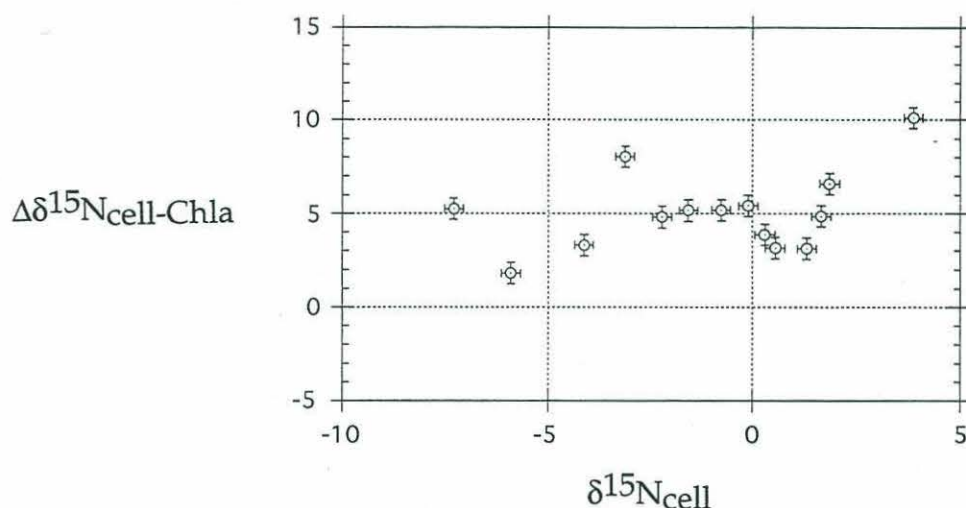
## 4.4 Results

### 4.4.1 Nitrogen Isotopes

When the nitrogen isotopic composition of purified chlorophyll from 14 cultures representing 5 classes and 8 species of marine algae is compared to the  $\delta^{15}\text{N}$  of the whole cells (e.g., bulk PON) a constant relationship is found. A linear regression analysis of  $y$  on  $x$ , or  $\Delta\delta^{15}\text{N}_{\text{cell-Chl}a}$  on  $\delta^{15}\text{N}_{\text{cell}}$ , yields a slope,  $m = 0.27$  and an intercept,  $b = 5.34$  with a correlation coefficient,  $r^2 = 0.15$  (figure 4.2). The  $y$ -error bar is the method precision of 0.57 per mil--the pooled standard deviation of replicate culture experiments on 6 algal species. The  $x$ -error bar is 0.23 per mil, which is the pooled standard deviation of 11 sets of replicate  $\delta^{15}\text{N}_{\text{PON}}$  determinations. The slope is not statistically different from zero (95% confidence interval (CI) for  $m = -0.10$  to  $0.63$ ), and the correlation coefficient is low. If a zero slope is assumed then the chlorophyll-cell N isotopic relationship for the 14 phytoplankton cultures is  $\Delta\delta^{15}\text{N}_{\text{cell-Chl}a} = 5.04 (\pm 2.15)$ . There is no dependence of  $\Delta\delta^{15}\text{N}$  on  $\delta^{15}\text{N}$ . In other words, on average, chlorophyll *a* is depleted by 5.04 per mil relative to the whole cell. The large standard deviation of this average (e.g., 2.15 per mil), as will be discussed below, appears to result from inter-species differences in the partitioning of N between non-protein biochemicals; not from variability between replicate culture



experiments, since the precision of the procedure, based on replicate analyses of 6 algal species, is 0.57 per mil.



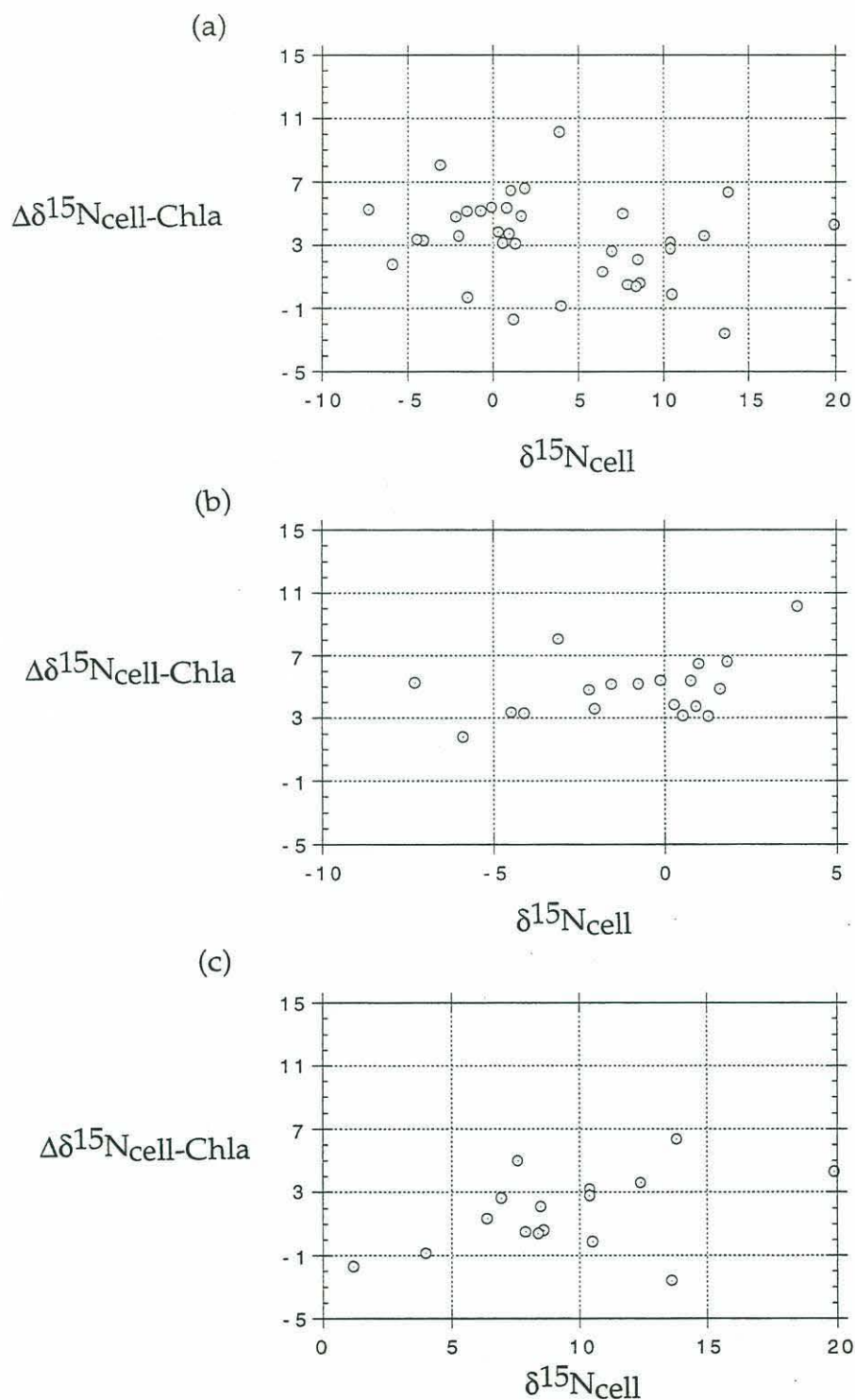
**Figure 4.2:** Plot of  $\Delta\delta^{15}\text{N}_{\text{cell-Chla}}$  vs  $\delta^{15}\text{N}_{\text{cell}}$  for the 14 algal cultures grown in this investigation. The y-error bar, 0.57 per mil, is the method precision for chlorophyll  $\delta^{15}\text{N}$  determinations in cultured phytoplankton. The x-error bar, 0.23 per mil, is the precision of  $\delta^{15}\text{N}_{\text{PON}}$  determinations in this study.

Table 4.3 shows the results of all known chlorophyll  $\delta^{15}\text{N}$  analyses from plants and cultures to date. The 35 data points consist of (1) 14 marine phytoplankton and one marine macroalga (*Fucus* sp. from Vineyard Sound, MA) from this study, (2) 5 marine phytoplankton from Dr. Ralf Goericke (personal communication), and (3) 10 terrestrial plants, 5 marine grasses, and one alga from Drs. R. Bidigare, M. Kennicutt, and S. Macko (Bidigare, et al., 1991; Kennicutt II, et al., 1992) (R. Bidigare, personal communication). The results of a linear regression of y on x, or  $\Delta\delta^{15}\text{N}$  on  $\delta^{15}\text{N}$ , for all the data, are  $m = -0.11$  (95% CI = -0.252 to 0.035),  $b = 3.74$  (2.70 to 4.77),  $r^2 = 0.06$  (Figure 4.3.a). Again the slope is not statistically different than zero and the correlation coefficient is low. The average  $\Delta\delta^{15}\text{N}_{\text{cell-Chla}}$  for



Sample	Avg Cell d15N	SD-Cell d15N	n-Cell d15N	Avg Chl d15N	SD-Chl d15N	n-Chl d15N	Dd15Ncell-chl	Avg Cell d13C	SD-Cell d13C	n-Cell d13C	Avg Chl d13C	SD-Chl d13C	n-Chl d13C	Dd13Ccell-chl
Sachs C#1														
IG1	0.55	0.07	2	-2.6	1.75	3	3.15	-10.75	0.07	2	-10.3	0.72	3	-0.45
TW1	-2.2	0.28	2	-7	1.01	3	4.80	-8.25	0.84	2	-8.2	0.62	3	-0.05
EH1	-5.9	0.14	2	-7.7	1.27	2	1.80	-11.1	0.14	2	-16.2	1.27	2	5.10
Sachs C#2														
PHA2	-3.1	0	2	-11.15	0.07	2	8.05	-9.15	0.07	2	-5.8	0	2	-3.35
PAV2	-4.1	0	2	-7.4	0.42	2	3.30	-16.2	0.14	2	-12.95	0.07	2	-3.25
DUN2	1.65	0.21	2	-3.2	0.1	3	4.85	-24.1	0	2	-24.6	0	3	0.50
AMP2	-1.55	0.07	2	-6.7	1.41	2	5.15	-24.75	0.07	2	-27	0.14	2	2.25
SYN2	3.88	0.64	2	-6.25	0.21	2	10.13	-15.65	0.78	2	-18.2	0	2	2.65
Sachs C#3														
IG3	1.3		1	-1.8		1	3.10	-14		1	-10.9		1	-3.10
Sachs C#4														
AMP4	-0.75	0.07	2	-5.93	1.19	3	5.18	-3.55	1.34	2	-14.13	2.6	3	10.58
DUN4	0.3	0	2	-3.55	0.07	2	3.85	-16.2	1.13	2	-20.2	1.56	2	4.00
PAV4	-0.1		1	-5.5		1	5.40	-14.5		1	-11.6		1	-2.90
TW4	-7.3		1	-12.55	0.21	2	5.25	-11.6		1	-13.05	0.07	2	1.45
PHA4	1.85	0.07	2	-4.75	0.35	2	6.60	-9.25	0.07	2	-7.75	3.04	2	-1.50
Sachs Fucus														
Fucus	6.96		1	4.33	0.1	4	2.63							
Sachs AVG		Measure. Precision		Method Precision		Meas. Prec.	5.04		Measure. Precision		Method Prec.		Meas. Prec.	0.10
Sachs Pooled SD		0.23		0.57		0.72	2.15		0.61		1.25		1.10	2.86
Sachs n		11		6		21	14.00		11		5		23	13.00
Goericke							>Not a pooled SD				>Excl AMP4			>Not a pooled SD
IG-G	-2.04		1.00	-5.629		1.00	3.59							>excl AMP4
CYC-G	1.022		1.00	-5.448		1.00	6.47							
TW-G	-4.481		1.00	-7.861		1.00	3.38							
DUN-G	0.946		1.00	-2.783		1.00	3.73							
AMP-G	0.787		1.00	-4.591		1.00	5.38							
Goericke AVG							4.51							
Goericke SD							1.35							
Goericke n							5.00							
Kennicutt, et al (1992)														
RAK-K	7.90			7.4			0.50	-30.1			-25.35			-4.75
PAR-K	4.00			4.85			0.85	-27.7			-27.25			-0.45
BS-K	8.60			8			0.60	-25			-24.65			-0.35
SOR-K	6.40			5.05			1.35	-16.3			-15.3			-1.00
BQ-K	19.90			15.6			4.30	-16.5			-15.55			-0.95
JK-K	13.80			7.45			6.35	-18.3			-15.85			-2.45
IG-K	-1.5			-1.2			-0.30	-13.5			-12.2			-1.30
Bidigare (para. comm.)														
Spinach	7.6			2.60			5.00							
Brussel Sprouts	8.4			8.00			0.40							
Spinach (org)	13.6			16.20			-2.60							
Spinach (reps)	1.2			2.90			-1.70							
Eel Grass	10.4			7.20			3.20							
Eel Grass	10.4			7.60			2.80							
Eel Grass	12.4			8.80			3.60							
Saicomia	10.5			10.60			-0.10							
Spartina	8.5			6.40			2.10							
Gallimov and Shirinsky (1975)														
Anabaena								-27.3			-28.4			1.10
Lupin								-27.6			-29.5			1.90
Laminaria								-18.2			-21.6			3.40
Phytoplankton AVG							4.90							0.10
Phytoplankton SD							1.95							2.86
Phytoplankton n							19.00							13.00
Higher Plant AVG							1.72							>excl AMP4
Higher Plant SD							2.47							-1.66
Higher Plant n							16.00							1.69
AlI AVG							3.35							>excl IG-K
AlI SD							2.73							-0.16
AlI n							35.00							2.58
														23.00
														>excl AMP4

Table 4.3: Compilation of all paired nitrogen and carbon isotopic measurements in plants and algae from this study and the literature.



**Figure 4.3: Plot of  $\Delta\delta^{15}\text{N}_{\text{cell-Chla}}$  vs  $\delta^{15}\text{N}_{\text{cell}}$  for all known paired chlorophyll and bulk  $\delta^{15}\text{N}$  determinations in (a) plants, (b) marine phytoplankton, and (c) higher plants.**

all 35 data points is  $3.35 (\pm 2.73)$ .

When just the marine phytoplankton are considered (e.g., data of Sachs and Goericke) the linear regression analysis of  $\Delta\delta^{15}\text{N}$  on  $\delta^{15}\text{N}_{\text{cell}}$  yields  $m = 0.28$  (-0.02 to 0.57),  $b = 5.18$  (4.29 to 6.07),  $r^2 = 0.17$  (Figure 4.3.b). Since the slope is not significantly different than zero and the correlation coefficient is low, the assumption of a zero slope allows the average marine phytoplankton  $\Delta\delta^{15}\text{N}_{\text{cell-Chla}}$  to be determined, and this value is  $4.90 (\pm 1.95, n = 19)$ .

When just the higher plant data are considered a linear regression analysis of  $\Delta\delta^{15}\text{N}$  on  $\delta^{15}\text{N}_{\text{cell}}$  for the 16 data points reveals  $m = 0.27$  (-0.01 to 0.54),  $b = -0.78$  (-3.57 to 2.02),  $r^2 = 0.21$  (figure 4.3.c). Since the slope is not significantly different than zero and the correlation coefficient is low, then a zero-slope assumption yields the relationship  $\Delta\delta^{15}\text{N}_{\text{cell-Chla}} = 1.72 (\pm 2.47, n = 16)$ .

It should be noted (1) that the data from Bidigare, et al averages isotope values for chlorophylls *a* and *b*, and (2) that the chlorophyll purification procedure used by Goericke is unpublished and relies solely on phase extractions without chromatography (R. Goericke, personal communication).

#### 4.4.2 Carbon Isotopes

When the carbon isotopic composition of purified chlorophyll from 13 cultures representing 5 classes and 8 species of marine algae is compared to the  $\delta^{13}\text{C}$  of the whole cells (e.g., bulk POC) a constant relationship is found. Specifically, a linear regression analysis of  $\Delta\delta^{13}\text{C}_{\text{cell-Chla}}$  on  $\delta^{13}\text{C}_{\text{cell}}$  yields a slope,  $m = -0.12$  and an intercept,  $b = -1.62$  with a correlation coefficient,  $r^2 = 0.05$  (figure 4.4.a). The y-error bar, 1.25 per mil, represent the precision of the  $\Delta\delta^{13}\text{C}_{\text{cell-Chla}}$  determination on 5 sets of replicate culture



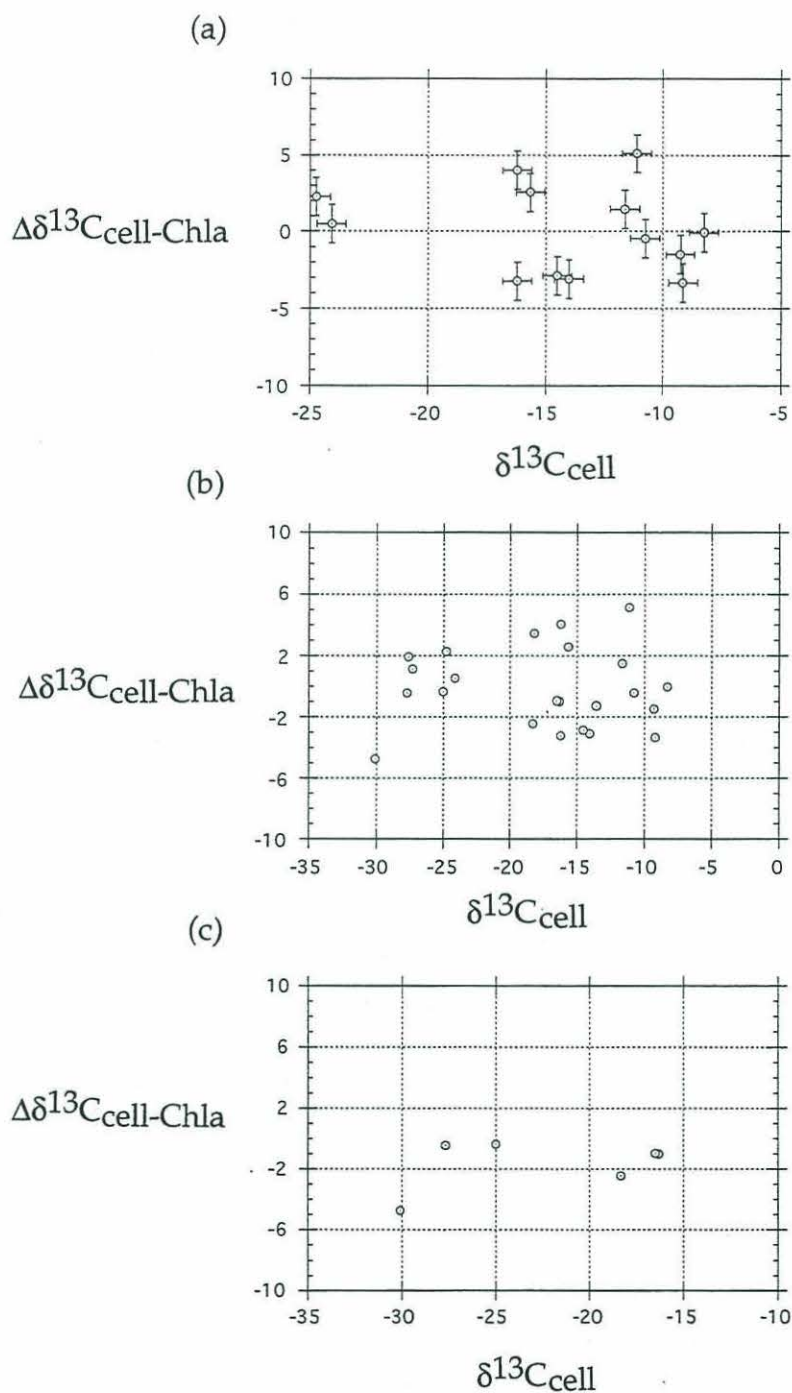


Figure 4.4: Plot of  $\Delta\delta^{13}\text{C}_{\text{cell-Chla}}$  vs  $\delta^{13}\text{C}_{\text{cell}}$  for (a) algal cultures grown in this study, (b) all plants and algae from this study and the literature, and (c) only the higher plants from (b). The x- and y-error bars are, respectively, the precision for POC and chlorophyll  $\delta^{13}\text{C}$  determinations in this study.

experiments, and the x-error bars, 0.61 per mil, represent the precision of the isotope determination on 11 sets of replicate POC samples. However, the slope is not statistically different than zero (95% confidence interval (CI) for  $m = -0.20$  to  $0.44$ ), and the correlation coefficient is low. If a zero slope is assumed then the chlorophyll-cell carbon isotopic relationship for the 13 phytoplankton cultures is  $\Delta\delta^{13}\text{C}_{\text{cell-Chla}} = 0.10 (\pm 2.86)$ . On average, then, chlorophyll  $a$  in the 8 species of marine phytoplankton studied here has the same carbon isotopic composition as the whole cell.

Table 4.3 shows the results of all available chlorophyll  $\delta^{13}\text{C}$  analyses from plants and cultures to date. The 24 data points are comprised of (1) 14 marine phytoplankton from this study, (2) 6 terrestrial plants and one alga from Kennicutt et al. (Bidigare, et al., 1991; Kennicutt II, et al., 1992), and (3) 3 plants from Galimov et al (Bogacheva, et al., 1979; Galimov and Shirinsky, 1975). The results of a linear regression analysis of  $\Delta\delta^{13}\text{C}$  on  $\delta^{13}\text{C}$  for all the data (excluding AMP4, which is considered an outlier) are  $m = -0.007$  (95% CI =  $-0.16$  to  $0.17$ ),  $b = -0.29$  ( $-2.85$  to  $3.43$ ),  $r^2 = 0.0004$  (figure 4.4.b). Again the slope is not significantly different than zero and the correlation coefficient is low. The average  $\Delta\delta^{13}\text{C}_{\text{cell-Chla}}$  for all 23 data points is  $-0.16 (\pm 2.58)$ .

When just the higher plant data are considered (e.g., data of Bidigare, et al (1991) and Kennicutt, et al. (1992)), a linear regression analysis of  $\Delta\delta^{13}\text{C}$  on  $\delta^{13}\text{C}$  for the 6 data points reveals  $m = 0.10$  ( $-0.16$  to  $0.36$ ),  $b = 0.65$  ( $-5.32$  to  $6.62$ ),  $r^2 = 0.14$  (figure 4.4.c). Since the slope is not significantly different than zero and the correlation coefficient is low, then a zero-slope assumption yields the relationship  $\Delta\delta^{13}\text{C}_{\text{cell-Chla}} = -1.66 (\pm 1.69, n = 6)$ .

It should be noted (1) that the data from Bidigare et al averages isotope values for chlorophylls  $a$  and  $b$ , and (2) that the data from Galimov et al does

not specify which type of chlorophyll was used or what the purity of that chlorophyll was.

## 4.5 Discussion

### 4.5.1 Nitrogen Isotopes

The 14 culture experiments with 8 different species of marine phytoplankton indicates that chlorophyll  $\delta^{15}\text{N}$  is, on average, 5.04 ( $\pm 2.15$ ,  $n = 14$ ) per mil depleted in  $^{15}\text{N}$  relative to total cellular nitrogen. Therefore, chlorophyll  $\delta^{15}\text{N}$  values in marine particulates and sediments can be used to determine algal  $\delta^{15}\text{N}$  values in contemporary and historical marine environments by adding 5 per mil. In this way the large and variable isotopic alteration of algal material during decomposition processes (i.e., senescence, grazing, remineralization) (Altabet, 1988; DeNiro and Epstein, 1981; Montoya, 1994; Wada, 1980) can be circumvented. Moreover, the isotopic difference between bulk material (i.e., sediments) and chlorophyll can yield information on the depositional environment at the time the material was sedimented. (See chapter 5 for a discussion of these applications.)

Two important questions, then, are (1) why is chlorophyll from marine algae consistently depleted in  $^{15}\text{N}$  relative to the whole cell, and (2) why is there variability in the magnitude of this depletion? These questions will be addressed in the following discussion.



#### 4.5.1.1 Overview of Chlorophyll Biosynthesis

The first committed precursor to chlorophyll in all plants, algae and cyanobacteria is  $\delta$ -aminolevulinic acid (ALA) (Beale and Weinstein, 1991). ALA is synthesized in a three-step process from glutamic acid (GLU), which derives from  $\alpha$ -ketoglutarate (figure 4.5). Two ALA molecules are then condensed to form the pyrrole monomer porphobilinogen (PBG). A complex condensation reaction of 4 PBG molecules yields uroporphyrinogen III, the precursor to all tetrapyrroles (i.e., chlorophylls, hemes and phycobilins) (Zubay, 1983) (figure 4.6). The pathway from glutamate to chlorophyll *a* is the same in all plants and algae, down to the individual enzymes required for each step (Beale and Weinstein, 1991; Leeper, 1991).

#### 4.5.1.2 Isotopic Fractionation During Chlorophyll Biosynthesis

There are five instances in the synthetic pathway from GLU to Chl<sub>a</sub> where bonds to nitrogen are formed or broken, and hence, where N isotopic fractionation might be expected to occur. These are: (1) the transamination of  $\alpha$ -ketoglutaric acid (AKA) to form GLU, (2) the transamination of glutamate-1-semialdehyde to yield ALA, (3) the condensation of 2 ALA's to form PBG, (4) the deamination of 4 PBG's to form hydroxymethylbilane, and (5) the insertion of Mg into protoporphyrin 9 to yield Mg protoporphyrin IX.

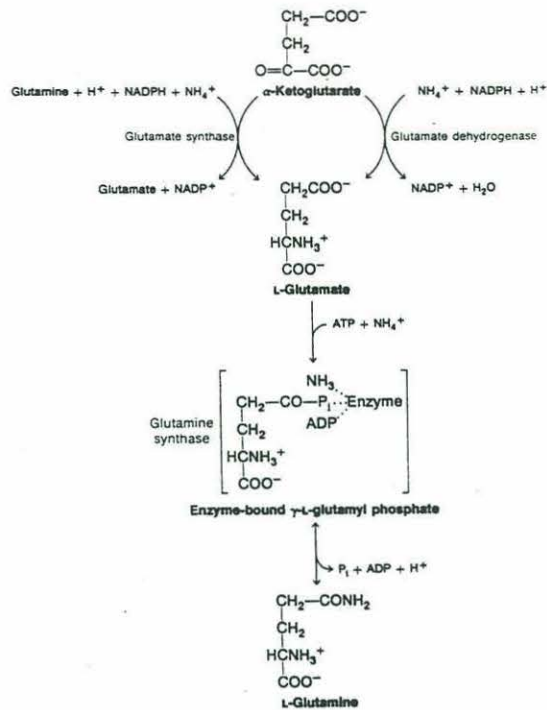


Figure 4.5: The conversion of ammonia into the  $\alpha$ -amino group of glutamate.  $\alpha$ -Ketoglutarate is the starting material for this conversion, and hence, for chlorophyll biosynthesis. Figure from Zubay (1983).

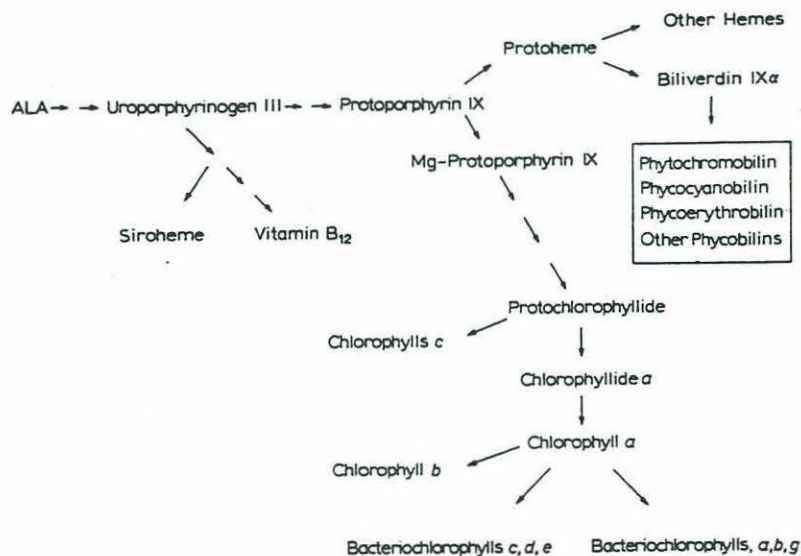


Figure 4.6: The biosynthetic pathway of chlorophyll and other tetrapyrroles. Figure from Beale and Weinstein (1991).

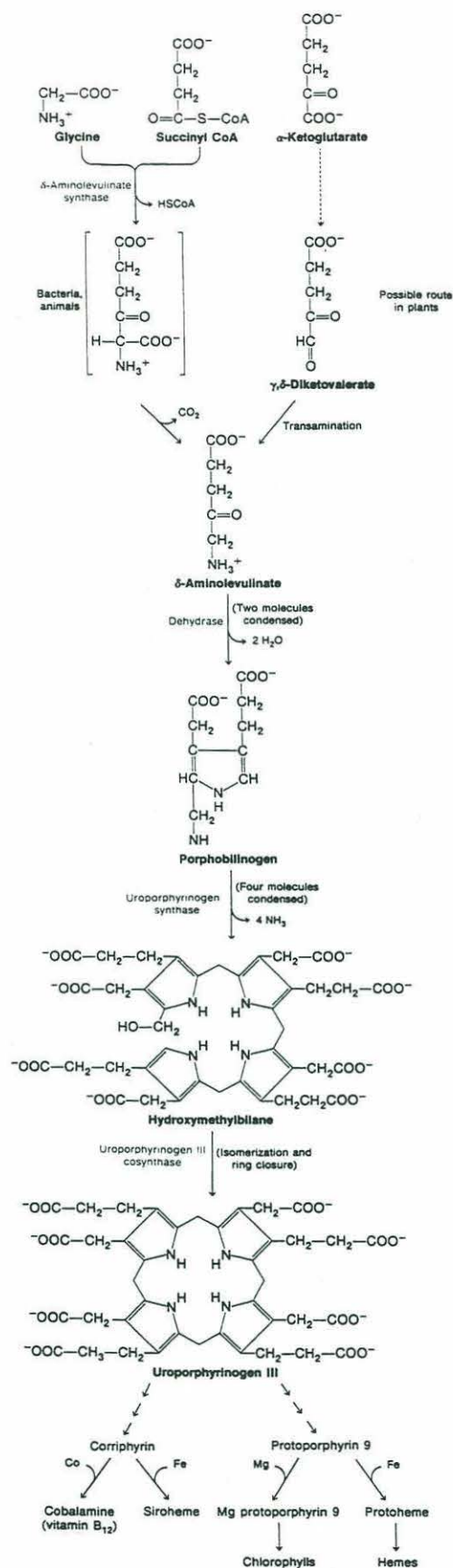


Figure 4.6: (continued). Figure from Zubay (1983).



#### 4.5.1.2.1 Transamination

Of these 5 enzyme-catalyzed reactions, the only one that has been studied for N isotopic fractionation is transamination (Macko, et al., 1986). In that study, Macko et al (1986) measured the isotopic fractionation associated with the forward and reverse transformations of GLU and oxalacetic acid (OAA), to  $\alpha$ -ketoglutaric acid (AKA) and aspartic acid (ASP), by the enzyme, porcine-heart glutamic oxaloacetic transaminase. Significant isotopic fractionation was found for both the forward and reverse reactions, with the transfer of  $^{14}\text{NH}_2$  being 1.0083 and 1.0017 times faster than the transfer of  $^{15}\text{NH}_2$  for the conversion of GLU to ASP and ASP to GLU, respectively. In other words the ASP from the transamination of GLU to ASP was found to be depleted in  $^{15}\text{N}$  by 8.3 per mil, while the GLU from the transamination of ASP to GLU was found to be depleted in  $^{15}\text{N}$  by 1.7 per mil.

Since the first two steps in chlorophyll biosynthesis are transamination reactions, it seems plausible that this is where some of the depletion in chlorophyll  $\delta^{15}\text{N}$  derives. As will be discussed below, it is the second of these transaminations that seems the most likely source of the  $^{15}\text{N}$  depletion, since GLU is the precursor to all amino acids and most cellular nitrogenous species (Zubay, 1983), and may accumulate in a pool. This appears to be a prerequisite for net isotopic fractionation in a biosynthetic product. If the conversion of a substrate to a product is complete, and the system is closed, then no net isotopic fractionation will be expressed in the product (Mariotti, et al., 1981).

#### 4.5.1.2.2 ALA Condensation to PBG

In the condensation reaction of two ALA molecules, catalyzed by the enzyme  $\delta$ -aminolevulinic acid dehydratase, to form PBG, the potential exists for

isotopic fractionation even if 100% of ALA is converted to PBG. This is the case because there are two identical amino groups at which the reaction can occur. So that if the ALA dehydration is more rapid for  $^{14}\text{NH}_2$  than for  $^{15}\text{NH}_2$ , then the pyrrole formed will be depleted in  $^{15}\text{N}$  relative to the 2 ALA's, and the  $^{15}\text{N}$ -enriched terminal amino group will be lost in the subsequent condensation. In fact, in the similar dehydration of GLU by glutamate dehydrogenase, a kinetic nitrogen isotope effect of 1.047 was found (Schimerlik, et al., 1975), thus resulting in an isotopic depletion of 47 per mil in the product relative to the substrate. Therefore, the dehydration of 2 ALA molecules to form PBG, in addition to the transamination reaction, seems like a likely step for chlorophyll  $^{15}\text{N}$ -depletion to occur.

#### 4.5.1.2.3 PBG Condensation to Form Hydroxymethylbilane

The next step in chlorophyll biosynthesis, the condensation and deamination of 4 PBG's, by the enzymes PBG deaminase and uroporphyrinogen cosynthetase (Leeper, 1991) (figure 4.7), is not expected to result in significant

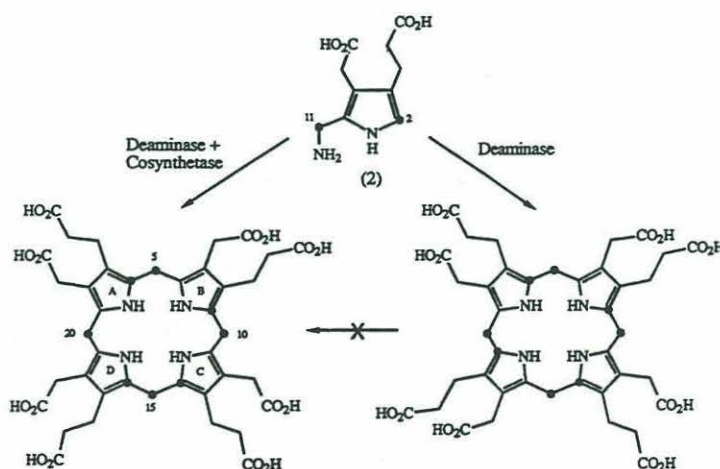


**Figure 4.7: Condensation of 4 PBG molecules to form hydroxymethylbilane.**  
Figure from Leeper (1991).



isotopic fractionation as long as the conversion of PBG to hydroxymethylbilane goes to completion. It can only be speculated that this is the case. Namely, (1) that tight feedbacks exist to prevent the accumulation of products not lying at biosynthetic branch points, and (2) that the energy expenditure for the synthesis of such products is large enough that their subsequent destruction (and the further energy expenditure thus required) seems unlikely. Radiolabeled pigment turnover experiments support these suppositions (Goericke and Welschmeyer, 1992).

However, if PBG is drawn from a pool to make hydroxymethylbilane there is the possibility of isotopic fractionation during the deamination and condensation. For instance, one or both of the enzymes involved in the deamination and condensation may bind to the pyrrolic nitrogen and may exhibit a kinetic isotope effect. This could result in isotopically-depleted hydroxymethylbilane relative to PBG.

#### 4.5.1.2.4 *Mg Insertion of Protoporphyrin IX to Form Mg-Protoporphyrin IX*

The final potential source of N isotopic fractionation during chlorophyll biosynthesis is during the metallation of protoporphyrin IX (PTP), by the enzyme Mg chelatase, to form Mg protoporphyrin IX (MPTP). PTP lies at a branch point in tetrapyrrole synthesis. It is the point at which metallation with either Mg or Fe occurs to form either the chlorophylls or the hemes and bilins, respectively (figure 4.6). All plants and algae contain the three common hemes (i.e., heme *a*, heme *b* and heme *c*) found in animals (Beale and Weinstein, 1991). The hemes are constituents of respiratory cytochromes and various oxidative enzymes. This suggests that different feedbacks may operate on the production of PTP for the heme pathway than for the chlorophyll pathway. In addition, many plants and



algae contain bilins, either as primary or accessory photosynthetic pigments (Scheer, 1981). Given PTP's role as the precursor to two, at least partially, independent branches of tetrapyrrole synthesis in plants and algae, it seems plausible that isotopic fractionation could occur there if the enzymes responsible for metal chelation demonstrate a kinetic isotope effect.

There are no known studies on the kinetic isotope effect of the enzyme Mg-chelatase. However, in equilibrium metal exchange reactions between Mg-meso-tetraphenylporphin (MTTP) and free-base meso-tetraphenylporphin (TTP), Macko (1981) found the free-base to be enriched in  $^{15}\text{N}$  by  $2.2 (\pm 0.3)$  per mil relative to the metallated product (Macko, 1981). Furthermore, in three (inadvertant!) chlorophyll demetallation experiments, in which harvested cultures of three marine algae (*Isochrysis galbana*, *Emiliana huxleyi* and *Thalassiosira weissflogii*) were stored at  $-20^{\circ}\text{C}$  for 9 months and the Chl $a$  allowed to partially demetallate to pheophytin  $a$ , it was found that the demetallated product was enriched in  $^{15}\text{N}$  by  $2.0 (\pm 0.39)$  per mil relative to the intact Chl $a$ . These reactions went to 53-65% of completion. (This explains why the standard deviation of the chlorophyll  $\delta^{15}\text{N}$  values for this first set of cultures was so high (table 4.3)).

It is unknown whether the *in vivo* demetallation of chlorophyll  $a$  is enzyme-catalyzed (Brown, et al., 1991), or whether it occurs nonenzymatically. However, *in vitro* experiments with several species of marine phytoplankton have demonstrated the existence of a Mg-releasing enzyme (Owens and Falkowski, 1982). Since the rate for enzyme-catalyzed reactions in biological systems tends to be faster for the light, relative to the heavy isotope, though, our results suggest the demetallation reaction occurred non-enzymatically in the frozen phytoplankton.

In the final analysis, any nitrogen isotopic fractionation imparted to chlorophyll during the enzyme-catalyzed insertion of Mg into protoporphyrin IX will most likely depend upon (1) the kinetic isotope effects associated with both Mg-chelatase and the enzyme responsible for iron chelation in the synthesis of hemes and bilins, and (2) the branching ratio of PTP to MPTP and protoheme.

#### *4.5.1.2.5 Fe Insertion to PTP and the Heme/Bilin Branch*

The kinetic isotope effect associated with Fe chelation by ferrochelatase in the synthesis of protoheme for the heme/bilin branch of tetrapyrrole synthesis could affect the  $\delta^{15}\text{N}$  of chlorophyll. As discussed in the preceding section, the impact of this reaction on chlorophyll  $\delta^{15}\text{N}$  will depend on the branching ratio of PTP to MPTP and protoheme, and on the magnitude of both isotope effects.

#### *4.5.1.2.6 Summation of Chlorophyll Biosynthesis and Isotopic Fractionation Discussion*

In conclusion, the  $^{15}\text{N}$  depletion in chlorophyll *a*, relative to whole-cells, of marine phytoplankton cultured in this study likely results from one or more of the five enzyme-catalyzed reactions involving bonds to nitrogen. Experimental evidence exists for substantial (e.g., 8.3 per mil) isotopic depletion in aspartic acid formed by transamination of glutamic acid (Macko, et al., 1986). Since the transamination of glutamic acid to form ALA is the first dedicated reaction in chlorophyll biosynthesis (Beale and Weinstein, 1991), it is likely that this is an important step in the isotopic depletion of chlorophyll. It is also likely that additional isotopic depletion is imparted during the dehydrogenation and condensation of 2 ALA molecules to form PBG. During this step one of two ALA



nitrogens becomes pyrrolic, and hence destined for chlorophyll (or heme/bilin). In addition, GLU dehydrogenase has been shown to result in substantial (47 per mil) isotopic depletion of the product (Schimerlik, et al., 1975).

Having addressed the question of how N isotopic depletion is imparted to chlorophyll in algae, I will now turn to a discussion of why variability exists in the magnitude of this isotopic depletion.

#### 4.5.1.3 Variability in Chlorophyll $^{15}\text{N}$ -Depletion Between Algal Species

The uncertainty of an algal  $\delta^{15}\text{N}$  value estimated from a measured chlorophyll  $\delta^{15}\text{N}$  value will likely be no better than the standard deviation of  $\Delta\delta^{15}\text{N}_{\text{cell-Chl}a}$  measurements in cultured phytoplankton. For the 14 cultures grown in this study, this value is 2.15 per mil. Given that (1) the reproducibility of the culture experiments ( $\pm 0.57$  per mil) is so much greater than that implied by this standard deviation, and (2) the biosynthetic route to chlorophyll is identical in all plants and algae (Beale and Weinstein, 1991; Leeper, 1991), it seems likely that there are interspecies differences in the partitioning of N between non-proteinaceous biochemicals.

This interspecies difference is shown graphically in figure 4.8. The bar graph shows the  $\Delta\delta^{15}\text{N}_{\text{cell-Chl}a}$ , grouped by species, for the cultures grown in this study. Also plotted is the average  $\Delta\delta^{15}\text{N}_{\text{cell-Chl}a}$  for the 8 species ( $= 5.16 \pm 2.40$  per mil). The error bars are the standard deviations of the individual replicate experiments, except in the cases of *E. huxleyi* (EH) and *Synechoccus* (SYN), for which no replicates were performed. The error bar used in these cases is 0.57 per mil, the pooled standard deviation of the 6 replicate experiments. Clearly there is interspecies variability in  $\Delta\delta^{15}\text{N}_{\text{cell-Chl}a}$  that cannot be ascribed to measurement precision.



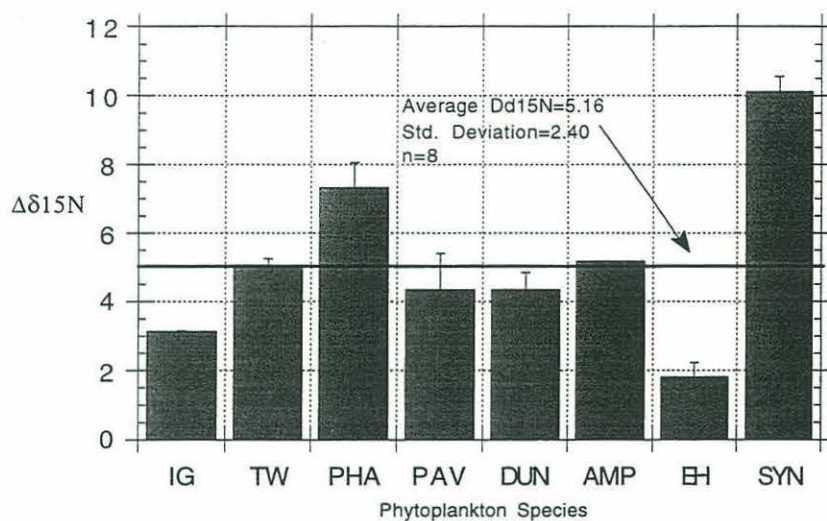


Figure 4.8: A plot of the nitrogen isotopic difference between chlorophyll and whole cells (e.g.,  $\Delta\delta^{15}\text{N}_{\text{cell-Chl}a}$ ) for 8 species of marine phytoplankton. See text for explanation of error bars, and table 4.1 for species abbreviations.

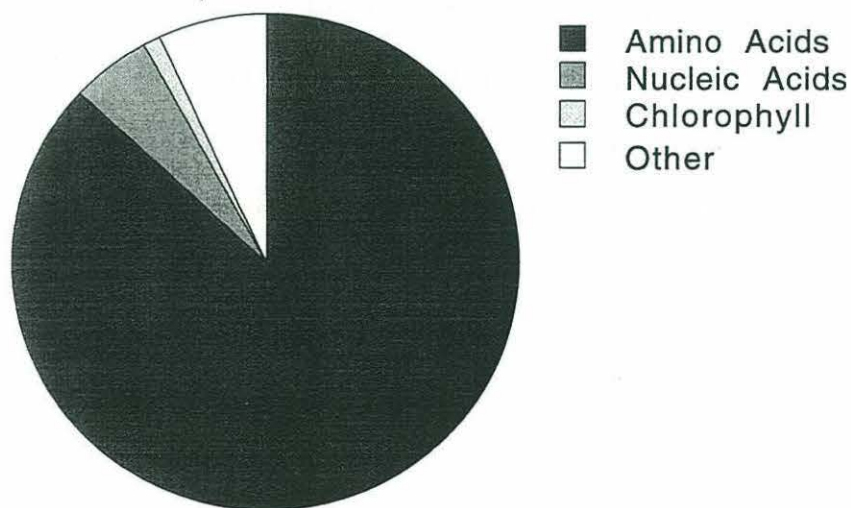


Figure 4.9: The distribution of nitrogen in phytoplankton as a percentage of total cellular nitrogen. Data from Parsons, et al. (1984).

#### 4.5.1.3.1 *A Model of the Distribution of N Isotopes in Phytoplankton*

Most of the cellular nitrogen in marine phytoplankton is amino acid nitrogen, constituting protein, with smaller amounts being contained in chlorophyll, nucleic acids, and other minor components such as amino sugars and ATP (figure 4.9). Using data from marine phytoplankton summarized in Parsons et al. (1984), and assuming a Redfield C:N ratio of 6.6, and a carbon:chlorophyll (w/w) ratio of 30 (Parsons, et al., 1984), the following cellular weight percentages of N can be calculated: amino acids, 86.8% ( $\pm 4.6\%$ ); nucleic acids, 1.5 to 10.5%; and chlorophyll, 1.2%. That leaves 1.5 to 10.5% of cellular nitrogen remaining in all other minor components such as amino sugars, AMP/ADP/ATP, histidine, tryptophan, carbamyl phosphate, cytidine triphosphate, etc. Some diatoms have been found to contain significant quantities of chitin, a polymer of the amino sugar *N*-acetyl-D-glucosamine, such that amino sugar nitrogen may amount to 15-20% of total cellular nitrogen in some instances (Smucker and Dawson, 1986). The compound from which these diverse biochemicals derive is glutamic acid (GLU) (Zubay, 1983).

A simple conceptual model is therefore proposed in which isotopic differences between cellular nitrogenous species stem from a hierarchy in the transfer of GLU to the biosynthetic pathways of proteins, nucleic acids, chlorophylls, and amino sugars. This model is based on nitrogen isotopic data, from numerous sources, of one or more of these components relative to the whole cell or tissue. Since so few measurements have been made on individual nitrogen-containing compounds in plants and algae it is necessary to use some animal data. The isotopic differences for plants may vary substantially. A summary of these data follows.

Protein was found to be enriched in  $^{15}\text{N}$  by  $3.53 (\pm 0.29)$  per mil, relative to whole cells, in 6 species of algae and macroalgae (Macko, et al., 1987). An earlier study by Gaebler et al. corroborated this finding (Gaebler, et al., 1963). Chlorophyll was found to be depleted in  $^{15}\text{N}$  by  $5.16 (\pm 2.40)$  per mil in 8 species of marine phytoplankton (this study). The amino sugar, N-acetylglucosamine, isolated from chitin, was found to be depleted in  $^{15}\text{N}$  by about 9 per mil relative to whole arthropods (Schimmelman and DeNiro, 1986). Insect chitin was also found to be depleted in  $^{15}\text{N}$  relative to the whole organism (Deniro and Epstein, 1981), as were zooplankton molts (Montoya, et al., 1992); the latter by 3.8 to 4.6 per mil. Chitin (e.g., poly-N -acetyl-D-glucosamine) is found in certain species of phytoplankton, especially diatoms (Smucker and Dawson, 1986). Finally, nucleic acids were reported to be depleted in  $^{15}\text{N}$  relative to whole algal cells by about 2 per mil (Dr. Luis Cifuentes, personal communication).

From mass balance considerations, it is apparent that non-amino acid nitrogenous species must, on average, be depleted in  $^{15}\text{N}$ . In fact, if the values for protein  $\delta^{15}\text{N}$  are accurate, this depletion must, on average, be 23.4 per mil. That is,

$$\delta^{15}\text{N}_{\text{cell}}(\%N) = \delta^{15}\text{N}_{\text{protein}}(\%N) + \delta^{15}\text{N}_{\text{chlorophyll}}(\%N) + \delta^{15}\text{N}_{\text{nucleic acid}}(\%N) + \delta^{15}\text{N}_{\text{amino sugar}}(\%N) + \delta^{15}\text{N}_{\text{other}}(\%N).$$

Then, by setting the whole-cell isotopic value to zero, and substituting the appropriate values for protein it is calculated that

$$0 = (3.5)(0.87) + \delta^{15}\text{N}_{\text{non-protein}}(0.13)$$

$$\delta^{15}\text{N}_{\text{non-protein}} = -23.4 \text{ per mil.}$$

The  $^{15}\text{N}$ -depletion in non-protein nitrogenous species becomes even larger if the experimentally-determined isotopic values for chlorophyll, nucleic acids and



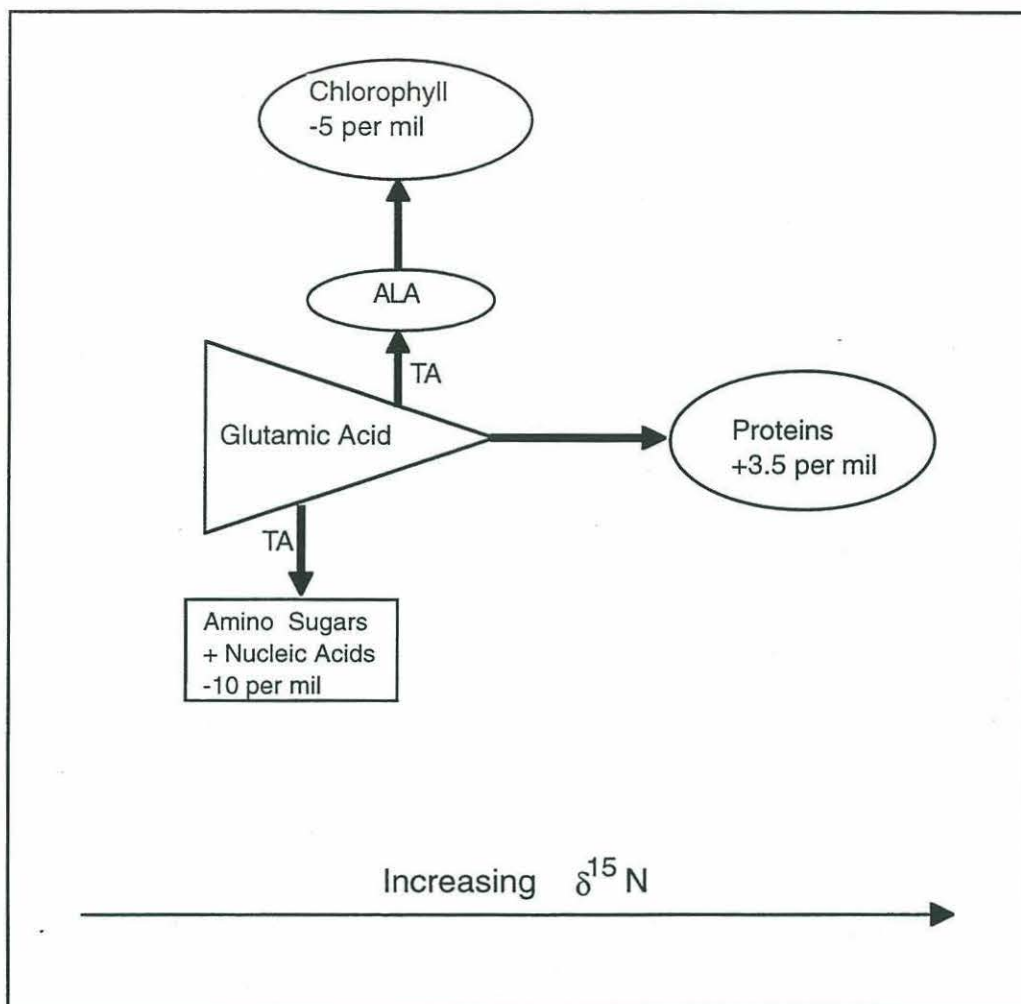


Figure 4.10: A conceptual model for the distribution of  $^{15}\text{N}$  in phytoplankton.

amino sugars are included:

$$0 = (3.5)(0.87) + (-5)(0.01) + (-10)(0.05) + \delta^{15}\text{N}_{\text{other}}(0.07)$$

$$\delta^{15}\text{N}_{\text{other}} = -35.6 \text{ per mil.}$$

(Here a value of 5% was chosen for the nucleic acid plus amino sugar contribution to total cellular N, and the associated average isotopic value was taken to be -10 per mil). Given this extreme isotopic depletion in the unspecified nitrogenous component it is likely that either the protein isotopic data or the average protein nitrogen fraction used here are inaccurate.

Figure 4.10 is a schematic of the model for  $^{15}\text{N}$  distribution in phytoplankton. It is proposed that the enzyme-catalyzed transaminations of glutamic acid (denoted by "TA" in the figure)--to form the precursors of nucleic acids, chlorophylls and amino sugars--are characterized by kinetic isotope effects that result in isotopic depletions of the reaction products and isotopic enrichments of the substrate (GLU). This has been demonstrated experimentally with the *in vitro* transamination of GLU, by porcine-heart glutamic oxaloacetic transaminase, to form aspartic acid. That transamination reaction resulted in an 8.3 per mil isotopic depletion of the product (Macko, et al., 1986). It is further proposed that the branch points for these non-protein biosynthetic pathways occur prior to that for protein synthesis. In this fashion, a pool of GLU would become increasingly enriched in  $^{15}\text{N}$  as the amino acid is removed, via transamination, for the synthesis of nucleic acids, amino sugars, chlorophylls, and other nitrogenous species. This would result in the observed isotopic enrichment of proteins formed from the residual pool of GLU.

#### 4.5.1.3.2 Interspecies Differences in $\Delta\delta^{15}\text{N}$ Based Upon Branching Ratios of Glutamate

The model can account for the observed interspecies variation in the chlorophyll-whole cell nitrogen isotopic difference. For instance, if the branching ratios for GLU upstream of the chlorophyll branch vary, even slightly, from species to species, then the  $\delta^{15}\text{N}$  of chlorophyll, relative to the whole cell, can vary substantially (see model results below). As mentioned above, the percentage of total nitrogen in marine phytoplankton that is nucleic acid can vary between 1.5 and 10.5% (Parsons, et al., 1984). Furthermore, the abundance of amino sugars can account for up to 15-20% of total cellular N in certain species of

diatoms (Smucker and Dawson, 1986). And the fraction of cellular N contained in chlorophyll can vary by at least a factor of 4, between 1.4% and 0.35%, for typical C:Chl ratios between 25 and 100 (Claustre and Marty, 1995; Goericke, 1990; Parsons, et al., 1984).

The model consists of the mass balance equation for cellular  $^{15}\text{N}$  (see above). The  $\delta^{15}\text{N}$  values are actually the isotopic differences between the cell and the biochemical, or  $\Delta\delta^{15}\text{N}_{\text{cell-component}}$  values. In the model, the percentages of cellular N that are protein and "other" are held constant at 87% and 7%, respectively. The latter was arbitrarily chosen as an intermediate value for nitrogenous compounds other than amino acids, nucleic acids, chlorophyll, and amino sugars. The  $\delta^{15}\text{N}$  values of protein, nucleic acids plus amino sugars, and "other" are also held constant at 3.5, -10, and -35.6 per mil. The  $\delta^{15}\text{N}$  value for "other" was derived from the mass balance when best guesses for all quantities for which some data is available were made. Those best guesses are: 87%, 5%, 1%, 7%, respectively, for the fraction of cellular N in protein, nucleic acids plus amino sugars, chlorophyll, and other; and 3.5, -10, -5 per mil, respectively, for protein, nucleic acids plus amino sugars, and chlorophyll.

As is shown in table 4.4, small variations in the percentage of cellular nitrogen that is contained in nucleic acids and amino sugars, relative to chlorophyll can cause large changes in the isotopic difference between

**Table 4.4: Cellular  $^{15}\text{N}$  distribution model output**

% Chlorophyll N	$\delta^{15}\text{N}$ -Chlorophyll	% Nucl. Acid + Amino Sugar N
1.4	-6.64	4.6
1	-5.30	5
0.75	-3.73	5.25
0.5	-0.60	5.5
0.35	3.43	5.65



chlorophyll and the whole cell. For example, holding all other parameters constant, if nucleic acid plus amino sugar N is 5.25% instead of 5% of total N, and chlorophyll is 0.75% instead of 1% of total N, then the  $\Delta\delta^{15}\text{N}_{\text{cell-Chla}}$  increases to -3.7 from -5.3 per mil.

The purpose of this exercise is not so much to accurately model cellular  $^{15}\text{N}$  distributions as it is a sensitivity analysis to demonstrate how small changes in the partitioning of cellular N between minor biochemicals can significantly alter the isotopic difference between chlorophyll and whole cells. Since the fraction of cellular N contained in nucleic acids, amino sugars and chlorophyll can vary by factors of at least 4 to 10 between species, it is not surprising that the N isotopic difference between whole cells and chlorophyll is somewhat variable. A similar explanation could account for the difference in  $\Delta\delta^{15}\text{N}_{\text{cell-Chla}}$  between higher plants and algae ( $1.72 \pm 2.47$  per mil vs.  $5.16 \pm 2.40$  per mil) (table 4.3). In the next section the possibility that growth rate can affect this difference is explored.

#### *4.5.1.4 Growth Rate and Nitrogen Isotopic Fractionation*

Growth rate has been implicated as an important factor in the study of nitrogen (Wada and Hattori, 1978) and carbon (Goericke, et al., in press; Laws, et al., 1995) isotopic fractionation in marine phytoplankton. For instance, it has been found that growth rate markedly affects nitrogen isotopic fractionation during nitrate assimilation in marine diatoms (Wada and Hattori, 1978) (figure 4.11). In that study larger isotopic fractionations were associated with slower growth rates. The duplicate cultures from this study of, the diatom

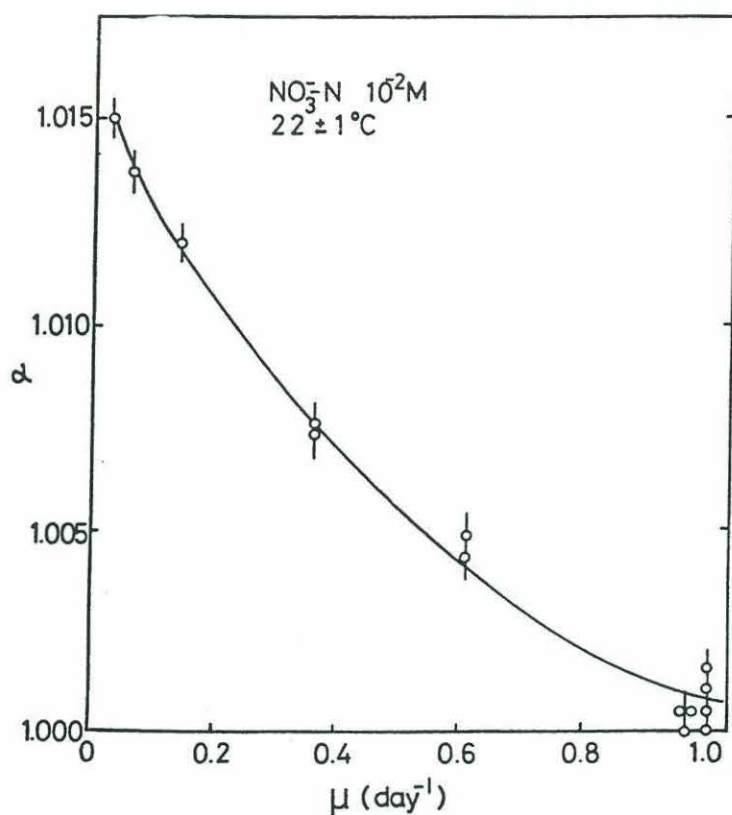


**Figure 4.11: Relationship between nitrogen isotopic fractionation during nitrate assimilation and growth rate. The fractionation factor,  $\alpha$ , is plotted versus the growth rate constant,  $\mu$ . Figure from Wada and Hattori (1978).**

*Phaeodactylum tricornutum*, demonstrated different isotopic fractionations associated with nitrate assimilation (e.g.,  $\epsilon = \delta^{15}\text{N}_{\text{NO}_3^-} - \delta^{15}\text{N}_{\text{cell}} = 3.6$  and  $1.8$ , respectively) (table 4.1). This suggests that the two cultures were harvested at different growth rates. Yet the standard deviation of the  $\Delta\delta^{15}\text{N}_{\text{cell-Chla}}$  determinations was  $0.7$  per mil. This value was not substantially different from the precision of the measurement ( $0.43$  per mil). Nevertheless, since growth rate has such a large effect on overall cellular isotopic fractionation, it may affect the isotopic difference between chlorophyll and whole cells.

Estimates of growth rate are available for 8 of the 14 cultures grown in this study (table 4.1). For two of the six species for which replicates were performed (e.g., *Dunaliella tertiolecta* and *Pavlova lutheri*), duplicate cultures were clearly

harvested at different growth rates. That is, one culture of *Dunaliella* and one culture of *Pavlova* were harvested during the exponential growth phase, and one culture of each was harvested during the stationary growth phase. The standard deviations for the two pairs were 0.50 and 1.05 per mil, respectively, for *Dunaliella tertiolecta* and *Pavlova lutheri*. Moreover, the two *Isochrysis galbana* cultures were grown at different temperatures (18 and 24°C), and in different light:dark cycles (12h:12h vs 24h:0h), yet the standard deviation of  $\Delta\delta^{15}\text{N}_{\text{cell-Chla}}$  for the replicates was 0.03 per mil.

Furthermore, aeration rate and illumination have been shown to affect nitrogen isotopic fractionation in marine diatoms via changes in growth rate (Wada and Hattori, 1978). These factors varied between all replicates, as a result of changing bubbling rate (when active aeration was used at all--i.e., in the 20 L cultures), flask size and light intensity. Yet the pooled standard deviation for replicate cultures was just 0.57 per mil.

Since quantitative measures of growth rate were not available it is not possible to conclude with certainty that chlorophyll-cell N isotopic differences were independent of growth rate. Nevertheless, given the range of conditions under which duplicate cultures were grown, it seems likely that growth rates did vary, leading to little intra-species  $\Delta\delta^{15}\text{N}_{\text{cell-Chla}}$  variation. It would be informative to conduct this experiment in the future with continuous cultures of phytoplankton grown at different rates to determine with certainty whether this parameter affects the isotopic difference between chlorophyll and whole cells.

#### 4.5.1.5 Nutrient Source and Chlorophyll-Cell N Isotopic Differences

It is unlikely that the source of nitrogen to an algal cell would affect the chlorophyll-cell N isotopic difference, unless that source were to change over the



lifetime of the cell. Ammonium is the form in which nitrogen is incorporated into all organic matter. Since it is rarely available in nature, though, due to rapid assimilation or oxidation by nitrifying bacteria, it must be produced in algae by nitrate and nitrite reductases (Zubay, 1983). The production of  $\text{NH}_4^+$  from the reduction of nitrate and nitrite within plants occurs "at a rate no greater than that required for synthesis of nitrogenous compounds during growth" (Zubay, 1983). So there is a tight coupling between nitrate and nitrite reduction, and ammonium assimilation, when cells grow. Ammonium does not accumulate. Since isotopic fractionation tends to be expressed in a product when incomplete reaction of a substrate occurs (Mariotti, et al., 1981), it seems unlikely that isotopic fractionation occurs during  $\text{NH}_4^+$  assimilation in phytoplankton.

However, N isotopic fractionation does occur during the enzyme-mediated reduction of  $\text{NO}_3^-$  to form  $\text{NH}_4^+$  in phytoplankton (Wada and Hattori, 1978). Wada and Hattori (1978) concluded that the isotopic fractionation occurred during the breaking of the N-O bond in the formation of nitrite by nitrate reductase. The second reduction, converting nitrite to ammonium, was found by those researchers to result in no net isotopic fractionation.

The important point from the standpoint of chlorophyll-cell N isotopic differences, is that ammonium is the precursor to all nitrogenous biochemicals, so isotopic fractionation imparted to  $\text{NH}_4^+$  should be transferred to all nitrogenous compounds produced in the cell. The only way the nitrogen source could affect that relationship would be if the cell produced different nitrogenous biochemicals in different nutrient regimes. That is, in fact, a real possibility.

For example, if a cell were to move from the lower euphotic zone, where C:Chl ratios tend to be low, to the upper euphotic zone, where those ratios tend to be high (Goericke, 1990), the cell would concurrently be moving from a relatively  $\text{NO}_3^-$ -rich,  $\text{NH}_4^+$ -poor environment to a relatively  $\text{NO}_3^-$ -poor,  $\text{NH}_4^+$ -

rich(er) environment. In the latter location, the phytoplankton would tend to grow with little additional chlorophyll production (Goericke and Welschmeyer, 1992). In other words, in the upper euphotic zone, protein would be added to the cell that derived from regenerated ammonium outside the cell, with little or no isotopic fractionation. At depth, however, the source of  $\text{NH}_4^+$  for chlorophyll biosynthesis would have been enzymatically-reduced nitrate--a process known to impart isotopic fractionation. If chlorophyll biosynthesis is offset in time (and space) from the synthesis of other nitrogenous biochemicals, differences in the chlorophyll-cell isotopic difference could arise, even amongst algae within a single species.

The cultures grown for this study had a large excess of nitrate (883  $\mu\text{M}$ ). It is not expected that more than 15% of this nitrate was consumed by any culture. Furthermore, the ammonium concentration was undetectable in the Vineyard Sound seawater used for 10 of the 14 cultures. It is therefore unlikely that a switch from one form of nitrogen to another occurred over time in the cultures. In the field, however--and especially in stratified locations--such a change in nutrient regime may be relevant.

#### 4.5.2 *Carbon Isotopic Differences Between Chlorophyll and Algae*

The results of 13 culture experiments with 8 different algal species suggest that chlorophyll has nearly the same isotopic composition as whole algae, being enriched by  $0.10 \pm 2.86$  per mil (table 4.3). Thus chlorophyll  $\delta^{13}\text{C}$  in particles and sediments can be used as a surrogate for algal  $\delta^{13}\text{C}$  in contemporary and historical marine environments.



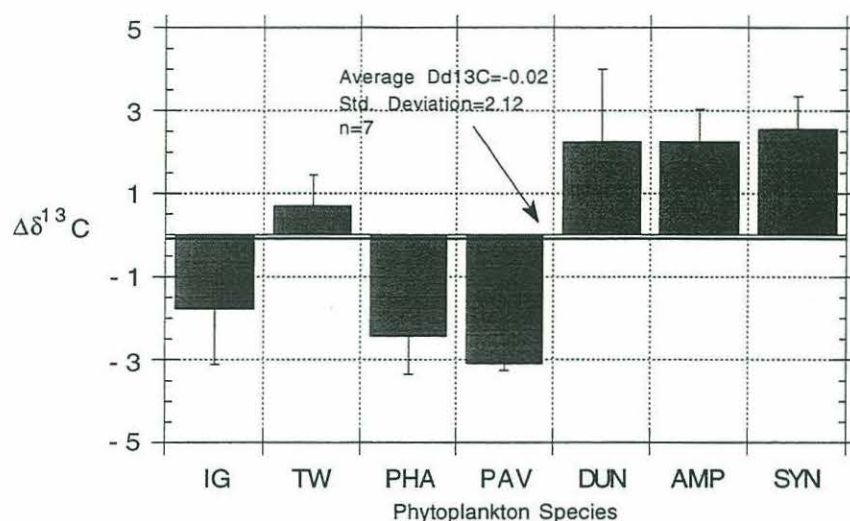


**Figure 4.12: The carbon isotopic difference between chlorophyll and whole cells,  $\Delta\delta^{13}\text{C}_{\text{cell-Chla}}$ , for 7 species of marine phytoplankton. See text for an explanation of error bars, and table 4.1 for species abbreviations.**

As was the case with nitrogen, there appears to be interspecies variation in  $\Delta\delta^{13}\text{C}_{\text{cell-Chla}}$  that cannot be attributed to measurement imprecision (figure 4.12). When  $\Delta\delta^{13}\text{C}_{\text{cell-Chla}}$  values for 7 species were averaged, then the isotopic difference between whole cells and chlorophyll *a* was  $-0.02 \pm 2.12$  per mil. The error bars in the figure are actual standard deviations of replicate culture experiments for IG, TW, PHA, PAV, and DUN. Duplicates were not performed for SYN. Duplicate *Amphidinium carterae* (AMP) cultures were grown, but AMP4 is considered an outlier ( $\Delta\delta^{13}\text{C}=10.58$ ), so it is not included in this discussion. The error bars on AMP and SYN are the pooled standard deviation ( $=1.25$  per mil) of the 5 replicate experiments. One additional point is that none of the POC samples were decarbonated before isotopic analysis. This likely resulted in an overly large  $\Delta\delta^{13}\text{C}_{\text{cell-Chla}}$  ( $=5.1$  per mil) value for *Emiliana huxleyi* (EH, clone CCMP 1516), since carbonate has a high  $\delta^{13}\text{C}$  relative to organic carbon (Craig, 1953). According to CCMP, the strain of *Emiliana huxleyi* used in this study



normally contains carbonate liths. Therefore this species was not included in the average.

A discussion on the biochemical basis for the observed interspecies  $\Delta\delta^{13}\text{C}_{\text{cell-Chla}}$  variability is beyond the scope of this investigation. The situation is likely to be complicated, relative to that for nitrogen, by the fact that the C<sub>20</sub> isoprenoid side chain (phytol) (Rudiger and Schoch, 1991) and the C<sub>35</sub> cyclic tetrapyrrole (macrocycle) of chlorophyll (Beale and Weinstein, 1991) derive their carbon from different biosynthetic pathways. Phytol is a lipid and is thus expected to be depleted in  $^{13}\text{C}$  relative to protein and carbohydrate (DeNiro and Epstein, 1977; Galimov and Shirinsky, 1975). A carbon isotopic depletion of 1.6 to 5.1 per mil in phytol relative to the macrocycle has, in fact, been demonstrated (Bogacheva, et al., 1979). Other investigators have noted a 0.01 to 0.73 per mil carbon isotopic enrichment of the chlorin macrocycle relative to whole plant or leaf material (Hayes, et al., 1987, and references therein). This isotopic enrichment should be accounted for when pheophorbides and other de-phytolated chlorophyll derivatives are isolated from sediments for carbon isotopic analysis.

#### 4.6 Conclusion

On average, chlorophyll *a* was 5.16 per mil depleted in  $^{15}\text{N}$  relative to total cellular nitrogen in eight species of cultured marine phytoplankton. Therefore, chlorophyll  $\delta^{15}\text{N}$  can be used as a proxy for algal  $\delta^{15}\text{N}$  after the addition of that quantity. No such correction is required in order to use the carbon isotopic composition of chlorophyll *a* as a surrogate for phytoplankton  $\delta^{13}\text{C}$ .

Interspecies variation in the partitioning of nitrogen between non-protein biochemicals is a likely cause for variations in the chlorophyll-whole cell  $\delta^{15}\text{N}$  difference. The magnitude of this interspecies variability was estimated to be 2.40 per mil, the standard deviation of  $\Delta\delta^{15}\text{N}_{\text{cell-Chla}}$  for 8 species of phytoplankton. The carbon isotopic difference between chlorophyll *a* and total cellular carbon also varied between phytoplankton species. The magnitude of this variation was estimated to be 2.12 per mil, the standard deviation of  $\Delta\delta^{13}\text{C}_{\text{cell-Chla}}$  for 7 species of phytoplankton.

#### References for Chapter 4

- Altabet, M.A. (1988) Variations in Nitrogen Isotopic Composition Between Sinking and Suspended Particles: Implications for Nitrogen Cycling and Particle Transformation in the Open Ocean. *Deep-Sea Research*, 35(4): 535-554.
- Altabet, M.A., W.G. Deuser, S. Honjo and C. Stienen (1991) Seasonal and Depth-Related Changes in the Source of Sinking Particles in the North Atlantic. *Nature*, 354: 136-139.
- Bada, J.L., M.J. Schoeninger and A. Schimmelmann (1989) Isotopic Fractionation During Peptide Bond Hydrolysis. *Geochimica et Cosmochimica Acta*, 53: 3337-3341.
- Baker, E.W. and J.W. Louda (1986) Porphyrins in the Geological Record. In: *Biological Markers in the Sedimentary Record*, (R. B. Johns, ed.), Elsevier, Amsterdam, pp. 125-225.
- Beale, S.I. and J.D. Weinstein (1991) Biochemistry and Regulation of Photosynthetic Pigment Formation in Plants and Algae. In: *Biosynthesis of Tetrapyrroles*, (P. M. Jordan, ed.), Elsevier, Amsterdam, pp. 155-235.
- Bidigare, R.R., M.C. Kennicutt II, W.L. Keeney-Kennicutt and S.A. Macko (1991) Isolation and Purification of Chlorophylls a and b for the Determination of Stable Carbon and Nitrogen Isotope Compositions. *Analytical Chemistry*, 63: 130-133.
- Bogacheva, M.P., L.A. Kodina and E.M. Galimov (1979) Intramolecular Carbon Isotope Distributions in Chlorophyll and Its Geochemical Derivatives. In: *Advances in Organic Geochemistry 1979*, (A. G. Douglas and J. R. Maxwell, ed.), Pergamon Press, Oxford, pp. 679-687.
- Boreham, C.J., C.J.R. Fookes, B.N. Popp and J.M. Hayes (1989) Origins of Etioporphyrins in Sediments: Evidence From Stable Carbon Isotopes. *Geochimica et Cosmochimica Acta*, 53: 2451-2455.



- Brown, S.B., J.D. Houghton and G.A.F. Hendry (1991) Chlorophyll Breakdown. In: *Chlorophylls*, (H. Scheer, ed.), CRC Press, Boca Raton, pp. 465-489.
- Claustre, H. and J.-C. Marty (1995) Specific Phytoplankton Biomasses and Their Relation to Primary Production in the Tropical North Atlantic. *Deep-Sea Research*, **42**(8): 1475-1493.
- Craig, H. (1953) The Geochemistry of the Stable Carbon Isotopes. *Geochimica et Cosmochimica Acta*, **3**: 53-92.
- DeNiro, M.J. and S. Epstein (1977) Mechanism of Carbon Isotope Fractionation Associated With Lipid Synthesis. *Science*, **197**: 261-263.
- DeNiro, M.J. and S. Epstein (1978) Influence of Diet on the Distribution of Carbon Isotopes in Animals. *Geochimica et Cosmochimica Acta*, **42**: 495-506.
- DeNiro, M.J. and S. Epstein (1981) Influence of Diet on the Distribution of Nitrogen Isotopes in Animals. *Geochimica et Cosmochimica Acta*, **45**: 341-351.
- Fry, B., W. Brand, F.J. Mersch, K. Tholke and R. Garritt (1992) Automated Analysis System for Coupled  $\delta^{13}\text{C}$  and  $\delta^{15}\text{N}$  Measurements. *Analytical Chemistry*, **64**: 288-291.
- Gaebler, O.H., H.C. Choitz, T.G. Vitti and R. Vukmirovich (1963) Significance of  $\text{N}^{15}$  Excess in Nitrogenous Compounds of Biological Origin. *Canadian Journal of Biochemistry and Physiology*, **41**(5): 1089-1097.
- Galimov, E.M. and V.G. Shirinsky (1975) Ordered Distributions of Carbon Isotopes in Compounds and Components of the Lipid Fraction in Organisms. *Geokhimiya*, **4**: 503-528.
- Goericke, R. (1990) Pigments as Ecological Tracers for the Study of the Abundance and Growth of Marine Phytoplankton. PhD, Harvard University.

Goericke, R., J.P. Montoya and B. Fry (1993) Physiology of Isotope Fractionation in Algae and Cyanobacteria. In: *Stable Isotopes in Ecology*, (K. Lajtha and B. Michener, ed.).

Goericke, R. and N.A. Welschmeyer (1992) Pigment Turnover in the Marine Diatom *Thalassiosira weissflogii*. I. The  $^{14}\text{CO}_2$ -Labeling Kinetics of Chlorophyll *a*. *Journal of Phycology*, **28**: 498-507.

Guillard, R.R.L. (1975) Culture of Phytoplankton for Feeding Marine Invertebrates. In: *Culture of Marine Invertebrate Animals*, (W. L. Smith and M. H. Chanley, ed.), Plenum Publishing Corporation, New York, pp. 29-60.

Hayes, J.M., K.H. Freeman, B.N. Popp and C.H. Hoham (1990) Compound-Specific Isotopic Analyses: A Novel Tool for Reconstruction of Ancient Biogeochemical Processes. *Organic Geochemistry*, **16**(4-6): 1115-1128.

Hayes, J.M., B.N. Popp, R. Takigiku and M.W. Johnson (1989) An Isotopic Study of Biogeochemical Relationships between Carbonates and Organic Carbon in the Greenhorn Formation. *Geochimica et Cosmochimica Acta*, **53**: 2961-2972.

Hayes, J.M., R. Takigiku, R. Ocampo, H.J. Callot and P. Albrecht (1987) Isotopic Compositions and Probable Origins of Organic Molecules in the Eocene Messel Shale. *Nature*, **329**: 48-51.

Hoering, T. (1955) Variations of Nitrogen-15 Abundance in Naturally Occurring Substances. *Science*, **122**: 1233-1234.

Keely, B.J., W.G. Prowse and J.R. Maxwell (1990) The Treibs Hypothesis: An Evaluation Based on Structural Studies. *Energy & Fuels*, **4**: 628-634.

Kennicutt II, M.C., R.R. Bidigare, S.A. Macko and W.L. Keeney-Kennicutt (1992) The Stable Isotopic Composition of Photosynthetic Pigments and Related Biochemicals. *Chemical Geology (Isotope Geoscience Section)*, **101**: 235-245.

Knoll, A.H. and M.R. Walter (1992) Latest Proterozoic Stratigraphy and Earth History. *Nature*, **356**(6371): 673-678.



- Krane, J., T. Skjetne, N. Telnaes, M. Bjoroy and H. Solli (1983) Nuclear Magnetic Resonance Spectroscopy of Petroporphyrins. *Tetrahedron*, **39**(24): 4109-4119.
- Laws, E.A., B.N. Popp, R.R. Bidigare, M.C. Kennicutt and S.A. Macko (1995) Dependence of Phytoplankton Carbon Isotopic Composition on Growth Rate and  $[CO_2]_{aq}$ : Theoretical Considerations and Experimental Results. *Geochimica et Cosmochimica Acta*, **59**(6): 1131-1138.
- Leeper, F.J. (1991) Intermediate Steps in the Biosynthesis of Chlorophylls. In: *Chlorophylls*, (H. Scheer, ed.), CRC Press, Boca Raton, pp. 407-431.
- Louda, J.W. and E.W. Baker (1986) The Biogeochemistry of Chlorophyll. In: *Organic Marine Geochemistry*, (H. L. Sohn, ed.), American Chemical Society, Washington D.C., pp. 107-126.
- Macko, S.A. (1981) Stable Nitrogen Isotope Ratios as Tracers of Organic Geochemical Processes. Ph.D., The University of Texas at Austin.
- Macko, S.A., M.L.F. Estep, M.H. Engel and P.E. Hare (1986) Kinetic Fractionation of Stable Nitrogen Isotopes during Amino Acid Transamination. *Geochimica et Cosmochimica Acta*, **50**: 2143-2146.
- Macko, S.A., M.L.F. Estep, P.E. Hare and T.C. Hoering (1987) Isotopic Fractionation of Nitrogen and Carbon in the Synthesis of Amino Acids by Microorganisms. *Chemical Geology (Isotope Geoscience Section)*, **65**: 79-92.
- Mariotti, A., J.C. Germon, P. Hubert, P. Kaiser, R. Letolle, A. Tardieux and P. Tardieux (1981) Experimental Determination of Nitrogen Kinetic Isotope Fractionation: Some Principles; Illustration for the Denitrification and Nitrification Processes. *Plant and Soil*, **62**: 413-430.
- Montoya, J.P. (1994) Nitrogen Isotope Fractionation in the Modern Ocean: Implications for the Sedimentary Record. In: *Carbon Cycling in the Glacial Ocean: Constraints on the Ocean's Role in Global Change*, (R. Zahn, M. A. Kaminski, L. Labeyrie and T. F. Pederson, ed.), Springer-Verlag, Berlin, pp. 259-279.



- Montoya, J.P. and J.J. McCarthy (1995) Isotopic Fractionation During Nitrate Uptake by Marine Phytoplankton Grown in Continuous Culture. *Journal of Plankton Research*, **17**: 439-464.
- Montoya, J.P., P.H. Wiebe and J.J. McCarthy (1992) Natural Abundance of  $^{15}\text{N}$  in Particulate Nitrogen and Zooplankton in the Gulf Stream Region and Warm-Core Ring 86A. *Deep-Sea Research*, **39**(Suppl. 1): S363-S392.
- Owens, T.G. and P.G. Falkowski (1982) Enzymatic Degradation of Chlorophyll *a* By Marine Phytoplankton *In Vitro*. *Phytochemistry*, **21**(5): 979-984.
- Parsons, T.R., M. Takahashi and B. Hargrave (1984) *Biological Oceanographic Processes*. Pergamon Press, Oxford, 330 pp.
- Rudiger, W. and S. Schoch (1991) The Last Steps of Chlorophyll Biosynthesis. In: *Chlorophylls*, (H. Scheer, ed.), CRC Press, Boca Raton, pp. 251-464.
- Scheer, H. (1981) Biliproteins. *Angew. Chem. Int. Ed. Engl.*, **20**: 241-261.
- Scheer, H. (1991) *Chlorophylls*. CRC Press, Boca Raton, 1257 pp.
- Schimerlik, M.I., J.E. Rife and W.W. Cleland (1975) Equilibrium Perturbation by Isotope Substitution. *Biochemistry*, **14**(24): 5347-5354.
- Schimmelman, A. and M.J. DeNiro (1986) Stable Isotopic Studies on Chitin, II. The  $^{13}\text{C}/^{12}\text{C}$  and  $^{15}\text{N}/^{14}\text{N}$  Ratios in Arthropod Chitin. *Contributions in Marine Science*, **29**: 113-130.
- Smucker, R.A. and R. Dawson (1986) Products of Photosynthesis by Marine Phytoplankton: Chitin in TCA "Protein" Precipitates. *Journal of Experimental Marine Biology and Ecology*, **104**: 143-152.
- Sun, M., R.C. Aller and C. Lee (1991) Early Diagenesis of Chlorophyll-*a* in Long Island Sound Sediments: A Measure of Carbon Flux and Particle Reworking. *Journal of Marine Research*, **49**: 379-401.

Sun, M.-Y., C. Lee and R.C. Aller (1993) Laboratory Studies of Oxic and Anoxic Degradation of Chlorophyll-*a* in Long Island Sound Sediments. *Geochimica et Cosmochimica Acta*, **57**: 147-157.

Treibs, A. (1936) Chlorophyll and Hemin Derivatives in Organic Mineral Substances. *Angew. Chem.*, **49**(38): 682-686.

Wada, E. (1980) Nitrogen Isotope Fractionation and its Significance in Biogeochemical Processes Occurring in Marine Environments. In: *Isotope Marine Chemistry*, (E. D. Goldberg, Y. Horibe and K. Saruhashi, ed.), Uchida Rokakuho, Tokyo, pp. 375-398.

Wada, E. and A. Hattori (1978) Nitrogen Isotope Effects in the Assimilation of Inorganic Nitrogenous Compounds by Marine Diatoms. *Geomicrobiology Journal*, **1**: 85-101.

Welschmeyer, N.A. and C.J. Lorenzen (1985) Chlorophyll Budgets: Zooplankton Grazing and Phytoplankton Growth in a Temperate Fjord and the Central Pacific Gyres. *Limnology and Oceanography*, **30**(1): 1-21.

Zubay, G. (1983) *Biochemistry*. Addison-Wesley Publishing Company, Reading, Massachusetts, 1268 pp.

### 5.1 Abstract

The nitrogen isotopic composition of chlorins from six Late Quaternary Eastern Mediterranean sapropels ( $-5.01 \pm 0.38$  per mil) was similar to the  $\delta^{15}\text{N}$  of chlorophyll *a* from the modern deep chlorophyll maximum at three Eastern Mediterranean locations ( $-6.38 \pm 1.80$  per mil). In addition, sapropel photoautotrophic material (calculated from the chlorin  $\delta^{15}\text{N}$ ) had the same  $\delta^{15}\text{N}$  (0.15 per mil) as bulk sapropel sediments ( $-0.08 \pm 0.53$  per mil) and deep water nitrate ( $-0.05$  per mil) in the modern Eastern Mediterranean, within the error of the measurements. These data suggest that (1) bottom waters were anoxic, (2) organic matter burial efficiency was enhanced, and (3) oligotrophic conditions similar to today persisted in the Eastern Mediterranean during sapropel deposition.

It is further suggested that Late Quaternary bulk sedimentary  $\delta^{15}\text{N}$  profiles record changes in the magnitude of diagenetic alteration of  $^{15}\text{N}/^{14}\text{N}$  ratios in organic matter. Large isotopic elevations of about 5.4 per mil are observed in organic-poor nannofossil marl oozes, while negligible diagenetic alteration is observed in organic-rich sapropel sequences. The diagenetic alteration under normal conditions in the Eastern Mediterranean is attributed to oxic diagenetic processes.

These results contradict an earlier interpretation (Calvert, et al., 1992) of Late Quaternary Eastern Mediterranean  $\delta^{15}\text{N}$  which concluded that the pattern of high values in marl oozes and low values in sapropels resulted from decreased



nutrient utilization (and hence, increased primary production) during sapropel events.

The modern Black Sea is demonstrated to be an excellent modern analog for the Eastern Mediterranean during sapropel events. In addition, it is suggested, based on chlorin  $\delta^{15}\text{N}$ , that the Black Sea was anoxic during deposition of the Holocene sapropel (e.g., Unit II).

## 5.2 Introduction

The burial of organic matter in marine sediments controls the oxygen content of the atmosphere (Walker, 1974) and leads to the formation of petroleum (Tissot and Welte, 1984). Yet our understanding of the controls on organic matter preservation is limited. The classical model maintains that the establishment of anoxia in bottom water is a principal control (Canfield, 1989; Correns, 1939; Demaison and Moore, 1980; Emerson, 1985; Hunt, 1979; Richards and Redfield, 1954; Tissot and Welte, 1984). More recently, this model has been challenged (Betts and Holland, 1991; Calvert, et al., 1991; Cowie and Hedges, 1992), and the roles of productivity (Calvert and Pedersen, 1992; Pedersen and Calvert, 1990; Bertrand and Lallier-Verges, 1993) sedimentation rate (Henrichs and Reeburgh, 1987) and sediment texture (Mayer, 1993), have been championed as primary controls on organic matter preservation. The major impediment to our assessment of these controls is their interdependence (Emerson and Hedges, 1988).

One of the more intriguing instances of enhanced organic matter preservation in marine sediments occurs in the Mediterranean Sea, where organic-rich sapropel layers have been periodically deposited since at least the middle Miocene (Kidd, et al., 1978; Olausson, 1961). These layers, the most

recent of which was deposited between 9 and 7 kyr BP (Troelstra, et al., 1991), have organic carbon concentrations between 2 and 17%, and durations of 1-10 kyr (Kidd, et al., 1978). The two competing hypotheses regarding their formation call on either increased production or increased preservation of organic matter.

Sapropel formation has been linked to the Indian Ocean monsoon (Rossignol-Strick, 1985; Rossignol-Strick, et al., 1982). During the monsoon, heavy precipitation in east Africa increases Nile River discharge to the Eastern Mediterranean. The decreased salinity in surface waters resulting from the additional freshwater may have caused a density stratification, perhaps inhibiting deep water ventilation (figure 5.1.c). This would have promoted the establishment of anoxic bottom water, much as in the modern Black Sea (Olausson, 1961). Such conditions are frequently cited as being conducive to the preservation of organic matter and the formation of organic-rich sediments (Canfield, 1989; Demaison and Moore, 1980).

The oxygen isotopic composition and distribution of planktonic foraminifera support a freshening of surface waters during sapropel formation (Cita, et al., 1977; Thunell and Williams, 1983; Thunell, et al., 1977; Vergnaud-Grazzini, et al., 1977; Williams and Thunell, 1979). Moreover, the lack of benthic foraminifera (Thunell, et al., 1977) and other benthic fauna (Kidd, et al., 1978) in most Late Quaternary sapropels indicates that bottom waters were anoxic during these times. (A small number of benthic foraminifera have been reported on the extremes of two sapropels (Mullineaux and Lohmann, 1981). It was speculated, though, that the species encountered are partially pelagic, and therefore able to float or swim above a narrow oxygen-depleted bottom layer of water at the onset or termination of a sapropel event.)

An alternative route to organic-rich sediments may be an increase in biological productivity (Pedersen and Calvert, 1990). This may have resulted, in



the Eastern Mediterranean, from an increased discharge of nutrient-rich riverine water (Calvert, 1983; Calvert, et al., 1992; Olausson, 1961; Sutherland, et al., 1984). In addition, elevated surface water nutrient concentrations may have been augmented by increased upwelling of nutrient-rich deep water resulting from a switch from anti-estuarine (e.g., that of today) to estuarine circulation (Calvert, et al., 1992).

The circulation of the modern Eastern Mediterranean is driven by an excess of evaporation over precipitation (Bethoux, 1979). Nutrient-depleted North Atlantic surface waters flow in from the west and sink in the east as their salinity is increased through intense evaporation. That inflow is balanced by an outflow of nutrient-enriched subsurface water at the Strait of Sicily (figure 5.1.a). This circulation pattern results in what has been termed a "nutrient desert"--the extreme nutrient-impoverishment of Eastern Mediterranean surface and deep waters. During sapropel deposition, however, it is possible that surface waters became sufficiently fresh to cause a reversal in this circulation pattern, resulting in a "nutrient trap" (Sarmiento, et al., 1988a). According to this scenario, low salinity surface water from increased river discharge would flow west over the Strait of Sicily (Muerdter, 1984; Stanley, et al., 1975) and be replaced by eastward flowing nutrient-enriched subsurface water (figure 5.1.b).

Some evidence exists for increased productivity during sapropel deposition. However, much of the evidence is localized in area and pertains only to certain sapropels. For instance, high abundances of diatom frustules have been identified in certain sapropels (Olausson, 1961; Schrader and Matherne, 1981; Thunell and Williams, 1982; Thunell and Williams, 1983). In addition, the abundance and distribution of coccolithophorids in a suite of cores from the eastern basin were suggestive of higher productivity (Castradori, 1993). Other evidence came from organic carbon concentration



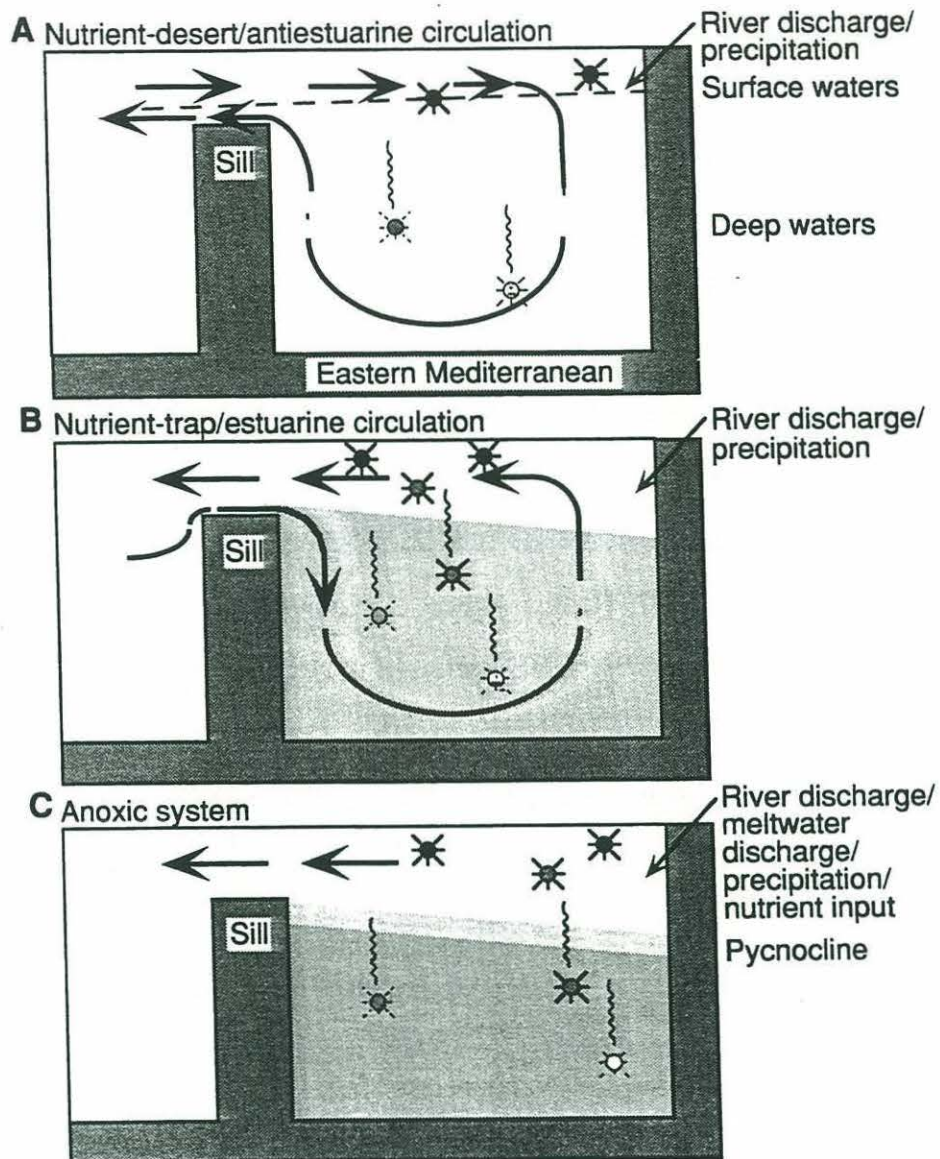


Figure 5.1: Schematic diagrams of (a) the circulation in the modern Eastern Mediterranean, a nutrient desert, (b) an estuarine circulation and nutrient trap that may have resulted from a freshening of surface waters by increased monsoon-derived Nile runoff, and (c) an anoxic basin resulting from reduced ventilation of deep waters caused by a strong salinity gradient. A switch to estuarine circulation need not result in increased biological production (Sarmiento, et al., 1988). Figure from Emeis, et al (1996).

(de Lange and ten Haven, 1983) and accumulation rate (Howell and Thunell, 1992) measurements, as well as theoretical arguments based on the dissolved oxygen balance in the Eastern Mediterranean (Jenkins and Williams, 1983/84).

Recently, sedimentary nitrogen isotopic evidence has been called upon to support the increased productivity hypothesis (Calvert, et al., 1992). Low  $\delta^{15}\text{N}$  values in sapropels and high values in interbedded marl oozes were interpreted to result from the preferential uptake of  $^{14}\text{N}$  by phytoplankton living in nutrient-enriched surface waters. Other investigators have shown a good inverse correlation between  $\delta^{15}\text{N}$  values in particles (Altabet, et al., 1991; Rau, et al., 1991; Saino and Hattori, 1985) and sediments (Altabet and Francois, 1994; Francois and Altabet, 1992), and nutrient availability in surface waters.

This chapter describes the results of nitrogen isotopic measurements in chlorophyll-related pigments from Late Quaternary sapropels in the Eastern Mediterranean. Chlorin  $\delta^{15}\text{N}$  is believed to reflect the isotopic composition of phytoplankton at the time the sapropels were deposited. By comparing these values to  $\delta^{15}\text{N}$  measurements in whole sediments, modern phytoplankton, and deep-water nitrate it is suggested that, contrary to previous conclusions from nitrogen isotopic measurements, sapropels result primarily from the increased preservation of organic matter under anoxic bottom water. An analogy is then drawn to the modern Black Sea where, presently, organic-rich sediments are being deposited in an oligotrophic, anoxic basin.

### 5.3 Methods

The techniques for measuring nitrogen and carbon isotopic ratios in sedimentary and particulate chlorins are described in chapter 2. The procedures



for measuring whole sediment and particulate  $\delta^{15}\text{N}$  and  $\delta^{13}\text{C}$  are also described in that chapter.

### 5.3.1 Sample Collection

All Eastern Mediterranean Sea sediments (except for surface samples) were collected from the Drilling Vessel *JOIDES Resolution*, during Ocean Drilling Program Leg 160, in March and April, 1995. The samples analyzed in this study came from two locations. Site 964F ( $36^{\circ}15.638'\text{N}$ , longitude  $17^{\circ}45.025'\text{E}$ ), at a water depth of 3657 m, was located at the foot of the Calabrian Ridge, about 200 m above and 35 km to the northwest of the Ionian Abyssal Plain (figure 5.2). Site 969C ( $33^{\circ}50.323'\text{N}$ ,  $24^{\circ}53.005'\text{E}$ ), at a water depth of 2196 m, was located about 100 km south of Crete, on the Mediterranean Ridge that separates the Ionian Basin in the west from the Levantine Basin in the east (figure 5.2). All the samples for which isotopic determinations were made are listed in table 5.6. Those samples for which chlorin isotopic measurements were made are listed in table 5.1. Sediment samples from ODP were stored frozen until analysis.

Suspended particulate, sediment trap and water samples were collected between May 22nd and June 5th, 1996, aboard R/V Suroit during the Minos Cruise from Toulon, France to Heraklion, Greece. The type and location of the samples used in this study are listed in table 5.2. Station locations are shown in figure 5.3. Suspended particulate samples were collected by drawing water from the deep chlorophyll maximum (DCM) (a depth of 70-110 m) with a 3/4" garden hose connected to a pneumatic pump (Lutz Pumps, Inc, Norcross, GA) on deck. A 53  $\mu\text{m}$  screen was placed across the hose intake. The outflow from the pump was passed through a 293 mm pre-combusted ( $450^{\circ}\text{C}$ , > 8 hours) Gelman A/E filter. Between 500 and 1500 L seawater was pumped through each filter at a rate



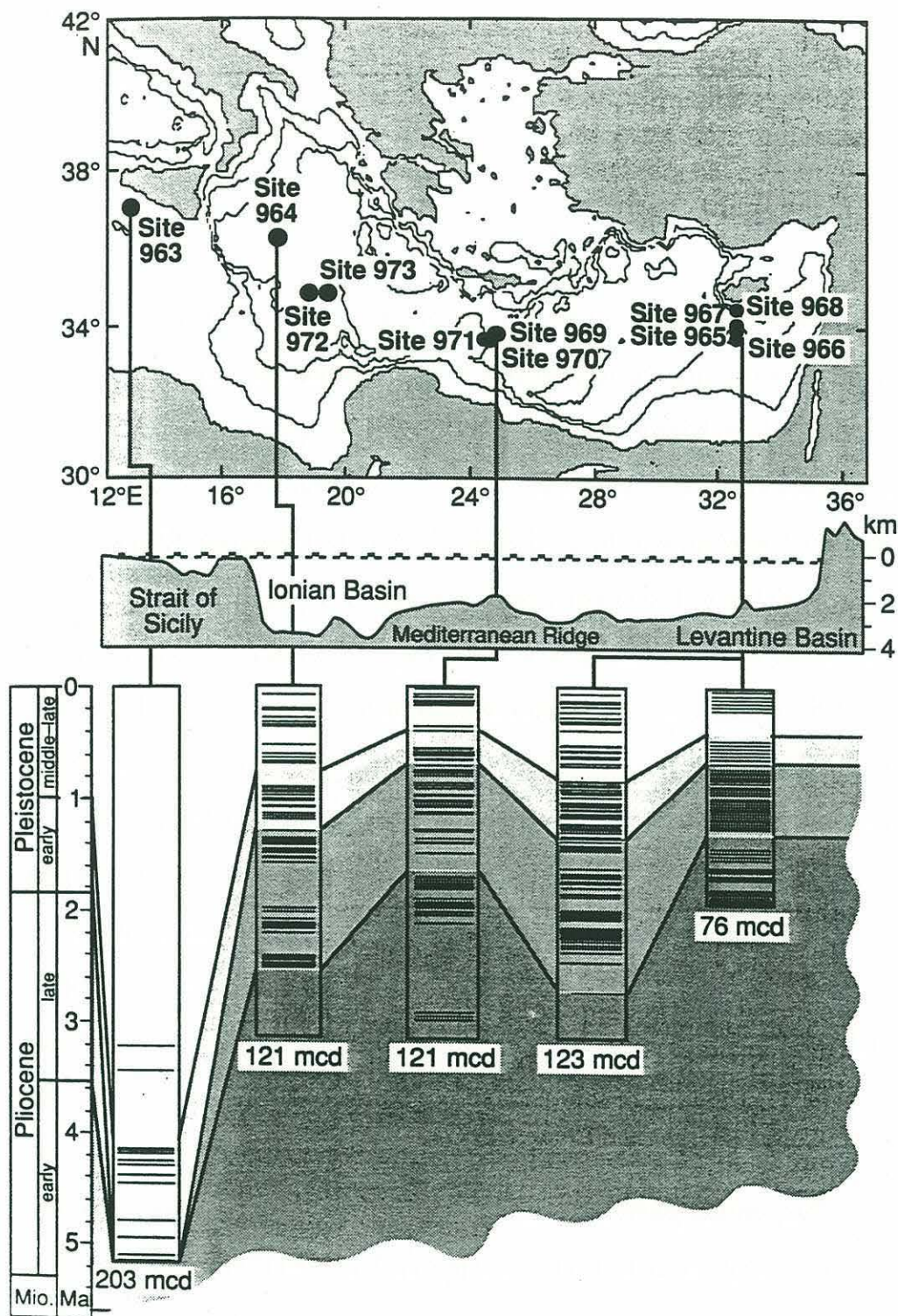


Figure 5.2: Overview map of the Eastern Mediterranean Sea with schematics showing the widespread occurrence of sapropels in that basin. Cores from sites 164 and 169 were used in this study. Figure from Emeis, et al. (1996).

**Table 5.1: Sapropel samples from ODP leg 160 for which chlorin N and C isotopic determinations were made.**

Sample Hole/Core/Sec	Interval (cm)	Depth (mbsf) <sup>1</sup>	Sapropel <sup>1</sup>	Approx. <sup>2</sup> Age (kyr)	Dry Wt. (g) <sup>3</sup>
964F/1H/05	38-48	6.38	S2	55	26.6
964F/1H/05	114-126	7.14	S3	81	42.6
964F/2H/01	40-48	11.02	S4	95	28.3
964F/2H/01	48-58	11.02	S4	98	34.4
969C/1H/01	119-125	5.62	S5	123	55.9
	130-136				
969C/1H/02	29-35	6.22	S6	175	23.5
969C/1H/02	76-82	6.68	S7	193	44.1
	87-93				

<sup>1</sup> Composite depths and sapropel numbers were from Dr. K. Emeis, chief scientist of Leg 160 (personal communication). <sup>2</sup> Ages are estimated from Cita, et al (1977), and Emeis, et al (1996). <sup>3</sup> Dry weights were measured after solvent extraction.

of about 500 L/hour. The filters were frozen at -40°C immediately following the filtration.

The sediment trap sample was collected using a 1/8 m<sup>2</sup> floating trap deployed at 200 m. The deployment was for 8 hours, between 0600 and 1400 local time. No poison or preservative was used.

Water samples (table 5.2) were collected from 10 L Niskin bottles arranged on a rosette. The rosette was equipped with a CTD, as well as an oxygen probe and a fluorometer. The depth of the DCM was estimated by the fluorescence maximum. Water samples were either acidified with HCl (1.0 mL 12 N HCl/250 mL seawater), or preserved with HgCl<sub>2</sub> (~200 µL saturated HgCl<sub>2</sub> (aq)/1500 mL seawater), and stored at room temperature until analysis.



Figure 5.3: Minos Cruise station locations.

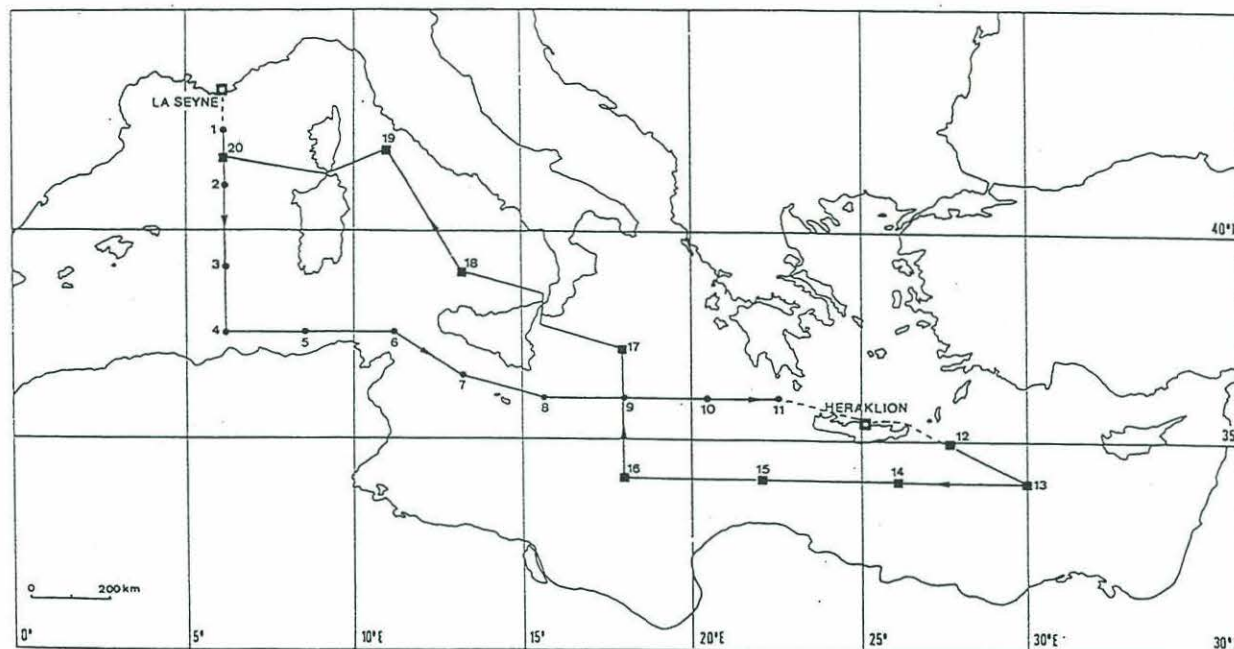


Table 5.2: Samples from the Mediterranean Sea collected during R/V *Le Suroit* Minos Cruise, 5/22/96-6/5/96 and used in this study.

Type	Latitude	Longitude	Stn.	Water Depth	Description
Susp. Partic.	39°13' N	6°09' E	3	2800	2722 L @ 70 m
Susp. Partic.	36°00' N	17°59' E	9	3935	1056 L @ 110 m
Susp. Partic.	36°00' N	20°20' E	10	2975	1927 L @ 75 m
Susp. Partic.	36°00' N	22°16' E	11	3885	2003 L @ 80 m
Water	36°00' N	22°16' E	11	3885	1.5 L @ 1000 m
Water	36°00' N	22°16' E	11	3885	0.25 L @ 1000 m
Sed. Trap	36°00' N	20°20' E	10	2975	1/8 m <sup>2</sup> , 8 hrs @ 200 m
Surf. Sed.	35°43' N	15°27' E	8	410	0-15 cm, bulk



Eastern Mediterranean surface sediment samples (table 5.2) were collected by gravity corer, and immediately stored frozen in the core liner at -40°C. Sediments remained frozen until analysis.

**Figure 5.4: Map of the Black Sea showing sample locations.**

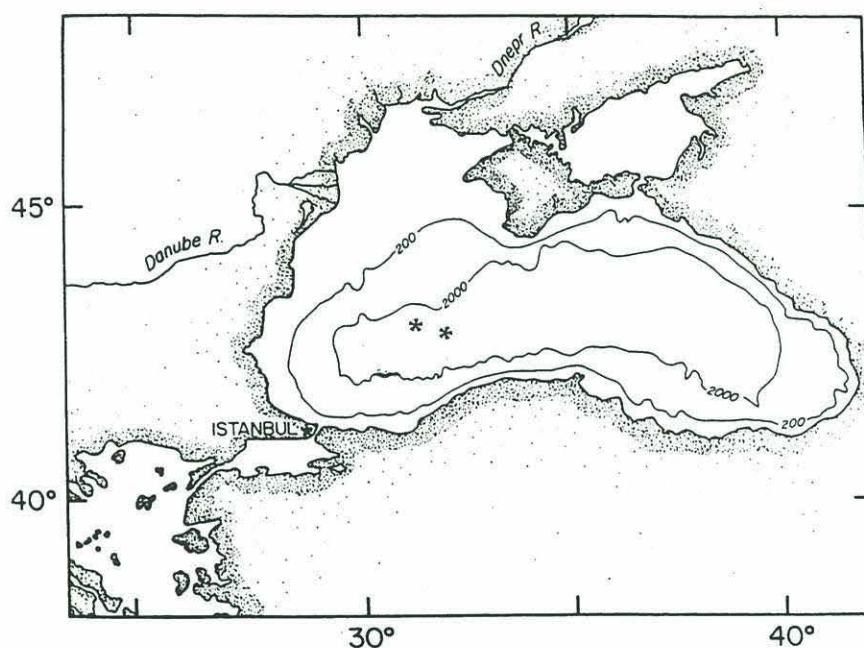


**Table 5.3: Description of Black Sea sediment samples used in this study.**

Core	Latitude	Longitude	Water Depth	Interval (cmbsf)	Strat. Unit <sup>1</sup>	Dry Wt. (g) <sup>2</sup>
KNR134-09 BC2	42°51' N	31°57' E	2129	0-10	I	217
KNR134-08 BC17	42°58' N	31°25' E	2066	36-42	II	
KNR134-08 BC17	42°58' N	31°25' E	2066	42-47	II	31.7
KNR134-08 BC17	42°58' N	31°25' E	2066	50-56	II	

<sup>1</sup> Stratigraphic unit as defined by Hay, et al. (1991); stratigraphy from Jones and Gagnon (1994). <sup>2</sup> Dry weights were from extracted sediment.

Black Sea sediments were collected from the Euxine Abyssal Plain, at a water depth of about 2100 m, using an Ocean Instruments Mark-III box corer during R/V *Knorr* cruise 134, in May, 1988. The sample locations are shown in figure 5.4 and listed in table 5.3.

### 5.3.2 Nitrogen Isotopic Measurements on Small Samples: Cryofocussing

Since the minimum sample size required to measure nitrogen isotopic ratios at the Marine Biological Laboratory Isotope Facility was 1  $\mu\text{mol N}$ , samples smaller than that were measured at the Boston University Stable Isotope Facility using a cryofocussing technique (Fry, et al., in preparation). Samples were combusted in an elemental analyzer and cryogenically purified before being degassed into the mass spectrometer. The manual continuous flow system used helium as a carrier gas. A precision of 0.38 per mil was achieved with glycine standards ranging in size from 41 to 6000 nmol N. The average precision for 2 sets of triplicate measurements of sedimentary chlorins was 0.54 per mil, which is the presumed precision for this study. The nitrogen blank associated with the measurement averaged 90 nmol N, and this blank had a  $\delta^{15}\text{N}$  of  $-6.15 (\pm 0.45)$  per mil. Cryofocus  $\delta^{15}\text{N}$  values were blank-corrected.

All Eastern Mediterranean suspended particulate chlorophyll  $\delta^{15}\text{N}$  measurements were performed using the cryofocussing technique. On a second occasion, the chlorin  $\delta^{15}\text{N}$  values from sapropels S2 and S7, in addition to the sediment trap sample, were determined by this technique. The latter values were corrected for a bias of  $1.625 (\pm 0.43)$  per mil. This bias was determined by averaging the difference between the  $\delta^{15}\text{N}$  values measured by cryofocussing, and those determined independently at the Marine Biological Laboratory Isotope Facility on 6 different sedimentary chlorin samples.

### *5.3.3 Preparation of Nitrate Samples for Isotopic Analysis*

Nitrate samples were prepared for isotopic analysis by Daniel Sigman at the Woods Hole Oceanographic Institution (Sigman, et al., submitted). In brief, 400 mL of seawater were incubated for 5 days at 65°C with 1.2 g MgO. This acted as a buffer and raised the pH of the seawater to 9.7. Samples were then concentrated to 60 to 80 mL by boiling. Then 36 to 48 mg of Devarda's alloy was added to each sample. This converted nitrate to ammonia. In addition, a "diffusion packet" consisting of an acidified glass fiber filter within an envelope of teflon tape, was added to each sample. Ammonia diffused onto the acidified filter. The samples were then incubated at 65°C for 4 days, then on a shaker at 60 rpm for 8 days at room temperature, to facilitate the diffusion. The packet was then removed, dipped into 10% HCl, then distilled water, and dried in a dessicator containing silica gel and an open vial of H<sub>2</sub>SO<sub>4</sub> (to remove any ammonia in the air). Filters were removed from the packets and placed into Sn boats just prior to isotopic analysis.

### *5.3.4 Precision of Isotopic Measurements*

The precision of N and C isotopic determinations in sedimentary and particulate chlorin samples is discussed in detail in chapter 2. The precision for isotopic determinations in bulk particulate and sedimentary samples is listed in table 5.4. The precisions represent the pooled standard deviations of multiple sets of replicate analyses.



**Table 5.4: Precision of nitrogen and carbon isotopic determinations in different sample types. PSD is the pooled standard deviation of multiple sets of replicate measurements. Values are in per mil.**

Sample Type	PSD - $\delta^{15}\text{N}$	PSD - $\delta^{13}\text{C}$
Chlorin	0.12	0.09
Particulate	0.26	0.39
Sediment	0.17	0.04
Seawater Nitrate <sup>1</sup>	0.2	
Cryofocus <sup>1</sup>	0.54	

<sup>1</sup> Values are average standard deviations of replicates.

## 5.4 Results

### 5.4.1 Nitrogen and Carbon Isotopes in the Mediterranean Sea

#### 5.4.1.1 Water Column Particulate Samples

The N and C isotopic composition of chlorophyll and bulk suspended particulates was measured at the deep chlorophyll maximum (DCM) at 4 stations in the Mediterranean Sea between May 25th and June 4th, 1996 (table 5.5, figure 5.11.a and figure 5.5.6-1.a). Station 3 was in the western basin, while stations 9, 10 and 11 were in the eastern basin (see table 5.2 and figure 5.3 for station locations and descriptions). Chlorophyll  $\delta^{15}\text{N}$  values in suspended particles

from the eastern basin (e.g., Stations 9, 10 and 11) were made by cryofocus irMS. Therefore, no  $\delta^{13}\text{C}$  values were available for those samples.

**Table 5.5: Nitrogen and carbon isotopic composition of chlorophyll, suspended particulate and nitrate samples from the Mediterranean Sea. All chlorophyll samples are from the deep chlorophyll maximum. Station locations are shown in figure 5.3.**

Station	Sample	Depth (m)	$\delta^{15}\text{N}$	$\delta^{13}\text{C}$
3	Chlorophyll <i>a</i>	70	-2.2	-26.6
3	POM	70	2.15	-25.75
3	POM	4	0.15	-24.65
9	Chlorophyll <i>a</i>	110	-8.6	
9	POM	110	-0.7	-24.4
10	Chlorophyll <i>a</i>	75	-6.5	
10	POM	75	-0.7	-24.2
10	Sinking PON <sup>1</sup>	200	5.0	
11	Chlorophyll <i>a</i>	80	-6.2	
11	Chlorophyll <i>a'</i>	80	-4.2	
11	POM	80	-0.5	-24.15
11	Nitrate	1000	-0.05	

<sup>1</sup> A gelatinous plankton specimen (i.e., swimmer) was in this sample, but could not be removed. Therefore, this value may not be representative of sinking PON.

Chlorophyll  $\delta^{15}\text{N}$  values in suspended particles from the DCM fell in a range between -8.6 and -2.2 per mil. In the eastern basin (e.g., Stations 9, 10 and 11) they averaged -6.38 ( $\pm 1.80$ ) per mil. Therefore, applying the relationship between chlorophyll and whole cell  $\delta^{15}\text{N}$  in phytoplankton (determined in chapter 4), it is calculated that phytoplankton in the eastern basin DCM had an

average  $\delta^{15}\text{N}$  of -1.22 per mil. The origin of a possible east-west gradient in  $\delta^{15}\text{N}_{\text{Chla}}$  is discussed in section 5.5.5. Bulk suspended particulate  $\delta^{15}\text{N}$  values from the DCM fell in a range between -0.7 and 2.15 per mil. In the eastern basin they averaged  $-0.63 (\pm 0.12)$  per mil.

The one chlorophyll  $\delta^{13}\text{C}$  value measured was in the western basin. The sample from the DCM at Station 3 had a  $\delta^{13}\text{C}$  value of -26.6 per mil. Suspended particulate  $\delta^{13}\text{C}$  values from the DCM fell in a range between -25.75 and -24.15. The average of those values was  $-24.63 (\pm 0.76)$ . When only the samples from the eastern basin were included, the average  $\delta^{13}\text{C}_{\text{POC}}$  was  $-24.25 (\pm 0.13)$ . Since the POC sample from which the Stn. 3 chlorophyll was extracted had a  $\delta^{13}\text{C}$  of -25.75 (i.e., 1.5 per mil less than the average  $\delta^{13}\text{C}_{\text{POC}}$  in the eastern basin), it may be possible to estimate the  $\delta^{13}\text{C}$  of eastern basin DCM chlorophyll by adding 1.5 per mil to the measured chlorophyll  $\delta^{13}\text{C}$  in the western basin. This yields an estimate of -25.1 per mil for the average  $\delta^{13}\text{C}_{\text{Chla}}$  at the DCM in the eastern basin.

The  $\delta^{15}\text{N}$  value of two chlorophyll *a* structural isomers was determined at Station 11. The 10(S)- stereoisomer of chlorophyll *a*, chlorophyll *a'*, comprised 28% of the total Chla+a' in that sample. Therefore the weighted average  $\delta^{15}\text{N}$  of chlorophyll at Station 11 is taken to be -5.64 ( $= (0.28) \times (-4.2) + (0.72) \times (-6.2)$ ). The chlorophyll  $\delta^{15}\text{N}$  determinations for Stations 9 and 10 were made on the combined Chla+a', because samples were small. A discussion about the origin of this isotopic difference can be found in chapter 2 (section 2.5.2.2).

The average N isotopic difference between PON and chlorophyll in the 4 DCM samples was  $5.78 (\pm 1.54)$  per mil. This compares favorably with the  $\Delta\delta^{15}\text{N}_{\text{cell-Chla}}$  difference of  $5.16 (\pm 2.40)$  per mil in axenic phytoplankton cultures (see chapter 4). This suggests that most of the PON sampled was algal, since higher trophic levels are enriched in  $^{15}\text{N}$  (DeNiro and Epstein, 1981; Fry,



1988). The C isotopic difference between POC and chlorophyll in the one sample from the western basin was 0.85 per mil. This falls within the range of values found in cultured phytoplankton,  $-0.02 (\pm 2.12)$  per mil (see chapter 4).

#### 5.4.1.2 Water Samples

The N isotopic composition of deep-water nitrate was measured at Station 11 in the Eastern Mediterranean. The  $\delta^{15}\text{N}$  value for nitrate from a depth of 1000 m was  $-0.05$  per mil. The nitrate concentration in that sample was  $3.64 \mu\text{M}$  (Dr. Patrick Rimbault, personal communication). Profiles of nitrate and phosphate at station 11 are shown in figure 5.5.

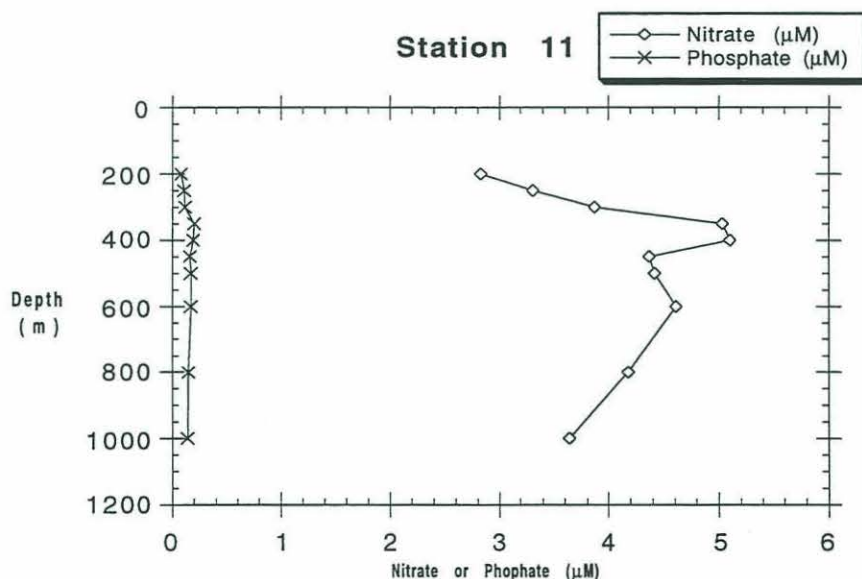


**Figure 5.5: Nitrate and phosphate profiles at Station 11 in the E. Mediterranean. Data were provided by Dr. Patrick Rimbault.**

#### 5.4.1.3 Sediment Samples

The N and C isotopic composition of chlorins and whole sediments was measured in two cores from ODP Leg 160 in the Eastern Mediterranean (see map in figure 5.2). Sediments received from hole 964F (3657 m water depth, 36°15.638'N, 17°45.025'E), located at the base of the Calabrian Ridge, 35 km northwest of the Ionian Abyssal Plain, contained 3 sapropels: S2, S3 and S4 (Dr. K. Emeis, personal communication). Sediments received from hole 969C (2196 m water depth, 33°50.323'N, 24°53.005'E), located on the Mediterranean Ridge, 100 km south of Crete, also contained 3 sapropels: S5, S6 and S7 (Dr. K. Emeis, personal communication). The stratigraphic position of these sapropels within the SPECMAP stacked  $\delta^{18}\text{O}$  record (Imbrie, et al., 1984) and the orbital precession index (Berger and Loutre, 1991) is shown in figure 5.6.

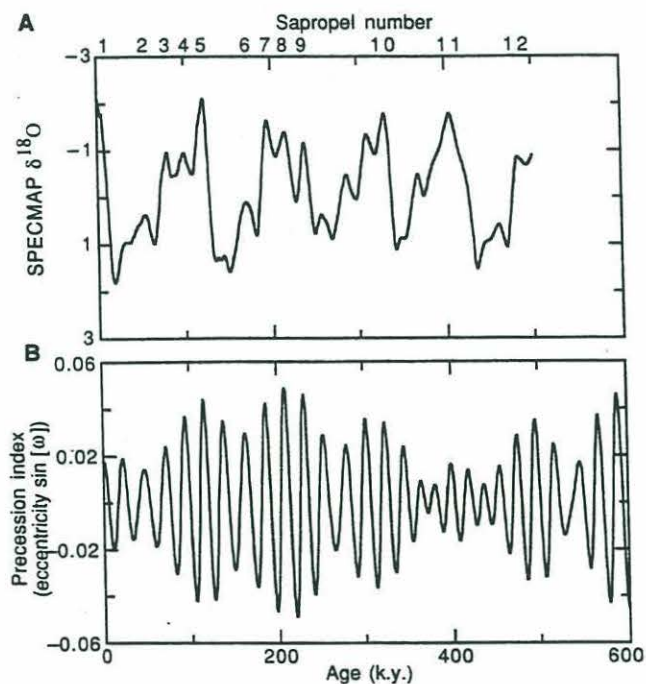


**Figure 5.6: Stratigraphic position of Late Quaternary Eastern Mediterranean sapropels within (a) the SPECMAP stacked  $\delta^{18}\text{O}$  record of Imbrie, et al (1984), and (b) the orbital precession index of Berger and Loutre (1991). Sapropels S2 through S7 were included in this study. Figure from Emeis, et al (1996).**

Table 5.6: Nitrogen and carbon isotopic ratios in Eastern Mediterranean sediments.

Sapropel	Leg	Hole	Core	Sect	Interval	Comp. Depth (mbsf)	$\delta^{15}\text{N}$	$\delta^{13}\text{C}$	Spread Dupl.	Spread Dupl.
S2-6	160	964F	1H	5	32-34	6.33	4.8			
S2-4	160	964F	1H	5	34-36	6.35	5.1			
S2-2	160	964F	1H	5	36-38	6.37	4.7			
S2	160	964F	1H	5	38-39	6.385	0.8	-22.3		
S2	160	964F	1H	5	40-41	6.405	1.4	-23		
S2	160	964F	1H	5	42-43	6.425	1.8	-22.4		
S2	160	964F	1H	5	44-45	6.445	2.1	-21.9		
S2	160	964F	1H	5	46-47	6.465	1.8	-22.1		
S2+2	160	964F	1H	5	48-50	6.49	4.4			
S2+4	160	964F	1H	5	50-52	6.51	4.1			
S2+6	160	964F	1H	5	52-54	6.53	4.2			
S3-12	160	964F	1H	5	102-104	7.03	5.6			
S3-10	160	964F	1H	5	104-106	7.05	5.75		0.1	
S3-8	160	964F	1H	5	106-108	7.07	5.7			
S3-6	160	964F	1H	5	108-110	7.09	5.6			
S3-4	160	964F	1H	5	110-112	7.11	4.8			
S3-2	160	964F	1H	5	112-114	7.13	4.8			
S3	160	964F	1H	5	114-115	7.145	-1.1	-22		
S3	160	964F	1H	5	116-117	7.165	-0.8	-21.5		
S3	160	964F	1H	5	118-119	7.185	-0.7	-21.8		
S3	160	964F	1H	5	120-121	7.205	-0.6	-21.8		
S3	160	964F	1H	5	122-123	7.225	0.8	-22.7		
S3	160	964F	1H	5	124-125	7.245	1.5	-22.3		
S3+2	160	964F	1H	5	128-130	7.29	5.1			
S3+4	160	964F	1H	5	130-132	7.31	5		0.2	
S4-8	160	964F	2H	1	32-34	9.43	4.9			
S4-6	160	964F	2H	1	34-36	9.45	1		0	
S4-4	160	964F	2H	1	36-38	9.47	1.4			
S4-2	160	964F	2H	1	38-40	9.49	4.6			
S4a	160	964F	2H	1	40-41	9.505	0.5	-24.2		
S4a	160	964F	2H	1	42-43	9.525	0.2	-23.7		
S4a	160	964F	2H	1	44-45	9.545	1	-23.3		
S4a	160	964F	2H	1	46-47	9.565	0.9	-23.4		
S4b	160	964F	2H	1	48-49	9.585	0.6	-23.7		
S4b	160	964F	2H	1	50-51	9.605	0.4	-23.6		
S4b	160	964F	2H	1	52-53	9.625	-0.8	-22.6		
S4b	160	964F	2H	1	54-55	9.645	0.3	-22.8		
S4b	160	964F	2H	1	56-57	9.665	0.7	-21.8		
S4+2	160	964F	2H	1	58-60	9.69	5			
S4+4	160	964F	2H	1	60-62	9.71	5			
S4+6	160	964F	2H	1	62-64	9.73	4.5			
S4+8	160	964F	2H	1	64-66	9.75	4.85		0.1	
S5-17	160	969C	1H	1	81-87	5.24	6.5			
S5	160	969C	1H	1	122-123	5.625	-0.2	-23.7		
S5	160	969C	1H	1	127-128	5.675	-0.45	-16.85	0.5	0.3
S5	160	969C	1H	1	133-134	5.735	-1.5	-23.9		
S5+7	160	969C	1H	1	142-148	5.85	6.2			
S6-9	160	969C	1H	2	16-22	6.11	4.2			
S6	160	969C	1H	2	31-32	6.235	-0.15	-21.3	1.5	
S6+19	160	969C	1H	2	54-60	6.49	6.8			
S7	160	969C	1H	2	78-79	6.705				
S7	160	969C	1H	2	84-85	6.765	0	-23.3		
S7	160	969C	1H	2	90-91	6.825	0.4	-24.7		
S7+15	160	969C	1H	2	106-112	7.01	6.3		0.2	



High-resolution (2 cm) sampling of bulk sediment in hole 964F was performed, and the N and C isotopic results are listed in table 5.6 and shown in figures 5.11.b and 5.13.b. In addition, table 5.6 lists the bulk sediment isotopic determinations from hole 969C, and those results are shown in figures 5.11.c and 5.13.c.

The chlorin isotopic results from sapropels are listed in table 5.7 and shown in figures 5.11 and 5.13. A single chlorophyll degradation product, pyropheophorbide *a*, was found to be the most abundant chlorin in all 6 sapropels (figure 5.7) investigated in this study. This identification was based upon the visible spectrum and coelution with an authentic standard. Also listed in table 5.7 are the N and C isotopic ratios in the bulk sediment from which the chlorins were extracted. Those values represent the average sapropel  $\delta^{15}\text{N}$  and  $\delta^{13}\text{C}$ .

Sapropel  $\delta^{15}\text{N}$  values fell in a narrow range between -1.5 and 2.1 per mil, and averaged  $-0.08 (\pm 0.53)$  per mil. Non-sapropel sediment  $\delta^{15}\text{N}$  values were between 4.2 and 6.8 per mil, and averaged  $5.30 (\pm 0.97)$  per mil. Therefore, on average, sapropels are depleted in  $^{15}\text{N}$  by 5.38 per mil relative to non-sapropel sediments. As discussed below, this quantity represents the diagenetic alteration of nitrogen isotope ratios in marine organic matter in oxic waters.

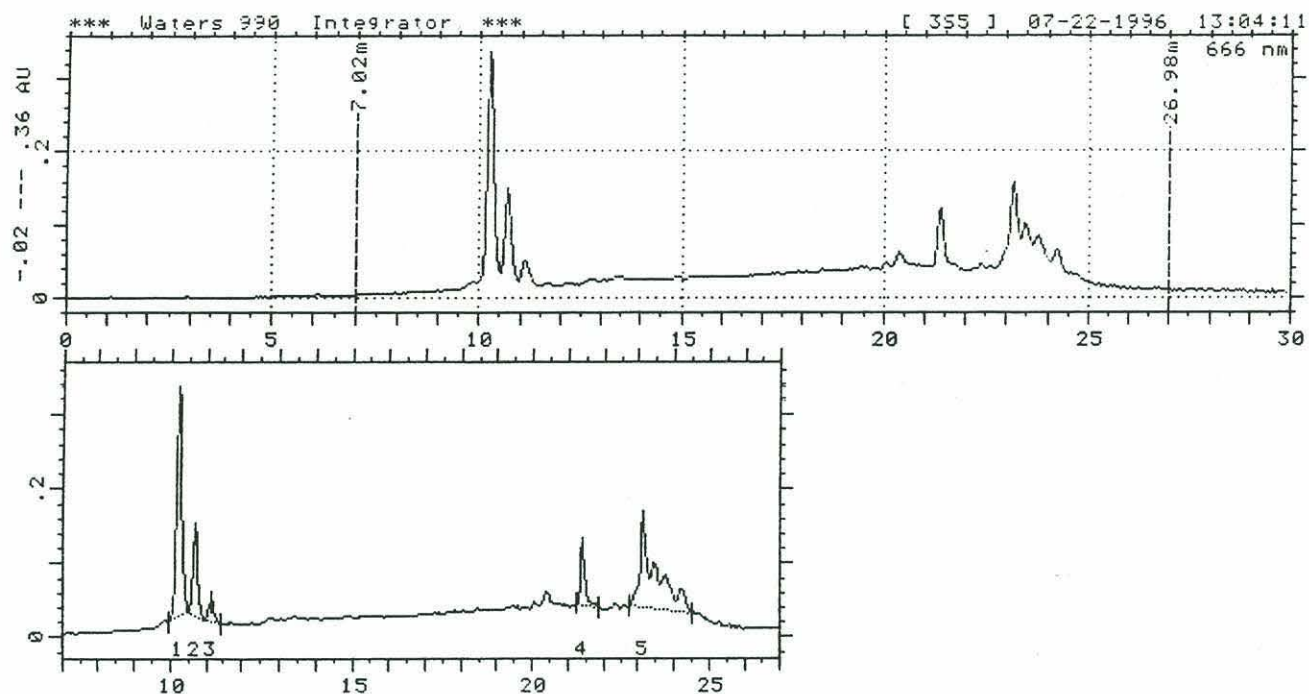
Chlorin  $\delta^{15}\text{N}$  values from sapropels fell in a narrow range between -5.65 and -4.6, and averaged  $-5.01 (\pm 0.38)$  per mil. Therefore, using the chlorophyll-cell isotopic relationship established in chapter 4, it is calculated that phytoplankton living during sapropel events had average  $\delta^{15}\text{N}$  values of 0.15 per mil. This value is surprisingly close to the modern  $\delta^{15}\text{N}$  of phytoplankton in the eastern basin, -1.2 per mil (see section 5.4.1.1), given that the  $\Delta\delta^{15}\text{N}_{\text{cell-Chla}}$  relationship has a standard deviation of 2.40 per mil.

Furthermore, on average, chlorins were depleted in  $^{15}\text{N}$  by 4.95 per mil relative to the sapropels from which they were extracted. This difference

**Table 5.7: Nitrogen and carbon isotopic ratios in chlorins and sediments from Eastern Mediterranean sapropels. All values were measured in composite samples of the entire sapropel. For samples measured in duplicate, the  $\delta^{15}\text{N}$  and  $\delta^{13}\text{C}$  spread of the measurements is shown.**

Sapropel	Sample	$\delta^{15}\text{N}$	$\delta^{15}\text{N}$ Spread	$\delta^{13}\text{C}$	$\delta^{13}\text{C}$ Spread
S2	Chlorin <sup>1</sup>	-5.26	0.60		
S2	Sediment	-0.05	0.9	-23.6	1.8
S3	Chlorin	-5.65	0.1	-20.5	0
S3	Sediment	-0.3	0.2	-22.05	0.1
S4a	Chlorin	-4.8		-22.1	
S4a	Sediment	0.75	0.3	-23.8	0
S4b	Chlorin	-4.9		-22.4	
S4b	Sediment	-0.2	0.2	-23.1	0
S5	Chlorin	-4.6	0	-22.9	0
S5	Sediment	-0.55	0.1	-23.2	0
S6	Chlorin	-5.2		-18.1	
S6	Sediment	-0.15	1.5	-21.3	0
S7	Chlorin <sup>1</sup>	-4.66	0.47		
S7	Sediment	-0.05	0.1	-24.1	0
AVG	Chlorin <sup>2</sup>	-5.01	0.38		

<sup>1</sup> Measured in triplicate by cryofocussing, and corrected by -1.625 per mil for a bias (section 5.3.2).  $\delta^{15}\text{N}$  Spread is the standard deviation of the 3 measurements. <sup>2</sup> The average value for all 6 sapropels, S2-S7, and the standard deviation of that average.



[666 nm]							
No.	Retention time	Height [AU]	Left time	Right time	Area [AU*min]	Area [%]	Mark
1	10.25	0.2937	9.95	10.50	0.056338	35.023	I
2	10.70	0.1093	10.50	10.95	0.020729	12.886	I
3	11.15	0.0253	10.95	11.40	0.005451	3.388	I
4	21.40	0.0768	21.25	21.85	0.014037	8.726	I
5	23.15	0.1172	22.75	24.50	0.064308	39.977	I

Figure 5.7: Typical reverse-phase HPLC chromatogram of a sapropel solvent extract after solid-phase extraction. Visible absorbance detection was at 666 nm. In this sapropel (S5), PPBDa (retention time=10.25 mins) accounted for 35% of the total chlorins in the sample. Tentative identifications of the other chlorins, their retention times and their relative abundance in the sample are as follows: mesopyropheophorbide *a* (10.7 mins, 13%), methyl pyropheophorbide *a* (11.15 mins, 3%), pyropheophytin *a* (21.4 mins, 9%), and chlorin steryl esters (23-25 mins, 40%).



compares favorably with the measured  $\Delta\delta^{15}\text{N}_{\text{cell-Chla}}$  of 5.16 per mil in axenic phytoplankton cultures (see chapter 4), and with the  $\Delta\delta^{15}\text{N}_{\text{PON-Chla}}$  of 5.78 per mil at the DCM in the modern E. Mediterranean.

Sapropel  $\delta^{13}\text{C}_{\text{org}}$  values fell in a range between -24.1 and -21.3, and averaged -23.0 ( $\pm 1.00$ ) per mil. Chlorin  $\delta^{13}\text{C}$  values from sapropels were between -22.9 and -18.1, and averaged -21.2 ( $\pm 1.95$ ) per mil. If the glacial sapropel S6 (Castradori, 1993) is excluded, then the average chlorin  $\delta^{13}\text{C}$  is -21.98 ( $\pm 1.04$ ) per mil and the average sapropel  $\delta^{13}\text{C}_{\text{org}}$  is -23.3 ( $\pm 0.72$ ) per mil. Therefore, on average, chlorins are enriched in  $^{13}\text{C}$  by 1.33 per mil relative to sapropelic organic matter.

The N and C isotopic composition of a surface (0-15 cm, bulk) sediment collected at Station 8 on the Minos Cruise (see map in figure 5.3) was measured. The site (35°43'N, 15°27'E), at a water depth of 410 m, was located on the eastern flank of the Strait of Sicily. The  $\delta^{15}\text{N}$  of that sample was 4.3 per mil (spread of 2 measurements was 0.2), and the  $\delta^{13}\text{C}$  was -21.5 per mil. This  $\delta^{15}\text{N}$  value was in the range of those for non-sapropel sediments in the ODP cores (see table 5.6).

#### 5.4.2 Nitrogen and Carbon Isotopes in the Black Sea

The nitrogen and carbon isotopic compositions of chlorins and whole sediments from a Black Sea surface sediment (Unit I) and an underlying sapropel (Unit II) were measured (see table 5.3 and figure 5.4 for descriptions and locations of sites). The results are listed in table 5.8.

Table 5.8: Nitrogen and Carbon isotopic ratios in sediments and chlorins from the Black Sea.

Core	Interval (cm)	Strat Unit	$^{14}\text{C}$ Age (yr BP) <sup>1</sup>	Sample	$\delta^{15}\text{N}$	$\delta^{13}\text{C}$
BC2	0-10	I	1000	Chlorin	-4.51	-24.1
BC2	0-10	I	1000	Sediment	1.3	-23.3
BC17	36-42	II	3768	Sediment	0.6	-24.4
BC17	42-47	II	4515	Chlorin	-5.8	-23.2
BC17	42-47	II	4515	Sediment	0.45	-24.1
BC17	50-56	II	5670	Sediment	1.5	-23.1

<sup>1</sup> Unit I age is approximated from Jones and Gagnon (1994). Unit II ages are interpolated from age vs. depth plot (see figure 5.8)

Whole sediment  $\delta^{15}\text{N}$  values in Units I and II from the Black Sea fell in a range between 0.45 and 1.5, averaging 0.96 ( $\pm 0.52$ ) per mil. Whole sediment  $\delta^{13}\text{C}$  values were between -24.4 and -23.1, averaging -23.73 ( $\pm 0.62$ ) per mil.

The average chlorin  $\delta^{15}\text{N}$  value in Unit I sediments was -4.51 per mil (see chapter 2), resulting in a mean phytoplankton  $\delta^{15}\text{N}$  of 0.65. Bulk Unit I (0-10 cm) sediment had a  $\delta^{15}\text{N}$  of 1.3 per mil. In the middle of Unit II, chlorin  $\delta^{15}\text{N}$  was -5.8 per mil, resulting in a mean phytoplankton  $\delta^{15}\text{N}$  of -0.64. The associated bulk sediment had  $\delta^{15}\text{N}$  equal to 0.45 per mil. Therefore, the average difference between chlorin and whole sediment  $\delta^{15}\text{N}$  in Units I and II of the Black Sea is 6.03 ( $\pm 0.31$ ) per mil. This is similar to the difference between Chla and whole cells in axenic phytoplankton cultures, 5.16 ( $\pm 2.40$ ) per mil.

The  $^{14}\text{C}$  ages of Unit II sedimentary organic matter from core BC17 were determined (Dr. Timothy Eglinton, personal communication). A plot of those ages versus depth in the core is shown in figure 5.8. The linear relationship

suggests that the mean sedimentation rate in BC17 during deposition of the sapropel was 7.4 cm/kyr. This figure is in close agreement with the value of 7.7 cm/kyr determined for a core located 300 km to the east of our site (Calvert, et al., 1987). Therefore, ages of Unit II samples in this study were interpolated from the linear relationship. The age of Unit I sediments in core BC2 was estimated from Jones and Gagnon (1994). Those investigators found similar  $^{14}\text{C}$  ages in multiple core-top (0-10 cm) sediments from water depths > 2000 m (Jones and Gagnon, 1994).

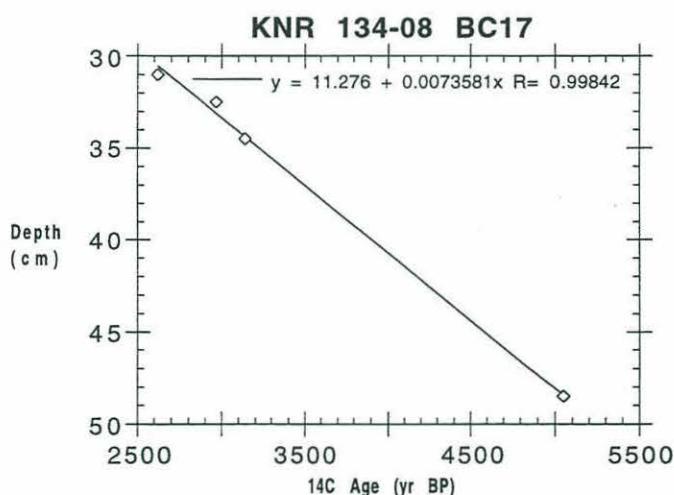


**Figure 5.8: Age versus depth relationship for Unit II sediments from the Black Sea, core KNR 134-08 BC17. Data provided by Dr. Timothy Eglinton.**

Nitrogen isotopic ratios in the Black Sea are shown in figure 5.12. The modern Black Sea isotopic values are averages of published data. Suspended particulate  $\delta^{15}\text{N}$  values averaged  $2.77 (\pm 1.31)$  per mil in 6 samples from depths between 5 and 35 m at two central Black Sea locations (R/V *Knorr* 134-09: Leg 2, Stn. BS2-2 at  $42^{\circ}50'\text{N}$ ,  $32^{\circ}00'\text{E}$  (Fry, et al., 1991); and Leg 3, Stns. BS3-2 at  $42^{\circ}50'\text{N}$ ,  $32^{\circ}00'\text{E}$  and BS3-6 at  $43^{\circ}04'\text{N}$ ,  $34^{\circ}00'\text{E}$  (Velinsky and Fogel, unpubl.). The deep



water  $\text{NH}_4^+$   $\delta^{15}\text{N}$  was 1.7 per mil and was invariant from 500 m to the seafloor (~2200 m) at stations BS3-2 and BS3-6 (Velinsky, et al., 1989).

## 5.5 Discussion

The single published study of nitrogen isotopes in Late Quaternary sediments of the Eastern Mediterranean (Calvert, et al., 1992) concluded that sapropels resulted from increased primary production. Our results suggest a markedly different interpretation. Based on measurements of chlorophyll  $\delta^{15}\text{N}$  values in sapropels and in the modern Eastern Mediterranean we conclude that sapropels formed as a result of improved organic matter preservation under anoxic bottom waters. In addition, it is suggested that Late Quaternary bulk sediment nitrogen isotopic variations in the Eastern Mediterranean are the result of diagenesis.

The term "anoxic" is used in this work to describe oxygen concentrations of less than 0.3 mL/L. The term thus includes, but is not limited to, euxinic environments which are characterized by the complete lack of oxygen and the existence of  $\text{H}_2\text{S}$  in the water.

### 5.5.1 Prior Nitrogen Isotope Studies in the Eastern Mediterranean

A profile of sedimentary  $\delta^{15}\text{N}$  was published by Calvert et al. (1992) for an 11.6 m core from the Eastern Mediterranean (MD 84641; 1,375 m water depth; 33°02'N, 32°38'E) (figure 5.9). That record spanned the last 450 kyr and included 9 sapropels. The results of that study were similar to those in this study. Namely,  $\delta^{15}\text{N}$  values were low (0-2 per mil) in sapropel sequences, and high (5-7 per mil) in non-sapropel sections.

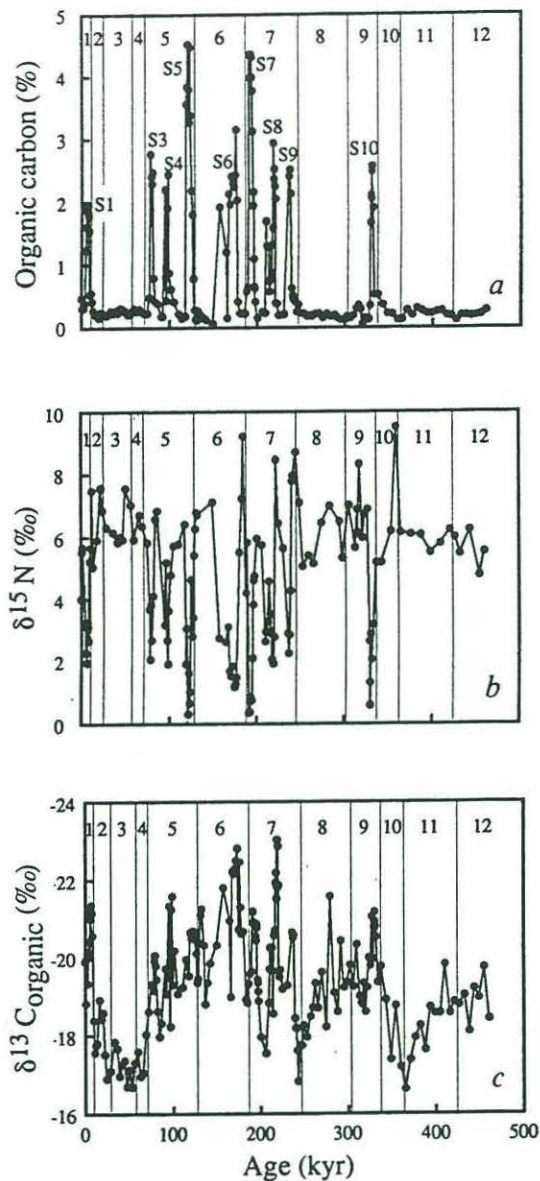


**Figure 5.9: Profiles of (a) organic carbon concentration, (b) sedimentary  $\delta^{15}\text{N}$ , and (c)  $\delta^{13}\text{C}$  of organic carbon in core MD 84641 from the Eastern Mediterranean. Figure from Calvert, et al. (1992).**

Those investigators concluded (1) that the sedimentary  $\delta^{15}\text{N}$  values reflected those of phytoplankton, (2) that phytoplankton  $\delta^{15}\text{N}$  was low during sapropel events due to the incomplete utilization of dissolved nitrogen, and (3) that this implied productivity was higher because major nutrients are typically only underutilized in high productivity regions (i.e., upwelling regions and polar oceans). Below we present evidence refuting these conclusions.

### 5.5.2 *N Isotopic Fractionation During Biological Transformations*

Most biologically-mediated transformations of nitrogen occur more rapidly with  $^{14}\text{N}$  than with  $^{15}\text{N}$  as a result of higher vibrational frequency of bonding in the former (Owens, 1987). This results in isotopic depletion in products relative to substrates. Examples of such processes are the uptake of DIN by phytoplankton (Montoya and McCarthy, 1995; Wada and Hattori, 1978), and microbial denitrification (Delwiche and Steyn, 1970; Mariotti, et al., 1981; Miyazaki, et al., 1980). Field measurements in the marine environment of  $\delta^{15}\text{N}$  in products (Richards and Benson, 1961) (Altabet, et al., 1991; Goering, et al., 1990) and substrates (Cline and Kaplan, 1975; Horrigan, et al., 1990) have borne out the laboratory findings. Recently, attempts have been made to exploit these kinetic isotope effects to reconstruct nutrient utilization (Farrell, et al., 1995; Francois and Altabet, 1992; Francois, et al., 1993; Nakatsuka, et al., 1995) and denitrification (Altabet, et al., 1995; Ganeshram, et al., 1995) patterns in the past.

#### 5.5.2.1 *Nitrogen Isotopes as Tracers of Nutrient Utilization*

Field studies have demonstrated an inverse correlation between nitrate (Goering, et al., 1990; Miyake and Wada, 1967; Saino and Hattori, 1985; Saino and Hattori, 1987; Wada and Hattori, 1976) and ammonium (Montoya, et al., 1991; Rau, et al., 1991) concentrations in surface waters and the  $\delta^{15}\text{N}$  of suspended and sinking (Altabet, et al., 1991; Altabet and Francois, 1994; Nakatsuka, et al., 1992) particles, and surface sediments (Altabet and Francois, 1994). When DIN concentrations are high, as is the case on the equator and in the Southern Ocean, south of the polar front, particulate (Altabet and Francois, 1994; Rau, et al., 1991)



and sedimentary (Altabet and Francois, 1994)  $\delta^{15}\text{N}$  is low. In latitudinal transects from these nutrient-enriched to nutrient-depleted surface waters (i.e., north and south of the equator and north of the polar front), the  $\delta^{15}\text{N}$  of both particles and surface sediments increased (figure 5.10).

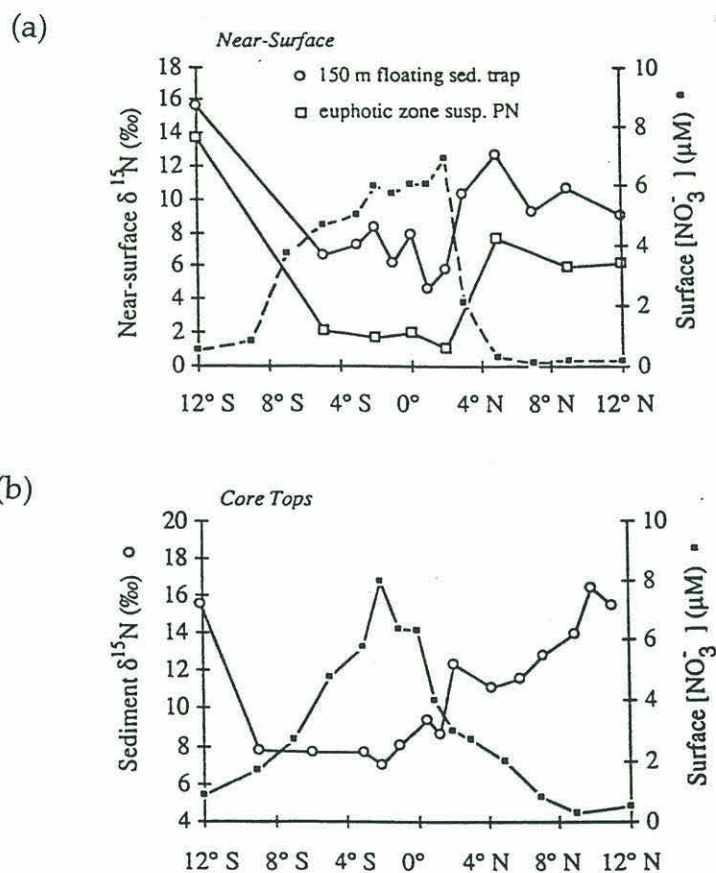


**Figure 5.10: Nitrogen isotopes in the Equatorial Pacific. An inverse relationship between nitrate concentration and (a) suspended and sinking particles, and (b) surface sediments was observed in latitudinal transects across the equator between 135° and 140° West longitude. Figure from Altabet and Francois (1994).**

An extrapolation of these spatial trends to temporal (i.e., downcore) patterns has been attempted in the Southern Ocean (Francois and Altabet, 1992; Francois, et al., 1993), the Eastern Equatorial Pacific (Farrell, et al., 1995), the

Bering Sea (Nakatsuka, et al., 1995), and the Eastern Mediterranean (Calvert, et al., 1992). In those studies, Late Quaternary changes in sedimentary  $\delta^{15}\text{N}$  were interpreted in terms of changing nutrient utilization by phytoplankton. A fundamental assumption in each of those studies was that diagenetic alteration of N isotopic ratios was either insignificant or unchanging in space and time. Contrary to such assumptions, we suggest sedimentary  $\delta^{15}\text{N}$  variations in locations such as these can result entirely from diagenetic processes.

### *5.5.3 Diagenetic Alteration of Nitrogen Isotopic Ratios*

Laboratory (Macko and Estep, 1984; Wada, 1980) and field (Benner, et al., 1991; Zieman, et al., 1984) experiments have demonstrated that  $^{15}\text{N}/^{14}\text{N}$  ratios can be altered during the decomposition of marine organic matter. In addition, the  $\delta^{15}\text{N}$  of suspended (Fry, et al., 1991; Libes and Deuser, 1988; Saino and Hattori, 1980) and sinking (Wada, et al., 1987b) particles in the ocean has been shown to change dramatically with depth (Altabet, 1988; Altabet, 1989; Altabet, et al., 1991; Saino and Hattori, 1987). Furthermore, the isotopic difference between surface sediments and material from deep water sediment traps is frequently large and variable, with sediments being enriched by 2-8 per mil relative to deep sinking particles (Francois and Altabet, 1992; Schafer and Ittekkot, 1993; Wada, et al., 1987b; Altabet, personal communication). This suggests that downcore variations in bulk sediment  $\delta^{15}\text{N}$  are subject to misinterpretation if the magnitude of diagenetic alteration of that quantity is unknown.

Of primary concern is the magnitude of these observed isotopic alterations. They are is similar to the kinetic isotope effects (e.g., the signal) of

the processes being investigated. For instance, the fractionation factor for nitrate uptake by phytoplankton has been between 5 and 9 per mil in field studies (Altabet, et al., 1991; Biggs, et al., 1988; Wada, 1980).

#### 5.5.3.1 Eastern Mediterranean Sedimentary $\delta^{15}\text{N}$ : An Artefact of Diagenesis

Our measurements of chlorin  $\delta^{15}\text{N}$  suggest that the pattern of Late Quaternary sedimentary  $\delta^{15}\text{N}$  in the Eastern Mediterranean is the result of diagenesis. First, bulk sapropel  $\delta^{15}\text{N}$  values ( $-0.08 \pm 0.53$ ) are virtually identical to the calculated  $\delta^{15}\text{N}$  of phytoplankton (0.15 per mil) at the time of their deposition (i.e.,  $\delta^{15}\text{N}_{\text{phyt}} = \delta^{15}\text{N}_{\text{Chla}} + 5.2$  per mil). Today, however, sediments being deposited (4.30 per mil) are enriched by 5.52 per mil relative to phytoplankton (-1.22 per mil) in the overlying water. This indicates that phytoplanktonic material is isotopically altered during decompositional processes characterizing non-sapropel depositional conditions like today. During sapropel events, phytoplankton isotopic values are preserved.

Second, chlorophyll  $\delta^{15}\text{N}$  values in the Eastern Mediterranean today ( $-6.38 \pm 1.80$  per mil) are remarkably similar to chlorin  $\delta^{15}\text{N}$  values in all six sapropels ( $-5.01 \pm 0.38$  per mil) studied (figure 5.11). This indicates that phytoplankton isotopic values, unlike bulk sediment  $\delta^{15}\text{N}$  values, have remained essentially constant over the last 200 kyr.

Finally, modern-day suspended particles from the DCM ( $-0.63 \pm 0.12$  per mil) and deep water nitrate ( $-0.05$  per mil) both have nitrogen isotopic compositions similar to bulk  $\delta^{15}\text{N}$  values in sapropels ( $-0.08 \pm 0.53$  per mil). This indicates that sapropelic organic matter may have been produced in a nutrient regime similar to today--a stratified, oligotrophic setting.



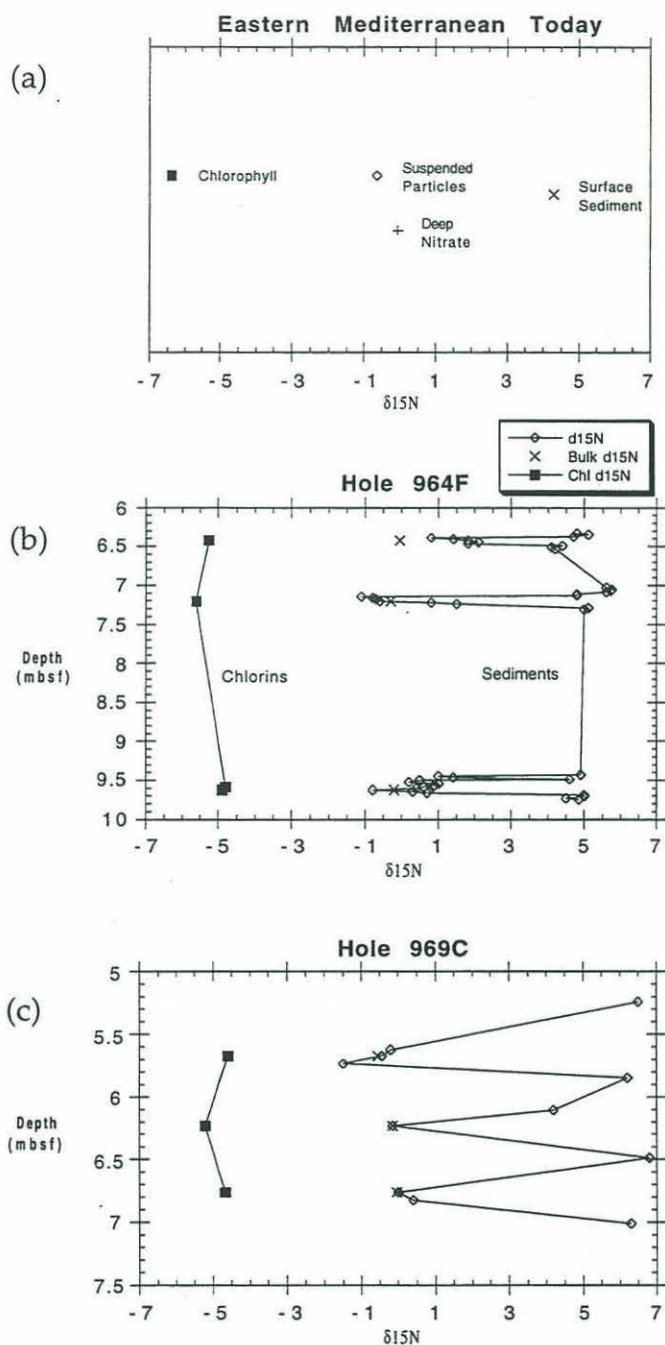


Figure 5.11: Nitrogen isotopes in (a) the modern Eastern Mediterranean, and (b,c) Late Quaternary Eastern Mediterranean sediments. Sapropels S2, S3 and S4 are contained in hole 964F, while sapropels S5, S6 and S7 are contained in hole 969C. Modern-day particulate and chlorophyll  $\delta^{15}\text{N}$  values are from the deep chlorophyll maximum and are averages of values from three stations.

If the  $\delta^{15}\text{N}$  of primary producers has been constant in the Late Quaternary, then the observed pattern of high  $\delta^{15}\text{N}$  in non-sapropel sediments and low  $\delta^{15}\text{N}$  in sapropels resulted from secondary (i.e., non-autotrophic) processes. Examples of such processes are diagenesis and the marine deposition of terrestrial nitrogen.

The fraction of terrestrial organic matter in sapropels has been widely debated, with some studies concluding it is significant (Calvert, 1983; Deroo, et al., 1978; Shaw and Evans, 1984; Sigl, et al., 1978) and others that it is minor (Fontugne and Calvert, 1992; Poutanen and Morris, 1985; Smith, et al., 1986; ten Haven, et al., 1987). Evidence for the existence of a significant terrestrial component to sapropel organic matter came from elemental ratios (i.e., high C/N; Calvert, 1983; Sigl, et al., 1978), terrestrial biomarkers (i.e., high n-alkane carbon numbers and a high odd/even n-alkane predominance; Deroo, et al., 1978), and bulk characteristics of the organic matter (i.e., high concentrations of humic material (Deroo, et al., 1978) and high abundances of pollen and higher plant debris (Shaw and Evans, 1984; Sigl, et al., 1978)). Evidence against a significant terrestrial component to sapropel organic matter came from elemental ratios (i.e., low C/N; Sutherland, et al., 1984), carbon isotopes (i.e., high  $\delta^{13}\text{C}$  values; Fontugne and Calvert, 1992; Sutherland, et al., 1984), marine biomarkers (i.e., high alkenone abundances (prymnesiophytes) and large amounts of dinosterol and 4-methyl sterols (dinoflagellates); Smith, et al., 1986; ten Haven, et al., 1987), and bulk characteristics of the organic matter (i.e., high humic acid to fulvic acid ratios; Poutanen and Morris, 1985)

Our chlorin nitrogen isotope data argues for a minor terrestrial nitrogen contribution to sapropels. Chlorins in marine sediments are thought to derive entirely from marine photoautotrophs (Baker and Louda, 1986). The average phytoplankton  $\delta^{15}\text{N}$  in sapropels, calculated from the chlorin  $\delta^{15}\text{N}$  values, was



0.15 per mil. This compares to an average  $\delta^{15}\text{N}$  for whole sapropel sediments of  $-0.08 \pm 0.53$  per mil. When it is considered that terrestrial nitrogen averages about 2 per mil (Mariotti, et al., 1984; Owens, 1987; Peters, et al., 1978; Sweeney and Kaplan, 1980; Sweeney, et al., 1978), it is apparent that nitrogen in sapropels is predominantly marine in origin.

Since the input of terrestrial nitrogen to sapropels does not appear to be the cause of their low  $\delta^{15}\text{N}$  values, it is likely that diagenesis was responsible for elevated  $\delta^{15}\text{N}$  values in non-sapropel sequences. And, conversely, that minor diagenetic alteration allowed the preservation of phytoplanktonic  $\delta^{15}\text{N}$  during sapropel deposition.

As mentioned, the 5.5 per mil isotopic enrichment of surface sediments (4.3 per mil) relative to phytoplankton (-1.2 per mil) in the Eastern Mediterranean today indicates that oxic diagenetic processes are causing nitrogen isotopic enrichments in decomposing organic matter. Conversely, the isotopic similarity between phytoplanktonic (0.15 per mil) and bulk sapropel material (-0.08 per mil) demonstrates a complete lack of nitrogen isotopic alteration of primary organic matter during sapropel events, and suggests that oxic diagenesis was not occurring at those times.

Evidence for a diagenetic origin of elevated  $^{15}\text{N}/^{14}\text{N}$  ratios in non-sapropel sediments was recently presented by Dr. Gregory Cowie (poster at the 17th International Meeting on Organic Geochemistry, September 4-8, 1995, Donostia-San Sebastian, Spain). He showed high-resolution measurements of bulk sedimentary  $\delta^{15}\text{N}$  through an oxidized zone at the top of the most recent Eastern Mediterranean sapropel (e.g., S1). (The phenomenon of post-depositional sapropel oxidation is thought to be general (Higgs, et al., 1994; Troelstra, et al., 1991) and can confound attempts to reconstruct primary geochemical signals (Pruyser, et al., 1991; van Os, et al., 1991)). In the unoxidized



zone of the sapropel,  $\delta^{15}\text{N}$  values were low and similar to those in other sapropel sediments discussed in this work. In non-sapropel sequences immediately above and below the sapropel, isotopic values were high, similar to those in other non-sapropel sediments from the Eastern Mediterranean. In the oxidized portion of the sapropel, however,  $\delta^{15}\text{N}$  values rose as organic carbon concentrations declined from typical sapropel to typical non-sapropel values.

#### 5.5.3.2 *Preservation of Sedimentary $\delta^{15}\text{N}$ Under Anoxic Bottom Water*

A substantial amount of evidence has been gathered (most in unpublished studies) suggesting that much of the diagenetic alteration of  $^{15}\text{N}/^{14}\text{N}$  ratios in marine organic matter occurs at the sediment-water interface, probably as a result of the activities of benthic fauna (Dr. Mark Altabet, personal communication). When bottom waters are anoxic, and benthic animal communities absent--such as in the Black Sea, the Gulf of California and the Santa Barbara Basin--surface sediment  $\delta^{15}\text{N}$  values are similar to  $\delta^{15}\text{N}$  values in sinking particles collected in deep water sediment traps. However, when bottom waters are oxygenated, surficial sediments tend to be significantly enriched in  $^{15}\text{N}$  relative to deep sinking particles.

The available data demonstrating these trends are shown in table 5.9, along with approximate bottom water oxygen concentrations. Also shown in the table are data for surface water suspended particles and phytoplankton, when available. As is the case for deep sinking particles,  $\delta^{15}\text{N}$  values in both suspended particles and phytoplankton tend to be similar to surface sediments when bottom waters are anoxic, and depleted in  $^{15}\text{N}$  relative to sediments when bottom waters are oxygenated.

Table 5.9: The link between bottom water oxygen concentrations and the diagenetic alteration of  $^{15}\text{N}/^{14}\text{N}$  ratios in marine organic matter. Values are expressed as the difference between the  $\delta^{15}\text{N}$  of surface sediments and the  $\delta^{15}\text{N}$  of either deep water sediment trap material (trap), suspended particles in overlying surface waters (susp), or phytoplankton (phyt). The phytoplankton  $\delta^{15}\text{N}$  value is calculated from the measured chlorophyll  $\delta^{15}\text{N}$  value, as described in chapter 4. Approximate bottom water oxygen concentrations are shown in mL/L.

Location	$\Delta\delta^{15}\text{N}_{\text{sed-trap}}$	$\Delta\delta^{15}\text{N}_{\text{sed-susp}}$	$\Delta\delta^{15}\text{N}_{\text{sed-phyt}}$	[O <sub>2</sub> ]	Ref.
<b>Oxic Bottom Water</b>					
Southern Ocean	7.5	4.5		5.2	1,10
E. Mediterranean		5	5.5	4.3	5,9
Equatorial Pacific	4	6		3.6	2,3,10
Arabian Sea	2-4			2	4,12
<b>Anoxic Bottom Water</b>					
Gulf of California	1			n.d.	2
Santa Barbara Basin	0.5			0.3	2,13
Peru Margin		2	-0.5	< 0.2	5,7,11
Black Sea	-1	-1	-1	0	2,5,6,14
Cariaco Trench		-1.5		0	6,15
Framvaren Fjord		-1.5		0	8,16

- |                                |                              |
|--------------------------------|------------------------------|
| 1. Wada, et al. (1987)         | 9. Miller, et al. (1970)     |
| 2. M. Altabet, personal comm.  | 10. Broecker and Peng (1982) |
| 3. Altabet and Francois (1994) | 11. Suess, et al. (1988)     |
| 4. Schafer and Ittekkot (1993) | 12. Shimmield, et al. (1990) |
| 5. This study                  | 13. Emery (1960)             |
| 6. Fry, et al. (1991)          | 14. Canfield (1989)          |
| 7. Libes and Deuser (1988)     | 15. Wakeham (1990)           |
| 8. D. Velinsky, personal comm. | 16. Jacobs, et al. (1987)    |



Since sapropel  $\delta^{15}\text{N}$  values ( $-0.08 \pm 0.53$  per mil) were virtually identical to calculated phytoplankton  $\delta^{15}\text{N}$  values (0.15 per mil), it is suggested that sapropels S2 through S7 were deposited when bottom waters in the Eastern Mediterranean were anoxic (i.e.,  $< 0.3 \text{ mL/L O}_2$ ). While recognizing that a strict interpretation of the limited data presented in table 5.9 would allow only the conclusion that bottom water during sapropel events contained  $< 2 \text{ mL/L O}_2$ , there is a positive correlation between  $\Delta\delta^{15}\text{N}$  values and decreasing oxygen concentrations that suggests bottom water  $[\text{O}_2]$  will be very low when phytoplankton  $\delta^{15}\text{N}$  values are identical to sediment  $\delta^{15}\text{N}$  values. In addition, the late Quaternary bulk sediment  $\delta^{15}\text{N}$  record published by Calvert, et al. (1992; figure 5.9) frequently shows a gradual transition into and out of sapropels. If it is assumed that the onset of anoxia--i.e., sapropel deposition--and the reintroduction of oxygen in bottom waters is gradual (Mullineaux and Lohmann, 1981), then sediment  $\delta^{15}\text{N}$  values would be expected to gradually decrease then increase at the beginning and end of an event. Additional measurements of  $\Delta\delta^{15}\text{N}_{\text{sed-Chla}}$  in low oxygen (i.e.,  $< 2 \text{ mL/L}$ ) environments would help to elucidate the exact relationship between the nitrogen isotopic difference between phytoplankton and sediments and bottom water  $[\text{O}_2]$ .

Further evidence that benthic fauna are responsible for the observed elevation of sedimentary  $\delta^{15}\text{N}$  relative to deep sinking particles is the 4.5 per mil  $^{15}\text{N}$  enrichment of surface sediments from the Equatorial Pacific, relative to the floc lying just above those sediments (Dr. Mark Altabet, personal communication). In that study, the floc had about the same  $\delta^{15}\text{N}$  as both the deep trap material (3700 m) and material from a floating sediment trap at 150 m (Altabet and Francois, 1994). This suggests that, in the presence of oxygen, much of the isotopic alteration of sedimenting nitrogen occurs at the sediment-water interface.



#### 5.5.3.3 *Origin of Diagenetic $^{15}\text{N}$ -Enrichment in Sediments*

The process(es) responsible for the observed  $^{15}\text{N}$  enrichment in sediments underlying oxygenated bottom water is (are) unknown. There are three possibilities frequently cited in the literature. The first is preferential removal, by heterotrophs, of nitrogenous components depleted in  $^{15}\text{N}$  (Altabet and McCarthy, 1985; Libes and Deuser, 1988; Saino and Hattori, 1980). The second is isotopic fractionation during the incomplete consumption of nitrogenous components of sedimenting material (Montoya, et al., 1992). And the third is a trophic effect whereby grazers excrete  $^{15}\text{N}$ -depleted dissolved metabolites (Checkley and Miller, 1989) while producing isotopically-enriched fecal material (Altabet, 1988; Altabet and Small, 1990; Checkley and Entzeroth, 1985; Montoya, et al., 1992). It is important to note, though, that since only a small fraction of organic nitrogen produced in the euphotic zone is buried in sediments, it would not require a large isotope effect (or fractionation factor) to impart a significant isotopic signal to residual sedimentary  $\text{N}_{\text{org}}$ .

#### 5.5.4 *The Origin Of Eastern Mediterranean Sapropels*

It has been demonstrated that phytoplankton  $\delta^{15}\text{N}$  values are about the same today as they were in all six Late Quaternary sapropels studied. Since the main factors that have been shown to effect phytoplankton  $\delta^{15}\text{N}$  in the marine environment are nitrogen source (Checkley and Miller, 1989; Saino and Hattori, 1987) and concentration, or more specifically, extent of utilization (Altabet, et al., 1991; Altabet and Francois, 1994; Saino and Hattori, 1985), it is proposed that these factors have remained essentially unchanged over the last 200 kyr in the

Eastern Mediterranean. It is further suggested that sapropels formed primarily as a result of increased organic carbon accumulation caused by improved preservation of organic matter under anoxic bottom water.

#### *5.5.4.1 Persistence of Oligotrophic Conditions in the E. Mediterranean During the Past 200 kyr*

Today, the Mediterranean Sea is oligotrophic. Concentrations of dissolved inorganic phosphorous and nitrogen (DIN) are at or near their limits of detectability for much of the year (Miller, et al., 1970). DIN is completely utilized by phytoplankton. This explains why the  $\delta^{15}\text{N}$  of phytoplankton from the DCM ( $-1.22 \pm 1.80$  per mil)--calculated from the measured chlorophyll  $\delta^{15}\text{N}$ --is similar to the  $\delta^{15}\text{N}$  of deep water nitrate ( $-0.05$  per mil). Deep water nitrate is generally thought to fuel new production in much of the world ocean (Dugdale and Goering, 1967)(Eppley and Peterson, 1979). With that nitrate being completely utilized at the base of the euphotic zone (i.e., the top of the nitracline) in the oligotrophic Eastern Mediterranean, there is little or no net isotopic fractionation, relative to deep nitrate, expressed in phytoplankton from the DCM.

Since chlorin  $\delta^{15}\text{N}$  values in sapropels S2-S7 ( $-5.01 \pm 0.38$  per mil) were about the same as those in the modern Eastern Mediterranean ( $-6.38 \pm 1.80$  per mil) (figure 5.11), it is proposed that nutrient utilization and the isotopic composition of deep water nitrate have remained nearly constant over time. In addition, bulk sediment  $\delta^{15}\text{N}$  values in all 6 sapropels (S2-S7;  $-0.08 \pm 0.53$  per mil) were virtually identical to the  $\delta^{15}\text{N}$  of deep nitrate today ( $-0.05$  per mil), suggesting that new nitrogen had the same isotopic composition during sapropel events as it does today. In other words, oligotrophic conditions in which



nutrients are completely utilized in the euphotic zone have characterized the Eastern Mediterranean throughout the Late Quaternary.

Other explanations for constant phytoplankton  $\delta^{15}\text{N}$  in the Late Quaternary can be imagined. For instance, nutrient utilization could have decreased during sapropel events, as Calvert, et al. (1992) suggested, and the  $\delta^{15}\text{N}$  of the nitrogen source to phytoplankton could have increased, exactly offsetting that decrease. However, in the absence of compelling evidence for such a scenario, a simpler explanation consistent with the  $\delta^{15}\text{N}$  data is that oligotrophic conditions similar to today have persisted in the Eastern Mediterranean during the Late Quaternary.

#### *5.5.4.2 Higher Carbon Accumulation Through Improved Preservation*

If the Eastern Mediterranean was oligotrophic when sapropels S2-S7 were deposited, what was the mechanism that resulted in such organic-rich sedimentary deposits? It is proposed that improved preservation of organic matter under anoxic water bottom water led to increased organic carbon accumulation and the formation of sapropels.

One popular model of sapropel formation is characterized by a reversal of the circulation at the Strait of Sicily, such that nutrient-rich deep waters flow into, instead of out of, the eastern basin (Sarmiento, et al., 1988a). Such a reversal would likely result from a freshening of surface waters caused by enhanced river runoff (Rossignol-Strick, 1985; Rossignol-Strick, et al., 1982). A "nutrient trap" would have resulted from such a circulation change as inflowing nutrient-rich deep water was balanced by outflowing nutrient-depleted surface water at the Strait of Sicily. The eastern basin would then have become anoxic as the ratio of



organic matter to oxygen exported from surface to deep layers increased (Sarmiento, et al., 1988a; Sarmiento, et al., 1988b). Significantly, as noted by Sarmiento, et al. (1988a,b), an increase in this ratio need not result from a change in biological productivity or new production.

The modern Eastern Mediterranean is characterized as a "nutrient desert." Westward flowing nutrient-enriched deep waters are lost over the Strait of Sicily, to be replaced by highly nutrient-depleted surface waters from the Western Mediterranean. In addition, deep waters of the eastern basin are well-oxygenated (Miller, et al., 1970) as a result of deep convection that occurs as an excess of evaporation over precipitation elevates surface salinities (Bethoux, 1979). This oxygenation of the deep eastern basin is countered by relatively little oxygen demand from decomposing organic matter (Sarmiento, et al., 1988a) since surface nutrient impoverishment supports low rates of new production (Claustre, 1994).

If surface waters were sufficiently freshened during sapropel events, such that deep water formation in the eastern basin ceased, then the oxygen demand, relative to supply, would have increased in the deep water, even in the absence of a change in new production (Bethoux, 1993; Sarmiento, et al., 1988a). Indeed, the modelled response time of deep water anoxia to such a circulation change was only about 1400 years, irrespective of the biological productivity (Sarmiento, et al., 1988a). Another modelling study indicated that a salinity decrease in the Adriatic Basin of a mere 0.2 per mil would be sufficient to cause anoxia in the deep Eastern Mediterranean in 150 years given current rates of primary production there (Mangini and Schlosser, 1986). This response time is consistent with observations of a rapid onset of sapropel events (Cita, et al., 1977; Kidd, et al., 1978).

Once anoxic deep waters had been established, organic carbon accumulation in sediments would have increased as a result of improved preservation of organic matter (Canfield, 1989; Demaison and Moore, 1980; Emerson, 1985). A modern analog for this scenario is the Black Sea. That anoxic, oligotrophic basin is characterized by low primary productivity (100-200 g C/m<sup>2</sup>/year (Deuser, 1971; Sorokin, 1983); on the order of that in the Mediterranean Sea (Claustre, 1994)) and by organic-rich sediments (3-5% C<sub>org</sub> (Glenn and Arthur, 1985)). There, the burial efficiency of organic carbon is high compared to oxygenated environments with similarly low sedimentation rates (Canfield, 1989). This may result from anaerobic bacteria being incapable of decomposing the entire range of organic compounds in sedimenting material (Canfield, 1989). Or it may result from the lack of grazers in anoxic environments (Demaison and Moore, 1980; Lee, 1992). Benthic animals enhance C<sub>org</sub> remineralization rates by fragmenting and remineralizing POM and by prolonging the exposure of organic matter to oxidants through bioturbation and irrigation. Their absence may leave some constituents of sedimentary POM unavailable to bacteria, and would also allow large amounts of organic carbon to be sequestered in bacterial biomass.

#### *5.5.4.3 Toward a Unified Picture of Eastern Mediterranean Sapropel Formation*

A growing body of evidence now exists suggesting (1) that surface waters freshened, (2) that the circulation pattern over the Strait of Sicily reversed, (3) that bottom waters were anoxic, and (4) that oligotrophic conditions persisted during sapropel formation events in the Eastern Mediterranean. That evidence is reviewed here.



Freshening of surface waters in the Eastern Mediterranean appears to be climatically linked to monsoonal precipitation in Africa which flows to the basin via the Nile (Rossignol-Strick, 1985; Rossignol-Strick, et al., 1982). Lower surface water salinities have been inferred from dramatic  $^{18}\text{O}$  depletions in planktonic foraminifera (Vergnaud-Grazzini, et al., 1977; Williams, et al., 1978) and changes in faunal abundances (Cita, et al., 1977; Thunell and Williams, 1983; Thunell, et al., 1977; Williams and Thunell, 1979).

A reversal of the circulation at the Strait of Sicily during sapropel deposition, resulting from the freshening of eastern basin surface water, has been inferred from sedimentologic, isotopic and faunal evidence (Huang and Stanley, 1972; Muerdter, 1984; Stanley, 1978; Stanley, et al., 1975). For instance, the low-salinity assemblage of planktonic foraminifera found in late Quaternary Eastern Mediterranean sapropels was found in coeval horizons from the western entrance of the Strait of Sicily where sapropels are not formed (Muerdter, 1984). This "indicates that low surface salinities extended through the strait, a condition requiring a surface water flow from east to west, a reversal of the present-day circulation pattern" (Muerdter, 1984). In addition to the circulation reversal, sedimentologic evidence suggests that the waters flowing over the Strait remained well-oxygenated and that circulation has been vigorous throughout the late Quaternary (Stanley, et al., 1975). For instance, sediments from the three deep (1300-1700 m) basins within the Strait of Sicily were bioturbated, and hence oxygenated, during sapropel events at those depths in the Eastern basin. In addition, early Holocene radiocarbon dates of core-tops at intermediate depths within the strait indicate non-deposition and/or erosion during the last ~10 kyr, consistent with a strong current regime during a period which includes the deposition of the most recent sapropel (i.e., S1). "Thus, it appears that vertical mixing prevailed on an almost continuing basis as a result of water mass



movement across the Strait of Sicily" during the late Quaternary (Stanley, et al., 1975).

Deep water anoxia in the eastern basin has been inferred from the absence of benthic microfossils in sapropel layers (Cita, et al., 1977; Kidd, et al., 1978; Thunell, et al., 1977) and the presence of iron sulfides and other minerals typically associated with reducing environments (Calvert, 1983; Sutherland, et al., 1984). To this evidence is added the chlorophyll nitrogen isotopic data presented above. The close similarity between phytoplankton and whole sediment  $\delta^{15}\text{N}$  values in sapropels is strongly suggestive of bottom water anoxia.

In addition, the similarity between chlorophyll  $\delta^{15}\text{N}$  values in the modern Eastern Mediterranean and in all six sapropels studied suggests that both nutrient utilization and new nitrogen source have remained essentially constant over the last 200 kyr. In other words, oligotrophic conditions similar to today persisted through the deposition of Late Quaternary sapropels.

This body of evidence supports a sapropel formation scenario whereby circulation changes induced anoxia which led to enhanced burial efficiency of organic matter (Sarmiento, et al., 1988a). A modern analog for this depositional environment is the Black Sea (Olausson, 1961; Sarmiento, et al., 1988a; Southam, et al., 1982).

#### *5.5.4.4 Comparison of E. Mediterranean Sapropels to the Modern Black Sea*

The modern Black Sea is a nutrient trap (Sarmiento, et al., 1988a). Low salinity surface waters are not dense enough to sink into deep waters made saline by inflow from the Bosphorous. Nutrients added by rivers and the atmosphere accumulate in the deep water to very high concentrations ( $[\text{PO}_4^{3-}] \sim 7 \mu\text{M}$ ). Burial of organic matter (e.g., reduced nutrients) in sediments keeps the system

in balance (Sarmiento, et al., 1988a). Even though primary production in the Black Sea is low ( $100\text{--}200\text{ g C/m}^2\text{/yr}$ ), and the surface waters oligotrophic, the export of carbon to deep waters exceeds their import of oxygen (Sarmiento, et al., 1988b). Thus, anoxia results. Significantly, as noted by Southam, et al. (1982), the Black Sea is not a stagnant basin. The residence time of deep water is between 475 and 935 years (Ostlund, 1974), and the vertical velocity in the interior of the basin is about  $0.5\text{ m/yr}$ , values not unlike the world ocean (Southam, et al., 1982).

The similarities to the Eastern Mediterranean during sapropel deposition are striking. As discussed above, the Eastern Mediterranean was not stagnant during anoxic events. Circulation through the Strait of Sicily was vigorous (Stanley, et al., 1975). In addition, surface waters were relatively fresh and sediments accumulated vast amounts of organic matter. This appears to have occurred in conjunction with oligotrophic surface waters.

Nitrogen isotopic evidence from the Black Sea supports this analogy. As shown in figure 5.12 and table 5.8, the  $\delta^{15}\text{N}$  of surface (0-10 cm) sediments in the Black Sea is 1.3 per mil. This is very close to the  $\delta^{15}\text{N}$  of phytoplankton (calculated from the chlorin  $\delta^{15}\text{N}$ ) in those sediments, 0.65 per mil. The similarity is expected since little nitrogen isotopic alteration occurs when bottom waters are anoxic (see section 5.5.3.2). In addition, the  $\delta^{15}\text{N}$  of deep water ammonium (there is no nitrate since it is completely denitrified in the sulfate reducing abyss) is 1.7 per mil (Velinsky, et al., 1989). This value is also similar to the  $\delta^{15}\text{N}$  of phytoplanktonic material in sediments and confirms (1) that new production in the Black Sea is supported by deep water ammonium (Velinsky, et al., 1991), and (2) that the biological uptake of that ammonium (e.g., nutrient utilization) is essentially complete (Velinsky, et al., 1991).

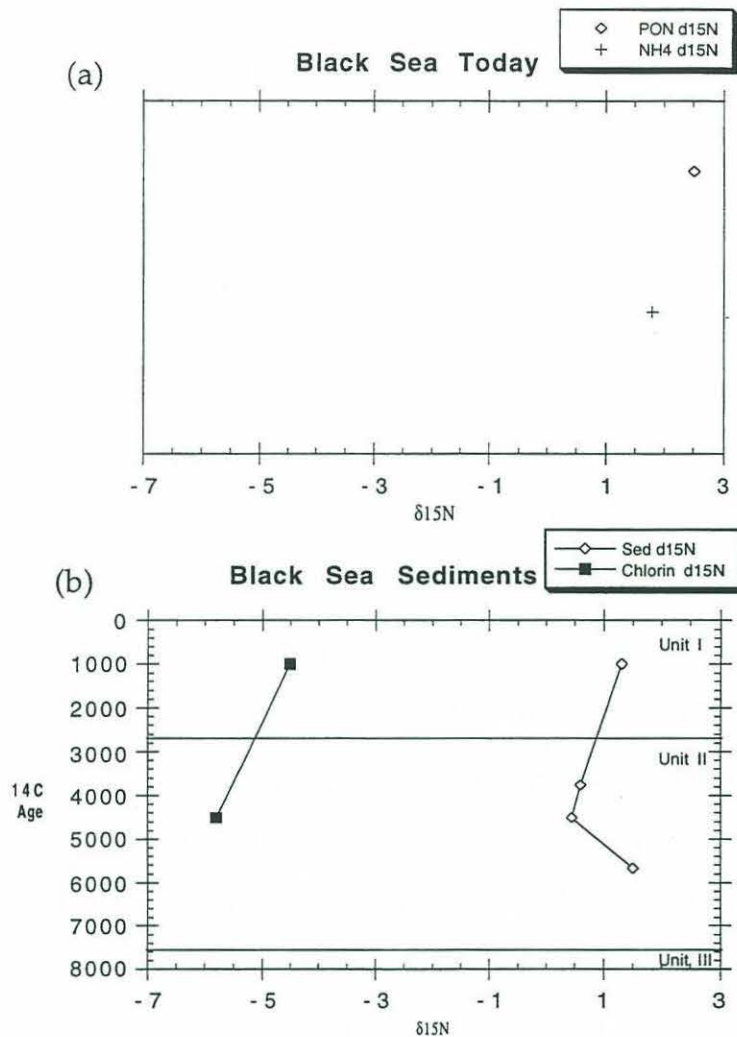


**Figure 5.12: Nitrogen isotopes in (a) the modern Black Sea, and (b) Unit I and II sediments.** The particulate  $\delta^{15}\text{N}$  value is a euphotic zone average from (Fry, et al., 1991) and Velinsky and Fogel (unpubl.). Ammonium  $\delta^{15}\text{N}$  was constant below 500 m (Velinsky, et al., 1989).

The similarity between the sediment-chlorin  $\delta^{15}\text{N}$  difference in Unit I and Unit II sediments is evidence that bottom waters of the Black Sea were anoxic during the deposition of the Unit II sapropel. The nitrogen isotopic composition of algal material in Unit II, as calculated from the measured chlorin  $\delta^{15}\text{N}$ , was -0.64 per mil. This was similar to the  $\delta^{15}\text{N}$  of the whole sediment, 0.45 per mil. This suggests that algal material was not exposed to oxic decomposition



processes during deposition of the sapropel, since such processes elevate the  $\delta^{15}\text{N}$  of residual material by several per mil (see section 5.5.3.2). The existence of anoxic bottom water in the Black Sea during the deposition of the Holocene sapropel (Unit II) contradicts the results of Calvert (1990), who concluded, based on Mn, I and Br distributions, that bottom waters were oxygenated during that time (Calvert, 1990).

Nitrogen isotopic values of chlorins and sediments in the Black Sea increased by about 1 per mil between the middle of Unit II and Unit I (figure 5.12 and table 5.8). Over this interval,  $\delta^{13}\text{C}$  values of sediments also increased by about 1 per mil. (A comparison between Unit I and Unit II chlorin  $\delta^{13}\text{C}$  values is not possible since the Unit II chlorin was a pheophorbide derivative that lacked the phytyl ester side-chain which is known to be depleted in  $^{13}\text{C}$  relative to the macrocycle (Bogacheva, et al., 1979).) This suggests that terrestrial organic matter constituted a larger fraction of sedimentary organic matter in Unit II (Pelet and Bebyser, 1977; Simoneit, 1977) than in the modern facies. Terrestrial organic matter is generally depleted in  $^{15}\text{N}$  (Sweeney and Kaplan, 1980; Sweeney, et al., 1978) and  $^{13}\text{C}$  (Calvert and Fontugne, 1987) relative to marine organic matter (Mariotti, et al., 1984; Peters, et al., 1978).

#### *5.5.4.4.1 The Effect of Denitrification and Nitrification on $\delta^{15}\text{N}$ Values in the Black Sea and in Eastern Mediterranean Sapropels*

A large kinetic isotope effect of about 20 to 40 per mil is associated with microbial denitrification (Cline and Kaplan, 1975; Delwiche and Steyn, 1970; Mariotti, et al., 1981; Richards and Benson, 1961). This can result in high  $\delta^{15}\text{N}$  values of organic matter in oceanic regimes, such as the eastern tropical Pacific

Ocean and the western Arabian Sea, characterized by mid-depth oxygen minima and a vigorous circulation. In such locations the supply of nitrate from depth to the denitrifying zone (i.e., the OMZ) is greater than the rate of denitrification (i.e., the loss rate of nitrate). Thus, the partial denitrification results in the transport of  $^{15}\text{N}$ -enriched nitrate to the euphotic layer, a signal that is incorporated into the food web (Saino and Hattori, 1987) and transferred to the sediments (Altabet, et al., 1995; Ganeshram, et al., 1995).

Similar isotopic enrichments of organic matter are not observed when the denitrification rate exceeds the supply rate of nitrate, such as in most marine sediments and in the water column of the Black Sea. In those locations, nitrate is completely removed by denitrification, and no net isotopic fractionation is expressed as a result of that process. Hence, organic matter produced in the euphotic zone of the Black Sea has an isotopic composition similar to the deep-water ammonium; the source of new nitrogen to phytoplankton (Velinsky, et al., 1991).

An important distinction between the modern Black Sea and the Eastern Mediterranean during sapropel events is the minimum depth of the presumed anoxic water. Sapropels are generally not found at depths above 800-1,000 m (Stanley, 1978) in the Eastern Mediterranean, suggesting a deeper anoxic layer than in the Black Sea today, where the anoxic water impinges upon the euphotic zone (i.e., 100-150 m water depth). In the Black Sea, ammonium concentrations increase with depth below the  $\text{O}_2/\text{H}_2\text{S}$  interface as a result of consumption in the euphotic zone and production during anaerobic fermentation and sulfate reduction in the euxinic abyss (Velinsky, et al., 1991). Little nitrification-- the microbially-mediated oxidation of ammonium to nitrite or nitrate--occurs before the ammonium is completely utilized by photoautotrophs (Velinsky, et al., 1991).



In the Eastern Mediterranean during sapropel events the cycling of nitrogen in the upper kilometer may have been quite different. One possible scenario would be that denitrification at depths below 800-1,000 m completely exhausted the nitrate supply to the deep water. In that case, no net isotopic fractionation from denitrification would be expected. Then, between the euphotic depth and the top of the anoxic zone, nitrification could have gone to completion, oxidizing all  $\text{NH}_4^+$  to nitrate. Although nitrification, like denitrification, is associated with a large kinetic isotope effect of about 20 to 40 per mil (Delwiche and Steyn, 1970; Mariotti, et al., 1981), no net fractionation would be expected if the process went to completion.

A more complex scenario might occur during the onset of a sapropel event, when the deep waters are gradually depleted of oxygen (Mullineaux and Lohmann, 1981), and nitrate is not yet exhausted. An increase in organic matter  $\delta^{15}\text{N}$  values would be expected during that time, as the residual,  $\text{N}^{15}$ -enriched nitrate is upwelled from depth. This effect may actually be discernible in the bulk sediment  $\delta^{15}\text{N}$  values published by Calvert, et al. (1992; figure 5.9) where positive spikes of one to several per mil are observed just prior to sapropels S1, S6, S8, S9. Unfortunately, neither the sampling interval of that record nor the chlorin  $\delta^{15}\text{N}$  record is fine enough to conclude with certainty that denitrification-derived increases in organic matter  $\delta^{15}\text{N}$  values occurred during the onset of sapropel events.

#### 5.5.4.5 *The Origin of Sedimentary Chlorins*

The chlorophyll isotopic data from the modern Mediterranean came from samples collected at the deep chlorophyll maximum, at the base of the euphotic



zone. If sedimentary chlorins do not derive from the DCM, and chlorophyll  $\delta^{15}\text{N}$  varies with depth in the euphotic layer, then the comparison between DCM-derived chlorophyll  $\delta^{15}\text{N}$  and sedimentary chlorin  $\delta^{15}\text{N}$  values would not be valid. Pigment data from sediment traps is not available yet for the Eastern Mediterranean. However, there is reason to believe that pigments in sedimenting particles derive primarily from the DCM.

In the Black Sea, for instance, pigment distributions in sediment trap samples were almost identical to those in suspended particles at the base of the euphotic zone (Repeta and Simpson, 1991). In addition, in stratified oligotrophic systems like the Eastern Mediterranean, small phytoplankton cells (i.e., prochlorophytes, cyanobacteria) tend to dominate the upper part of the euphotic layer (Claustre and Marty, 1995). The microzooplankton grazers of this community produce small, slowly sinking fecal pellets (SooHoo and Kiefer, 1982). The pigments in these fecal pellets may be susceptible to photooxidation as a result of their long residence time in the euphotic zone (SooHoo and Kiefer, 1982; Welschmeyer and Lorenzen, 1985). In the DCM, where there is more nitrate available, algal cells tend to be larger (i.e., diatoms, flagellates; Claustre, 1994; Claustre and Marty, 1995). These larger cells are grazed by macrozooplankton that produce large, rapidly sinking fecal pellets that dominate new production and would be more likely to transport chlorins to the seafloor (Claustre and Marty, 1995; Welschmeyer and Lorenzen, 1985; Dr. Herve Claustre, personal communication).

#### *5.5.5 Origin of Low Nitrogen Isotopic Ratios in the Eastern Mediterranean*

The  $\delta^{15}\text{N}$  of deep water (1000 m) nitrate in the Eastern Mediterranean was -0.05 per mil. This value is substantially lower than the mean global deep ocean

(>1500 m) value of  $5.7 \pm 0.7$  per mil (Liu and Kaplan, 1989). It also falls well below the lower limits of 4-6 per mil found in shallower layers (200-1500 m) of both the Atlantic and Pacific oceans (Liu and Kaplan, 1989). There are two likely sources for this isotopically depleted nitrate. One is rivers, the other is nitrogen fixation.

Today, the flux of phosphate to the Eastern Mediterranean comes from the surface inflow through the Strait of Sicily (62%), rivers (29%), atmospheric deposition (6.2%), and the Bosphorous (2.7%) (Bethoux, 1981; Sarmiento, et al., 1988a). These inputs are balanced by the deep outflow of water at the Strait of Sicily (and presumably negligible losses to sediments). Assuming that fluxes of nitrate are fractionally similar to those of phosphate, then about 40% of nitrate may derive from atmospheric and riverine input. This is close to the percentage calculated from a nitrogen budget for the entire Mediterranean Sea (e.g., 41%) (Bethoux and Copin-Montegut, 1986).

The limited data available suggests that the  $\delta^{15}\text{N}$  of riverine DIN is between 0 and 4 per mil (Mariotti, et al., 1984; Owens, 1987; Wada, et al., 1987a), while that of rain is between 0 and 1 per mil (Hoering, 1957; Owens, 1987). There don't appear to be any published measurements of riverine or rain  $\delta^{15}\text{N}$  in the Mediterranean region. If a value of 1.5 per mil is assumed for the riverine- plus precipitation-derived nitrate, then, from mass balance considerations, the  $\delta^{15}\text{N}$  of nitrate from other sources must be -1 per mil. The most likely source for such isotopically depleted nitrogen is biological nitrogen fixation.

Currently, the nitrogen budget of the Mediterranean sea is not balanced (Bethoux, 1981; Bethoux and Copin-Montegut, 1986). The net loss of nitrogen at the Strait of Gibraltar ( $19.7 \times 10^{10}$  mol N/yr) exceeds combined inputs from rivers ( $11.3 \times 10^{10}$  mol N/yr) and the atmosphere ( $1.3 \times 10^{10}$  mol N/yr) by  $7.1 \times 10^{10}$  mol N/yr (Bethoux and Copin-Montegut, 1986). This imbalance could be



maintained by a large contribution to the Mediterranean Sea nitrogen inventory from biological N<sub>2</sub>-fixation (Bethoux and Copin-Montegut, 1986). This source of nitrogen would also explain the high N/P ratio observed in deep waters (= 21-23) of the Mediterranean Sea compared to the global ocean, the Atlantic inflow (= 15) and terrestrial discharges (= 11) (Bethoux, et al., 1992). The calculations of Bethoux, et al. (1986, 1992) suggest that the primary source of nitrate, and as much as 36% of the nitrogen supply, to the Mediterranean Sea may be from fixation by seagrasses and the cyanobacterium, *Synechococcus*. Cyanobacteria are characterized by high protein contents, low C/N ratios, and are likely to have high N/P ratios, therefore accounting for the high N/P ratio of deep waters of the Mediterranean (Bethoux, et al., 1992).

Biological nitrogen fixation, which converts atmospheric N<sub>2</sub> to organic nitrogen, is generally characterized by a small isotopic fractionation effect, with the product being depleted in <sup>15</sup>N by 0 to 4 per mil relative to the substrate ( $\delta^{15}\text{N}_{\text{air}} \equiv 0$ ) (Delwiche and Steyn, 1970; Hoering and Ford, 1960; Macko, et al., 1987).

If an average  $\delta^{15}\text{N}$  value for organic matter produced by nitrogen fixers is taken to be -2 per mil, and inflowing surface waters from the North Atlantic are taken to be 4 per mil, then mass balance considerations require that nitrogen fixation provide 83% of nitrogen in the Eastern Mediterranean not supplied by rivers and atmospheric deposition. In other words, nitrogen fixation may supply on the order of 50% of the nitrogen in the modern Eastern Mediterranean. This is somewhat larger than the estimate of 36% for the entire Mediterranean basin suggested by the data of Bethoux and Copin-Montegut (1986).

The eastern basin might be expected to derive a larger fraction of nitrogen from fixation than the western basin or the Mediterranean Sea as a whole. The western basin receives 47% of its total phosphate flux from North Atlantic



surface water (Bethoux, 1981; Sarmiento, et al., 1988a). DIN from this source is expected to have a  $\delta^{15}\text{N}$  in the 4-6 per mil range (Liu and Kaplan, 1989). If nitrogen fixation is occurring in the western basin it would presumably act to decrease the  $\delta^{15}\text{N}$  of nitrogen in the surface layer as those waters age and flow eastward to the Strait of Sicily. The lower  $\delta^{15}\text{N}$  of phytoplankton from the eastern basin, relative to the western basin, supports this scenario (table 5.5). Phytoplankton in the western basin had a  $\delta^{15}\text{N}$  value, calculated from the chlorophyll  $\delta^{15}\text{N}$ , of 2.96 per mil, while those in the eastern basin averaged -1.22 per mil.

Such high rates of nitrogen fixation have not yet been measured in the Mediterranean Sea. However, in the Caribbean Sea, nitrogen fixation by the blue-green alga *Oscillatoria* (*Trichodesmium*) spp. has been measured to account for 60% of the chlorophyll *a* in the upper 50 m, and up to 27% of nitrogen primary production (Carpenter and Price IV, 1977). In addition, an analysis of nutrient budgets in the Red Sea has suggested that nitrogen fixation may account for up to 6% of the total primary production in that basin (Naqvi, et al., 1986). Furthermore, in nitrogen-limited lakes,  $\text{N}_2$ -fixation has been observed to contribute up to 38% of the total nitrogen requirements (Capone and Carpenter, 1982). Finally, it has been observed that floating diatom (i.e., *Rhizosolenia*) mats in oligotrophic ocean waters can fulfill all of their nitrogen requirements through  $\text{N}_2$ -fixation by symbiotic bacteria (Martinez, et al., 1983). In some cases this nitrogen was 14% of the nitrogen primary production in the North Pacific locations studied. However, nitrogen fixation does not occur in all *Rhizosolenia* mats (Villareal, et al., 1993).

At present, it is not known what environmental factors are necessary for large-scale nitrogen fixation to occur, though it has been suggested that "warm, nearshore zones of low export productivity" are conducive environments

(Codispoti, 1989). These regions are often characterized by low turbulence and enrichments of trace metals, such as iron, from land and sediments.

#### 5.5.6 Carbon Isotopic Ratios in Eastern Mediterranean Sapropels

The carbon isotopic composition of pyropheophorbide *a* from sapropels S3-S6 is shown in figure 5.13. Also depicted are the  $\delta^{13}\text{C}$  of bulk sediment from sapropels S2-S7. The top panel (figure 5.13.a) shows the  $\delta^{13}\text{C}$  of chlorophyll *a* and suspended particles from the modern DCM (the chlorophyll sample was from the Western Mediterranean), as well as the  $\delta^{13}\text{C}$  of surface sediments from the Eastern Mediterranean. Excluding the glacial sapropel, S6, sapropel  $\delta^{13}\text{C}$  values averaged  $-23.3 (\pm 0.72)$  per mil, and sapropel chlorins averaged  $-21.98 (\pm 1.04)$  per mil. Therefore, on average, chlorins were enriched in  $^{13}\text{C}$  by 1.33 per mil, relative to whole sediments.

Although results from axenic phytoplankton cultures suggest chlorophyll and whole cells have about the same  $\delta^{13}\text{C}$  (see chapter 4), the chlorin isolated from sapropels, pyropheophorbide *a*, lacks a phytyl-ester side chain. Therefore PPBDa is expected to be enriched in  $^{13}\text{C}$  relative to whole phytoplankton (Bogacheva, et al., 1979) (see discussion in section 4.5.2), and to bulk sedimentary organic matter, since little C isotopic alteration is expected during diagenesis (Dean, et al., 1986; Fontugne and Duplessy, 1986). (In a Black Sea surface sediment, for instance, a dephytylated chlorin was enriched in  $^{13}\text{C}$  by 1.85 per mil relative to intact pheophytins (see section 2.5.1)).

Sapropels are uniformly depleted in  $^{13}\text{C}$ , relative to surface sediments (excluding S6). This depletion has been attributed to the freshening of surface waters during sapropel deposition (Fontugne and Calvert, 1992). Freshwater

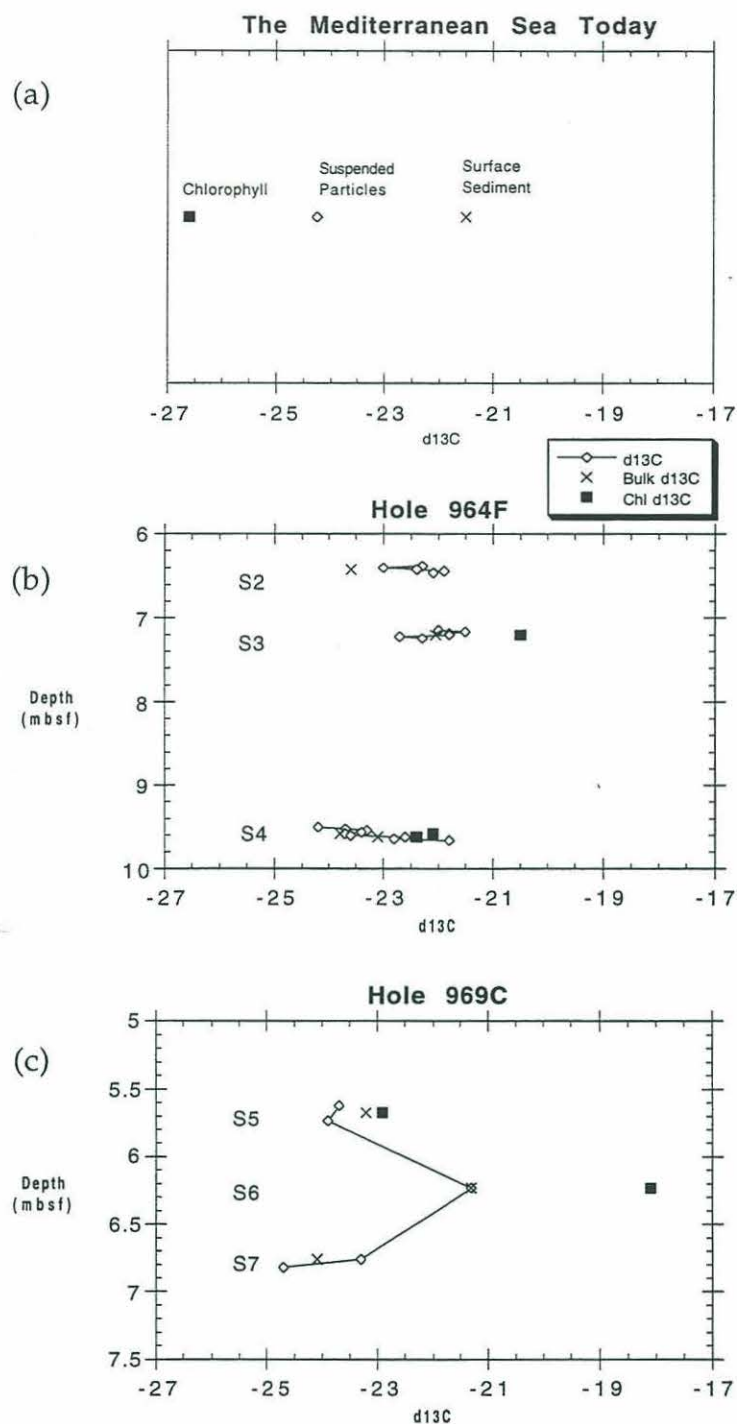


**Figure 5.13: Carbon isotopes in (a) the modern Mediterranean Sea, and (b,c) Late Quaternary Eastern Mediterranean sediments. The particulate  $\delta^{13}\text{C}$  value is an average of 3 samples from the Eastern Mediterranean. The chlorophyll  $\delta^{13}\text{C}$  value is a single measurement from the western basin (see text).**



DIC is depleted in  $^{13}\text{C}$  relative to seawater DIC by about 5-10 per mil (Fontugne and Calvert, 1992). Therefore, the input of freshwater would have lowered the  $\delta^{13}\text{C}$  of Eastern Mediterranean DIC.

Particulate samples from the DCM at four stations in the eastern basin averaged  $-24.25 (\pm 0.13)$  per mil, whereas surface sediments were  $-21.5$  per mil and sapropels averaged  $-23.3 (\pm 0.72)$  per mil. It is suggested that the isotopic depletion in particles is a result of low growth rates of phytoplankton at the deep chlorophyll maximum. Although chlorophyll concentrations are high at the DCM, phytoplankton growth rates are low (both due to low light intensities) (Parsons, et al., 1984). Furthermore, isotopic fractionation associated with carbon fixation by phytoplankton is inversely correlated with growth rate (Laws, et al., 1995). Suspended particles from the DCM are therefore expected to be depleted in  $^{13}\text{C}$  relative to suspended particles closer to the surface, where growth rates are higher.

The suspended particulate chlorophyll  $\delta^{13}\text{C}$  value ( $-26.6$  per mil) shown in figure 5.13.a represents a single sample from the Western Mediterranean. The isotopic composition of bulk suspended particulate matter associated with that chlorophyll was  $-25.75$  per mil. These low values, again, are attributed to low phytoplankton growth rates at the DCM. Suspended particles at the surface (4 m) at the same station had a  $\delta^{13}\text{C}$  value of  $-24.65$ , suggesting that growth rates were higher at shallower depths.

## 5.6 Conclusion

The nitrogen isotopic composition of pyropheophorbide *a* in six Late Quaternary sapropels from the Eastern Mediterranean was nearly constant at

-5.01 ( $\pm 0.38$ ) per mil. This value was similar to the  $\delta^{15}\text{N}$  of chlorophyll *a* from the present day deep chlorophyll maximum at three stations in the Eastern Mediterranean, -6.38 ( $\pm 1.80$ ) per mil. In addition, the  $\delta^{15}\text{N}$  of algal material in sapropels, calculated from the chlorophyll  $\delta^{15}\text{N}$ , was 0.15 per mil. This was nearly identical to both the  $\delta^{15}\text{N}$  of bulk sediment from sapropels ( $-0.08 \pm 0.53$  per mil), and to the  $\delta^{15}\text{N}$  of deep water nitrate (-0.05 per mil) in the modern Eastern Mediterranean. Contrary to previous interpretations of the nitrogen isotopic record in sediments of the Eastern Mediterranean, these data suggest that sapropels formed as a result of improved organic matter preservation. The downcore variation in whole sediment  $\delta^{15}\text{N}$  between sapropel and non-sapropel sequences is largely an artefact of diagenesis.

The similarity between algal  $\delta^{15}\text{N}$  values in sapropels S2-S7 and (1) bulk sapropel  $\delta^{15}\text{N}$ , (2) present day phytoplankton, and (3) deep water nitrate suggests that oligotrophic conditions similar to those of today have persisted in the Eastern Mediterranean for at least the last 200 kyr. This argues against any large changes in export production brought on by the decreased utilization (Calvert, et al., 1992) of an enlarged nutrient pool. Furthermore, these data are consistent with the existence of anoxic bottom waters in the Eastern Mediterranean during sapropel events. It is suggested that this condition fostered improved burial efficiency of organic matter, much like in the modern Black Sea (Canfield, 1989).

The likely mechanism for the establishment of anoxic bottom water in the Eastern Mediterranean was a freshening of surface water by monsoonal rains delivered by the Nile (Rossignol-Strick, 1985; Rossignol-Strick, et al., 1982). This freshening would have caused a reversal of the normal circulation pattern in the Eastern Mediterranean such that low-salinity surface waters flowed westward through the Strait of Sicily, to be replaced by nutrient-rich deep waters flowing



east. The ensuing nutrient trap would have resulted in bottom water anoxia since the oxygen demand from exported carbon would not have been compensated by the downward transport of oxygen (Sarmiento, et al., 1988a). The deep convection that occurs today as a result of excess evaporation over precipitation would not have been operable. Significantly, no change in biological productivity would be required to deplete bottom waters of oxygen on the observed timescales (Bethoux, 1993; Sarmiento, et al., 1988a).

The available evidence suggests that a modern analog for the Eastern Mediterranean during sapropel events is the Black Sea. That oligotrophic, anoxic basin has surface sediments containing 3-5% organic carbon. And, as pointed out by Southam, et al. (1982), the Black Sea is not stagnant. As in the Eastern Mediterranean sapropels, the nitrogen isotopic composition of algal material in Black Sea surface sediments, calculated from the chlorin  $\delta^{15}\text{N}$ , is similar to that of the bulk sediment and to deep water ammonium (there is no nitrate). It is the enhanced burial efficiency of organic matter under anoxic bottom waters that results in such organic-rich sediments (Canfield, 1989).

In addition, the chlorin  $\delta^{15}\text{N}$  value from the Holocene Black Sea sapropel (i.e., Unit II), -0.64 per mil, was similar to that of the bulk sediment, 0.45 per mil. This suggests that bottom waters of the Black Sea were anoxic during deposition of that sequence, a point that has been challenged by Calvert (1990).

Finally, it is proposed that the anomalously low  $\delta^{15}\text{N}$  value of deep water nitrate in the Eastern Mediterranean, -0.05 per mil, is a consequence of high rates of nitrogen fixation in that basin. Although nitrogen isotopic data for dissolved phases in the Mediterranean region are limited, a mass balance calculation suggests that 50% of Eastern Mediterranean DIN may derive from biological nitrogen fixation. Such high rates have not yet been measured, although nitrogen balances for the Mediterranean Sea (Bethoux, et al., 1992; Bethoux and



Copin-Montegut, 1986) suggested as much as 36% of dissolved nitrogen may derive from fixation.

This work has demonstrated the utility of a biomarker, such as chlorophyll, in environmental studies using nitrogen isotopes. Secondary processes occurring after photoautotrophic uptake and incorporation of nitrogen can result in isotopic alterations of the same magnitude as the primary signals often being sought. The measurement of chlorophyll  $\delta^{15}\text{N}$  allows the isotopic composition of primary producers to be determined. In addition, its comparison with bulk phases allows the quantification of isotopic alteration associated with secondary processes.

## References for Chapter 5

- Altabet, M.A. (1988) Variations in Nitrogen Isotopic Composition Between Sinking and Suspended Particles: Implications for Nitrogen Cycling and Particle Transformation in the Open Ocean. *Deep-Sea Research*, **35**(4): 535-554.
- Altabet, M.A. (1989) A Time-Series Study of the Vertical Structure of Nitrogen and Particle Dynamics in the Sargasso Sea. *Limnology and Oceanography*, **34**(7): 1185-1201.
- Altabet, M.A., W.G. Deuser, S. Honjo and C. Stienen (1991) Seasonal and Depth-Related Changes in the Source of Sinking Particles in the North Atlantic. *Nature*, **354**: 136-139.
- Altabet, M.A. and R. Francois (1994) Sedimentary Nitrogen Isotopic Ratio As a Recorder for Surface Ocean Nitrate Utilization. *Global Biogeochemical Cycles*, **8**(1): 103-116.
- Altabet, M.A., R. Francois, D.W. Murray and W.L. Prell (1995) Climate-Related Variations in Denitrification in the Arabian Sea from Sediment  $^{15}\text{N}/^{14}\text{N}$  Ratios. *Nature*, **373**: 506-509.
- Altabet, M.A. and J.J. McCarthy (1985) Temporal and Spatial Variations in the Natural Abundance of  $^{15}\text{N}$  in PON from a Warm-Core Ring. *Deep-Sea Research*, **32**(7): 755-772.
- Altabet, M.A. and L.F. Small (1990) Nitrogen Isotopic Ratios in Fecal Pellets Produced by Marine Zooplankton. *Geochimica et Cosmochimica Acta*, **54**: 155-163.
- Baker, E.W. and J.W. Louda (1986) Porphyrins in the Geological Record. In: *Biological Markers in the Sedimentary Record*, (R. B. Johns, ed.), Elsevier, Amsterdam, pp. 125-225.

- Benner, R., M.L. Fogel and E.K. Sprague (1991) Diagenesis of Belowground Biomass of *Spartina alterniflora* in Salt-Marsh Sediments. *Limnology and Oceanography*, **36**(7): 1358-1374.
- Berger, A.L. and M.F. Loutre (1991) Insolation Values for the Climate of the Last 10 Million Years. *Quaternary Science Reviews*, **10**: 297-317.
- Bertrand, P. and E. Lallier-Verges (1993) Past Sedimentary Organic Matter Accumulation and Degradation Controlled by Productivity. *Nature*, **364**: 786-788.
- Bethoux, J.P. (1979) Budgets of the Mediterranean Sea. Their Dependence on the Local Climate and On the Characteristics of the Atlantic Waters. *Oceanologica Acta*, **2**(2): 157-163.
- Bethoux, J.P. (1981) Le Phosphore et L'Azote en Mer Méditerranée, Bilans et Fertilité Potentielle. *Marine Chemistry*, **10**: 141-158.
- Bethoux, J.-P. (1993) Mediterranean Sapropel Formation, Dynamic and Climatic Viewpoints. *Oceanologica Acta*, **16**(2): 127-133.
- Bethoux, J.P. and G. Copin-Montegut (1986) Biological Fixation of Atmospheric Nitrogen In the Mediterranean Sea. *Limnology and Oceanography*, **31**(6): 1353-1358.
- Bethoux, J.P., P. Morin, C. Madec and B. Gentili (1992) Phosphorous and Nitrogen Behavior in the Mediterranean Sea. *Deep-Sea Research*, **39**(9): 1641-1654.
- Betts, J.N. and H.D. Holland (1991) The Oxygen Content of Ocean Bottom Waters, the Burial Efficiency of Organic Carbon, and the Regulation of Atmospheric Oxygen. *Paleogeography, Paleoclimatology, Paleoecology*, **97**: 1-14.
- Biggs, D.C., S.P. Berkowitz, M.A. Altabet, R.R. Bidigare, D.J. DeMaster, R.B. Dunbar, A. Leventer, S.A. Macko, C.A. Nittrouer and M.E. Ondrusek (1988) A Cooperative Study of Upper-Ocean Particulate Fluxes in the Weddell Sea. In: *Proceedings of the Ocean Drilling Program - Initial Reports*, ed.), NSF Joint Oceanographic Institutions Inc., College Station, TX, pp. 77-86.



Bogacheva, M.P., L.A. Kodina and E.M. Galimov (1979) Intramolecular Carbon Isotope Distributions in Chlorophyll and Its Geochemical Derivatives. In: *Advances in Organic Geochemistry 1979*, (A. G. Douglas and J. R. Maxwell, ed.), Pergamon Press, Oxford, pp. 679-687.

Broecker, W.S. and T.H. Peng (1982) *Tracers in the Sea*. Lamont-Doherty Geological Observatory, Palisades, NY, 689pp.

Bustillos-Guzman, J., H. Claustre and J.-C. Marty (1995) Specific Phytoplankton Signatures and Their Relationship to Hydrographic Conditions in the Coastal Northwestern Mediterranean Sea. *Marine Ecology Progress series*, **124**: 247-258.

Calvert, S.E. (1983) Geochemistry of Pleistocene Sapropels and Associated Sediments from the Eastern Mediterranean. *Oceanologica Acta*, **6**(3): 255-267.

Calvert, S.E. (1990) Geochemistry and Origin of the Holocene Sapropel in the Black Sea. In: *Facets of Modern Biogeochemistry*, (V. Ittekkot, S. Kempe, W. Michaelis and A. Spitz, ed.), Springer-Verlag, Berlin, pp. 326-352.

Calvert, S.E. and M.R. Fontugne (1987) Stable Carbon Isotopic Evidence for the Marine Origin of the Organic Matter in the Holocene Black Sea Sapropel. *Chemical Geology (Isotope Geoscience Section)*, **66**: 315-322.

Calvert, S.E., R.E. Karlin, L.J. Toolin, D.J. Donahue, J.R. Southon and J.S. Vogel (1991) Low Organic Carbon Accumulation Rates in Black Sea Sediments. *Nature*, **350**: 692-695.

Calvert, S.E., B. Nielsen and M.R. Fontugne (1992) Evidence From Nitrogen Isotope Ratios for Enhanced Productivity During Formation of Eastern Mediterranean Sapropels. *Nature*, **359**(6392): 223-225.

Calvert, S.E. and T.F. Pedersen (1992) Organic Carbon Accumulation and Preservation in Marine Sediments: How Important Is Anoxia? In: *Organic Matter: Productivity, Accumulation, and Preservation in Recent and Ancient Sediments*, (J. K. Whelan and J. W. Farrington, ed.), Columbia University Press, New York, pp. 231-263.

- Calvert, S.E., J.S. Vogel and J.R. Southon (1987) Carbon Accumulation Rates and the Origin of the Holocene Sapropel in the Black Sea. *Geology*, **15**: 918-921.
- Canfield, D.E. (1989) Sulfate Reduction and Oxidic Respiration in Marine Sediments: Implications for Organic Carbon Preservation in Euxinic Environments. *Deep-Sea Research*, **36**(1): 121-138.
- Capone, D.G. and E.J. Carpenter (1982) Nitrogen Fixation in the Marine Environment. *Science*, **217**: 1140-1142.
- Carpenter, E.J. and C.C. Price IV (1977) Nitrogen Fixation, Distribution, and Production of *Oscillatoria* (*Trichodesmium*) spp. in the Western Sargasso and Caribbean Seas. *Limnology and Oceanography*, **22**(1): 60-72.
- Castradori, D. (1993) Calcareous Nonnofossils and the Origin of Eastern Mediterranean Sapropels. *Paleoceanography*, **8**(4): 459-471.
- Checkley, D.M., Jr. and L.C. Entzeroth (1985) Elemental and Isotopic Fractionation of Carbon and Nitrogen By Marine, Planktonic Copepods and Implications to the Marine Nitrogen Cycle. *Journal of Plankton Research*, **7**(4): 553-568.
- Checkley, D.M., Jr. and C.A. Miller (1989) Nitrogen Isotope Fractionation By Oceanic Zooplankton. *Deep-Sea Research*, **36**(10): 1449-1456.
- Cita, M.B., C. Vergnaud-Grazzini, C. Robert, H. Chamley, N. Ciaranfi and S. D'Onofrio (1977) Paleoclimatic Record of a Long Deep Sea Core from the Eastern Mediterranean. *Quaternary Research*, **8**: 205-235.
- Claustre, H. (1994) The Trophic status of Various Oceanic Provinces as Revealed by Phytoplankton Pigment Signatures. *Limnology and Oceanography*, **39**(5): 1206-1210.
- Claustre, H. and J.-C. Marty (1995) Specific Phytoplankton Biomasses and Their Relation to Primary Production in the Tropical North Atlantic. *Deep-Sea Research*, **42**(8): 1475-1493.



- Cline, J.D. and I.R. Kaplan (1975) Isotopic Fractionation of Dissolved Nitrate During Denitrification in the Eastern Tropical North Pacific Ocean. *Marine Chemistry*, 3: 271-299.
- Codispoti, L.A. (1989) Phosphorous vs. Nitrogen Limitation of New and Export Production. In: *Productivity of the Ocean: Present and Past*, (W. H. Berger, V. S. Smetacek and G. Wefer, ed.), John Wiley & Sons, Chichester, pp. 377-394.
- Correns, C.W. (1939) Pelagic Sediments of the North Atlantic Ocean. In: *Recent Marine Sediments*, (P. D. Trask, ed.), The American Association of Petroleum Geologists, Tulsa, Oklahoma, pp. 373-395.
- Cowie, G.L. and J.I. Hedges (1992) The Role of Anoxia in Organic Matter Preservation in Coastal Sediments: Relative Stabilities of the Major Biochemicals Under Oxic and Anoxic Depositional Conditions. *Organic Geochemistry*, 19(1-3): 229-234.
- de Lange, G.J. and H.L. ten Haven (1983) Recent Sapropel Formation in the Eastern Mediterranean. *Nature*, 305: 797-798.
- Dean, W.E., M.A. Arthur and G.E. Claypool (1986) Depletion of  $^{13}\text{C}$  in Cretaceous Marine Organic Matter: Source, Diagenetic, or Environmental Signal? *Marine Geology*, 70: 119-157.
- Delwiche, C.C. and P.L. Steyn (1970) Nitrogen Isotope Fractionation in Soils and Microbial Reactions. *Environmental Science & Technology*, 4(11): 929-935.
- Demaison, G.J. and G.T. Moore (1980) Anoxic Environments and Oil Source Bed Genesis. *The American Association of Petroleum Geologists Bulletin*, 64(8): 1179-1209.
- DeNiro, M.J. and S. Epstein (1981) Influence of Diet on the Distribution of Nitrogen Isotopes in Animals. *Geochimica et Cosmochimica Acta*, 45: 341-351.
- Deroo, G., J.P. Herbin and J. Roucache (1978) Organic Geochemistry of Some Neogene Cores from Sites 374, 375, 377, and 378: Leg 42A, Eastern Mediterranean Sea. In: *Initial Reports of the Deep Sea Drilling Project*, (R. B. Kidd



and P. J. Worstel, ed.), U.S. Government Printing Office, Washington, D.C., pp. 465-572.

Deuser, W.G. (1971) Organic-Carbon Budget of the Black Sea. *Deep-Sea Research*, **18**: 995-1004.

Dugdale, R.C. and J.J. Goering (1967) Uptake of New and Regenerated Forms of Nitrogen in Primary Productivity. *Limnology and Oceanography*, **12**: 196-206.

Emeis, K.-C., A.H.F. Robertson, C. Richter, et al. (1996) Paleoceanography and Sapropel Introduction. In: *Proceedings of the Ocean Drilling Program, Initial Reports*, (E. Kapitan-White, ed.), Ocean Drilling Program, College Station, Texas, pp. 21-26.

Emerson, S. (1985) Organic Carbon Preservation in Marine Sediments. In: *The Carbon Cycle and Atmospheric CO<sub>2</sub>: Natural Variations Archean to Present*, (E. T. Sundquist and W. S. Broecker, ed.), American Geophysical Union, Washington, DC, pp. 78-87.

Emerson, S. and J.I. Hedges (1988) Processes Controlling the Organic Carbon Content of Open Ocean Sediments. *Paleoceanography*, **3**(5): 621-634.

Emery, K.O. (1960) *The Sea Off Southern California*. John Wiley & Sons, Inc., New York, 366 pp.

Eppley, R.W. and B.J. Peterson (1979) Particulate Organic Matter Flux and Planktonic New Production in the Deep Ocean. *Nature*, **282**: 677-680.

Farrell, J.W., T.F. Pedersen, S.E. Calvert and B. Nielsen (1995) Glacial-Interglacial Changes in Nutrient Utilization in the Equatorial Pacific Ocean. *Nature*, **377**(6549): 514-517.

Fontugne, M.R. and S.E. Calvert (1992) Late Pleistocene Variability of the Carbon Isotopic Composition of Organic Matter in the Eastern Mediterranean: Monitor of Changes in Carbon Sources and Atmospheric CO<sub>2</sub> Concentrations. *Paleoceanography*, **7**(1): 1-20.

Fontugne, M.R. and J.-C. Duplessy (1986) Variations of the Monsoon Regime During the Upper Quaternary: Evidence from Carbon Isotopic Records of Organic Matter in North Indian Ocean Sediment Cores. *Palaeogeography, Palaeoclimatology, Palaeoecology*, **56**(1/2): 69-88.

Francois, R. and M.A. Altabet (1992) Glacial to Interglacial Changes in Surface Nitrate Utilization in the Indian Sector of the Southern Ocean as Recorded by Sediment  $\delta^{15}\text{N}$ . *Paleoceanography*, **7**(5): 589-606.

Francois, R., M.P. Bacon, M.A. Altabet and L.D. Labeyrie (1993) Glacial/Interglacial Changes in Sediment Rain Rate in the SW Indian Sector of Subantarctic Waters as Recorded by  $^{230}\text{Th}$ ,  $^{231}\text{Pa}$ , U, and  $\delta^{15}\text{N}$ . *Paleoceanography*, **8**(5): 611-629.

Fry, B. (1988) Food Web Structure on Georges Bank from Stable C, N, and S Isotopic Compositions. *Limnology and Oceanography*, **33**(5): 1182-1190.

Fry, B., R. Garritt, K. Tholke, C. Neill and R.H. Michener (in preparation) Cryofocussing Nannomole Amounts of  $\text{CO}_2$ ,  $\text{N}_2$ , and  $\text{SO}_2$  for Stable Isotopic Analysis.

Fry, B., H.W. Jannasch, S.J. Molyneaux, C.O. Wirsen, J.A. Muramoto and S. King (1991) Stable Isotope Studies of the Carbon, Nitrogen and Sulfur Cycles in the Black Sea and the Cariaco Trench. *Deep-Sea Research*, **38**(Suppl. 2): S1003-S1019.

Ganeshram, R.S., T.F. Pedersen, S.E. Calvert and J.W. Murray (1995) Large Changes in Oceanic Nutrient Inventories from Glacial to Interglacial Periods. *Nature*, **376**: 755-758.

Glenn, C.R. and M.A. Arthur (1985) Sedimentary and Geochemical Indicators of Productivity and Oxygen Contents in Modern and Ancient Basins: The Holocene Black Sea as the "Type" Anoxic Basin. *Chemical Geology*, **48**: 325-354.



- Goering, J., V. Alexander and N. Haubenstock (1990) Seasonal Variability of Stable Carbon and Nitrogen Isotope Ratios of Organisms in a North Pacific Bay. *Estuarine and Coastal Shelf Science*, **30**: 239-260.
- Henrichs, S.M. and W.S. Reeburgh (1987) Anaerobic Mineralization of Marine Sediment Organic Matter: Rates and the Role of Anaerobic Processes in the Oceanic Carbon Economy. *Geomicrobiology Journal*, **5**(3/4): 191-237.
- Higgs, N.C., J. Thomson, T.R.S. Wilson and I.W. Croudace (1994) Modification and Complete Removal of Eastern Mediterranean Sapropels by Postdepositional Oxidation. *Geology*, **22**: 423-426.
- Hoering, T. (1957) The Isotopic Composition of the Ammonia and the Nitrate Ion in Rain. *Geochimica et Cosmochimica Acta*, **12**: 97-102.
- Hoering, T.C. and H.T. Ford (1960) The Isotope Effects in the Fixation of Nitrogen by *Azotobacter*. *Journal of the American Chemical Society*, **82**: 376-378.
- Horrigan, S.G., J.P. Montoya, J.L. Nevins and J.J. McCarthy (1990) Natural Isotopic Composition of Dissolved Inorganic Nitrogen in the Chesapeake Bay. *Estuarine, Coastal and Shelf Science*, **30**: 393-410.
- Howell, M.W. and R.C. Thunell (1992) Organic Carbon Accumulation in Bannock Basin: Evaluating the Role of Productivity in the Formation of Eastern Mediterranean Sapropels. *Marine Geology*, **103**: 461-471.
- Huang, T.C. and D.J. Stanley (1972) Western Alboran Sea: Sediment Dispersal, Ponding and Reversal of Currents. In: *The Mediterranean Sea*, (D. J. Stanley, ed.), Dowden, Hutchinson and Ross, Stroudsburg, PA, pp. 521-559.
- Hunt, J.M. (1979) *Petroleum Geochemistry and Geology*. W.H. Freeman and Company, San Francisco, 498 pp.
- Imbrie, J., J.D. Hays, D.G. Martinson, A. McIntyre, A.C. Mix, J.J. Morley, N.G. Pisias, W.L. Prell and N.J. Shackleton (1984) The Orbital Theory of Pleistocene Climate: Support from a Revised Chronology of the Marine  $\delta^{18}\text{O}$  Record. In:



*Milankovitch and Climate, Part 1*, (A. Berger, J. Imbrie, J. Hays, G. Kukla and B. Saltzman, ed.), D. Reidel Publishing Co., Dordrecht, pp. 269-305.

Jacobs, L., S. Emerson and S.S. Husted (1987) Trace Metal Geochemistry in the Cariaco Trench. *Deep-Sea Research*, **34**(5/6): 965-981.

Jenkins, J.A. and D.F. Williams (1983/84) Nile Water as a Cause of Eastern Mediterranean Sapropel Formation: Evidence for and Against. *Marine Micropaleontology*, **8**: 521-534.

Jones, G.A. and A.R. Gagnon (1994) Radiocarbon Chronology of Black Sea Sediments. *Deep-Sea Research*, **41**(3): 531-557.

Kidd, R.B., M.B. Cita and W.B.F. Ryan (1978) The Stratigraphy of Eastern Mediterranean Sapropel Sequences Recovered During DSDP Leg 42A and Their Paleoenvironmental Significance. In: *Initial Reports of the Deep Sea Drilling Project*, (R. B. Kidd and P. J. Worstel, ed.), U.S. Government Printing Office, Washington, D.C., pp. 421-443.

Laws, E.A., B.N. Popp, R.R. Bidigare, M.C. Kennicutt and S.A. Macko (1995) Dependence of Phytoplankton Carbon Isotopic Composition on Growth Rate and  $[CO_2]_{aq}$ : Theoretical Considerations and Experimental Results. *Geochimica et Cosmochimica Acta*, **59**(6): 1131-1138.

Lee, C. (1992) Controls on Organic Carbon Preservation: The Use of Stratified Water Bodies to Compare Intrinsic Rates of Decomposition in Oxidic and Anoxic Systems. *Geochimica et Cosmochimica Acta*, **56**(8): 3323-3335.

Libes, S.M. and W.G. Deuser (1988) The Isotope Geochemistry of Particulate Nitrogen in the Peru Upwelling Area and the Gulf of Maine. *Deep-Sea Research*, **35**(4): 517-533.

Liu, K.-K. and I.R. Kaplan (1989) The Eastern Tropical Pacific as a Source of  $^{15}N$ -Enriched Nitrate in Seawater Off Southern California. *Limnology and Oceanography*, **34**(5): 820-830.

Macko, S.A. and M.L.F. Estep (1984) Microbial Alteration of Stable Nitrogen and Carbon Isotopic Composition of Organic Matter. *Organic Geochemistry*, **6**: 787-790.

Macko, S.A., M.L.F. Estep, P.E. Hare and T.C. Hoering (1987) Isotopic Fractionation of Nitrogen and Carbon in the Synthesis of Amino Acids by Microorganisms. *Chemical Geology (Isotope Geoscience Section)*, **65**: 79-92.

Mangini, A. and P. Schlosser (1986) The Formation of Eastern Mediterranean Sapropels. *Marine Geology*, **72**: 115-124.

Mariotti, A., J.C. Germon, P. Hubert, P. Kaiser, R. Letolle, A. Tardieux and P. Tardieux (1981) Experimental Determination of Nitrogen Kinetic Isotope Fractionation: Some Principles; Illustration for the Denitrification and Nitrification Processes. *Plant and Soil*, **62**: 413-430.

Mariotti, A., C. Lancelot and G. Billen (1984) Natural Isotopic Composition of Nitrogen as a Tracer of Origin for Suspended Organic Matter in the Scheldt Estuary. *Geochimica et Cosmochimica Acta*, **48**: 549-555.

Martinez, L.A., M. Silver, J.M. King and A.L. Alldredge (1983) Nitrogen Fixation by Floating Diatom Mats: A Source of New Nitrogen to Oligotrophic Ocean Waters. *Science*, **221**: 152-154.

Mayer, L.M. (1993) Surface Area Control of Organic Carbon Accumulation in Continental Shelf Sediments. *Geochimica et Cosmochimica Acta*, **58**(4): 1271-1284.

Miller, A.R., P. Tchernia, H. Charnock and D.A. McGill (1970) *Mediterranean Sea Atlas*. The Woods Hole Oceanographic Institution, Woods Hole, MA, 190 pp.

Miyake, Y. and E. Wada (1967) The Abundance Ratio of  $^{15}\text{N}/^{14}\text{N}$  in Marine Environments. *Journal of the Oceanographic Society of Japan*, **9**: 37-53.

Miyazaki, T., E. Wada and A. Hattori (1980) Nitrogen-Isotope Fractionation in the Nitrate Respiration by the Marine Bacterium *Serratia marnorubra*. *Geomicrobiology Journal*, **2**(2): 115-126.



- Montoya, J.P., S.G. Horrigan and J.J. McCarthy (1991) Rapid, Storm-induced Changes in the Natural Abundance of  $^{15}\text{N}$  in a Planktonic Ecosystem, Chesapeake Bay, USA. *Geochimica et Cosmochimica Acta*, **55**: 3627-3638.
- Montoya, J.P. and J.J. McCarthy (1995) Isotopic Fractionation During Nitrate Uptake by Marine Phytoplankton Grown in Continuous Culture. *Journal of Plankton Research*, **17**: 439-464.
- Montoya, J.P., P.H. Wiebe and J.J. McCarthy (1992) Natural Abundance of  $^{15}\text{N}$  in Particulate Nitrogen and Zooplankton in the Gulf Stream Region and Warm-Core Ring 86A. *Deep-Sea Research*, **39**(Suppl. 1): S363-S392.
- Muerdter, D.R. (1984) Low-Salinity Surface Water Incursions Across the Strait of Sicily During Late Quaternary Sapropel Intervals. *Marine Geology*, **58**: 401-414.
- Mullineaux, L.S. and G.P. Lohmann (1981) Late Quaternary Stagnations and Recirculation of the Eastern Mediterranean: Changes in the Deep Water Recorded by Fossil Benthic Foraminifera. *Journal of Foraminiferal Research*, **11**(1): 20-39.
- Nakatsuka, T., N. Handa, E. Wada and C.S. Wong (1992) The Dynamic Changes of Stable Isotopic Ratios of Carbon and Nitrogen in Suspended and Sedimented Particulate Organic Matter During a Phytoplankton Bloom. *Journal of Marine Research*, : 267-296.
- Nakatsuka, T., K. Watanabe, N. Handa, E. Matsumoto and E. Wada (1995) Glacial to Interglacial Surface Nutrient Variations of Bering Deep Basins Recorded by  $\delta^{13}\text{C}$  and  $\delta^{15}\text{N}$  of Sedimentary Organic Matter. *Paleoceanography*, **10**(6): 1047-1061.
- Naqvi, S.W.A., H.P. Hansen and T.W. Kureishy (1986) Nutrient Uptake and Regeneration Ratios in the Red Sea With Reference to the Nutrient Budgets. *Oceanologica Acta*, **9**(3): 271-275.
- Olausson, E. (1961) Sediment Cores from the Mediterranean and the Red Sea. *Reports of the Swedish Deep Sea Expedition*, **8**(6): 337-391.



- Ostlund, H.G. (1974) Expedition "Odysseus 65": Radiocarbon Age of Black Sea Deep Water. In: *The Black Sea--Geology, Chemistry, and Biology*, (E. T. Degens and D. A. Ross, ed.), The American Association of Petroleum Geologists, Tulsa, OK, pp. 127-132
- Owens, N.J.P. (1987) Marine Variation in  $^{15}\text{N}$ . *Advances in Marine Biology*, **24**: 390-451.
- Parsons, T.R., M. Takahashi and B. Hargrave (1984) *Biological Oceanographic Processes*. Pergamon Press, Oxford, 330 pp.
- Pedersen, T.F. and S.E. Calvert (1990) Anoxia vs. Productivity: What Controls the Formation of Organic-Carbon-Rich Sediments and Sedimentary Rocks? *The American Association of Petroleum Geologists Bulletin*, **74**(2): 454-466.
- Pelet, R. and Y. Bebyser (1977) Organic Geochemistry of Black Sea Cores. *Geochimica et Cosmochimica Acta*, **41**: 1575-1586.
- Peters, K.E., R.E. Sweeney and I.R. Kaplan (1978) Correlation of Carbon and Nitrogen Stable Isotope Ratios in Sedimentary Organic Matter. *Limnology and Oceanography*, **23**(4): 598-604.
- Poutanen, E.-L. and R.J. Morris (1985) Humic Substances in an Arabian Shelf Sediment an the S<sub>1</sub> Sapropel from the Eastern Mediterranean. *Chemical Geology*, **51**: 135-145.
- Pruyser, P.A., G.J. de Lange and J.J. Middleburg (1991) Geochemistry of Eastern Mediterranean Sediments: Primary Sediment Composition and Diagenetic Alterations. *Marine Geology*, **100**: 137-154.
- Rau, G.H., C.W. Sullivan and L.I. Gordon (1991)  $\delta^{13}\text{C}$  and  $\delta^{15}\text{N}$  Variations in Weddell Sea Particulate Organic Matter. *Marine Chemistry*, **35**: 355-369.
- Rau, G.H., T. Takahashi and D.J.D. Marais (1989) Latitudinal Variations in Plankton  $\delta^{13}\text{C}$ : Implications for CO<sub>2</sub> and Productivity in Past Oceans. *Nature*, **341**: 516-518.

- Repeta, D.J. and D.J. Simpson (1991) The Distribution and Recycling of Chlorophyll, Bacteriochlorophyll and Carotenoids in the black Sea. *Deep-Sea Research*, 38(Suppl. 2): S969-S984.
- Richards, F.A. and B.B. Benson (1961) Nitrogen/Argon and Nitrogen Isotope Ratios in Two Anaerobic Environments, the Cariaco Trench in the Caribbean Sea and Drømsfjord, Norway. *Deep-Sea Research*, 7: 254-264.
- Richards, F.A. and A.C. Redfield (1954) A Correlation Between the Oxygen Content of Sea Water and the Organic Content of Marine Sediments. *Deep-Sea Research*, 1(4): 279-281.
- Rosignol-Strick, M. (1985) Mediterranean Quaternary Sapropels, An Immediate Response of the African Monsoon to Variation of Insolation. *Palaeogeography, Palaeoclimatology, Palaeoecology*, 49: 237-263.
- Rosignol-Strick, M., W. Nesteroff, P. Olive and C. Vergnaud-Grazzini (1982) After the Deluge: Mediterranean Stagnation and Sapropel Formation. *Nature*, 295: 105-109.
- Saino, T. and A. Hattori (1980)  $^{15}\text{N}$  Natural Abundance in Oceanic Suspended Particulate Matter. *Nature*, 283: 752-754.
- Saino, T. and A. Hattori (1985) Variation of  $^{15}\text{N}$  Natural Abundance of Suspended Organic Matter in Shallow Oceanic Waters. In: *Marine and Estuarine Geochemistry*, (A. C. Sigleo and A. Hattori, ed.), Lewis Publishers, Inc., Chelsea, MI, pp. 1-13.
- Saino, T. and A. Hattori (1987) Geographical Variation of the Water Column Distribution of Suspended Particulate Organic Nitrogen and Its  $^{15}\text{N}$  Natural Abundance in the Pacific and its Marginal Seas. *Deep-Sea Research*, 34(5/6): 807-827.
- Sarmiento, J.L., T. Herbert and J.R. Toggweiler (1988a) Mediterranean Nutrient Balance and Episodes of Anoxia. *Paleoceanography*, 2(4): 427-444.



Sarmiento, J.L., T.D. Herbert and J.R. Toggweiler (1988b) Causes of Anoxia in the World Ocean. *Global Biogeochemical Cycles*, 2(2): 115-128.

Schafer, P. and V. Ittekkot (1993) Seasonal Variability of  $\delta^{15}\text{N}$  in Settling Particles in the Arabian Sea and Its Palaeochemical Significance. *Naturwissenschaften*, 80: 511-513.

Schrader, H. and A. Matherne (1981) Sapropel Formation in the Eastern Mediterranean Sea: Evidence from Preserved Opal Assemblages. *Micropaleontology*, 27(2): 191-203.

Shaw, H.F. and G. Evans (1984) The Nature, Distribution and Origin of a Sapropelic Layer in Sediments of the Cilicia Basin, Northeastern Mediterranean. *Marine Geology*, 61: 1-12.

Shimmield, G.B., N.B. Price and T.F. Pedersen (1990) The Influence of Hydrography, Bathymetry and Productivity on Sediment Type and Composition on the Oman Margin and in the Northwest Arabian Sea. In: *The Geology and Tectonics of the Oman Margin*, (M. P. Robertson and e. al., ed.), Geological Society Special Publication, pp. 759-769.

Sigl, W., H. Chamley, F. Fabricius, G.G. d'Argoud and J. Muller (1978) Sedimentology and Environmental Conditions of Sapropels. In: *Initial Reports of the Deep Sea Drilling Project*, (R. B. Kidd and P. J. Worstel, ed.), U.S. Government Printing Office, Washington, D.C., pp. 425-465.

Sigman, D.M., M.A. Altabet, R. Michener, D.C. McCorkle and R.M. Holmes (submitted) Natural Abundance-Level Measurement of the Nitrogen Isotopic Composition of Oceanic Nitrate: an Adaptation of the Ammonium Diffusion Method.

Simoneit, B.R.T. (1977) The Black Sea, a Sink for Terrigenous Lipids. *Deep-Sea Research*, 24: 813-830.



Smith, D.J., G. Eglinton and R.J. Morris (1986) The Lipid Geochemistry of a Recent Sapropel and Associated Sediments from the Hellenic Outer Ridge, Eastern Mediterranean Sea. *Philosophical Transactions of the Royal Society of London*, **A 319**: 375-415.

SooHoo, J.B. and D.A. Kiefer (1982) Vertical Distribution of Phaeopigments--I. A Simple Grazing and Photooxidative Scheme for Small Particles. *Deep-Sea Research*, **29**(12A): 1539-1551.

Sorokin, Y.I. (1983) The Black Sea. In: *Ecosystems of the World 26--Estuaries and Enclosed Seas*, (B. Ketchum, ed.), Elsevier, pp. 253-307.

Southam, J.R., W.H. Peterson and G.W. Brass (1982) Dynamics of Anoxia. *Palaeogeography, Palaeoclimatology, Palaeoecology*, **40**: 183-198.

Stanley, D.J. (1978) Ionian Sea Sapropel Distribution and Late Quaternary Paleooceanography in the Eastern Mediterranean. *Nature*, **274**: 149-152.

Stanley, D.J., A. Maldonado and R. Stuckenrath (1975) Strait of Sicily Depositional Rates and Patterns, and Possible Reversal of Currents in the Late Quaternary. *Palaeogeography, Palaeoclimatology, Palaeoecology*, **18**: 279-291.

Suess, E., R. von Huene and e. al. (1988) 1. Introduction, Objectives, and Principal Results. Leg 112, Peru Continental Margin. In: *Proc. ODP, Init. Repts.*, Ocean Drilling Program, College Station, TX, pp. 5-23.

Sutherland, H.E., S.E. Calvert and R.J. Morris (1984) Geochemical Studies of the Recent Sapropel and Associated Sediment from the Hellenic Outer Ridge, Eastern Mediterranean Sea. I: Mineralogy and Chemical Composition. *Marine Geology*, **56**: 79-92.

Sweeney, R.E. and I.R. Kaplan (1980) Natural Abundance of  $^{15}\text{N}$  as a Source for Near-Shore Marine Sedimentary and Dissolved Nitrogen. *Marine Chemistry*, **9**: 81-94.

Sweeney, R.E., K.K. Liu and I.R. Kaplan (1978) Oceanic Nitrogen Isotopes and Their Uses in Determining the Source of Sedimentary Nitrogen. *DSIR Bull.*, **220**: 9-26.

ten Haven, H.L. (1986) Organic and Inorganic Geochemical Aspects of Mediterranean Late Quaternary Sapropels and Messinian Evaporitic Deposits. PhD, University of Utrecht.

ten Haven, H.L., M. Baas, J.W. de Leeuw and P.A. Schenk (1987) Late Quaternary Mediterranean Sapropels, I--On the Origin of Organic Matter in Sapropel S7. *Marine Geology*, **75**: 137-156.

Thunell, R.C. and D.F. Williams (1982) Paleooceanographic Events Associated With Termination II in the Eastern Mediterranean. *Oceanologica Acta*, **5**(2): 229-233.

Thunell, R.C. and D.F. Williams (1983) Paleotemperature and Paleosalinity History of the Eastern Mediterranean During the Late Quaternary. *Palaeogeography, Palaeoclimatology, Palaeoecology*, **44**: 23-39.

Thunell, R.C., D.F. Williams and J.P. Kennett (1977) Late Quaternary Paleoclimatology, Stratigraphy and Sapropel History in Eastern Mediterranean Deep-Sea Sediments. *Marine Micropaleontology*, **2**: 371-388.

Tissot, B.P. and D.H. Welte (1984) *Petroleum Formation and Occurrence*. Springer-Verlag, Berlin, 538 pp.

Troelstra, S.R., G.M. Ganssen, K. van der Borg and A.F.M. de Jong (1991) A Late Quaternary Stratigraphic Framework for Eastern Mediterranean Sapropel S1 Based On AMS  $^{14}\text{C}$  Dates and Stable Oxygen Isotopes. *Radiocarbon*, **33**(1): 15-21.

van Os, B.J.H., J.J. Middleburg and G.J. de Lange (1991) Possible Diagenetic Mobilization of Barium in Sapropelic Sediment from the Eastern Mediterranean. *Marine Geology*, **100**: 125-136.



- Velinsky, D.J., M.L. Fogel and B.M. Tebo (1989) Dissolved Nitrogen Isotopic Distribution in the Black Sea. In: *Annual Report of the Director Geophysical Laboratory*, ed.), Carnegie Institution of Washington, Washington, D.C., pp. 123-130.
- Velinsky, D.J., M.L. Fogel, J.F. Todd and B.M. Tebo (1991) Isotopic Fractionation of Dissolved Ammonium at the Oxygen-Hydrogen Sulfide Interface in Anoxic Waters. *Geophysical Research Letters*, **18**(4): 649-652.
- Vergnaud-Grazzini, C., W.B.F. Ryan and M.B. Cita (1977) Stable Isotopic Fractionation, Climate Change and Episodic Stagnation in the Eastern Mediterranean During the Late Quaternary. *Marine Micropaleontology*, **2**: 353-370.
- Villareal, T.A., M.A. Altabet and K. Culver-Rymsza (1993) Nitrogen Transport by Vertically Migrating Diatom Mats in the North Pacific Ocean. *Nature*, **363**: 709-712.
- Wada, E. (1980) Nitrogen Isotope Fractionation and its Significance in Biogeochemical Processes Occurring in Marine Environments. In: *Isotope Marine Chemistry*, (E. D. Goldberg, Y. Horibe and K. Saruhashi, ed.), Uchida Rokakuho, Tokyo, pp. 375-398.
- Wada, E. and A. Hattori (1976) Natural Abundance in Particulate Organic Matter in the North Pacific Ocean. *Geochimica et Cosmochimica Acta*, **40**: 249-251.
- Wada, E. and A. Hattori (1978) Nitrogen Isotope Effects in the Assimilation of Inorganic Nitrogenous Compounds by Marine Diatoms. *Geomicrobiology Journal*, **1**: 85-101.
- Wada, E., M. Minagawa, H. Mizutani, T. Tsuji, R. Imaizumi and K. Karasawa (1987a) Biogeochemical Studies on the Transport of Organic Matter Along the Otsuchi River Watershed, Japan. *Estuarine and Coastal Shelf Science*, **25**: 321-336.
- Wada, E., M. Terazaki, Y. Kabaya and T. Nemoto (1987b)  $^{15}\text{N}$  and  $^{13}\text{C}$  Abundances in the Antarctic Ocean with Emphasis on the Biogeochemical Structure of the Food Web. *Deep-Sea Research*, **34**(5/6): 829-841.



Wakeham, S.G. (1990) Algal and Bacterial Hydrocarbons in Particulate Matter and Interfacial Sediments of the Cariaco Trench. *Geochimica et Cosmochimica Acta*, **54**: 1325-1336.

Walker, J.C.G. (1974) Stability of Atmospheric Oxygen. *American Journal of Science*, **274**: 193-214.

Welschmeyer, N.A. and C.J. Lorenzen (1985) Chlorophyll Budgets: Zooplankton Grazing and Phytoplankton Growth in a Temperate Fjord and the Central Pacific Gyres. *Limnology and Oceanography*, **30**(1): 1-21.

Williams, D.F. and R.C. Thunell (1979) Faunal and Oxygen Isotopic Evidence for Surface Water Salinity Changes During Sapropel Formation in the Eastern Mediterranean Sea. *Sediment Geology*, **23**: 81-93.

Williams, D.F., R.C. Thunell and J.P. Kennett (1978) Periodic Freshwater Flooding and Stagnation of the Eastern Mediterranean Sea During the Late Quaternary. *Science*, **201**: 252-254.

Zieman, J.C., S.A. Macko and A.L. Mills (1984) Role of Seagrasses and Mangroves in Estuarine Food Webs: Temporal and Spatial Changes in Stable Isotope Composition and Amino Acid Content during Decomposition. *Bulletin of Marine Science*, **35**(3): 380-392.



### 6.1 General Conclusions

Nitrogen isotopes are a new tool in paleoceanography. Since nitrogen is likely to be a limiting nutrient to primary production in the ocean on  $10^3$ - $10^4$  year timescales, and productivity may influence climate (McElroy, 1983), an understanding of marine nitrogen cycling in the present and historical oceans is important. The nitrogen isotopic composition of marine organic matter may help further this understanding.

Attempts to reconstruct the nitrogen isotopic composition of marine organic matter in the past by measuring the  $\delta^{15}\text{N}$  of whole sediments may, however, be subject to misinterpretation due to the alteration of isotopic ratios during diagenesis. The partial oxidation of marine organic matter can result in significant isotopic enrichment of the preserved residual. The magnitude of this enrichment appears to be large when bottom waters are well-oxygenated, and small when bottom waters are anoxic. Environments where large temporal redox changes have occurred are expected to be the most problematic for the interpretation of bulk sedimentary  $\delta^{15}\text{N}$ . In these environments, the diagenetic signal can be at least as large as the primary isotopic signal being sought. The Eastern Mediterranean Sea during the Late Quaternary appears to be one such environment.

The research presented in this thesis was undertaken in order to find a robust recorder of primary nitrogen isotopic signals in the marine environment. One not susceptible to varying degrees of diagenetic alteration. It was hoped that the measurement of nitrogen isotopic ratios in chlorins would allow the



determination of phytoplankton  $\delta^{15}\text{N}$  in modern and historical environments.

Progress has been made toward this goal. More work needs to be done.

Nevertheless, the following conclusions can be made:

(1) Chlorin  $\delta^{15}\text{N}$  and  $\delta^{13}\text{C}$  can be measured in marine particles and sediments with a precision greater than 0.15 per mil for both nitrogen and carbon. The procedure, which can be performed in about 4 hours for particulate and 8 hours for sediment samples, relies on multiple chromatographic purifications and can be performed on about 20 g of a moderately organic-rich sediment.

(2) Chlorin nitrogen and carbon isotopic ratios can be measured by isotope-ratio monitoring gas chromatography-mass spectrometry (irmGC-MS) by synthesizing the bis-(*tert.*-butyldimethylsiloxy)Si(IV) derivatives. However, yields for the 4-step synthesis were only about 5-6% and there was a net isotopic depletion of  $1.2 (\pm 0.3)$  per mil in the derivative, relative to the starting material.

(3) Chlorin  $\delta^{15}\text{N}$  can be used as a surrogate for phytoplankton  $\delta^{15}\text{N}$  after the addition of 5.16 per mil. Chlorin  $\delta^{13}\text{C}$  is equivalent to phytoplankton  $\delta^{13}\text{C}$ . However, there appears to be interspecies variability in both the nitrogen and carbon isotopic differences between chlorophyll and whole cells in cultured phytoplankton. Although the pooled standard deviation for repeated culture experiments was 0.57 and 1.25 per mil, respectively, for the determination of  $\Delta\delta^{15}\text{N}_{\text{cell-Chla}}$  and  $\Delta\delta^{13}\text{C}_{\text{cell-Chla}}$ , the standard deviation of the average values in 6 species (5 for carbon) was 2.40 and 2.12 per mil, respectively, for nitrogen and carbon.

(4) The average nitrogen isotopic composition of chlorins from six Late Quaternary Eastern Mediterranean sapropels ( $-5.01 \pm 0.38$  per mil) was very similar to the  $\delta^{15}\text{N}$  of chlorophyll from the modern deep chlorophyll maximum ( $-6.38 \pm 1.80$  per mil) in the Eastern Mediterranean. In addition, sapropel

photoautotrophic material, calculated from the chlorin  $\delta^{15}\text{N}$ , had the same isotopic composition (0.15 per mil) as bulk sapropel sediments ( $-0.08 \pm 0.53$  per mil) and deep water nitrate ( $-0.05$  per mil). These data suggest that (a) bottom waters were anoxic, (b) organic matter burial efficiency was enhanced, and (c) oligotrophic conditions similar to today persisted in the Eastern Mediterranean during sapropel deposition. These results contradict earlier interpretations of Late Quaternary bulk sedimentary  $\delta^{15}\text{N}$  in the Eastern Mediterranean. They concluded that the pattern of high  $\delta^{15}\text{N}$  values in intercalated marl oozes and low values in sapropels was the result of decreased nutrient utilization, and hence, increased primary production, during sapropel events.

## 6.1 Directions for Future Research

The measurement of stable isotopic ratios in biomarkers is a powerful approach that allows the circumvention of diagenetic signals while providing targeted information from a paleoenvironment. In conjunction with isotopic determinations in bulk phases, information about secondary processes can also be obtained. Chlorins are ideal biomarkers for such studies in the marine environment because they are produced by all phytoplankton and can be found in both recent and ancient sediments.

A worthwhile extension of the work presented in this thesis would be the development of a rapid and reliable technique for measuring chlorin  $\delta^{15}\text{N}$  and  $\delta^{13}\text{C}$  by irmGC-MS. A promising avenue down which to proceed is the direct gas chromatography of sedimentary chlorins. The methyl ester of pyropheophorbide *a*, a common sedimentary chlorin, was successfully chromatographed on a high-temperature column, eluting near n-C<sub>60</sub> (see section



3.6.5). If it is possible to operate irmGC-MS systems at temperatures near 400°C, it may be possible to measure chlorin stable isotopic values directly from sedimentary lipid extracts. The thin phases (0.1  $\mu\text{m}$ ) of high-temperature GC columns may result in a lower resolution than possible with traditional columns, but there may be less need for resolution at such high temperatures--e.g., there may be few interfering compounds with the low volatility of chlorins.

Another issue worth exploring further is the inter-species isotopic differences between chlorophyll and whole cells for both nitrogen and carbon. If chlorin isotopic values are to be used as proxies for phytoplankton isotopic values it is important to know how the two differ. Although the culture studies described in chapter 4 suggested the inter-species variability in this quantity was on the order of 2 to 2.5 per mil for both carbon and nitrogen, results from the field suggest there was much less variation in the chlorophyll-POC nitrogen isotopic difference. This may result from the fact that the marine environment is rarely monospecific. In other words, the interspecies variability may not be expressed because mixtures of the different species should tend toward the average. Culture studies with mixtures of phytoplankton species may help to resolve this issue.

The low nitrogen isotopic values in the Eastern Mediterranean are one of the more intriguing results of this work. The  $\delta^{15}\text{N}$  of deep water nitrate was found to be -0.05 per mil, significantly lower than the global mean value of 5.7 per mil. This suggests that nitrogen fixation is an important source of new nitrogen to the basin. Yet there are no measurements of such high rates of nitrogen fixation today. Additional  $\delta^{15}\text{N}$  measurements should be made on dissolved nitrogen species in the eastern and western basins, as well as in water from the major rivers draining into the Mediterranean Sea, and in precipitation. The  $\delta^{15}\text{N}$  of DON from these sources, as well as from North Atlantic water



flowing through the Strait of Gibraltar should also be measured since DON may be an important source of new nitrogen. The isotopic characterization of these new nitrogen sources, in conjunction with an accurate nitrogen budget, could help constrain the size of the fixation source.

Finally, a better understanding of nitrogen isotopic systematics in the modern-day Eastern Mediterranean would help to interpret the isotopic record in Late Quaternary sediments. The three eastern basin suspended particulate samples used for this study were collected during a three-day period in June, 1996, in one sector of the basin. Additional samples from different seasons, locations and water depths would help to constrain the isotopic composition of modern-day phytoplankton. The  $\delta^{15}\text{N}$  of chlorins in sinking particles, and of the particles themselves, would aid in understanding the origin of the diagenetic alteration of nitrogen isotopic ratios. In addition, it was argued (section 5.5.4.5) that sedimentary chlorins in stratified systems derive largely from the deep chlorophyll maximum. This should be tested by comparing the pigment distribution in sediment traps to that in suspended particles from the DCM.

McElroy, M.B. (1983) Marine Biological Controls on Atmospheric  $\text{CO}_2$  and Climate. *Nature*, **302**: 328-329.